

OCEANOGRAPHY, MESOSTRUCTURE, AND CURRENTS
OF THE PACIFIC MARGINAL SEA-ICE ZONE -
MIZPAC 75

William John Zuberbuhler

UDLEY KNOX LIBRARY,
NAVAL POSTGRADUATE SCHOOL
MONTEREY, CALIF. 93940

NAVAL POSTGRADUATE SCHOOL

Monterey, California



THESIS

OCEANOGRAPHY, MESOSTRUCTURE, AND CURRENTS
OF THE PACIFIC MARGINAL SEA-ICE ZONE -
MIZPAC 75

by

William John Zuberbuhler
and
John Alexander Roeder

September 1976

Thesis Advisors:

R. G. Paquette
R. H. Bourke

Approved for public release; distribution unlimited.

A report submitted to
Director, Arctic Submarine Laboratory
Naval Undersea Center, San Diego

T175009

REPORT DOCUMENTATION PAGE		READ INSTRUCTIONS BEFORE COMPLETING FORM
1. REPORT NUMBER NPS-58PA76091	2. GOVT ACCESSION NO.	3. RECIPIENT'S CATALOG NUMBER
4. TITLE (and Subtitle) OCEANOGRAPHY, MESOSTRUCTURE, AND CURRENTS OF THE PACIFIC MARGINAL SEA-ICE ZONE - MIZPAC 75	5. TYPE OF REPORT & PERIOD COVERED Final 1 July 1975-30 June 1976	
	6. PERFORMING ORG. REPORT NUMBER	
7. AUTHOR(s) William J. Zuberbuhler and John A. Roeder in conjunction with Robert G. Paquette and Robert H. Bourke	8. CONTRACT OR GRANT NUMBER(s) PO-00010	
9. PERFORMING ORGANIZATION NAME AND ADDRESS Naval Postgraduate School Monterey, California 93940	10. PROGRAM ELEMENT, PROJECT, TASK AREA & WORK UNIT NUMBERS Element: 62759N Project: F52-555 Task: ZF52-555-01Z Work: 9024909	
11. CONTROLLING OFFICE NAME AND ADDRESS Arctic Submarine Laboratory, Code 90 Bldg. 371, Naval Undersea Center San Diego, California 92132	12. REPORT DATE September 1976	
	13. NUMBER OF PAGES 203	
14. MONITORING AGENCY NAME & ADDRESS (if different from Controlling Office)	15. SECURITY CLASS. (of this report) Unclassified	
	15a. DECLASSIFICATION/DOWNGRADING SCHEDULE	
16. DISTRIBUTION STATEMENT (of this Report) Approved for public release; distribution unlimited.		
17. DISTRIBUTION STATEMENT (of the abstract entered in Block 20, if different from Report)		
18. SUPPLEMENTARY NOTES		
19. KEY WORDS (Continue on reverse side if necessary and identify by block number)		
Marginal Sea-Ice Zone	MIZPAC	Physical Oceanography
Arctic Ocean	Microstructure	Circulation
Chukchi Sea	Ice	
Thermal Mesostructure	Currents	
20. ABSTRACT (Continue on reverse side if necessary and identify by block number)		
<p>Currents and complex temperature inversions observed in the Chukchi Sea during MIZPAC 75 were investigated in a further effort to define the mechanisms for the formation of mesostructure. Data was collected using a conductivity-temperature-depth (CTD) recorder and a Savonius rotor current meter. Whereas in previous MIZPAC cruises mesostructure was typically observed in the vicinity of ice margins, during MIZPAC 75 it was primarily</p>		

found in regions of diffuse ice floes and in the open water ice-melt region up to 96 km south of the ice margin. The nature of the mesostructure varied fairly systematically with ice diffuseness and distance from the ice margin. There was little correlation of mesostructure with current direction but a possible correlation with current strength. Mesostructure existed in the same spot for as much as two days with little change, a finding of possible significance to theories of double diffusion. A highly unusual warm bottom water on the Chukchi shelf is presumed to have originated in the Atlantic Layer of the Arctic Ocean.

Oceanography, Mesosstructure, and Currents
of the Pacific Marginal Sea-Ice Zone -
MIZPAC 75

by

William John Zuberbuhler
Lieutenant Commander, United States Navy
B.S., Xavier University, 1962

and

John Alexander Roeder
Lieutenant, United States Navy
B.S., United States Naval Academy, 1969

Submitted in partial fulfillment of the
requirements for the degree of

MASTER OF SCIENCE IN OCEANOGRAPHY

from the

NAVAL POSTGRADUATE SCHOOL
September 1976

Thesis
276
c.1

NAVAL POSTGRADUATE SCHOOL
Monterey, California

Rear Admiral Isham Linder
Superintendent

Jack R. Borsting
Provost

This thesis is prepared in conjunction with research supported in part by the Arctic Submarine Laboratory, Naval Undersea Center, San Diego, under Project Order No. 00010.

Reproduction of all or part of this report is authorized.

ABSTRACT

Currents and complex temperature inversions observed in the Chukchi Sea during MIZPAC 75 were investigated in a further effort to define the mechanisms for the formation of mesostructure. Data was collected using a conductivity-temperature-depth (CTD) recorder and a Savonius rotor current meter. Whereas in previous MIZPAC cruises mesostructure was typically observed in the vicinity of ice margins, during MIZPAC 75 it was primarily found in regions of diffuse ice floes and in the open water ice-melt region up to 96 km south of the ice margin. The nature of the mesostructure varied fairly systematically with ice diffuseness and distance from the ice margin. There was little correlation of mesostructure with current direction but a possible correlation with current strength. Mesostructure existed in the same spot for as much as two days with little change, a finding of possible significance to theories of double diffusion. A highly unusual warm bottom water on the Chukchi shelf is presumed to have originated in the Atlantic Layer of the Arctic Ocean.

TABLE OF CONTENTS

I.	INTRODUCTION - - - - -	13
	A. OVERVIEW - - - - -	13
	B. BACKGROUND - - - - -	18
	1. General Oceanography - - - - -	18
	2. Circulation in the Chukchi Sea - - - - -	20
	C. OBJECTIVES - - - - -	27
II.	EQUIPMENT AND TECHNIQUES - - - - -	29
	A. CONDUCTIVITY-TEMPERATURE-DEPTH RECORDER (CTD)-	29
	B. CURRENT METER- - - - -	30
III.	RESULTS- - - - -	32
	A. MESOSTRUCTURE CLASS AND INTENSITY- - - - -	32
	B. GENERAL OCEANOGRAPHY - - - - -	33
	1. Temperature/Salinity Characteristics - - -	33
	2. Currents - - - - -	43
	C. REGIONAL MESOSTRUCTURE - - - - -	47
	1. Margin Crossings - - - - -	47
	2. Diffuse Ice Floe Region- - - - -	79
	3. Ice-Melt Zone- - - - -	87
	D. TIME AND SPACE VARIATIONS OF MESOSTRUCTURE - -	88
	E. MESOSTRUCTURE-CURRENT CORRELATION- - - - -	96
IV.	CONCLUSIONS- - - - -	-103
	BIBLIOGRAPHY - - - - -	-106

APPENDIX A	EXPLANATION OF HEADING CODES - - - - -	108
APPENDIX B	HEADING DATA FOR MIZPAC 75 STATIONS- - - - -	110
APPENDIX C	CTD DATA FOR MIZPAC 75 STATIONS- - - - -	121
APPENDIX D	MIZPAC 75 CURRENT DATA - - - - -	174
INITIAL DISTRIBUTION LIST-	- - - - -	197

LIST OF TABLES

TABLE I.	MIZPAC 75 Summary - - - - -	-17
TABLE II.	Mesostructure Intensity - - - - -	-33
TABLE III.	Ice Character - - - - -	-98

LIST OF FIGURES

FIGURE

1.	MIZPAC 75 station locations - - - - -	16
2.	BROWN BEAR current measurements, August 1960- - -	22
3.	WEBSEC 70 current measurements, September 1970- -	23
4.	OSHORO MARU current measurements, July, 1972- - -	24
5.	Upper level flow patterns - - - - -	25
6.	Lower level flow patterns - - - - -	26
7.	Temperature cross section through Bering Strait -	35
8.	Salinity cross section through Bering Strait- - -	36
9.	Maximum temperature in the water column - - - - -	37
10.	Ice concentration chart - - - - -	40
11.	Bottom isotherms in MIZPAC 75 area- - - - -	41
12.	Bottom isopycnals in MIZPAC 75 area - - - - -	42
13.	MIZPAC 75 current measurements- - - - -	44
14.	Current measurements during 24 hour time series -	45
15.	Crossings 1, 2, and 3 in relation to the ice margin- - - - -	49
16.	Crossings 4, 5, and 6 in relation to the ice margin- - - - -	50
17.	Temperature profiles for Crossing 1 - - - - -	51
18.	Temperature profiles for Crossing 2 - - - - -	52
19.	Temperature profiles for Crossing 3 - - - - -	53
20.	Temperature profiles for Crossing 4 - - - - -	54
21.	Temperature profiles for Crossing 5 - - - - -	55
22.	Temperature profiles for Crossing 6 - - - - -	56
23.	Temperature cross section, Crossing 1 - - - - -	58

FIGURE

24.	Temperature cross section, Crossing 2	- - - - -	59
25.	Temperature cross section, Crossing 3	- - - - -	60
26.	Temperature cross section, Crossing 4	- - - - -	61
27.	Temperature cross section, Crossing 5	- - - - -	62
28.	Temperature cross section, Crossing 6	- - - - -	63
29.	Density cross section, Crossing 1	- - - - -	65
30.	Density cross section, Crossing 2	- - - - -	66
31.	Density cross section, Crossing 3	- - - - -	67
32.	Density cross section, Crossing 4	- - - - -	68
33.	Density cross section, Crossing 5	- - - - -	69
34.	Density cross section, Crossing 6	- - - - -	70
35.	Rate of flow <u>vs</u> margin orientation, Crossing 1	- - -	73
36.	Rate of flow <u>vs</u> margin orientation, Crossing 2	- - -	74
37.	Rate of flow <u>vs</u> margin orientation, Crossing 3	- - -	75
38.	Rate of flow <u>vs</u> margin orientation, Crossing 4	- - -	76
39.	Rate of flow <u>vs</u> margin orientation, Crossing 5	- - -	77
40.	Rate of flow <u>vs</u> margin orientation, Crossing 6	- - -	78
41a.	Temperature profiles for 24 hour time series (1)	- -	81
41b.	Temperature profiles for 24 hour time series (2)	- -	82
41c.	Temperature profiles for 24 hour time series (3)	- -	83
41d.	Temperature profiles for 24 hour time series (4)	- -	84
42.	Density cross section for 24 hour time series	- - -	85
43.	Temperature/density profiles for selected paired stations	- - - - -	89
44.	Temperature cross section for 24 hour time series	-	92
45.	T-S grouping of stations 64, 65, 66, 68	- - - - -	94
46.	T-S grouping of stations 129K, 129L, and 129M	- - -	95
47.	Mesostructure-current correlation chart	- - - - -	99

ACKNOWLEDGEMENT

The authors wish to express their gratitude to the faculty and staff of the Naval Postgraduate School, in particular Drs. R. G. Paquette and R. H. Bourke, for their assistance in the preparation of this technical report. Our wives, Pat and Kathy, sustained the authors with their untiring moral support; additionally, Pat Zuberbuhler provided welcomed typing assistance.

FOREWORD

This joint thesis had its beginning as two separate studies: one concerning the effects of temperature, salinity, and density on the formation of mesostructure; the other on the effect of the current regime on mesostructure formation. As analysis proceeded, it became more apparent that these variables could not be treated separately. A complete picture of the dynamic processes at and near the ice margin could only be done by combining the results of the previous individual efforts.

The paper is joint in writing only. Each author contributed his own sections and the ideas of these sections are his own. The only common section is the Conclusions section. The order of the authors on the cover sheet is meant to imply neither seniority nor the major contributor. It is felt the resultant product is more concise, and presents a more complete study, than had it remained as two separate papers.

I. INTRODUCTION

A. OVERVIEW

This investigation had its origin in reports of significant deterioration of underwater sound propagation in the marginal sea-ice zone (MIZ) of the Chukchi and Beaufort Seas. The effects were presumably due to the violent fluctuations in temperature which were observed in the vicinity of the ice margin, producing corresponding fluctuations in sound speed. These violent perturbations have been defined as mesostructure (Corse, 1974). It is interesting to note that these phenomena were observed as early as 1947 (LaFond and Pritchard, 1952), but that extensive study began over 20 years later when the Arctic Submarine Laboratory, Naval Undersea Center, San Diego, California established Project MIZPAC. The overall purpose of this project is to develop arctic submarine technology and enhance understanding of the complex sound speed profiles and rapid changes in propagation conditions with distance in the vicinity of the MIZ.

Personnel at the Naval Postgraduate School have been associated with Project MIZPAC since 1971. They have participated in the MIZPAC 71, MIZPAC 72, MIZPAC 74, and MIZPAC 75 mid-summer cruises to the Chukchi Sea. The four MIZPAC cruises have resulted in a data bank of 350 salinity-temperature-depth recorder (STD), 200 conductivity-temperature-depth recorder (CTD), and 44 current meter measurements.

Paquette and Bourke (1973, 1974) described the MIZPAC 71 and MIZPAC 72 results demonstrating some of the characteristic

temperature structures near the ice margin, the two-layered structure south of the ice, the coastal current of northwestern Alaska, and the descent of that warm current into mid-depth along the continental slope and its intrusion into the Beaufort Sea.

Corse (1974) examined MIZPAC 71 data for evidence of mesostructure formation and its space-time distribution. He defined a mesostructure element as extending from the depth where the temperature gradient becomes positive to the depth at which the temperature is the same value as it had when the the gradient became positive. Two different types of mesostructure, "shallow" and "deep", were identified. These were regarded as separated by the 25.5 sigma-t surface with "deep" elements having greater sigma-t values. He found correlation between mesostructure elements in a time series over a period of several hours, but poor spatial correlation over distances as short as 1 km. He postulated that mesostructure elements were formed by the interaction of the northward flow with ice keels causing a mixing downward of warm surficial water. He suggested a correlation between internal waves and the type of mesostructure.

Karrer (1975) examined MIZPAC 74 data, made heat and ice-melt evaluations in the vicinity of the ice margin, and hypothesized that the local dynamic height gradient near the ice margin was a possible driving force for downward mixing. He also modified Corse's definition of shallow and deep mesostructure by utilizing the 26.0 sigma-t surface as the division between them.

Paquette and Bourke (1976) re-evaluated Karrer's analysis and expanded his findings. They showed in one case that mesostructure appeared to be formed by lateral mixing of southerly and northerly waters having nearly the same densities but different temperatures. Uneven mixing and interleaving of water types were hypothesized to be due to complex lateral pressures near the ice. They noted an apparent southward circulation in mid-depth under the ice and found evidence that strong mesostructure was associated with rapid melting processes and probably with rapid flow of warm water toward the ice. They also noted the relatively small fraction of ice-margin crossings which showed strong mesostructure and suggested that the difficulty in demonstrating spatial correlation of mesostructure elements might be because the ice-margin crossings were not oriented in the direction of propagation of the mesostructure forming process.

The MIZPAC 75 cruise was intended to overcome some of the previous difficulties. Wherever mesostructure was found, ice margin crossings were planned to explore it along two directions, including the direction of the current, and to look for a complex flow structure in these areas using direct current measurements. Less time was to be spent in routine ice-margin crossings than in the past. The cruise was conducted substantially in accordance with the cruise plan. Table 1 presents a summary of significant information pertaining to the cruise, and Figure 1 indicates stations taken during MIZPAC 75.

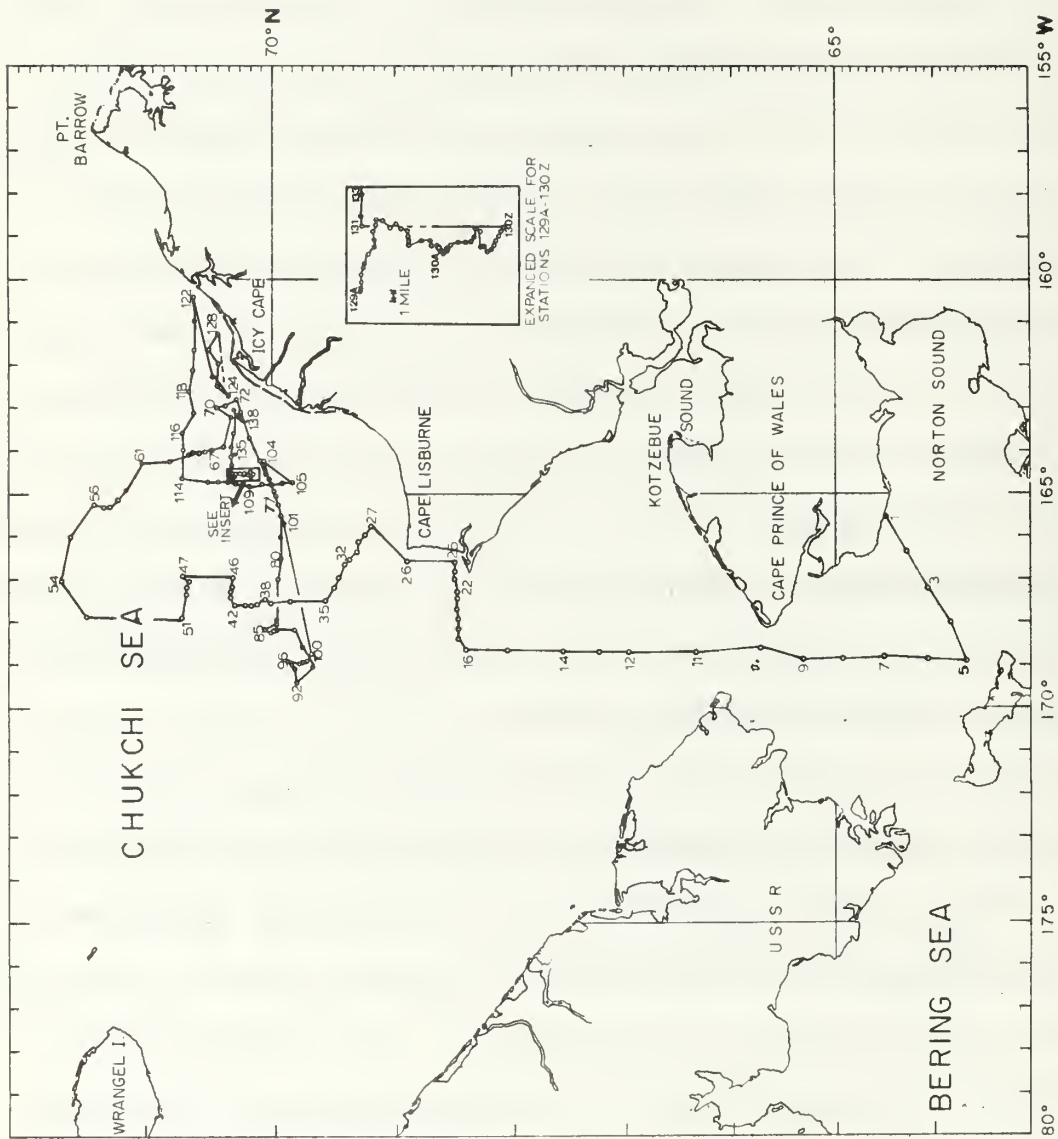


Figure 1. MIZPAC 75 station locations. Lines connecting stations represent only the idealized cruise track.

TABLE 1

MIZPAC 75 SUMMARY

EMBARKATION: 30 July 1975 Nome, Alaska

DEBARKATION: 14 August 1975 Pt. Barrow, Alaska

SHIP: USCGC GLACIER (WAGB-4)

OCEANOGRAPHIC EQUIPMENT:

1. Applied Physics Laboratory
University of Washington
Lightweight CTD System.
2. Hydro Products 400 Series
Current Measuring System.
3. Nansen Bottles and reversing
thermometers.

NAVIGATION SYSTEMS: NAVSAT/OMEGA/LORAN/RADAR

STATIONS OCCUPIED: 194

STATIONS WITH CTD DIGITAL
DIGITAL OUTPUT: 183

CURRENT MEASUREMENTS: 44

NOTE: All measurements were made from a drifting ship.

ICE MARGIN CROSSINGS: 6

SCIENTIFIC PARTY: Dr. M. A. Beal, Chief Scientist (NUC)

Dr. R. G. Paquette, Naval Post-
graduate School

Dr. R. H. Bourke, Naval Postgraduate
School

LCDR W. J. Zuberbuhler, Naval Post-
graduate School

LT J. A. Roeder, Naval Postgraduate
School

Mr. P. Becker, Applied Physics
Laboratory-University of Washington

The ice margin was approached from Nome via Bering Strait, making only enough measurements enroute to give some idea of the change of water properties from south to north. Two crossings were made of the coastal current region because this feature in the past seemed to be associated with mesostructure. Mesostructure was not found where it was expected. It was first found 96 km from the ice and was then regarded as atypical in this location. Therefore, a number of explorations were made along the ice margin before returning to the original mesostructure patch for time series measurements.

The most serious problem encountered during the cruise was recognition of the ice margin. This difficulty was caused either by fog or the failure to recognize the difference between an ice margin and a long line of large ice floes. The possibility exists that measurements were sometimes conducted in isolated patches of ice instead of in the ice margin. This problem was encountered in all previous MIZPAC cruises. Equipment problems during MIZPAC 75 were minimal.

This was the worst ice year in many years. When the time arrived to disembark, GLACIER had been unable to reach Barrow and the scientific group disembarked via helo at Wainwright and were flown to Barrow by courtesy of the Naval Arctic Research Laboratory.

B. BACKGROUND

1. General Oceanography

The Chukchi Sea is a shallow continental-shelf sea with an average depth of 45 m. In any sea as shallow as this

it becomes difficult to trace water types by their temperature and salinity properties because some degree of modification goes on all the time. However, several kinds of water have been identified in the Chukchi Sea:

- Two kinds of surficial water, one of them relatively low salinity, 28 ‰, and formed by extensive dilution of existing water by the melting of ice. This water is subsequently warmed by the sun to about 8°C. South of this water is another more saline surficial water which is similar to the water coming northward through the eastern side of Bering Strait. The temperature of this water is about 8° to 10°C and salinity of 31.5 ‰.
- Bottom water of two or three kinds, one of them at -1.5° to -1.8°C with salinity from 32.5 to 33.8 ‰ which can have had its origin in the convective overturn of the previous winter, either in the Bering Sea or the Chukchi Sea. South of the ice margin this bottom water is somewhat warmer and less saline.
- A third type of water, rarely found, is an anomalously warm and saline water of Atlantic origin which was observed during this cruise with temperatures of -1° to 1°C and salinities of about 32.9 to 33.6 ‰.
- Various transition waters: the waters between layers and the waters between distinct types.

Ice completely covers the Chukchi Sea from November to June. Commencing in June, the ice melts back rapidly in

an irregular fashion to a northerly extent of about 73°N , achieved in mid-September. During this phase the melting proceeds most rapidly along the Alaskan coast, but large areas extending northwestward to Herald Shoal are melted as well. There has been in the past no objective definition of ice margin diffuseness. We make a definition in Section C-2 which concentrates on the diffuseness within the one-okta contour and ignores scattered ice. By this definition the ice margin in MIZPAC 75 was more diffuse than during other MIZPAC cruises.

2. Circulation in the Chukchi Sea

An overview of circulation based upon historical measurements will be presented in this section in order to contrast these measurements with MIZPAC 75 current meter measurements.

Bering Strait is a narrow, shallow (30-50m deep) passage between Alaska and Siberia which connects the Bering and Chukchi Seas. The dominant feature of the mean flow through Bering Strait during summer is its generally northward direction. Coachman and Aagaard (1966) show the major driving force for this northward flow to be the sea surface sloping downward to the north due to regional winds. Normally, sea level in the southern Chukchi Sea is 0.5 m lower than in the Bering Sea. The winds drive water north from the Chukchi Sea and/or drive water from the south into the region north of St. Lawrence Island. The flow speeds in Bering Strait are always swiftest in the eastern channel (150 cm sec^{-1}). Coachman et al. (1976) computed the average transport through Bering.

Strait during summer as 1.7 Sv. Transport during winter is in considerable doubt. After passing through Bering Strait the water masses transverse the Chukchi Sea enroute to the Arctic Ocean.

There are few current measurements from the Chukchi Sea. Three previous surveys covered portions of the MIZPAC 75 region: August 1960 BROWN BEAR, east of 170°W ; September 1970 WEBSEC-70, coastal current from Cape Lisburne to Icy Cape; and July 1972 OSHORO MARU, sections from Cape Lisburne to Siberia and from Pt. Barrow to Herald Shoal. In all instances measurements were made while the ship was at anchor with a current meter reading out on deck. These measurements were made in open water, safely south of the ice margin, with a station time of less than one hour. These data are presented in Figures 2, 3, and 4.

Coachman, et al. (1976) have combined the above data to produce an integrated flow pattern for the Chukchi Sea (Figures 5 and 6). The current flows more rapidly ($20\text{-}30\text{ cm sec}^{-1}$) on the east side of the Chukchi Sea as it proceeds northward from Bering Strait. Over the south-central Chukchi Sea the average speed is $15\text{-}25\text{ cm sec}^{-1}$. This current bifurcates in the vicinity of Cape Lisburne with a northeast branch flowing toward Barrow Canyon, closely following the Alaskan coast. The northeast branch appears to accelerate to 30 cm sec^{-1} as it approaches the Alaskan coast near Icy Cape. Garrison, Pence, and Feldman (1973) noted speeds of 100 cm sec^{-1} along the coast northeast of Pt. Franklin. The Alaskan

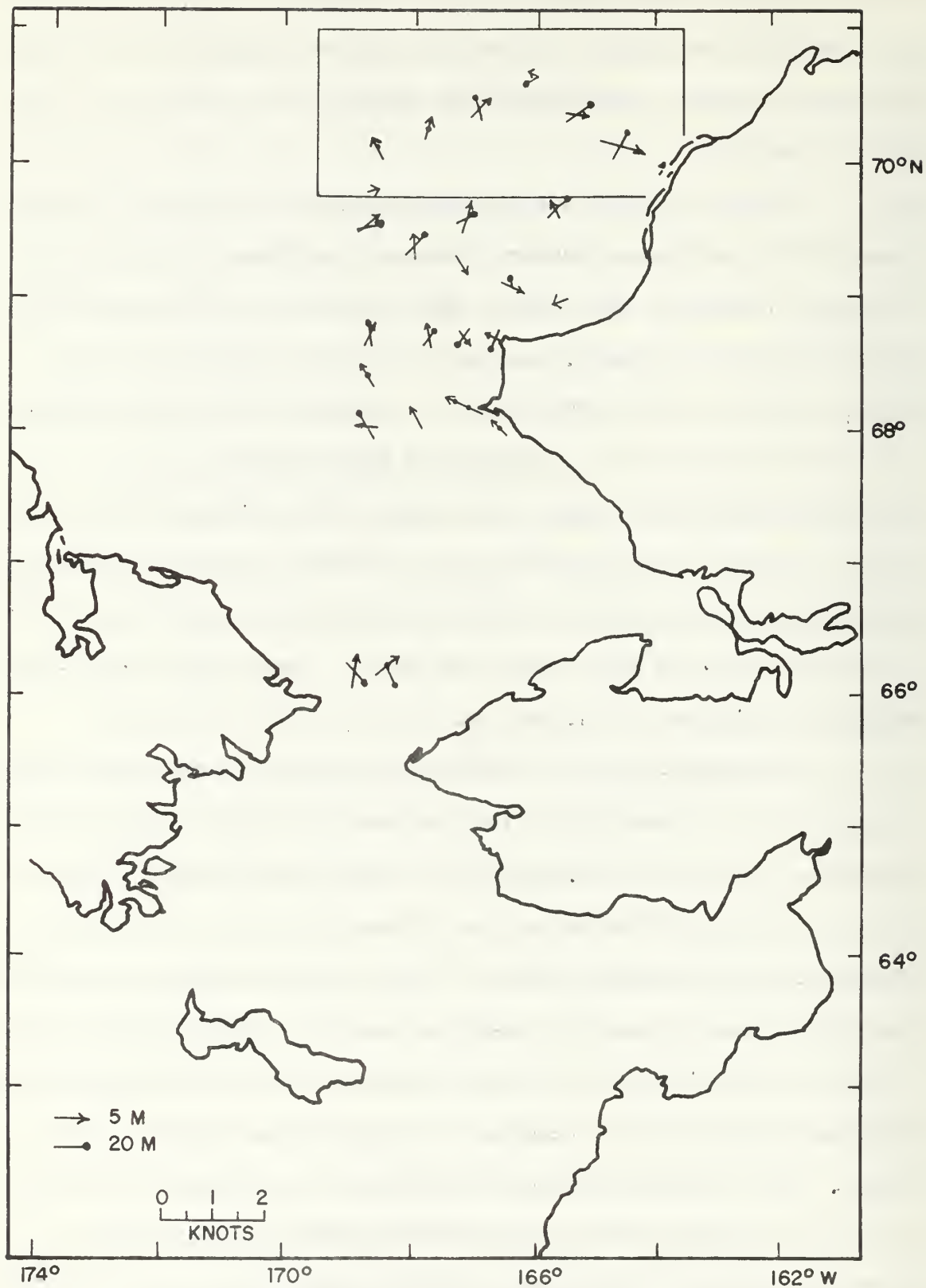


Figure 2. BROWN BEAR current measurements, August 1960. (Adapted from Coachman, et al., 1976) The rectangle shows the area where current measurements were made in 1975.

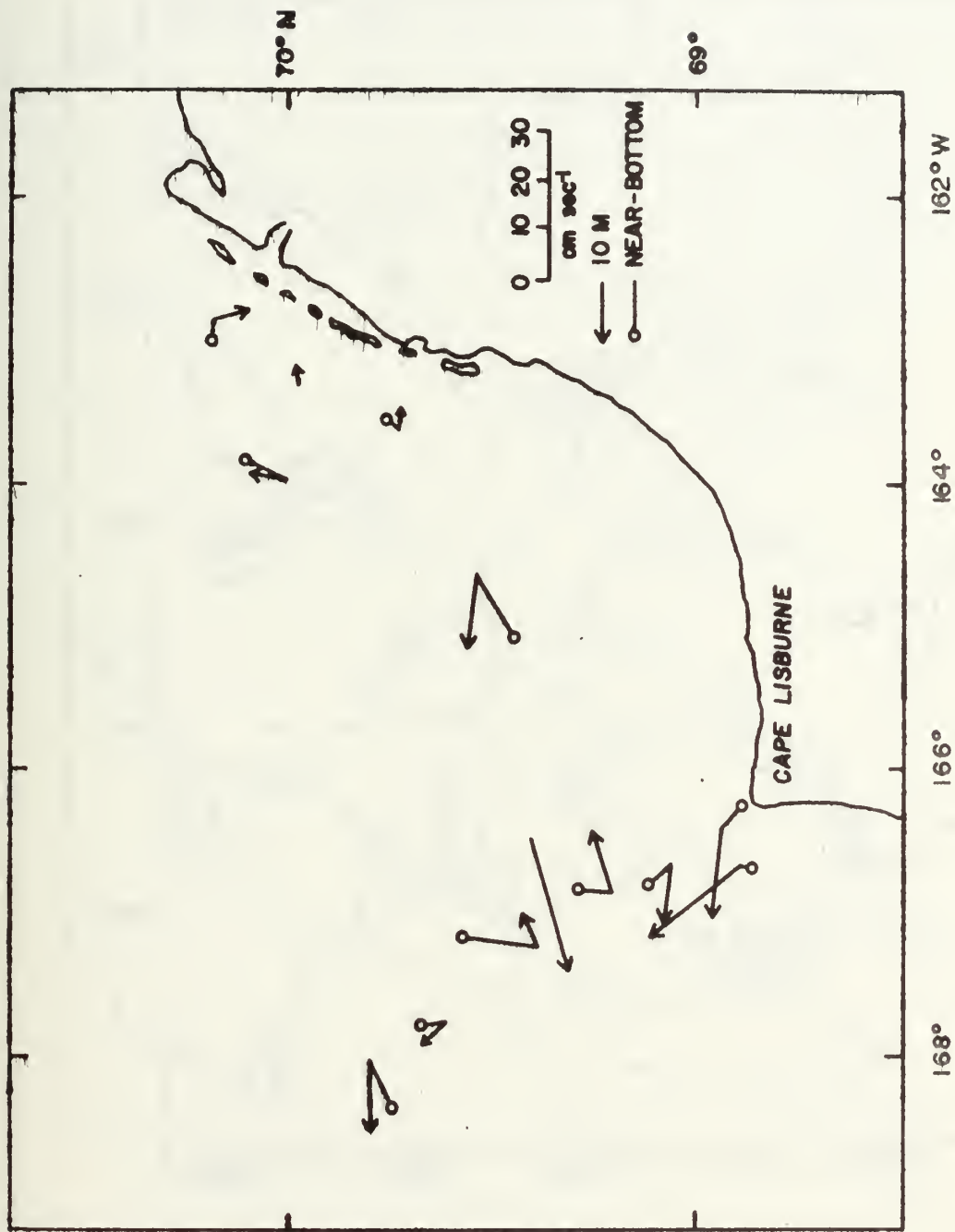


Figure 3. WEBSEC-70 current measurements, September 1970.
 (Adapted from Coachman, et al., 1976)

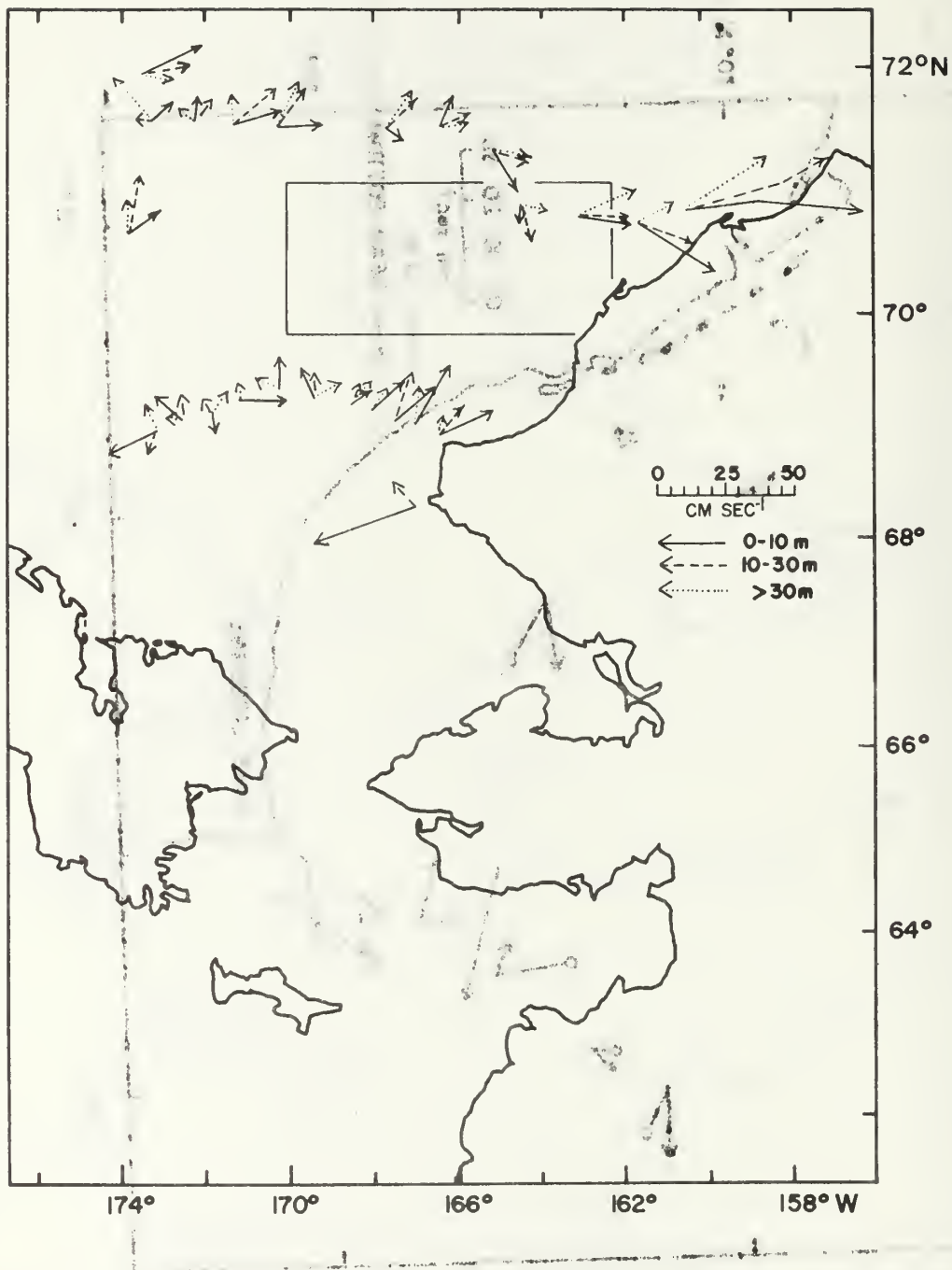


Figure 4. OSHORO MARU current measurements, July 1972.
 (Adapted from Coachman, et al., 1976)

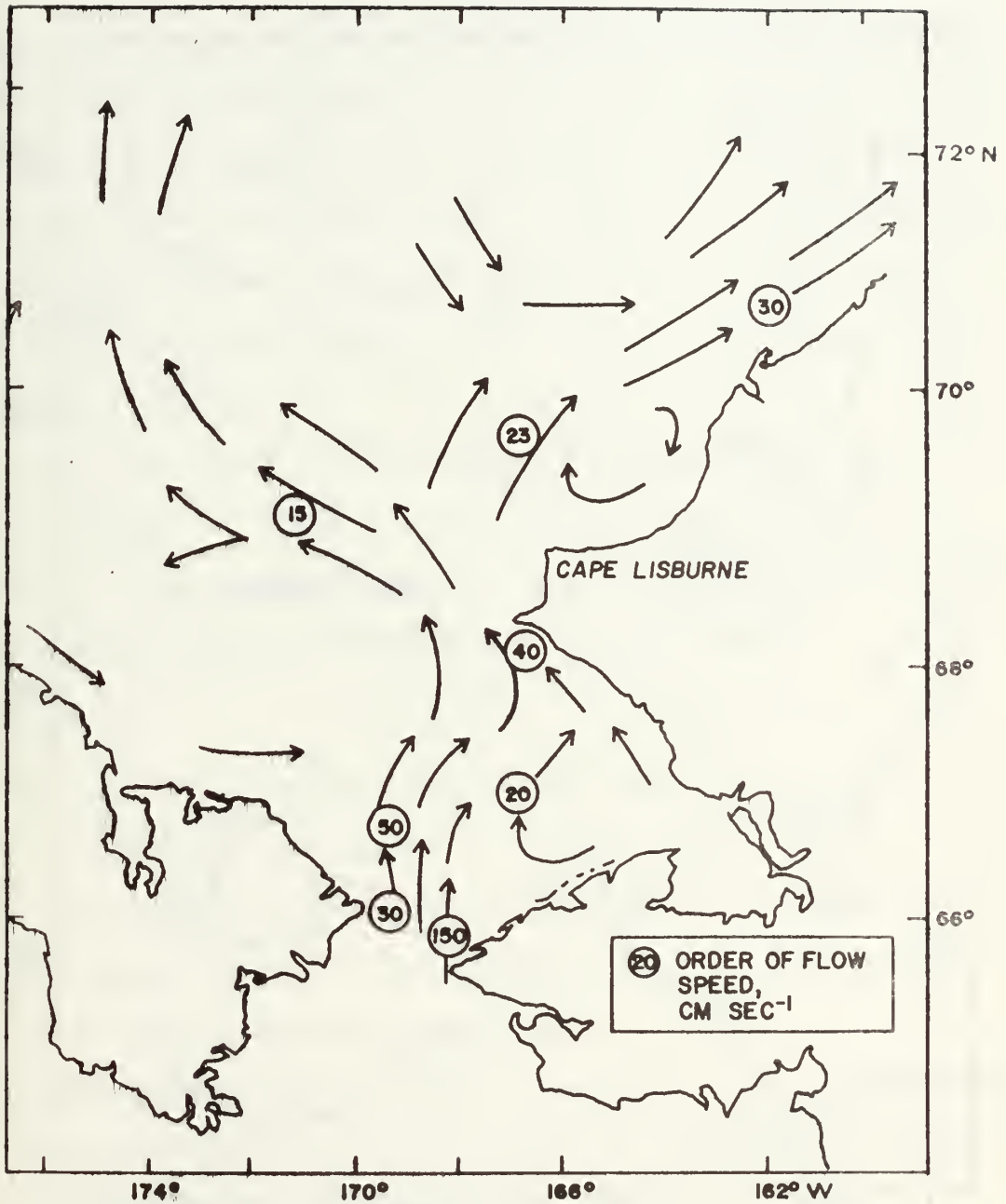


Figure 5. Upper level flow patterns. (Adapted from Coachman, et al., 1976)

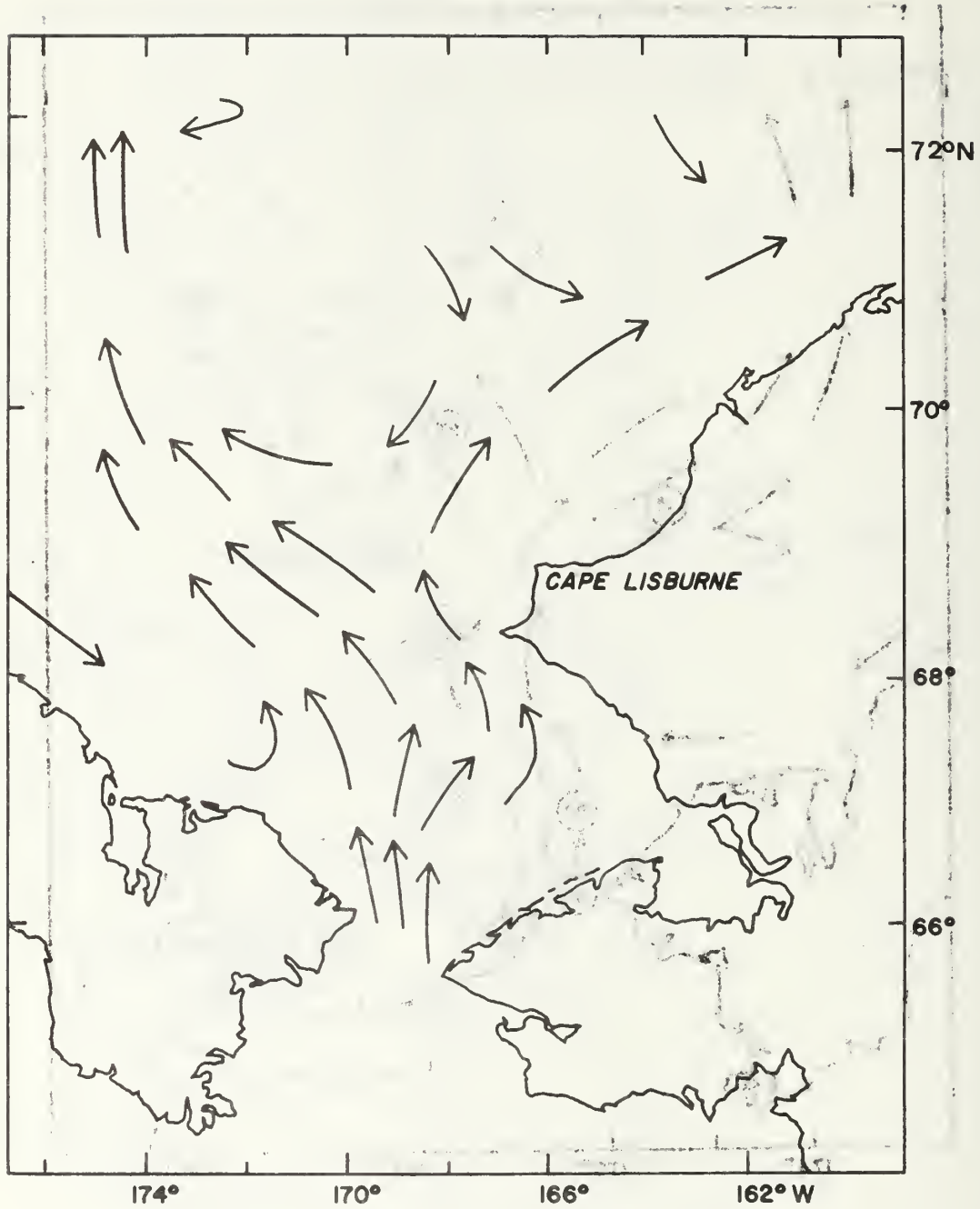


Figure 6. Lower level flow patterns. (Adapted from Coachman, et al., 1976)

Coastal Current, as this branch is known, follows the Barrow Sea Valley as it flows toward Barrow Canyon. Mountain (1974) estimated that the mean transport of flow through Barrow Canyon during summer is 0.75 Sv. This suggests that the flow through Barrow Canyon consists of almost the entire northeast branch of the flow through the Chukchi Sea. The relation between currents in Barrow Canyon and the local winds is similar to that found in Bering Strait. Mountain (1974) suggests that, between Bering Strait and Barrow Canyon, the oceanic system responds nearly simultaneously to the changing atmospheric pressure.

The existence of large gyres in the Chukchi Sea is evident in Figures 3 and 5. The anti-cyclonic gyre in the lee off the Cape Lisburne peninsula is pertinent to the analysis of mesostructure discussed in a later section.

C. OBJECTIVES

The objectives of this report are twofold:

1. To present the MIZPAC 75 cruise results;
2. To ascertain the dynamics involved in mesostructure formation using MIZPAC 75 data in conjunction with previous findings. Specifically this includes:
 - Defining the classes and intensities of mesostructure,
 - Establishing the relationship of mesostructure with ice character and currents.
 - Investigating the time and space scales of mesostructure.

Additionally, it is desired to relate MIZPAC 75 current measurements to previous measurements in the east-central Chukchi Sea and to amplify previous findings concerning the general oceanography of the Chukchi Sea.

II. EQUIPMENT AND TECHNIQUES

A. CONDUCTIVITY-TEMPERATURE-DEPTH RECORDER (CTD)

The CTD is a portable, hand lowered system developed by the Applied Physics Laboratory, University of Washington (APL-UW). The unit is built around a small hand-powered winch; the power supply and data cassette recorder are mounted within the winch drum itself thus avoiding the need for slip rings. The sensor group consists of a conductivity cell with platinized electrodes excited with a Wien-bridge oscillator, a thermistor, and a vibratron pressure sensor. The lowering rate of the CTD was about 1 m sec^{-1} in order to obtain a data rate of approximately three points per meter. The outputs were recorded digitally on 1/4 inch magnetic tape in serial order as groups of four-digit four-bit numerals.

Salinity spiking was observed in some of the profiles. However, it was considerably less than that recorded with the Bissett-Berman STD used on previous cruises. The possibility of encountering a density inversion was considered remote. Therefore, it was convenient to hand smooth the salinity traces where necessary.

The CTD was standardized by means of a Nansen bottle situated just above the instrument, which was tripped as the CTD sensor probe approached bottom. With the Nansen bottles as a standard, the salinity error averaged -0.03 ‰ and the temperature error -0.04°C . These errors were relatively constant for all samples taken.

Data obtained from each station lowering were immediately plotted, utilizing a Hewlett-Packard 9100 series computer/plotter system. These rough plots were used to make immediate assessments of the presence of mesostructure prior to departing from a station.

The data on the cassettes were eventually transferred to a single nine-track tape by the APL-UW. The tape, along with a computer printout of all the data, was sent to the Naval Postgraduate School for analysis. After editing the data for erroneous heading input and data sequencing errors, the tape was corrected for the instrument errors.

Plotting routines were utilized which presented a compact display of property profiles for each station: temperature, sound speed, salinity, and density (σ_t). These profiles, plotted four per page, along with the heading data printouts, are listed in Appendices B and C. The temperature trace is marked with crosses and the salinity trace with dots every 20 depth increments. Symbols (T,SV,S,ST) have been introduced to help distinguish curves of each property.

B. CURRENT METER

The current measurements attained during MIZPAC 75 were made using the Hydro-Products Series 400, self contained current-measuring system. The speed sensor of the underwater unit was a Savonius rotor and the direction sensor was a vane magnetically coupled to a micro-torque potentiometer oriented by a magnetic compass. The rotation rate of the rotor and the magnetic direction of the vane were telemetered to the

surface on four-conductor rubber-jacketed cable which read out on dial indicators located on deck. The cable was married to a weighted wire line by means of modified boat snaps.

The meter was suspended inside a weighted aluminum tetrapod, which permitted setting the assembly on the bottom, a procedure required to obtain absolute current velocities. With the tetrapod on the bottom the speed sensor was 48 cm above bottom and the direction vane 85 cm above bottom. Since the measurements were made from a drifting ship, the resulting relative currents were converted to absolute currents by means of comparison of the current measured with the meter just above bottom and a current measured with the tetrapod resting on the bottom, assuming the earth-referenced current vector to be the same at the two levels.

The manufacturer's claims for instrument accuracy were $\pm 3\%$ of the reading for the Savonius rotor, above a nominal threshold of 1 cm sec^{-1} , and $\pm 10^\circ$ for the direction vane. During calibration tests, the vane exhibited a stiction corresponding to a 10° lag. However, very small vibrations sufficed to reduce the lag considerably. It is believed that conditions in the field left this error smaller than 5° .

Current meter data are presented in Appendix D as follows: north and east components (cm sec^{-1}) at each measured depth; and the heading ($^\circ\text{T}$) and speed (cm sec^{-1}) averaged over 0-10m, 10-30m, and 30m-bottom.

III. RESULTS

A. MESOSTRUCTURE CLASS AND INTENSITY

This section is intended to define the various classes and intensities of mesostructure which will be referred to throughout the analysis of MIZPAC 75 temperature profiles.

Corse (1974) and Karrer (1975) described mesostructure as being divided into three classes: the nose feature, and shallow and deep structure. Corse (1974) defined the nose as any region of warmer water extending over more than 5m in depth. The authors feel that the nose feature, of itself, is not a class of mesostructure since it is not necessarily formed by the same dynamic processes that produce mesostructure. However, it is possible the nose feature can be associated with shallow mesostructure if the shallow elements are an integral part of the nose.

Corse (1974) and Karrer (1975) separated shallow mesostructure from deep mesostructure by means of a specified density surface. Corse placed the boundary between these mesostructure classes at a σ_t value of 25.5 while Karrer chose 26.0. The authors believe that a more realistic criterion is not a specific density surface but the relation of the mesostructure element to the thermocline. Therefore mesostructure is divided into two classes: shallow mesostructure, found above or in the main thermocline; and deep mesostructure, found below the main thermocline.

As will be seen, the lateral temperature excursion of any single mesostructure element varies from station to station and also within each station. The magnitude of this temperature excursion is defined as the mesostructure intensity. Paquette, Bourke, and Corse (1974) stated the minimal extent of this lateral temperature excursion, for it to be considered mesostructure, was 0.1°C . For analysis purposes it was convenient to define the intensity of mesostructure in three regimes: strong, moderate, and weak. The thermal excursion for these intensities is indicated in Table II. This excursion is measured from an estimated mean temperature curve to the extreme of the mesostructure element.

TABLE II. Mesostructure Intensity.

<u>Intensity</u>	<u>Temperature Excursion</u>
Weak	$0.1^{\circ} - 0.5^{\circ}\text{C}$
Moderate	$0.5^{\circ} - 1.0^{\circ}\text{C}$
Strong	$> 1.0^{\circ}\text{C}$

B. GENERAL OCEANOGRAPHY

1. Temperature/Salinity Characteristics

This section describes the general oceanography observed during MIZPAC 75 and emphasizes the salient features that differentiate it from the four previous MIZPAC cruises. The order of presentation of data is from south to north: south of Bering Strait, in the strait, north of the strait into the Chukchi Sea, and into the ice margin region.

The temperature of the surface waters south of Bering Strait were 10° - 12° C. These temperatures were slightly higher than those observed in previous MIZPAC cruises, although data from other cruises show temperatures of this magnitude. Surface salinities were about 31.5 to 32.0° /oo. The salinity has been shown to be lower toward the east side of the Bering Sea north of Norton Sound due to a concentration along the coast of warm relatively fresh water from Norton Sound (LaFond and Pritchard, 1952). These authors found the water column was highly stratified with a sharp temperature and salinity gradient at 10-12 m. The lower layer was fairly cold, 0° to 3° C, and had salinity values of 32.5 to 32.8° /oo. The MIZPAC 75 results are in agreement with these observations. Station property profiles for the stations south of Bering Strait, Stations 1-8, are presented in Appendix C.

Figure 7 shows the beginning of a decrease in temperature in the upper layers north of Station 10, which is in the throat of the strait. However, at Station 10 there is a pocket of warm water which will be seen to be also of low salinity in Figure 8. This is evidence of the large scale horizontal macro-turbulence which must exist in the Strait. Cooling was observed to continue toward the north. To show this, Figure 9, a plot of maximum temperatures in the water column, is presented. The concept of maximum temperatures will be useful later, but for the present purpose these temperatures may be regarded as surface temperatures south of Cape Lisburne. This cooling probably is due to the increasing

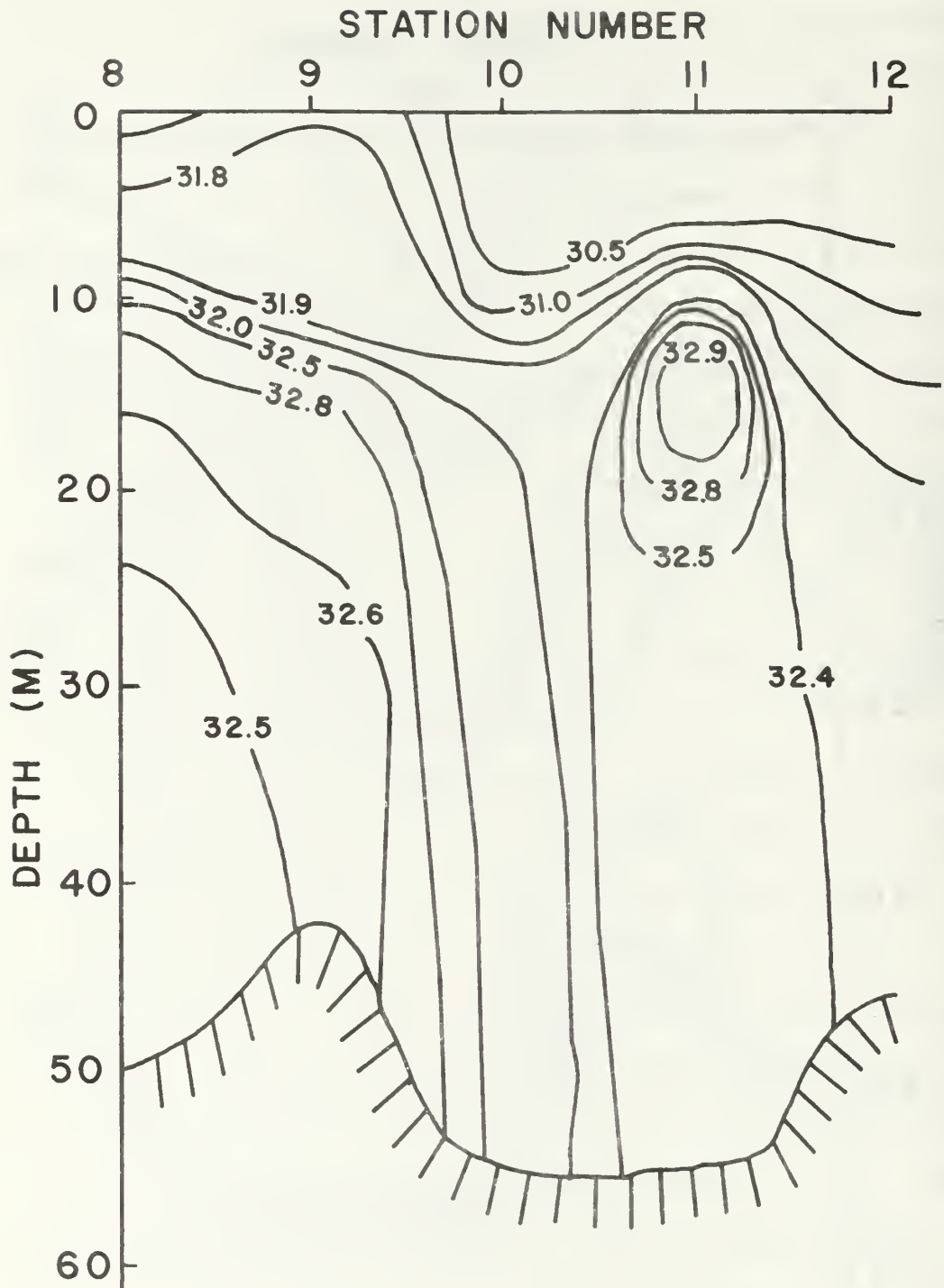


Figure 8. Salinity cross section through Bering Strait (South to North).

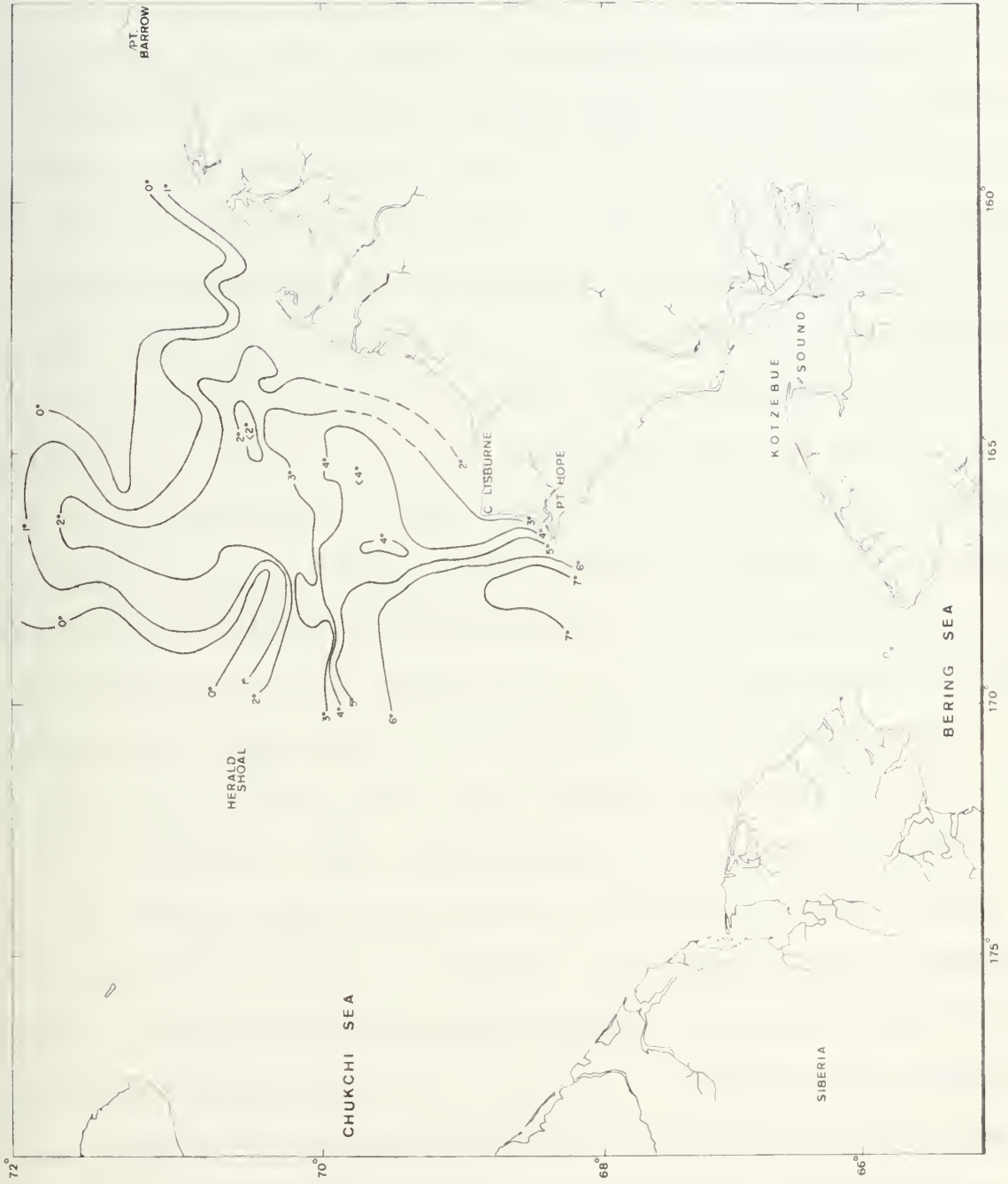


Figure 9. Maximum temperature in the water column.

importance of the effects of melting ice over those of insolation as the ice is approached, but admixtures of cold water from the East Siberian Current (Coachman, et al., 1976) may be a factor.

Proceeding north into the Chukchi Sea, the water structure was observed to be basically of two types. Most water columns north of Bering Strait were two-layered both in temperature and salinity, but at a point about 96 km south of the ice, near Cape Lisburne, the salinity of the upper layer decreased abruptly. This distinctive change in the surficial salinities may be seen by comparing Station 26 with the section off Cape Lisburne (Stations 27 to 35), where the stations exhibited reduced surficial salinities in the upper 2 to 8 m of the water column. The salinities ranged from 28.5-29.0 ‰, while just south of this section at Station 26, the surface salinity was 31.5 ‰. This area, to be designated as the ice-melt water zone after Paquette and Bourke (1976), will be described in greater detail in a later section. The ice melt-water boundary is at approximately 69°N latitude. This is nearly the same position it was found during MIZPAC 74 (Paquette and Bourke, 1976). However, 1975 was different in that mesostructure was observed throughout the ice-melt region, wherever it was sampled. It is also interesting that at this boundary the warm core of the coastal current was found covered from here northward by cooler, fresher water to a depth of about 10 m.

There are two other areas in which mesostructure was found; one is immediately outside the ice in a region of patchy ice floes (the areas < 1 okta in Figure 10) and the other is the ice-free ice-melt zone. As in past years, mesostructure was found in this zone near the ice. However, in 1975, mesostructure was found as far south as the southern limit of the zone.

In view of its importance to the formation of the mesostructure, a brief description of the ice margin in MIZPAC 75 follows. Mechanisms associated with mesostructure formation will be treated in a later section. The ice margin as observed from shipboard was, in general, diffuse by our definition, compared to 1971 or 1972. There was one segment of the ice margin which was compact for about 16 km, but the remainder was quite diffuse. The ice margin was generally coincident with the -1.6°C bottom isotherm. This suggests that the bottom water to the south has been modified by processes at the retreating ice edge (Paquette and Bourke, 1976).

An unusual water type was observed frequently near the ice. A relatively warm (near 0°C) but salty (> 33 ‰) bottom water was found underlying much colder water (-1.7°C). Figures 11 and 12 show the distribution and size of this anomalously dense water ($\sigma_t = 26.5$ to 26.9). It occurred in a lens near the coast near latitude 70° and also farther west near 70°N , 168°W . Water this salty is commonly found in the Chukchi as a result of brine release during ice formation in winter. However, such water is associated with cold

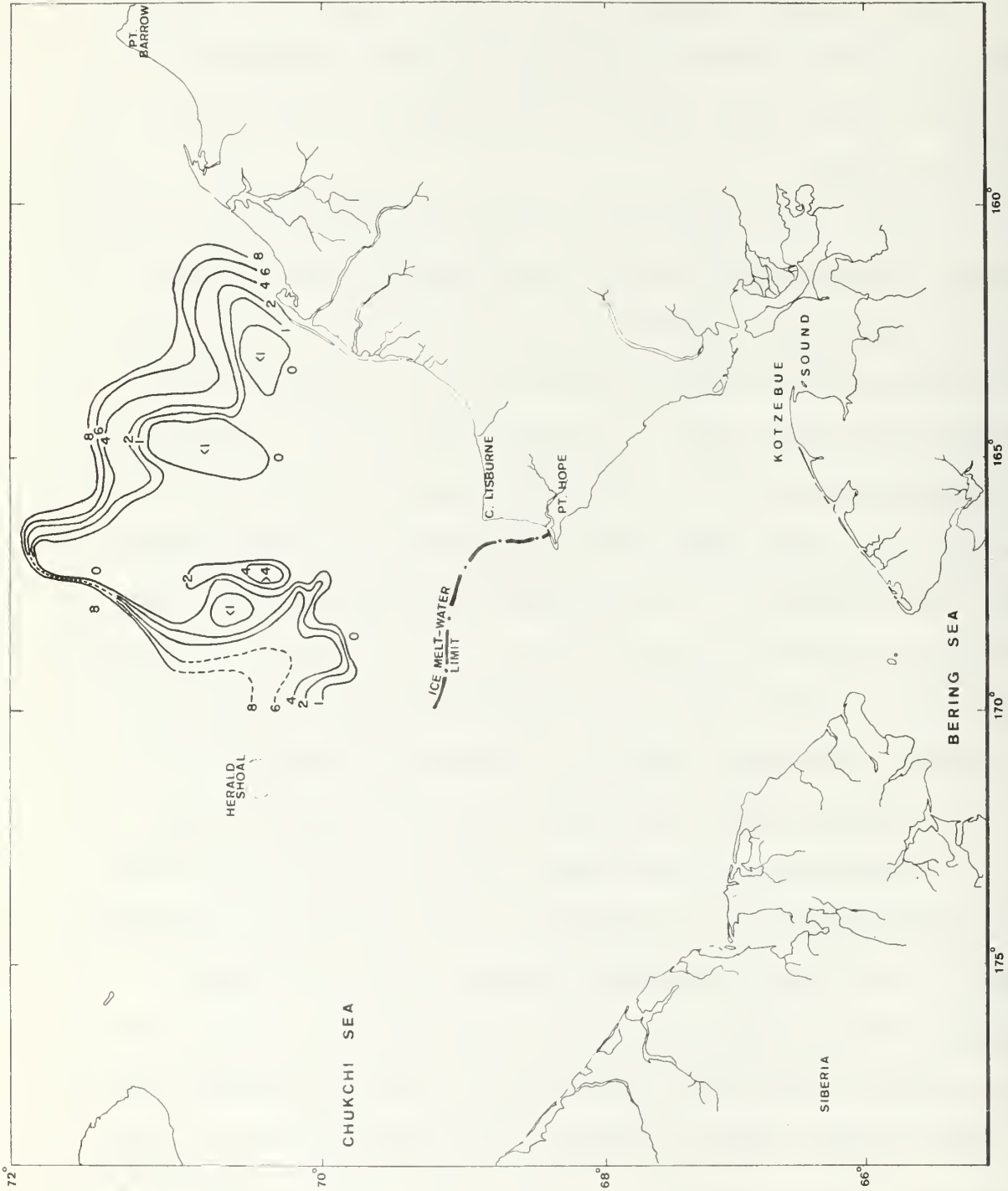


Figure 10. Ice concentration in oktas, including southern limit of ice melt-water region.

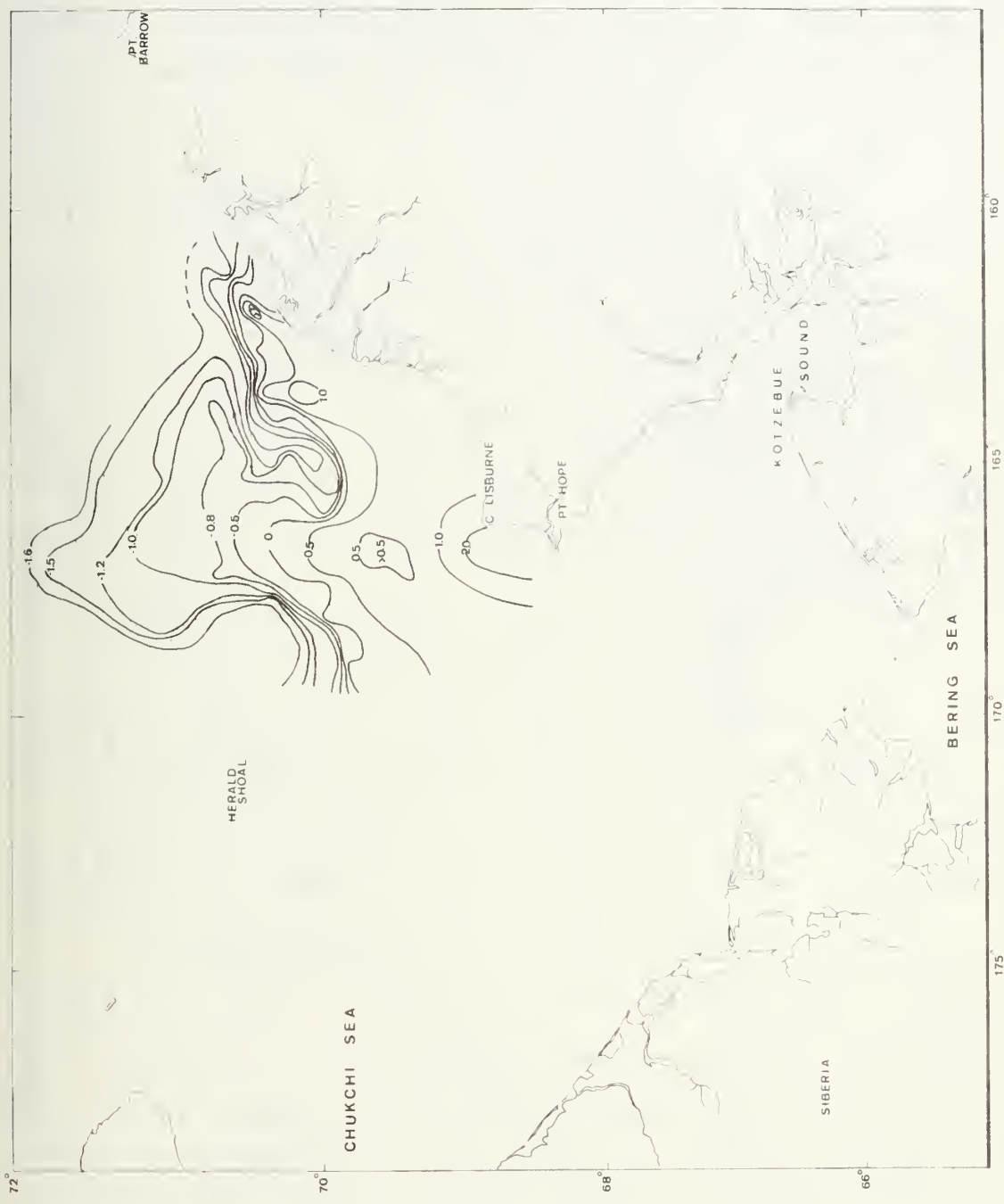


Figure 11. Bottom isotherms in MIZPAC 75 area. Temperatures are in °C.

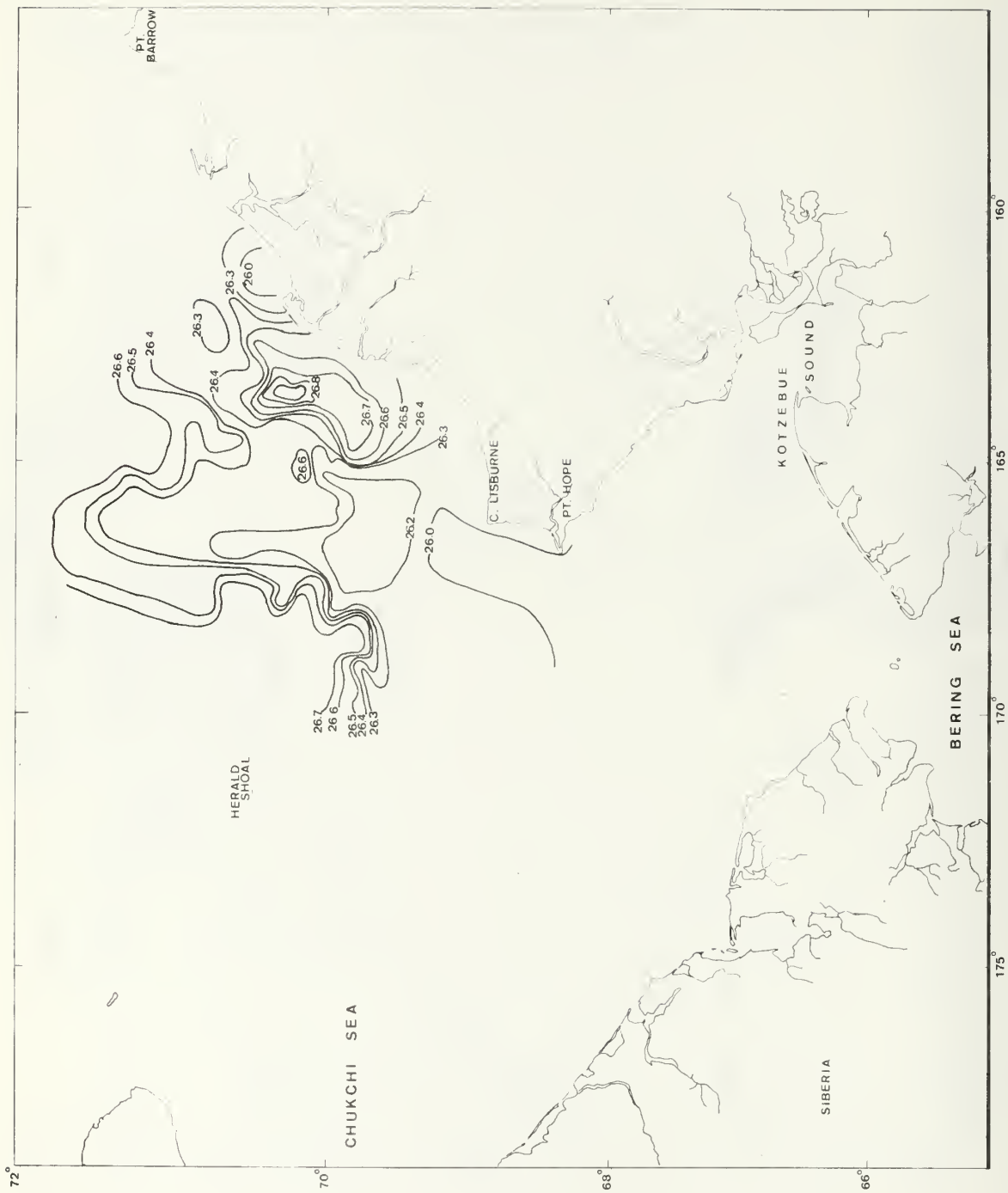


Figure 12. Bottom sigma-t in MIZPAC 75 area.

temperatures near the equilibrium freezing point (-1.7° to 1.8°C) and hence cannot be the origin of this anomalous bottom water. This water is most likely Atlantic water from the Arctic Ocean which has entered the Chukchi Sea via depressions or valleys in the sea floor, i.e., Barrow Canyon and the valley east of Herald Shoal (Bourke and Paquette, 1976).

2. Currents

Current measurements were taken at 44 stations during MIZPAC 75. Measurements were made in the vicinity of the ice to observe the local flow regime in areas where mesostructure existed. Depths of observation were every 5m from the surface to the bottom. The current measurements, averaged over 0-10m, 10-30m, and 30m-bottom, are shown as vectors in Figures 13 and 14.

These measurements were not designed to define the general circulation of the east-central Chukchi Sea. However, they do demonstrate a general northward flow of water which is in agreement with the few previous summer current measurements in this region of the Chukchi Sea. For a comparison with previous measurements the reader should refer back to Figures 2, 3 and 4. Figure 2 presents BROWN BEAR (1960) current vectors at 5m and 20m; Figure 3 presents the WEBSEC-70 current vectors at 10m and near bottom; and Figure 4 presents the OSHORO MARU (1972) averaged current vectors in the upper (0-10m), intermediate (10-30m), and bottom ($> 30\text{m}$) layers (Coachman, et al., 1976). The turning with depth of MIZPAC 75 current measurements was for the most part within

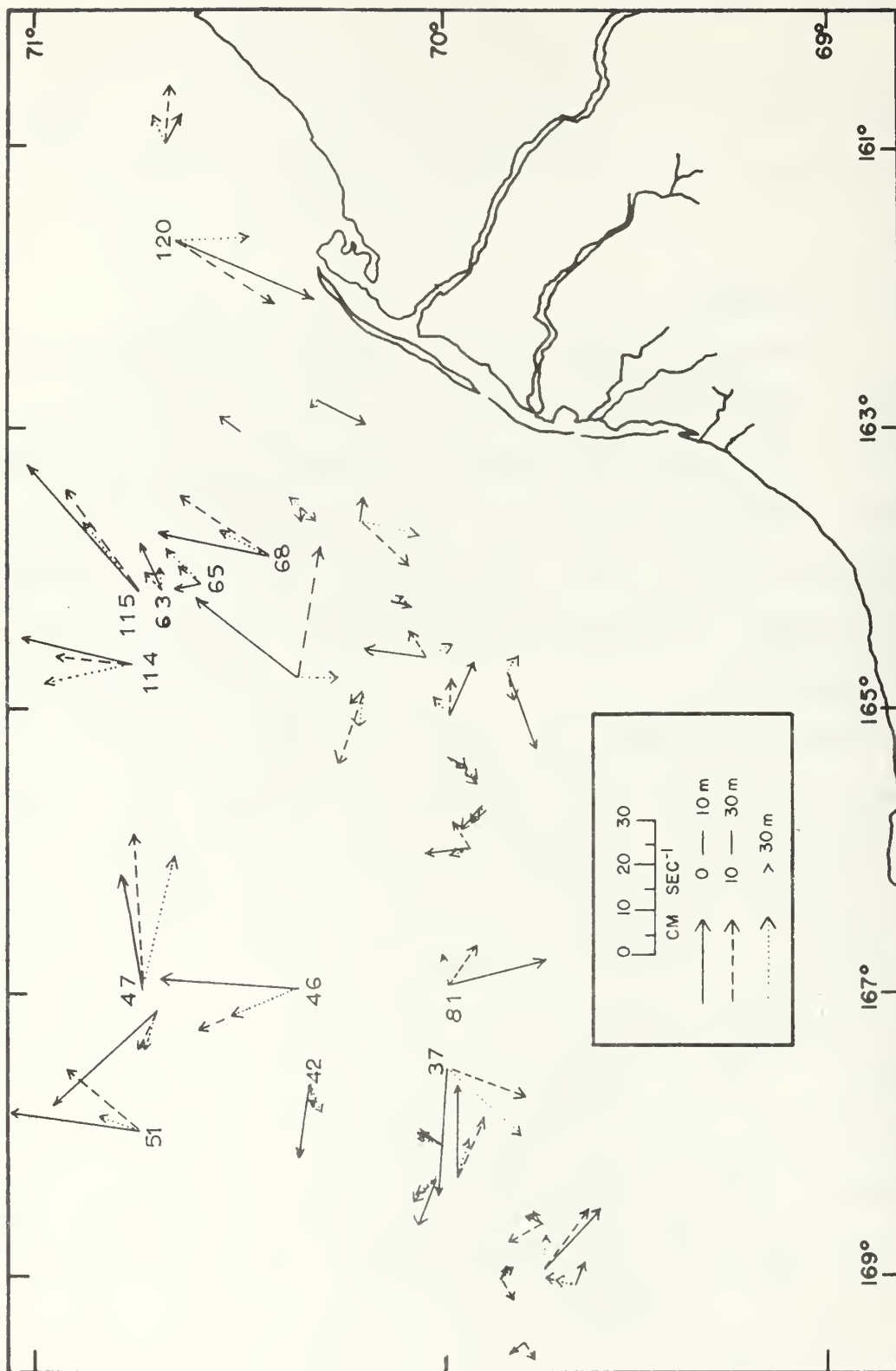


Figure 13. MIZPAC 75 current measurements.

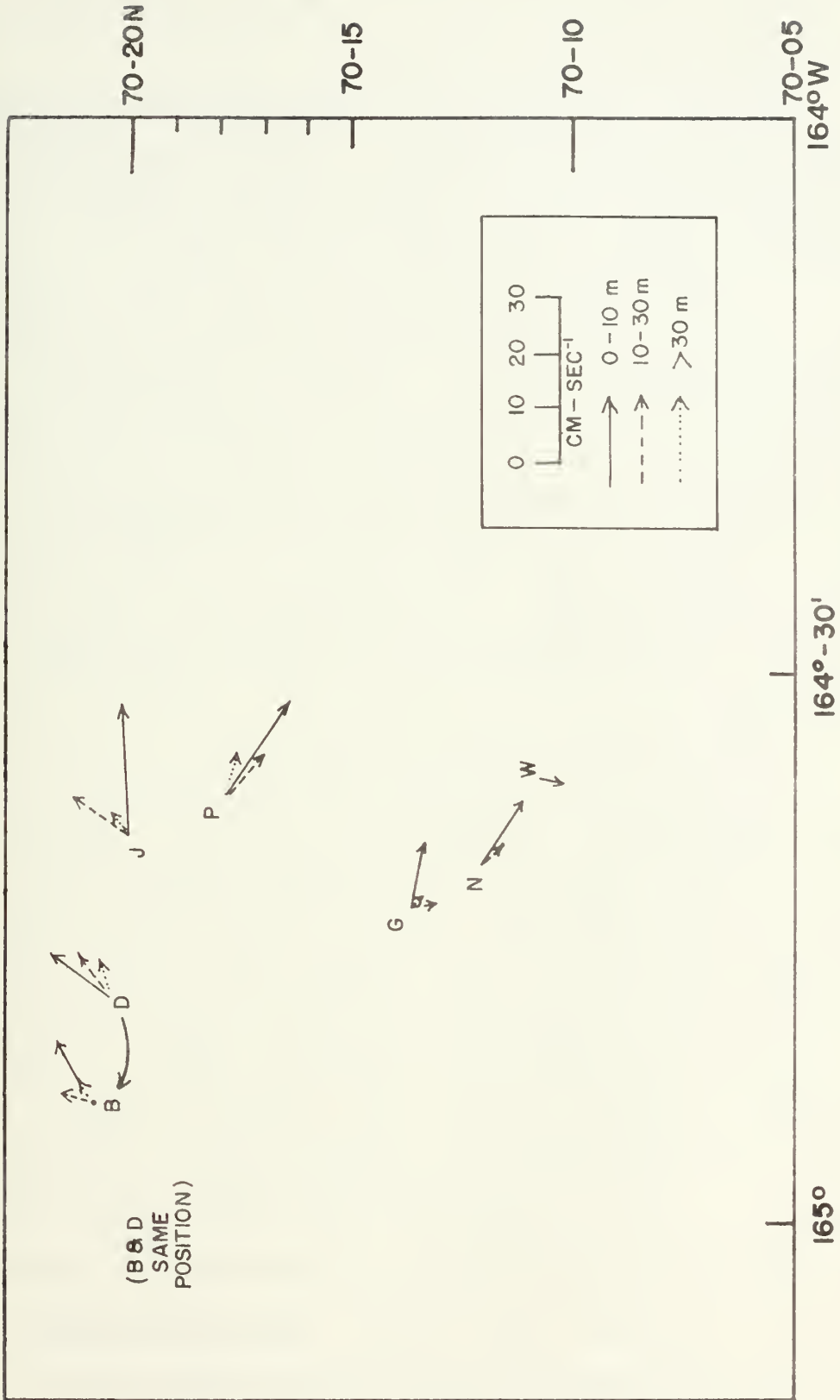


Figure 14. Current measurements during 24 hour time series. B, D, J and P have station numbers 129B, etc.; G, N and W are prefixed by 130.

a 60° sector which is consistent with the findings of the above authors. The turning was not generally clockwise, hence Ekman rotations are not important.

However, the rotation of direction between adjacent stations, demonstrated by MIZPAC 75 current measurements, was considerably greater than in previous measurements. These earlier measurements, which were made well south of the ice margin in open water, demonstrated rotations of less than 30° between adjacent stations. MIZPAC 75 measurements, made in the vicinity of ice, experienced rotations of up to 170° . This variability in direction between adjacent stations was greatest between closely spaced stations (10 km) taken during ice margin crossings. It is believed that this increased variability in direction was due to some dynamic effect of the ice margin.

The current measurements have been examined for evidence of large gyres. Coachman, et al. (1976) reported a gyre in the bight north of Cape Lisburne (Figures 3 and 5). Vectors somewhat consistent with such a gyre exist in the present data, but it is evident that the high degree of directional variability prevent an unequivocal support of the earlier data. During a 24-hour time series conducted in the vicinity of the reported gyre, GLACIER drifted to the east and south, as shown in Figure 14. The seven current meter measurements made during this drift shifted gradually from northward to southward flow. While a well defined rotation is clearly demonstrated, it is not clear whether it is a temporal or a spatial phenomenon.

The split in the northward flow of Bering Sea Water described by Coachman et al., (1976) is easily visible in the diagram of maximum temperatures (Figure 9). The westerly branch undoubtedly is the cause for the deep bight in the ice north of Cape Lisburne at longitude 166°W in Figure 10. The same kind of split may be seen at the same longitude in the current measurements (Figure 13).

The northeasterly branch, the Alaskan Coastal Current, was identified during MIZPAC 75 by the large finger of relatively warm water directed northeastward and the swift (15.4 cm/sec) northeastward flow demonstrated by the current measurements (Stations 63, 65, 68, 114, 115). The core of this current appears to be 74 km from the Alaskan Coast. Paquette and Bourke (1974), in their analysis of the coastal current during MIZPAC 71, show closely packed isotherms about 30 km off the Alaskan Coast in the vicinity of latitude 70°-30' N which appeared to be the core of the coastal current. Later, utilizing MIZPAC 74 data, Paquette and Bourke (1976) observed the core 65 km off the Alaskan Coast. The implication from MIZPAC data is that the position and relative strength of the core of the coastal current varies from year to year and possibly varies during the course of the summer season in response to the retreat of the ice.

C. REGIONAL MESOSTRUCTURE

1. Margin Crossings

Current measurements and CTD lowerings were made during six ice-margin crossings in MIZPAC 75. Mesostructure was

observed during each of the margin crossings and was examined in relation to the flow regime ascertained from current measurements. For convenience these crossings are numbered 1 through 6. The corresponding station sequences are 42-46, 47-51, 61-69, 82-85, 85-88, and 92-96 as shown in Figures 15 and 16. These ice-margin crossings do not extend on either side of the margin to the distances which were standard in previous cruises. They were not indeed intended as standard margin crossings but as explorations for mesostructure near the ice edge. Therefore, five of the six crossings cannot be expected to compare well with the ice crossings of previous years. Crossing 3 is the exception, being longer than the others and extending farther into open water.

The nested temperature profiles for each margin crossing are shown in Figures 17 through 22. The bottom temperature ($^{\circ}\text{C}$), position of the ice margin (M), and station number are displayed at the bottom of each trace, and the ice concentration, in oktas (eighths) or in exponential form, is indicated at the top. The figures present margin crossings from outside the ice (left) to inside the ice margin (right). Outside the ice margins the temperature profiles displayed a relatively warm surface layer with a maximum temperature of 2° to 5.5°C . This warm surface layer cooled rapidly in the immediate vicinity of the ice margin and disappeared or was greatly diminished well inside the ice margin. This is consistent with previous MIZPAC observations (Corse, 1974; Karrer, 1975).

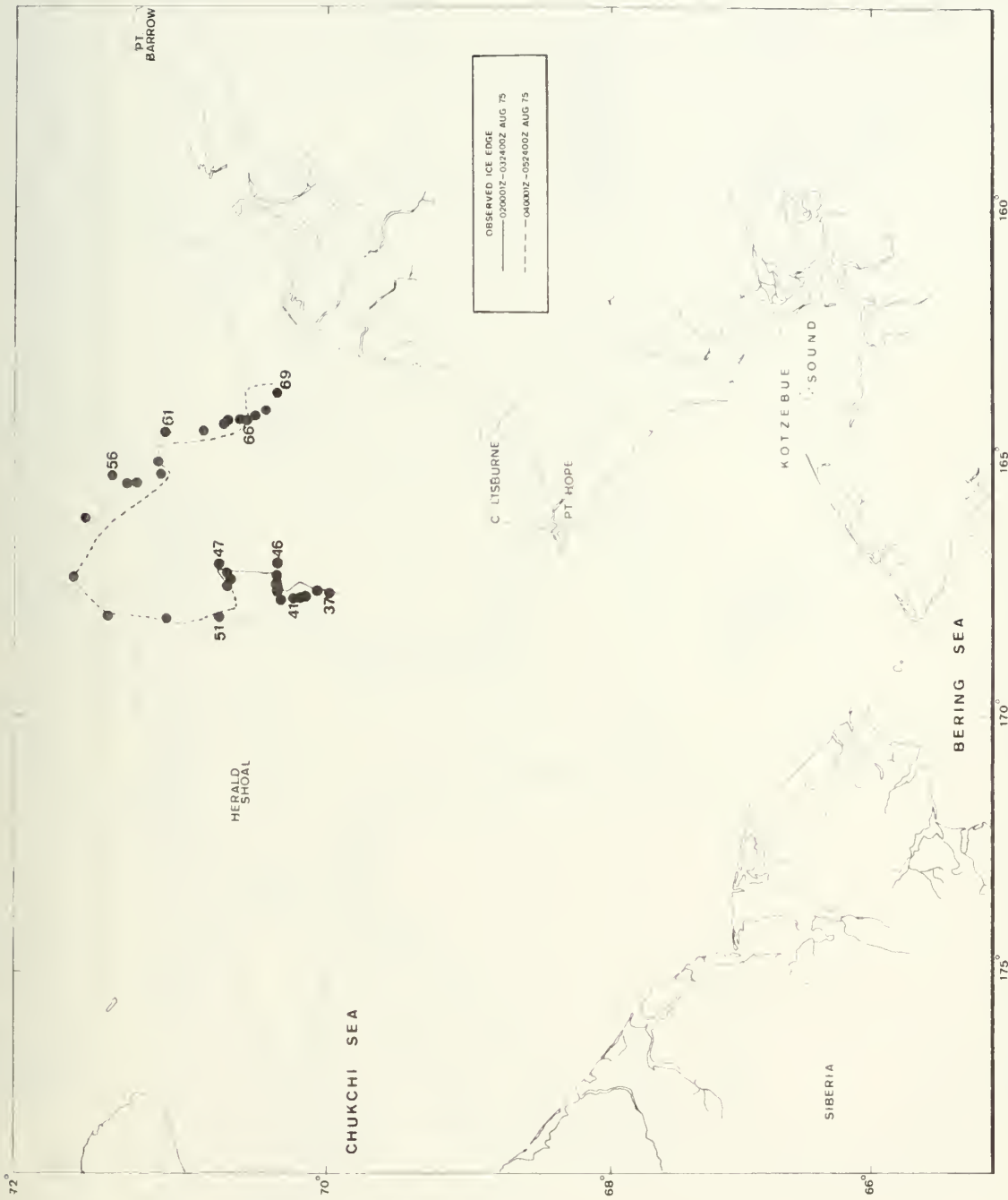


Figure 15. Crossings 1, 2, and 3 in relation to the ice margin. Only that part of the ice margin near the stations is shown. Crossing 1 is an egress from the ice, stations 42-46; crossing 2 is the group 47-51 and crossing 3 is the group 61-69.

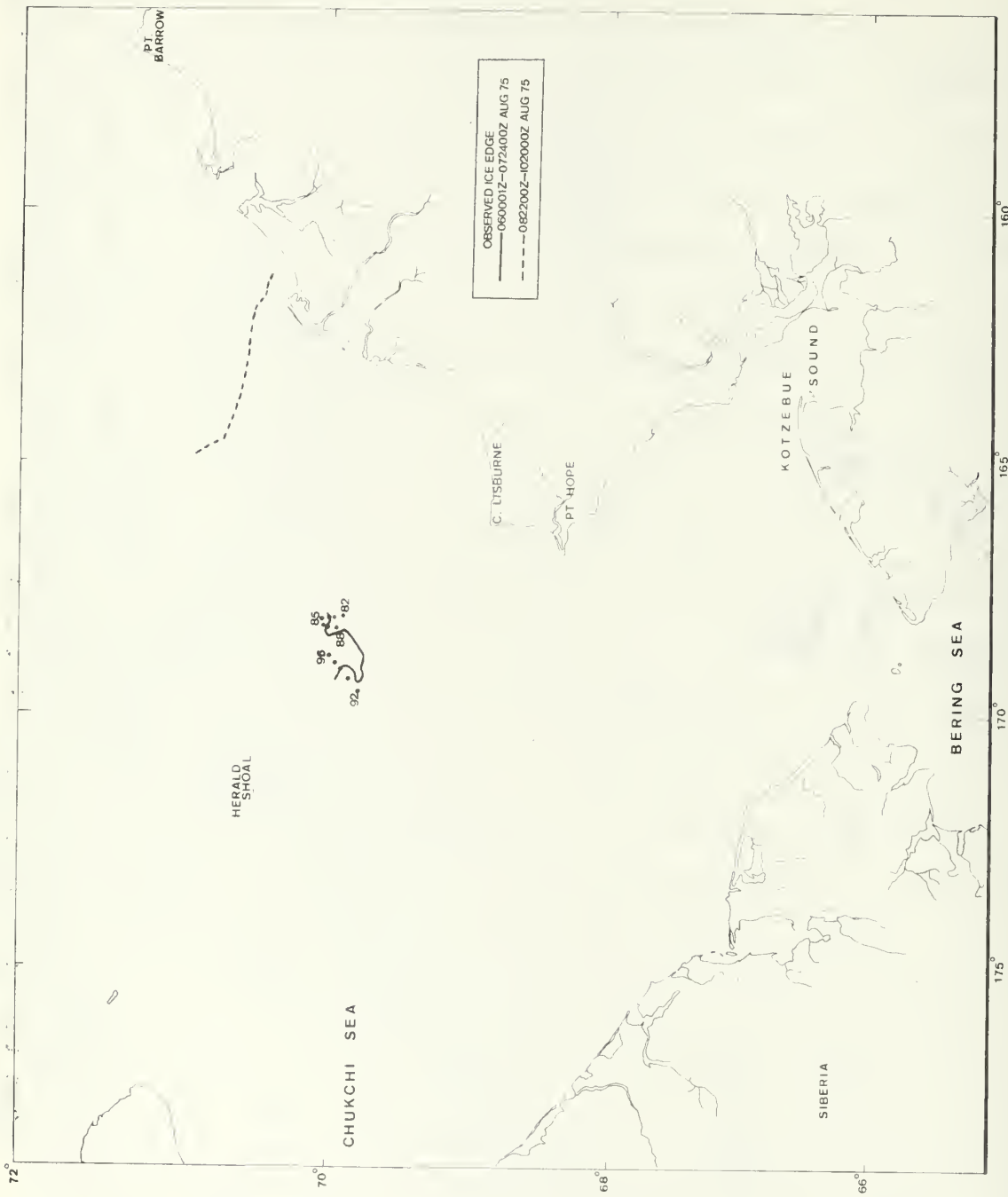


Figure 16. Crossings 4, 5, and 6 in relation to the ice margin. Only a portion of the ice margin is shown. Crossing 4 is the group 82-85, crossing 5 the group 85-88 and crossing 6 the group 92-96.

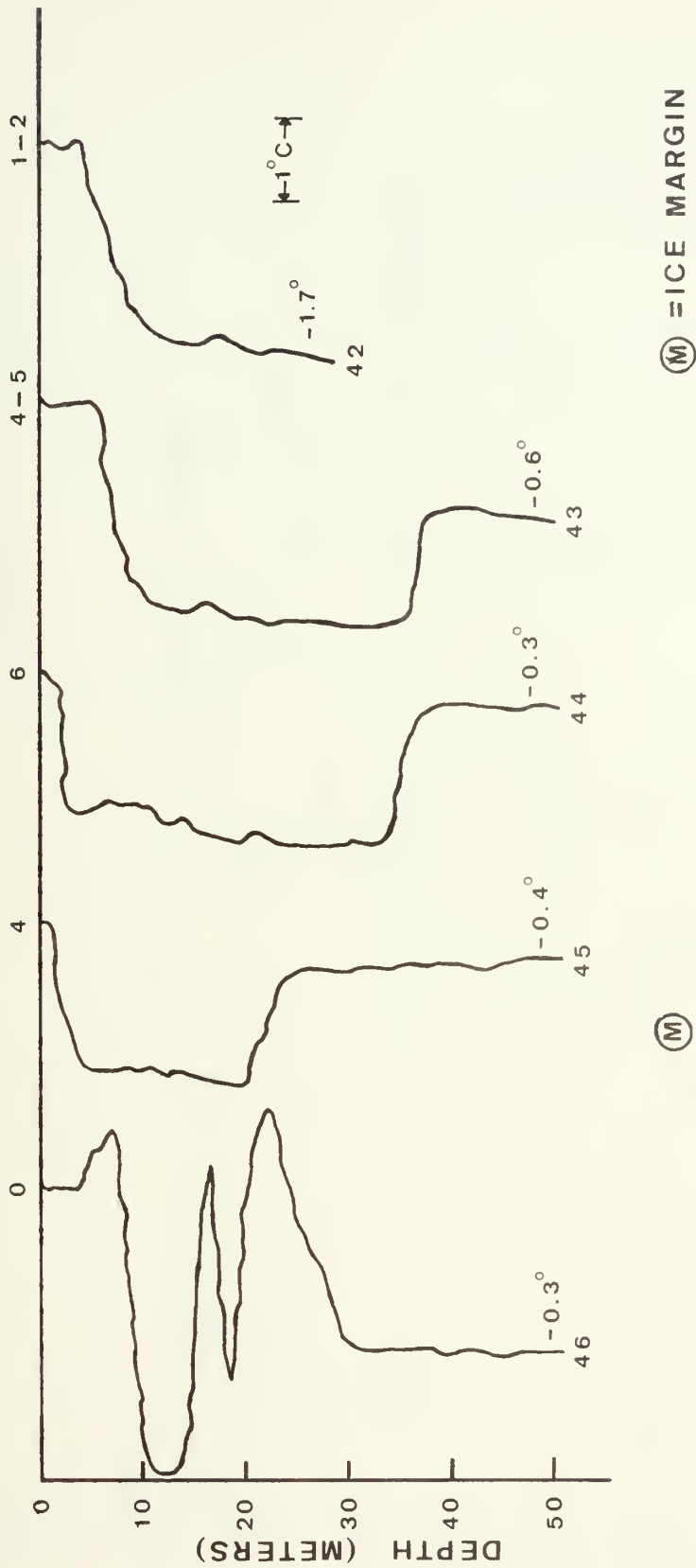


Figure 17. Temperature profiles for Crossing 1. Open water is toward the left. Ice concentrations in oktas are at the top and station numbers at the bottom of each curve. The temperature at the bottom of the curve in °C is shown.

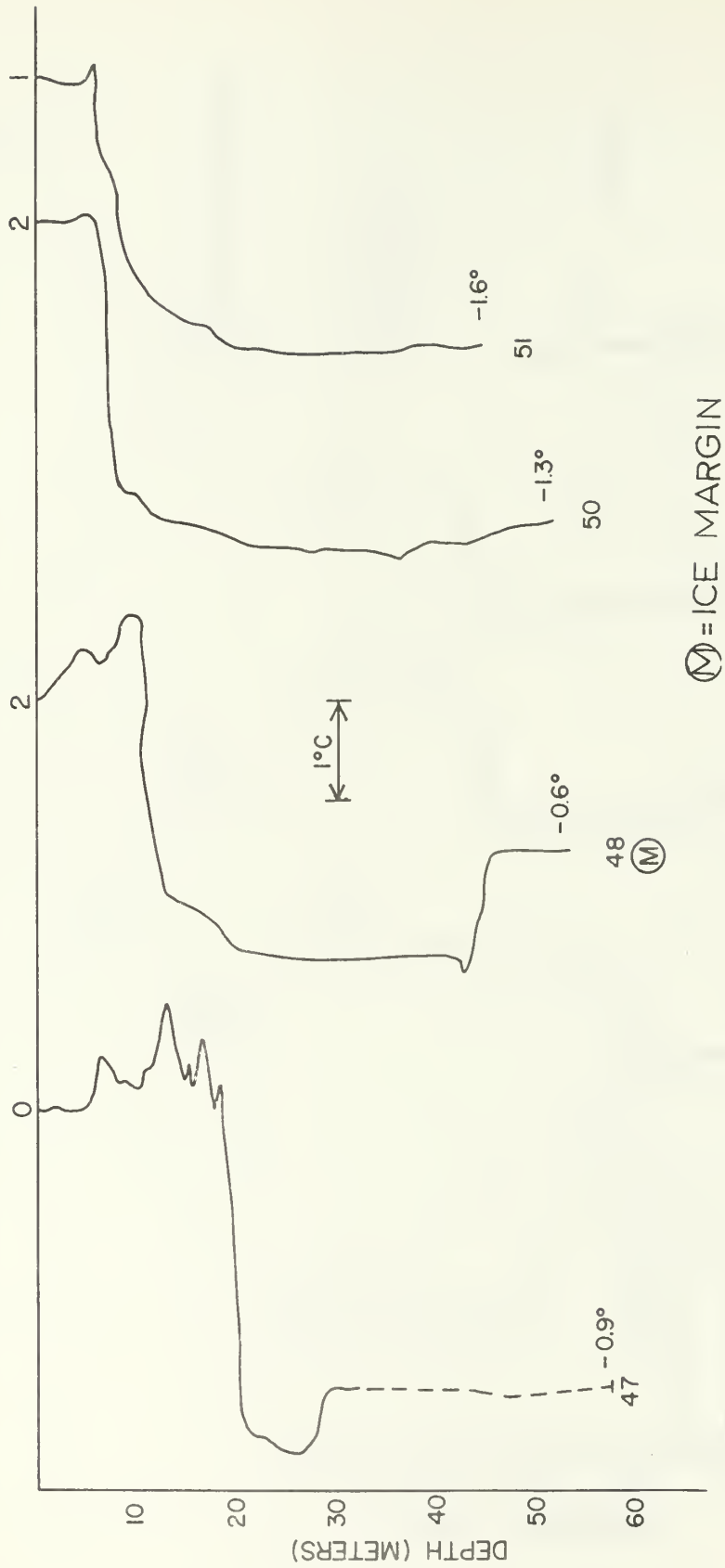


Figure 18. Temperature profiles for Crossing 2. Open water is toward the left. Ice concentrations in oktas are at the top and station numbers at the bottom of each curve. The temperature at the bottom of the curve in $^{\circ}\text{C}$ is shown.

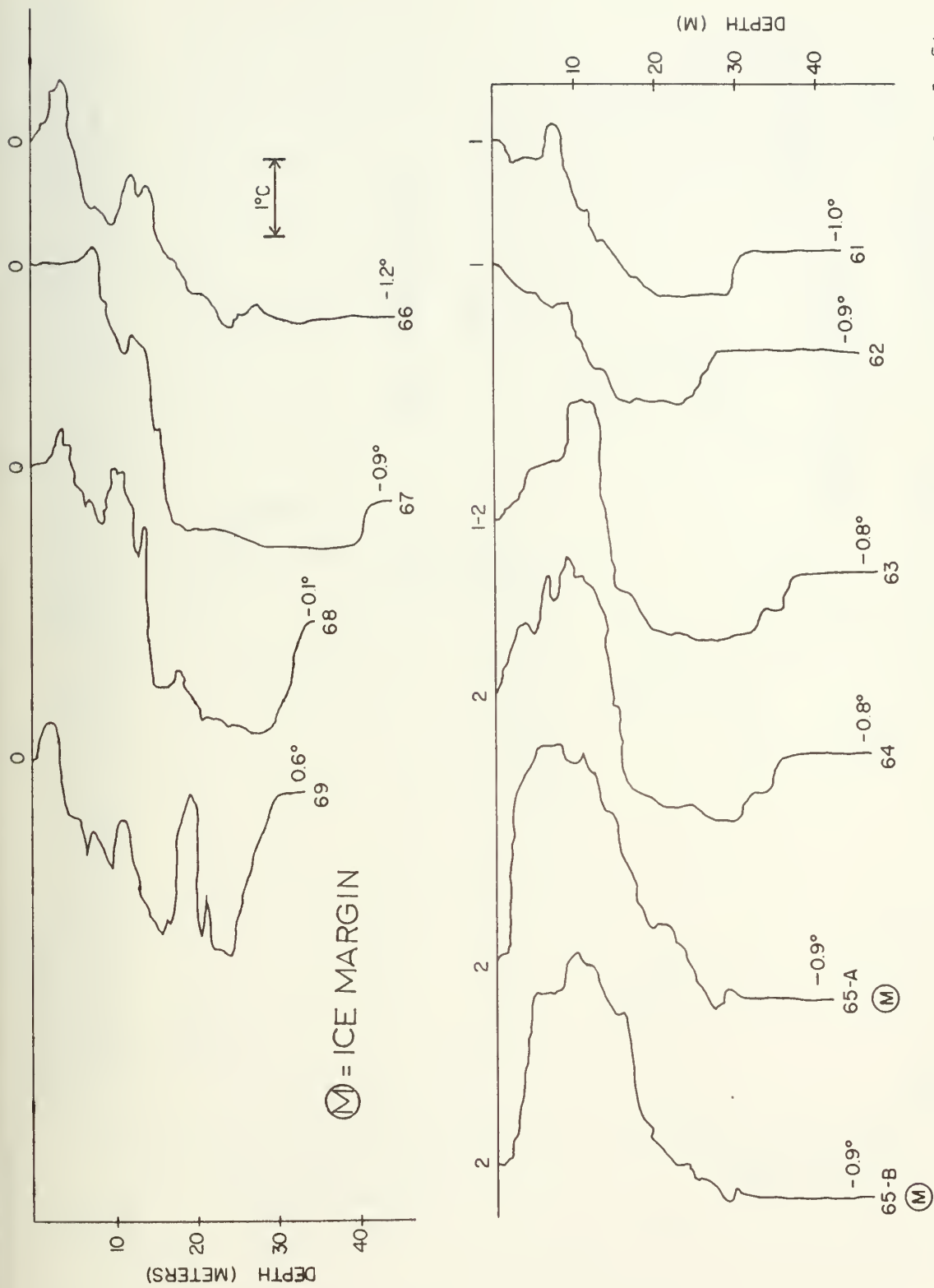


Figure 19. Temperature profiles for Crossing 3. Open water is toward the left. Ice concentrations in oktas are at the top and station numbers at the bottom of each curve. The temperature at the bottom of the curve in °C is shown.

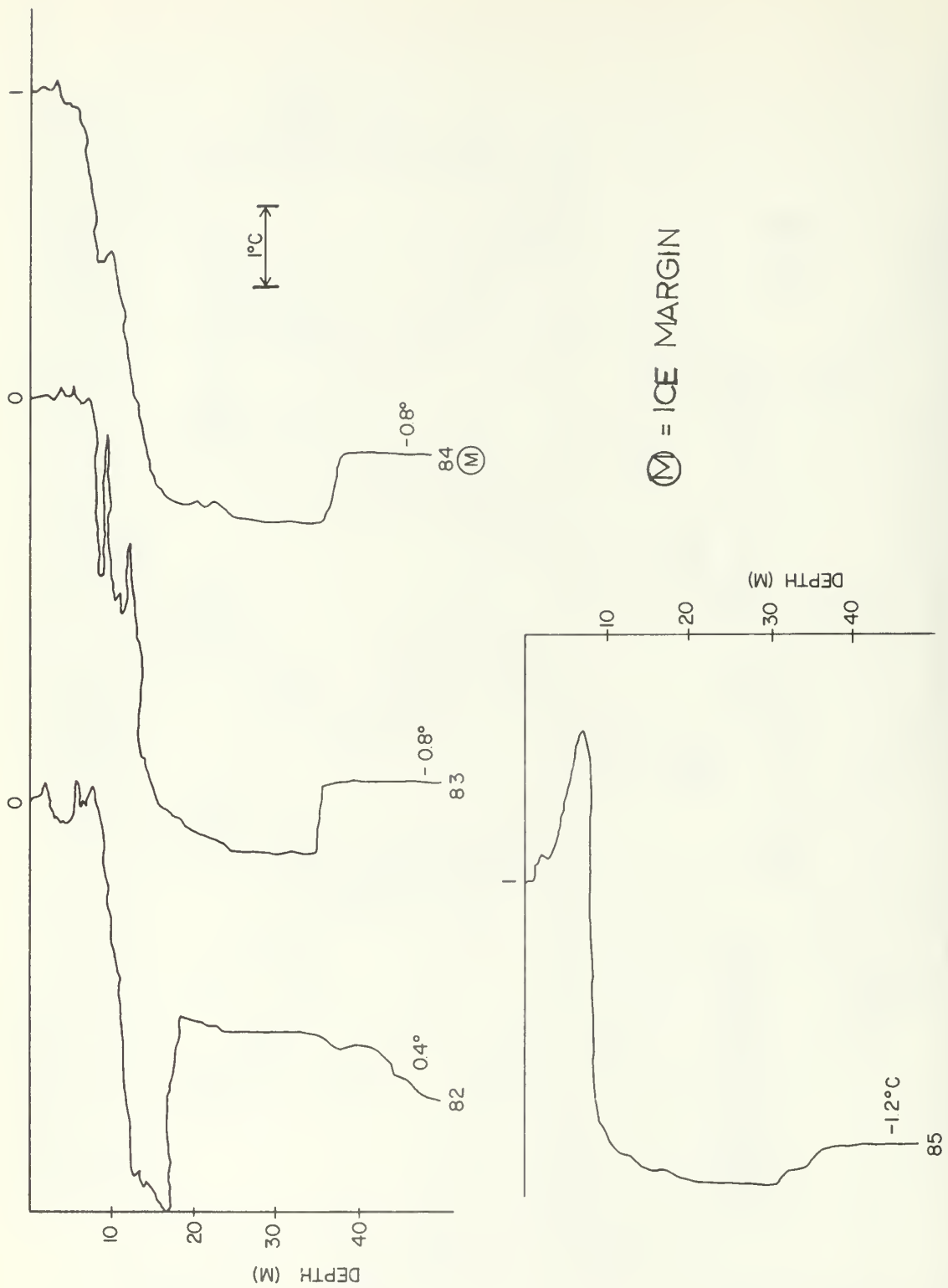


Figure 20. Temperature profiles for Crossing 4. Open water is toward the left. Ice concentrations in oktas are at the top and station numbers at the bottom of each curve. The temperature at the bottom of the curve in °C is shown.

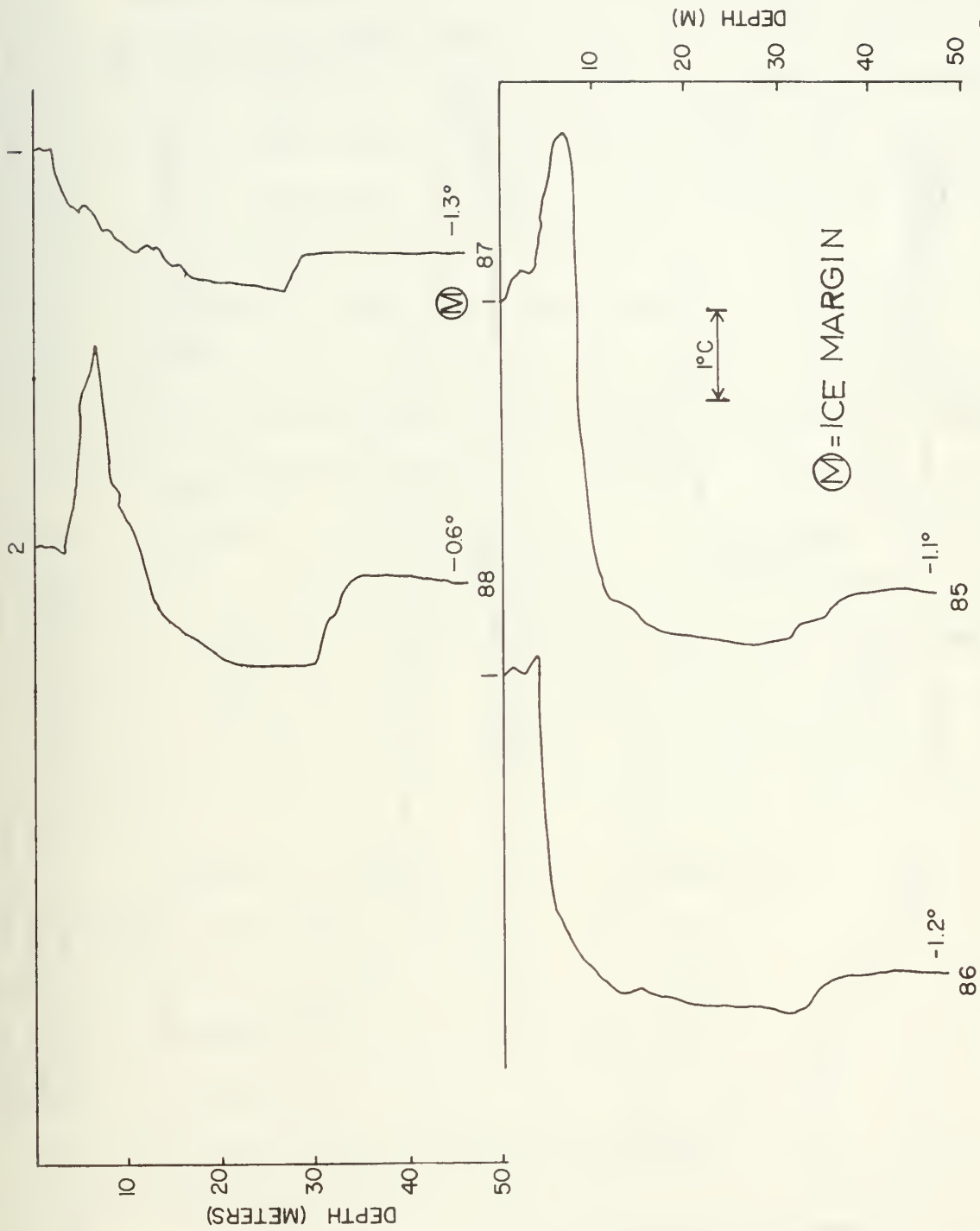


Figure 21. Temperature profiles for Crossing 5. Open water is toward the left. Ice concentrations in oktas are at the top and station numbers at the bottom of each curve. The temperature at the bottom of the curve in $^{\circ}\text{C}$ is shown.

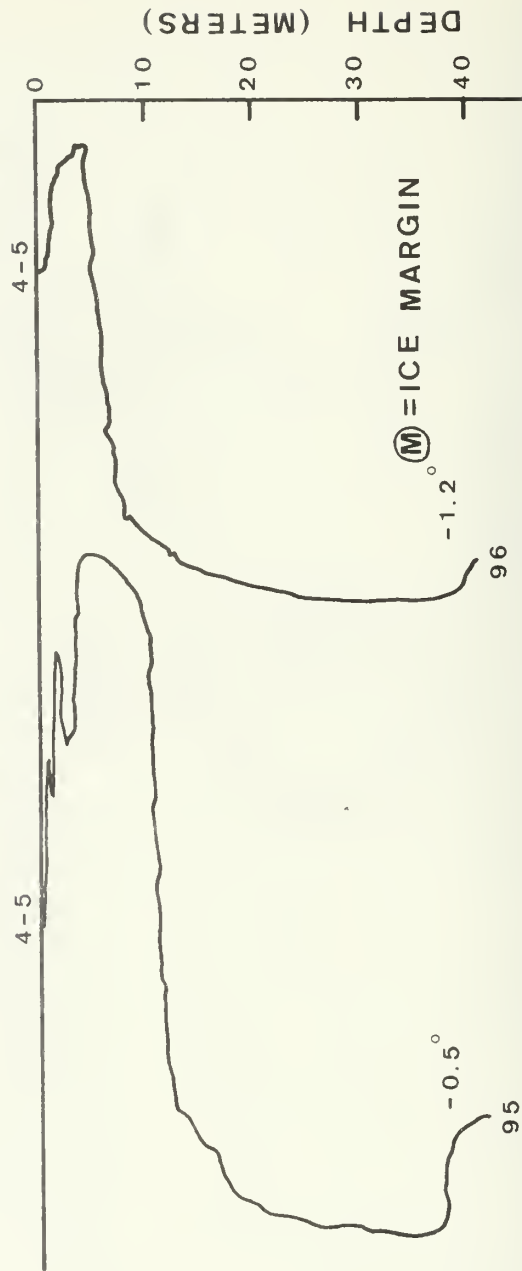
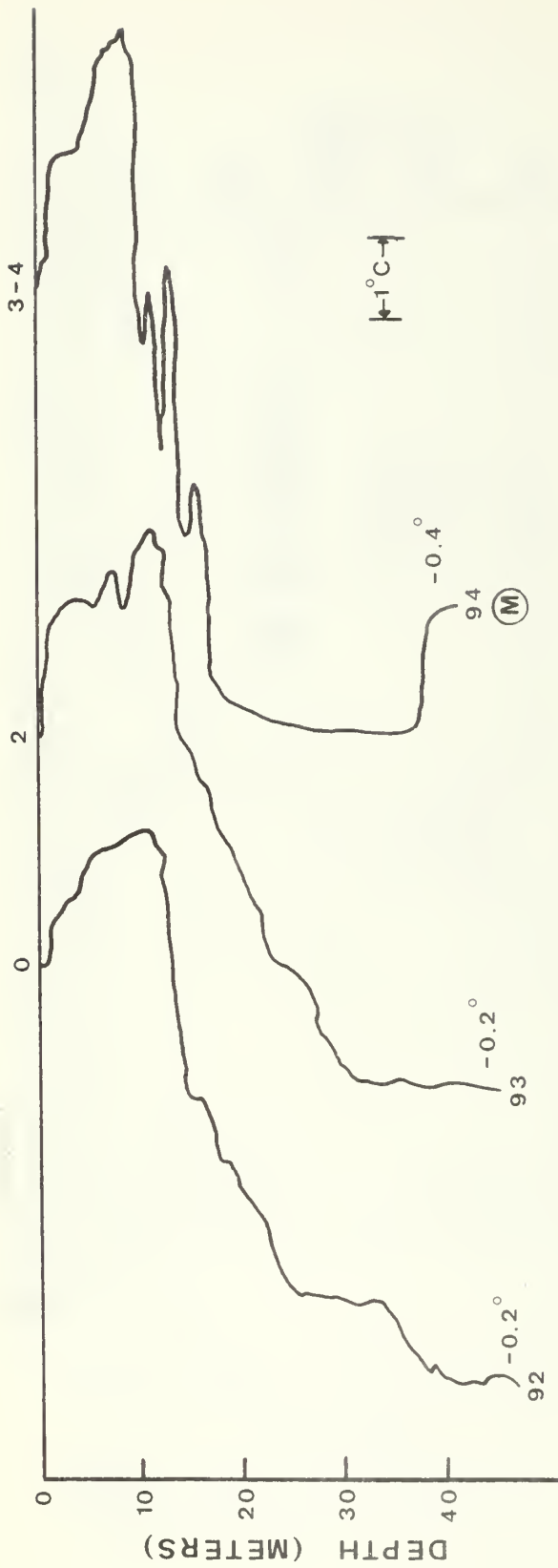


Figure 22. Temperature profiles for Crossing 6. Open water is toward the left. Ice concentrations in oktas are at the top and station numbers at the bottom of each curve. The temperature at the bottom of the curve in $^{\circ}\text{C}$ is shown.

Two forms of mesostructure were observed during the six crossings. Crossings 1 and 3 demonstrated shallow and deep mesostructure elements while Crossings 2, 4, 5, and 6 were dominated by a warm shallow nose with weak, shallow mesostructure elements in and near it. However, in Crossing 1 shallow and deep mesostructure was observed only at Station 46. The remaining stations in the crossing exhibited only a very weak deep mesostructure or none at all. Two conclusions may be drawn from these results. First, there is a tendency for the strongest mesostructure to appear toward the open-water end of the section, with the possible exception of Crossing 3. This seems to be true of results from previous cruises but has not been noted previously. Secondly, where there are adjacent stations with mesostructure, there is little station-to-station correlation between mesostructure elements, very likely due to the sections not being oriented along the direction of propagation, again possibly excepting Crossing 3.

Figures 23 through 28 are the temperature cross-sections for Crossings 1 through 6. Mesostructure is relatively weak except in Crossing 1 and 3. It appears that Crossing 1 missed all but the edge of the mesostructure which shows up only at Station 46. Situated south of the margin, this station has several warm tongues at mid-depth levels. There is a relatively weak thermocline at about 10 m. Crossing 3, on the other hand, has a very strong thermocline but at a deeper level (20 m). It is believed that the complexity of this

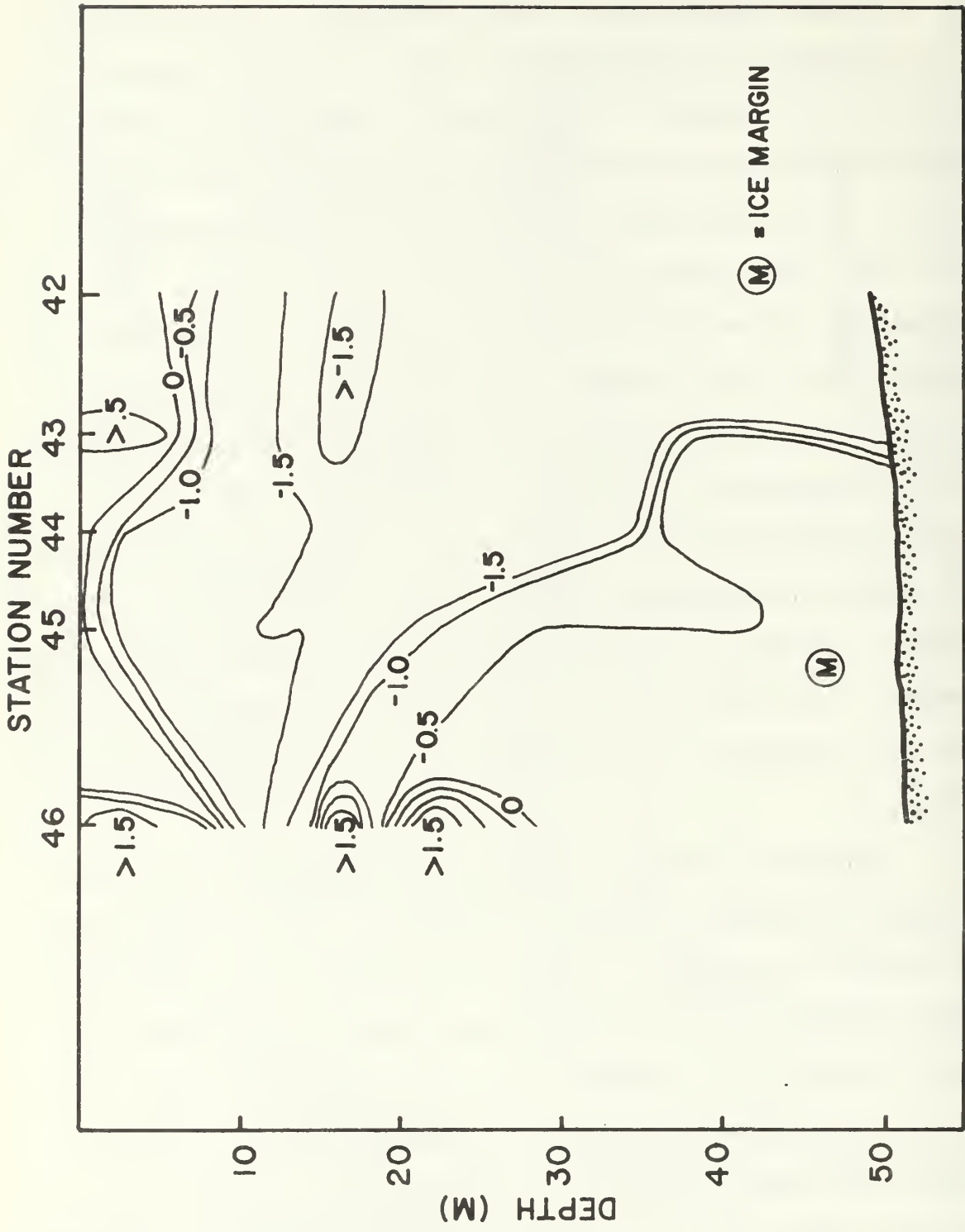


Figure 23. Temperature cross section, Crossing 1. Open water is toward the left. Temperatures are in °C.

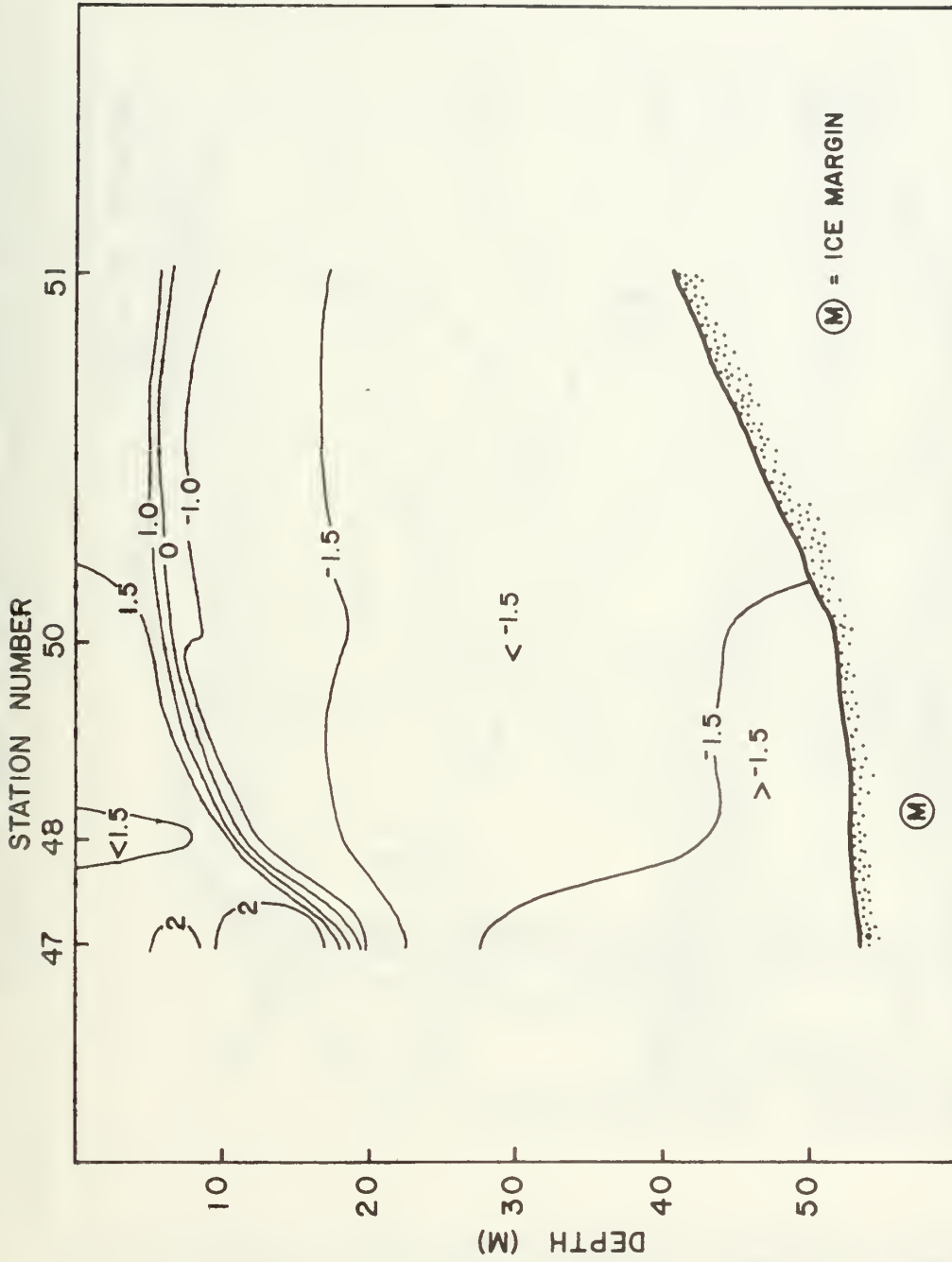


Figure 24. Temperature cross section, Crossing 2. Open water is toward the left. Temperatures are in °C.

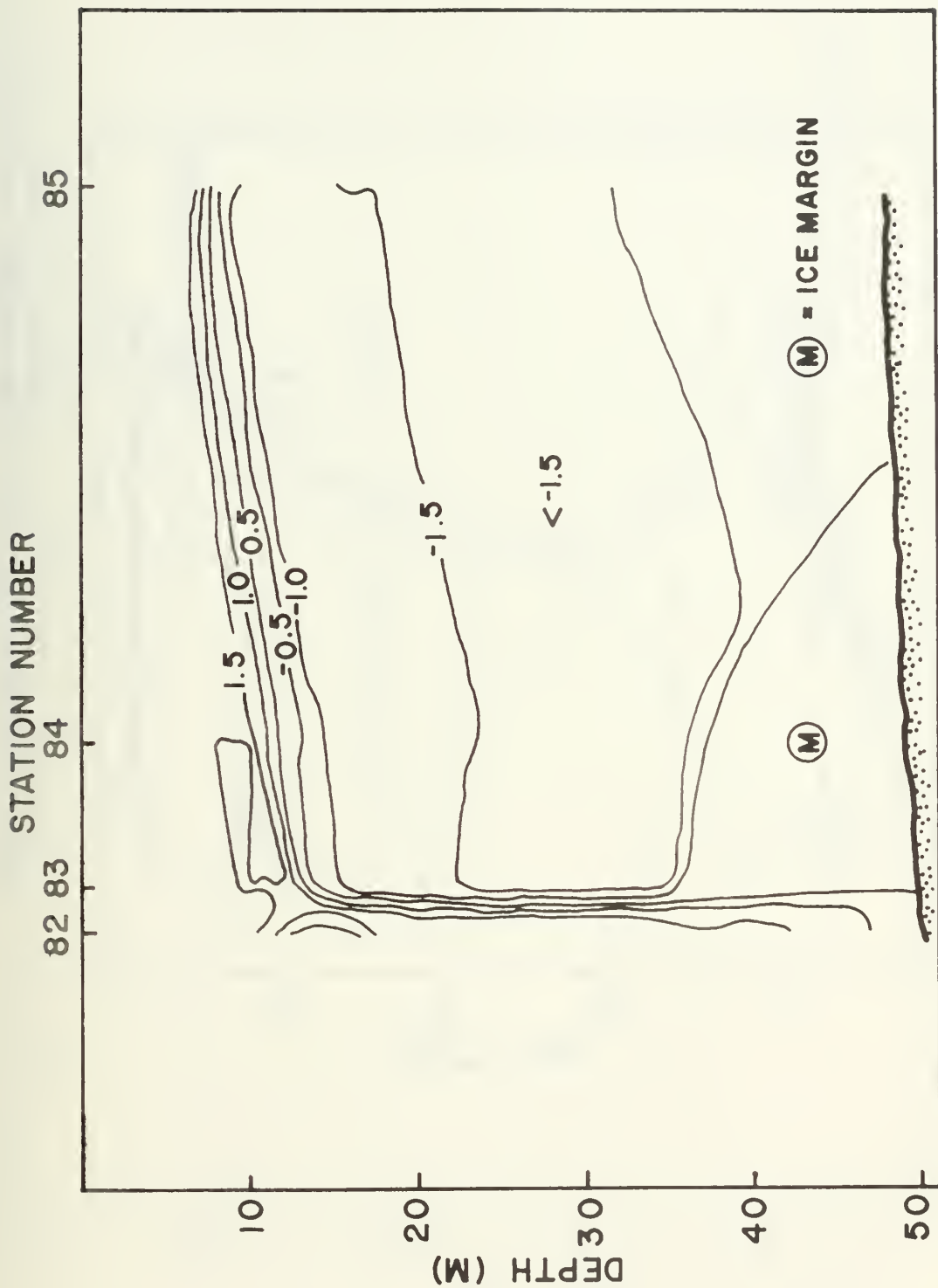


Figure 26. Temperature cross section, Crossing 4. Open water is toward the left. Temperatures are in °C.

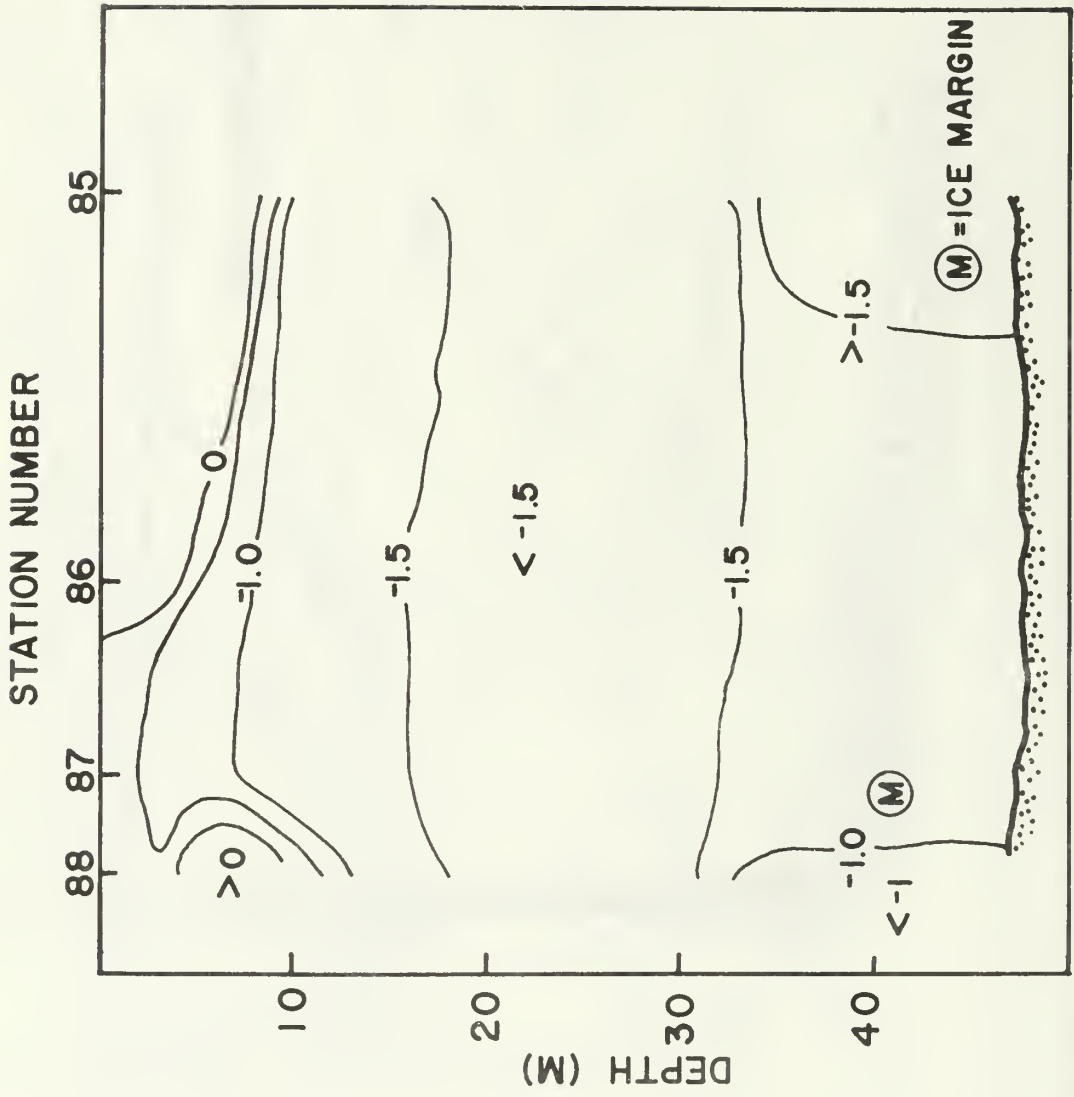


Figure 27. Temperature cross section, Crossing 5. Open water is toward the left. Temperatures are in °C.

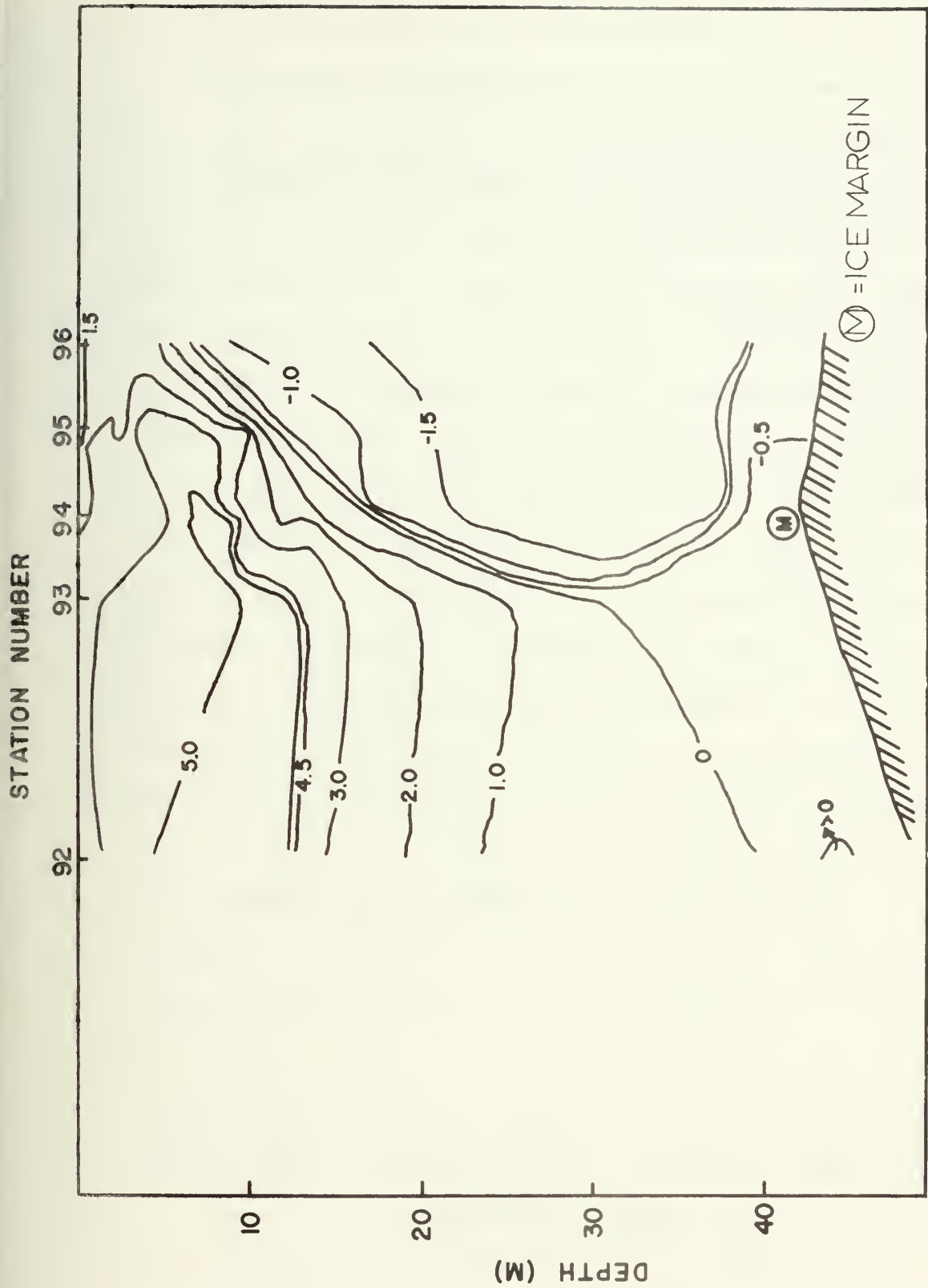


Figure 28. Temperature cross section, Crossing 6. Open water is toward the left. Temperatures are in °C.

section indicates that this crossing is not in line with the direction of flow. Evidence for this will be shown in the section on spatial and temporal variance of mesostructure.

Density cross-sections for Crossings 1 through 6 are shown in Figures 29 to 34. The remarkable difference in lateral density gradients in Crossings 1 and 3 is obvious, especially just outside the ice margin. The lateral density gradients of Crossing 3 were remarkably strong whereas Crossing 1 exhibited moderate to strong gradients. The mesostructure exhibited in both crossings is both shallow and deep. The mesostructure for Station 46, which is the only station in Crossing 1 with mesostructure, was strong in the 10-30 m level and relatively weak in the upper 10 m. This compares with Crossing 3 which also had weak structure in the upper level and strong structure at the deeper level. Also it can be seen that the intensity of the lateral density gradient does not necessarily correlate locally with the intensity of a mesostructure element.

As mentioned above the only crossing which can validly be compared with crossings in previous years is Crossing 3 (Figure 31). This is examined in comparison with Crossing 1 in 1974 (Karrer, 1975). In particular Karrer showed bottom isopycnals sloping up to the right, inside the ice margin. Crossing 3 shows this also if one ignores the lens of high-density water at the left of the diagram.

The high-density lens in Crossing 3 is part of the anomalous intrusion of dense Atlantic Water, a feature not

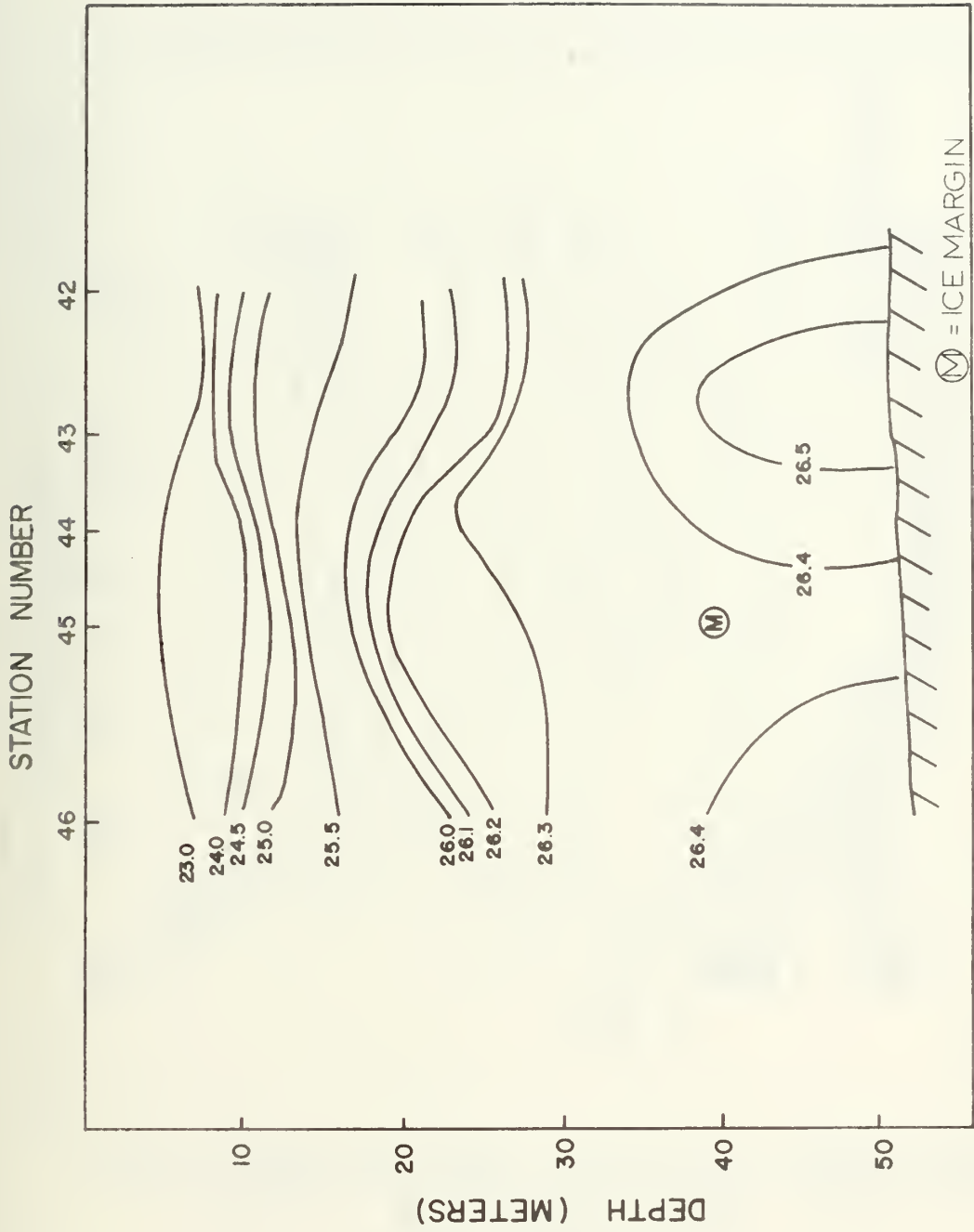


Figure 29. Sigma-t cross section, Crossing 1. Open water is toward the left.

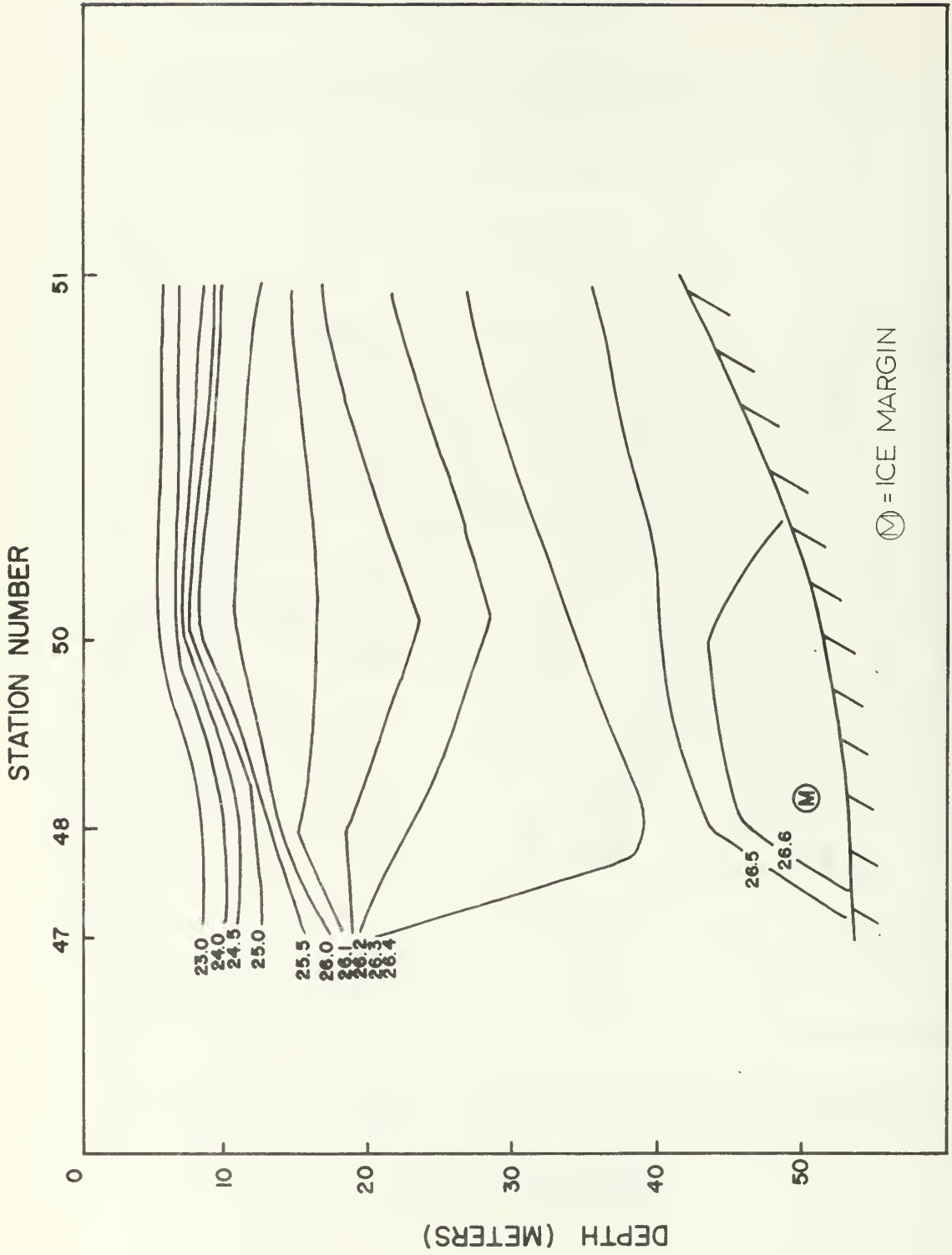


Figure 30. Sigma-t cross section, Crossing 2. Open water is toward the left.

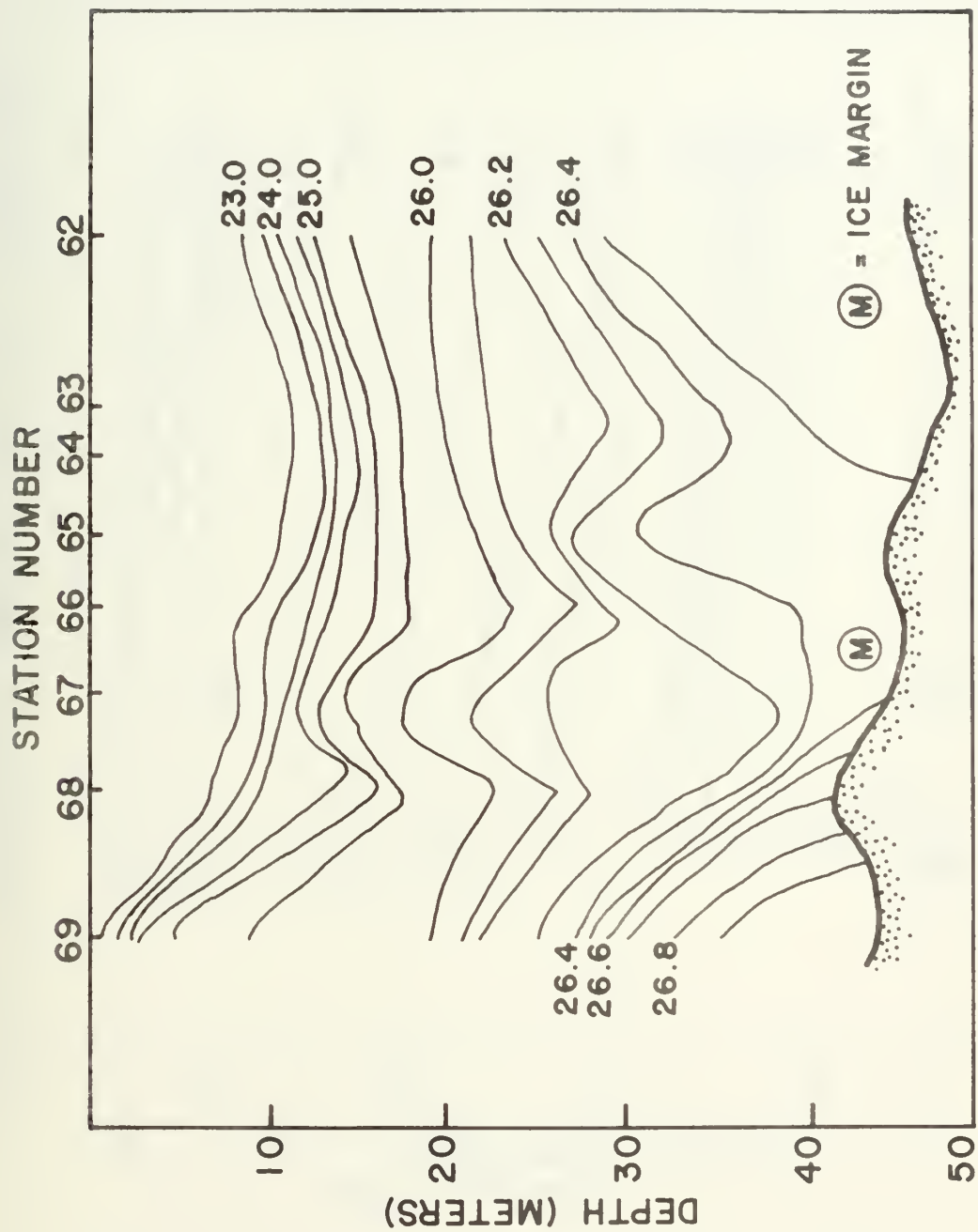


Figure 31. Sigma-t cross section, Crossing 3. Open water is toward the left.

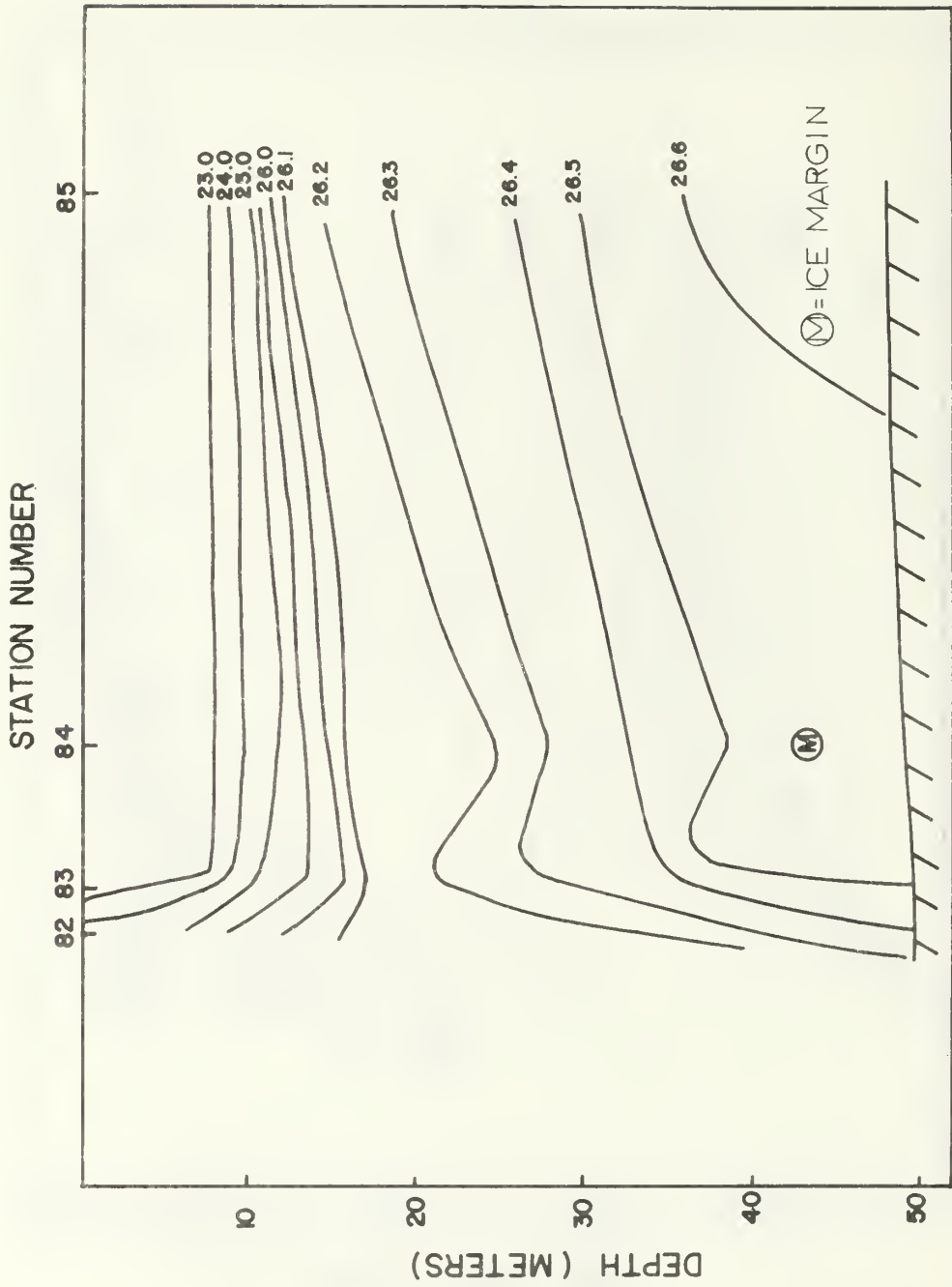


Figure 32. Sigma-t cross section, Crossing 4. Open water is toward the left.

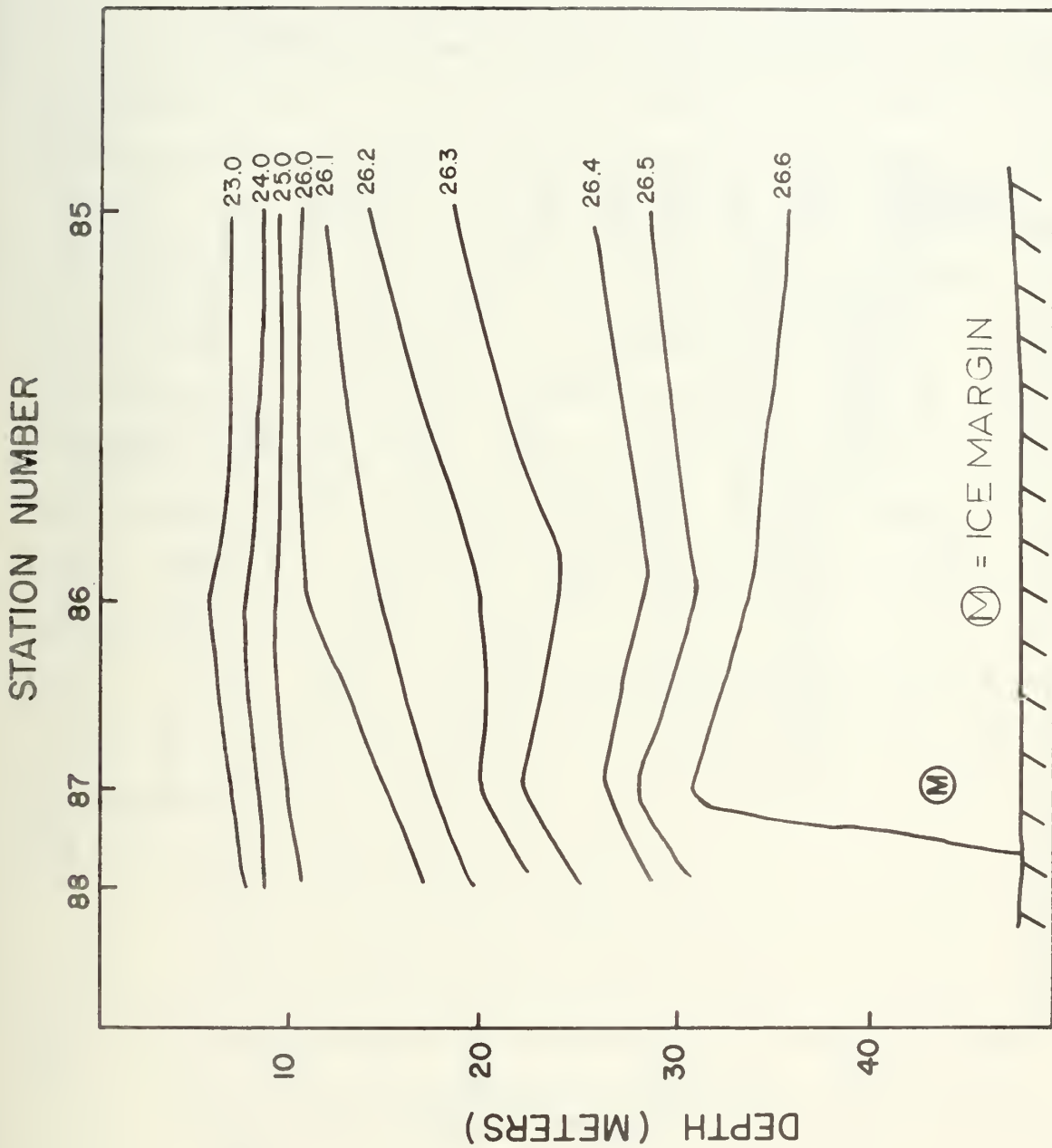


Figure 33. Sigma-t cross section, Crossing 5. Open water is toward the left.

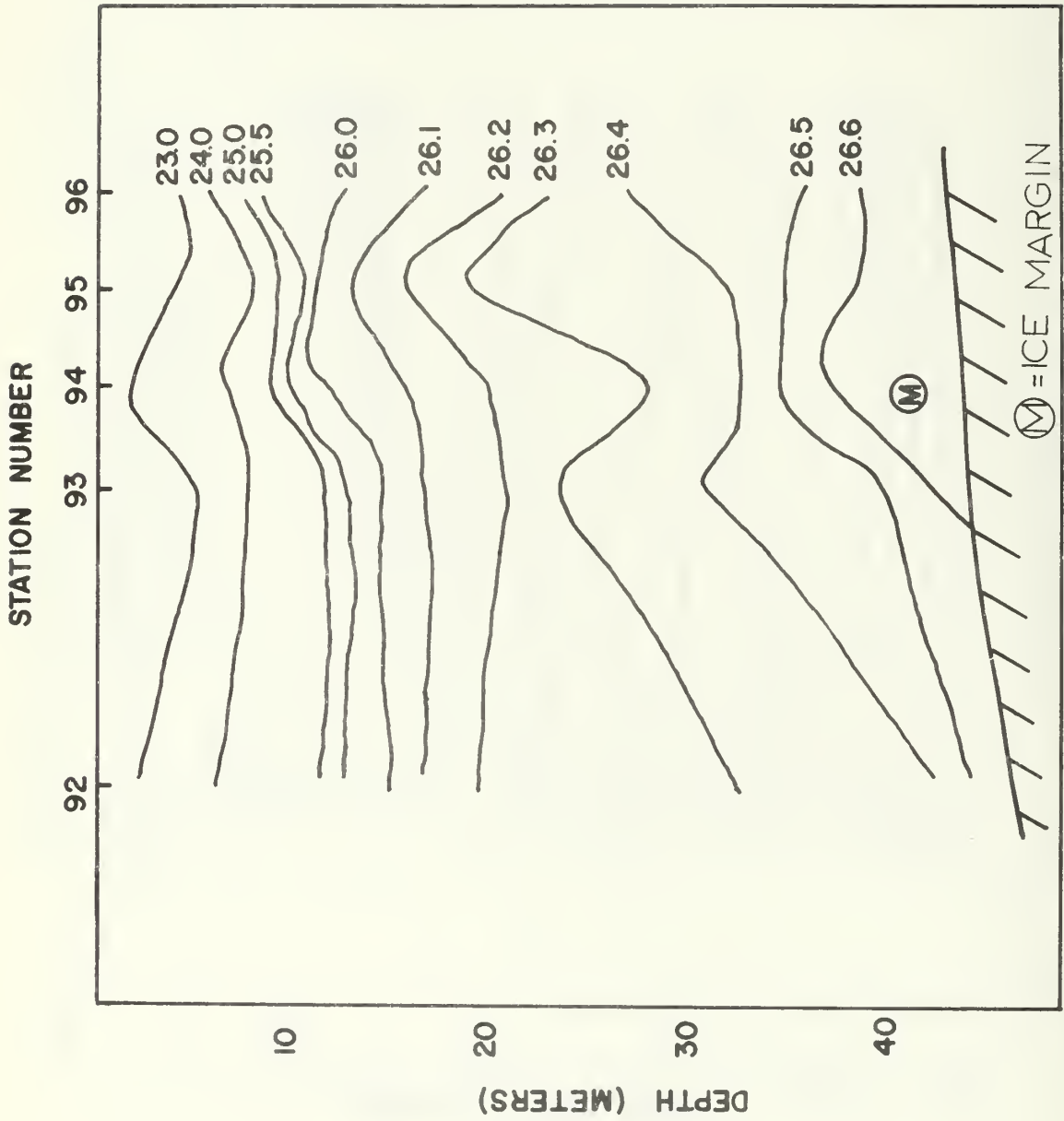


Figure 34. Sigma-t cross section, Crossing 6. Open water is toward the left.

observed during the previous MIZPAC cruises. It is not clear why this water type should be trapped in these areas on the Chukchi Sea shelf, but perhaps they are remnants of earlier surges of Atlantic Water up the Barrow Canyon.

Another interesting feature seen in MIZPAC 75 data is the presence of well-defined fronts at the ice margin in Crossings 4 and 6. These fronts appear in the temperature cross-sections (Figures 26 and 28) and less markedly in the density cross-sections (Figures 32 and 34). The crossings are within 20 km of each other, and it is probable that these fronts are portions of the same front. This can be further supported by noting that the temperature on respective sides of each front are almost the same for both crossings and have the same depth distribution. Density patterns, likewise, exhibit the same distribution and the isopycnals are matched closely with depth.

More data would be required to thoroughly analyze these frontal phenomena; however, the following interesting points may be made:

- This dramatically illustrates the idea of two water types of different temperatures existing near each other along a density surface with consequent potentiality for interleaving to form mesostructures.
- This may be a region of horizontal shear in the flow.
- There are two different water masses lying side by side, and not mixing with one another.

Paquette and Bourke (1976) suggest the relation of the flow regime to mesostructure in their analysis of MIZPAC 74 data. Crossings having deep mesostructure were thought to be associated with a strong flow of warm southerly water toward the ice. Crossings dominated by a warm shallow nose were thought to be related to a weaker flow toward the ice. To test this hypothesis an analysis was made of the rate of flow in the vicinity of the ice margin in relation to the class of mesostructure observed.

Specifically, it was desired to correlate the rate of flow with the orientation of the margin to test the idea that flow toward the margin was related to the class of mesostructure existing. Figures 35 through 40 display the rate of flow (cm sec^{-1}) relative to the orientation ($^{\circ}\text{T}$) of the ice margin for each of the six ice-margin crossings. Margin orientation, which varied considerably over distances as small as 16 km, is indicated for each station. In 70% of the current measurements there was a flow toward the margin. The shears in the relative flow rates were compared to temperature changes in the water column, displayed in the vertical cross-sections of temperature for the six margin crossings (Figures 23 through 28). However, throughout the water column, shear in the flow did not correlate with changes in temperature. Hence, it did not appear that there was a direct relationship between the class of mesostructure and flow relative to margin orientation. However, during this analysis it became apparent there was a relationship between the class of

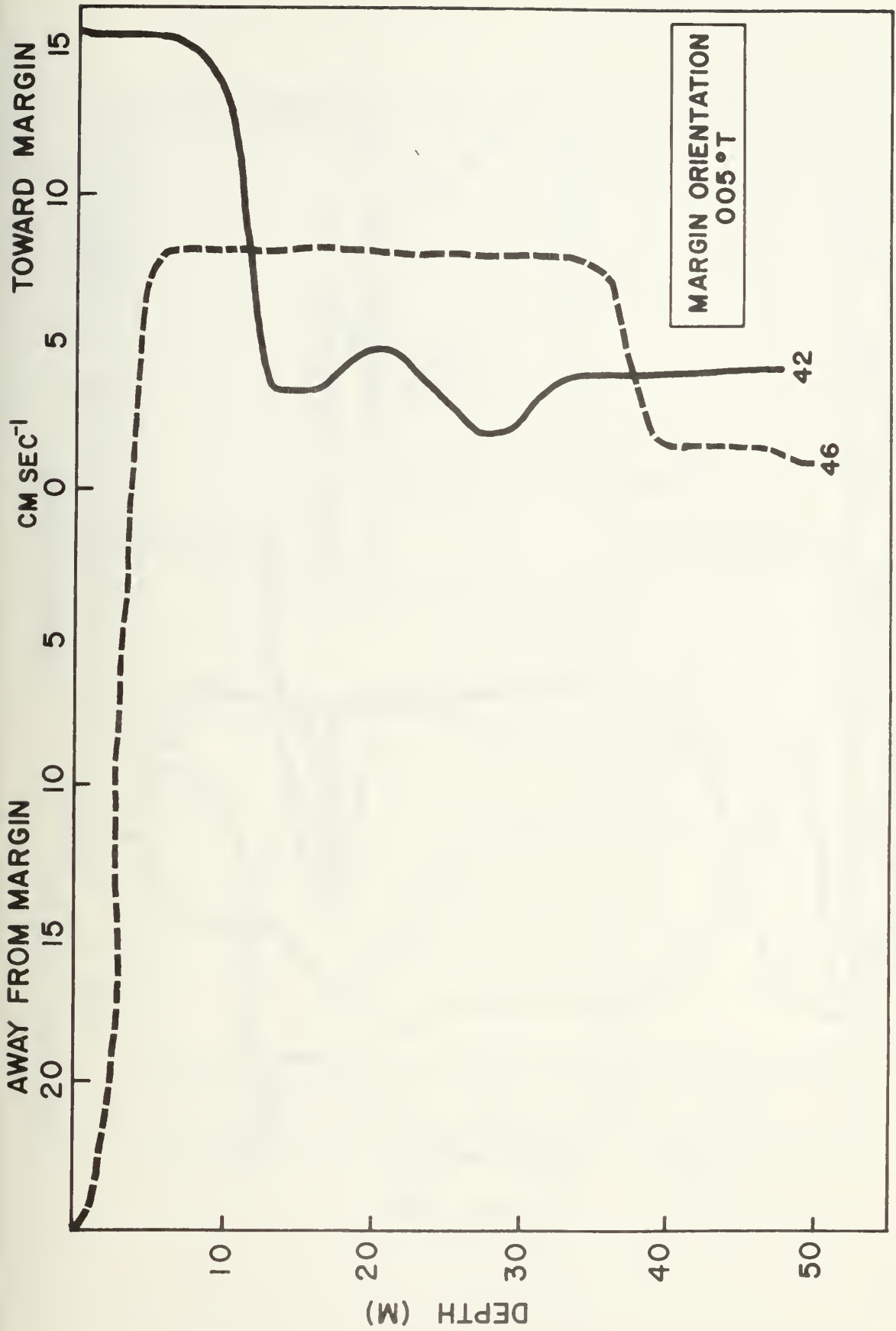


Figure 35. Rate of flow vs margin orientation, Crossing 1.

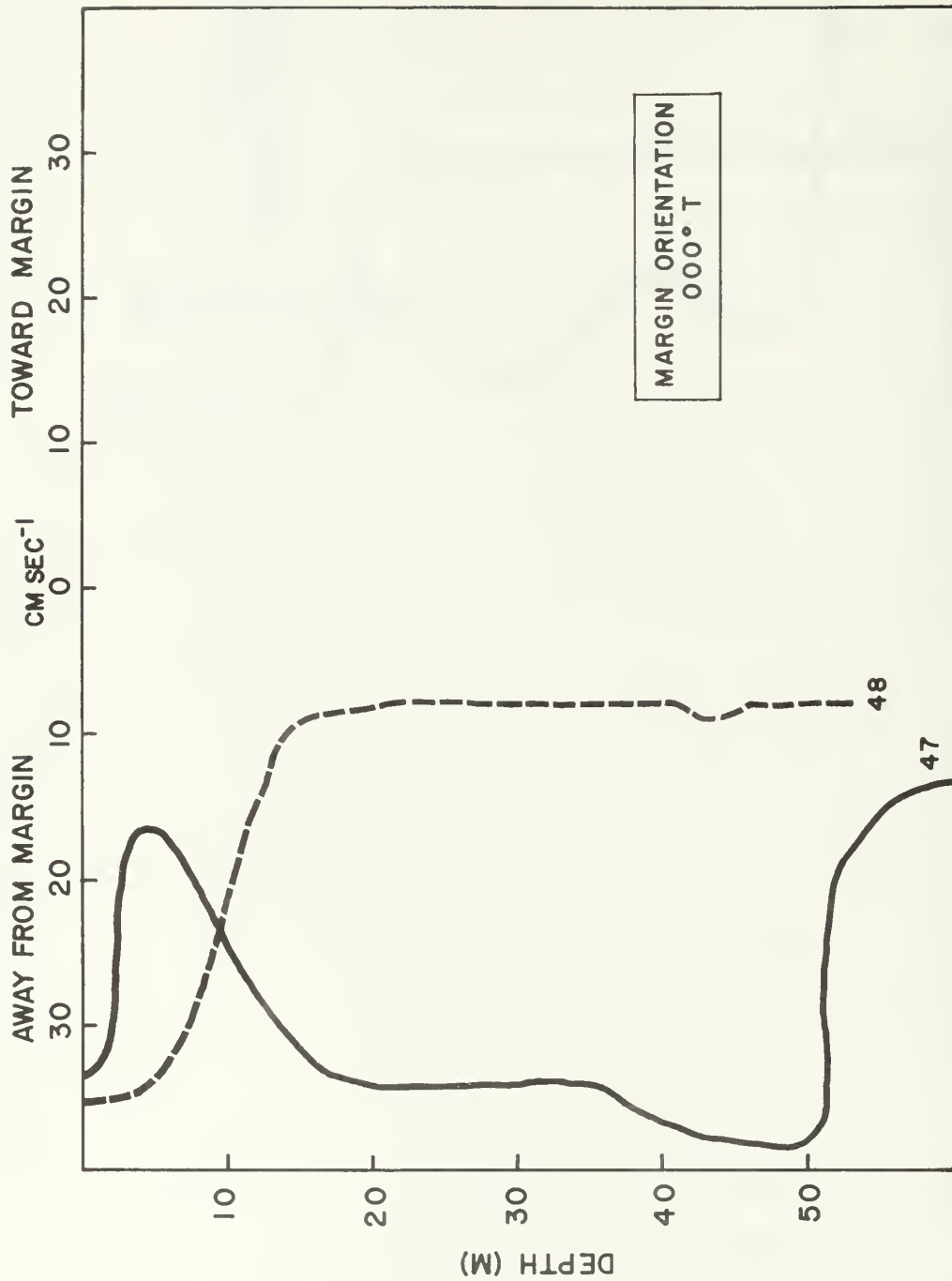


Figure 36. Rate of flow vs margin orientation, Crossing 2.

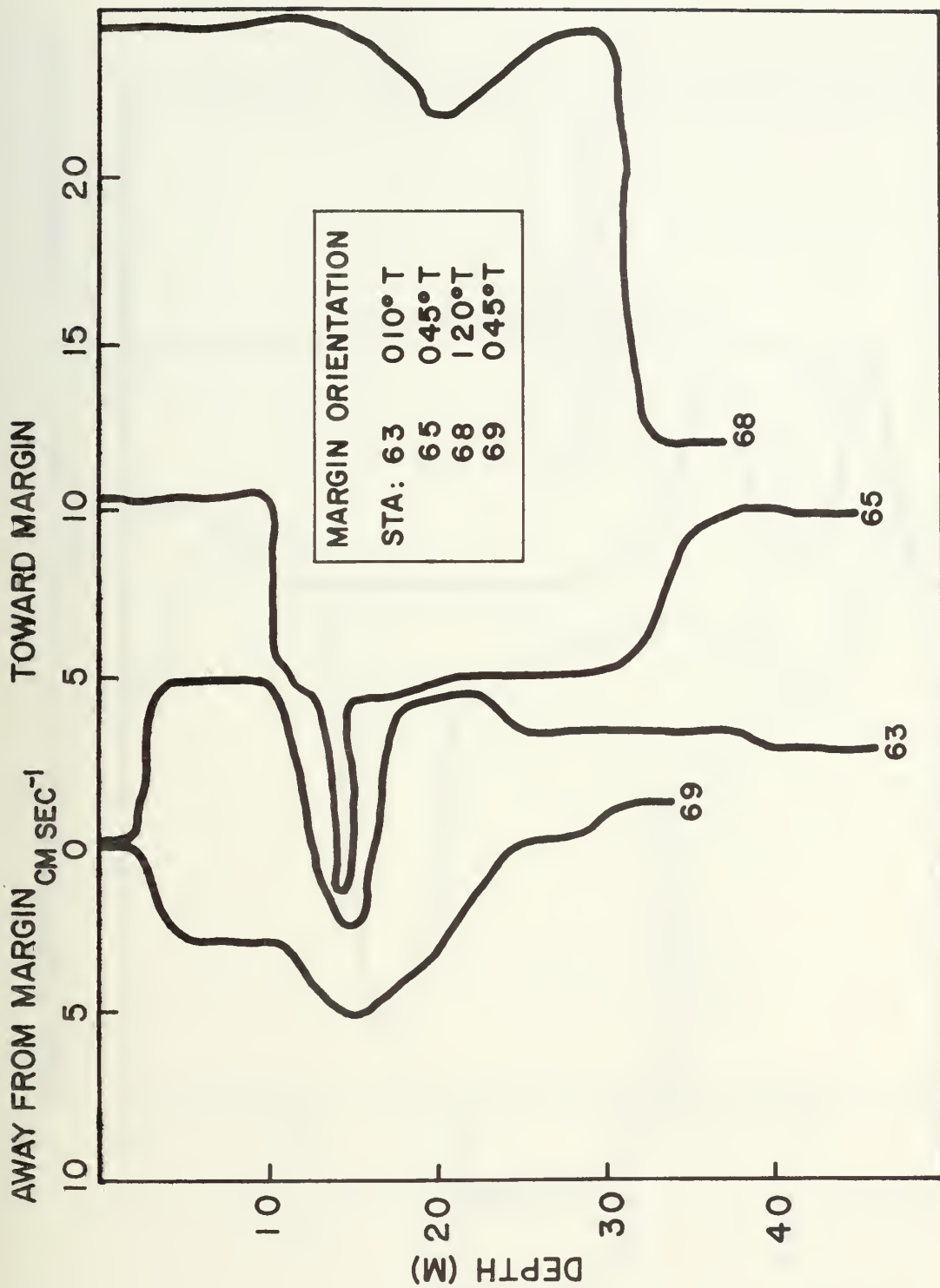


Figure 37. Rate of flow vs margin orientation, Crossing 3.

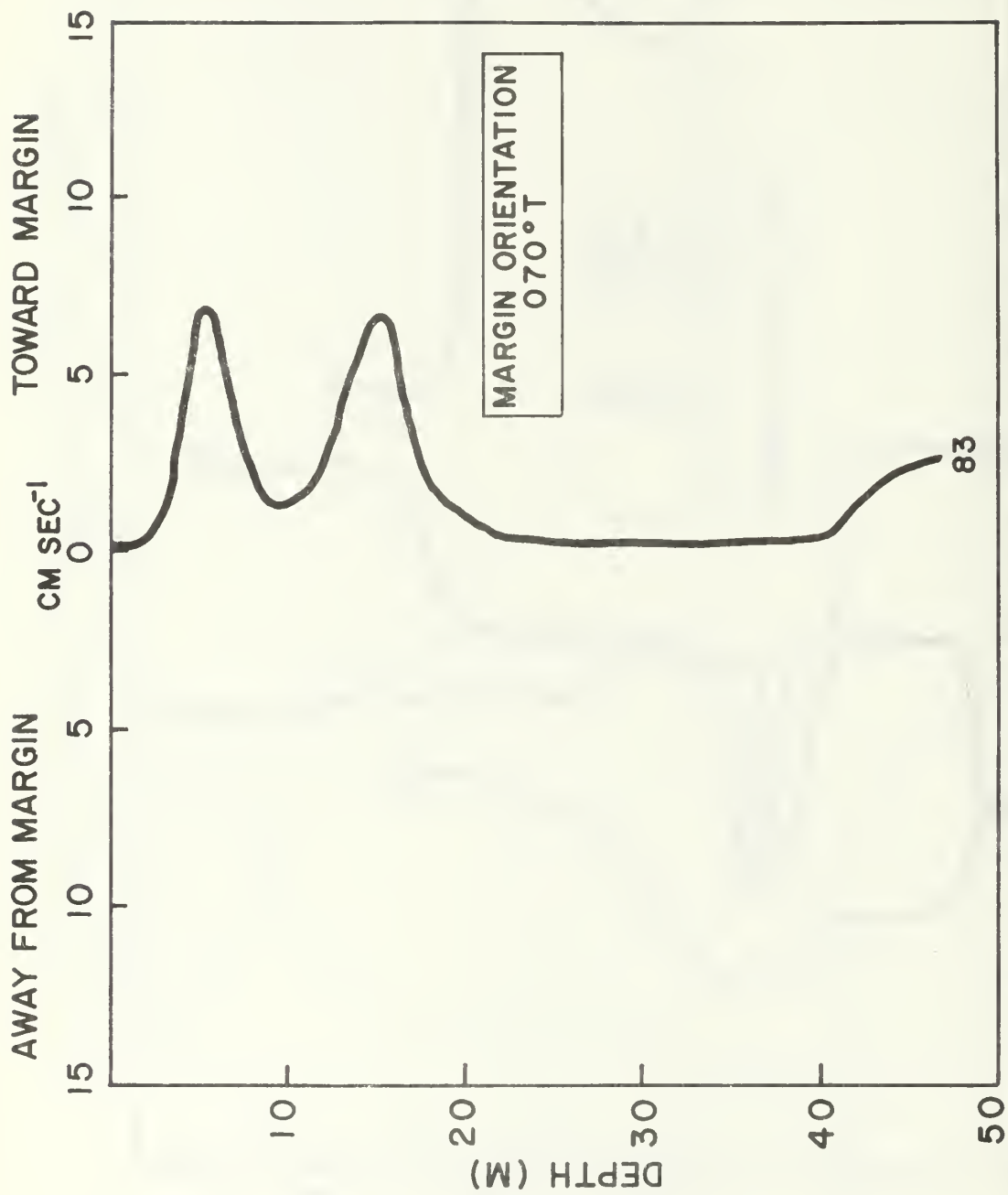


Figure 38. Rate of flow vs margin orientation, Crossing 4.

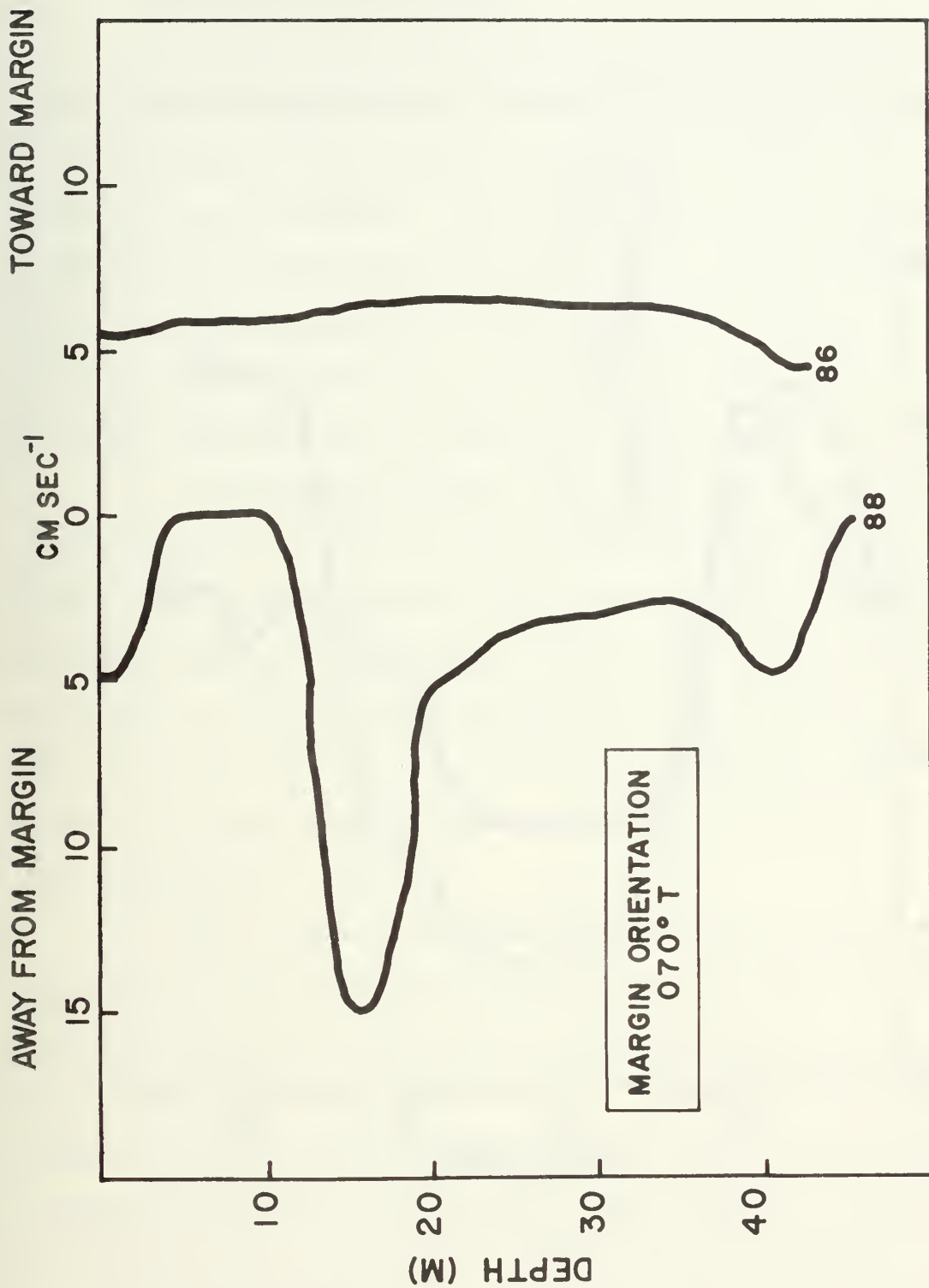


Figure 39. Rate of flow vs margin orientation, Crossing 5.

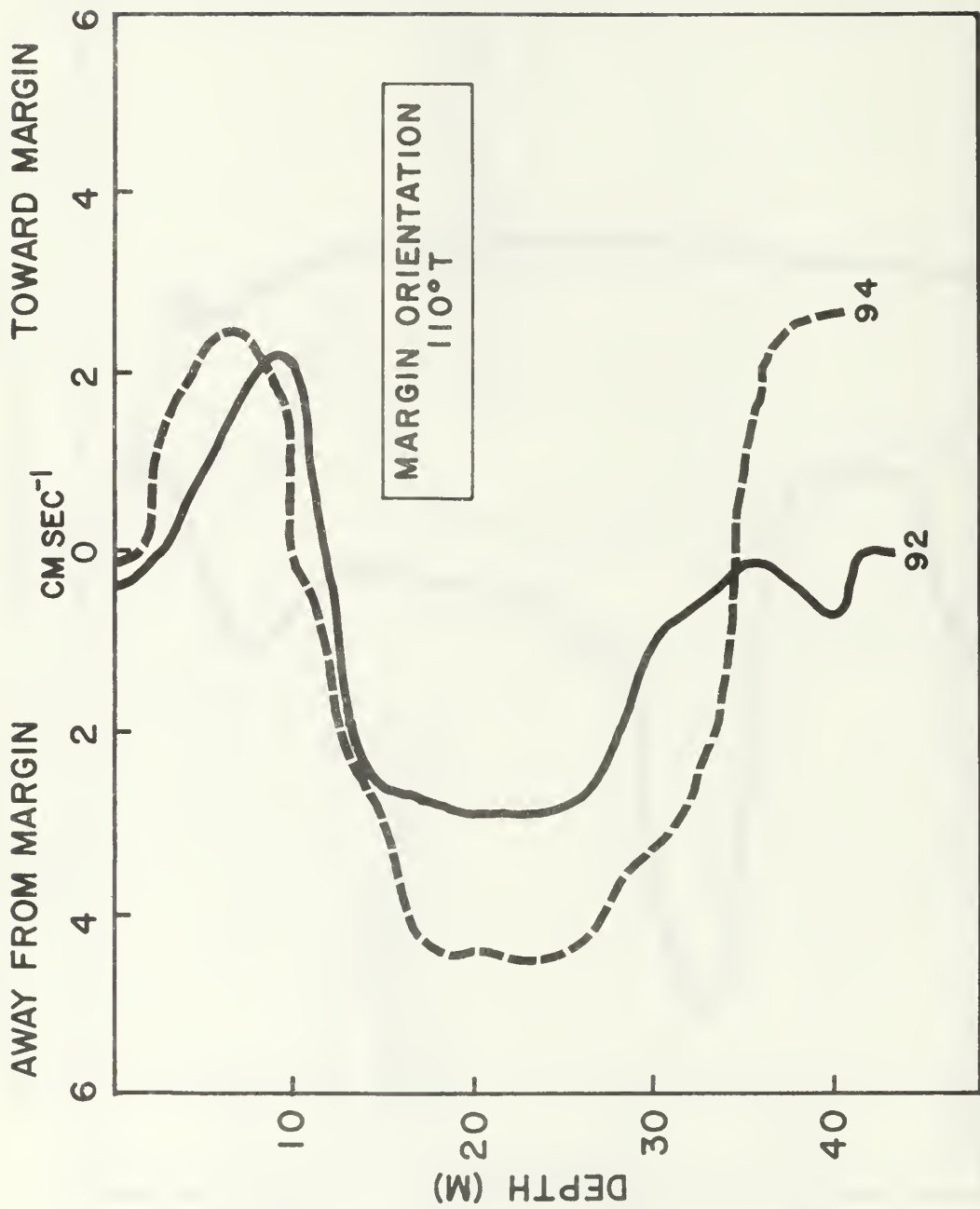


Figure 40. Rate of flow vs margin orientation, Crossing 6.

mesostructure and the northward component of flow, irrespective of margin orientation.

2. Diffuse Ice Floe Region

As mentioned in Section I, an unusual feature of MIZPAC 75 was the existence of mesostructure in the vicinity of scattered ice floes which were located as far as 40 km south of the ice margin. For the purpose of this analysis, a diffuse ice floe region is defined as a patch of scattered ice with a concentration of less than 1 okta and is described in exponential terms, e.g., 10^{-4} ice coverage. The location of these diffuse ice floe regions is shown in Figure 10.

Two extensive diffuse ice floe regions were observed south of the ice margin east of 166°W . The open area between these two regions coincided with the warm core of the coastal current described previously. As a result of finding mesostructure in these unexpected places, six stations were occupied, stations 69, 70, 72, 111, 114, and 115 (Appendix C). Shallow and deep mesostructure elements were observed at these stations.

Well defined deep mesostructure was noted at Station 110, just south of the westerly diffuse ice floe region. This led to the decision to return to the vicinity of this area and conduct a 24-hour time series. It commenced at Station 129-A, 48 hours after Station 110 was made and consisted of Stations 129A-129Z and 130A-130Z (See Appendix C) taken about 30 minutes apart except for a group of six at Station 129-O which were 5 minutes apart. These stations were characterized

by an isothermal layer with deep mesostructure below it. During the time series the ship drifted eastward for 12 hours under the influence of an eastward current and westerly winds. The winds were practically calm during the last 12 hours and GLACIER drifted south under the influence of a southerly current. Throughout the time series the surface current directions agreed well with the drift of the ship.

Temperature profiles, nested in sequence, for the time series are shown in Figures 41a through 41d. These profiles displayed several common characteristics. An isothermal layer (3.2° to 3.9°C) extended from the surface to 10-15 m and deep mesostructure existed below this layer in all cases. The upper layer was also isohaline in the same depth range. During the first 12 hours of the time series, the deep mesostructure elements were strong and located between 20-25 m depth. However, during the last 12 hours, beginning with Station 130C and coincident with the change in ship's drift, the deep mesostructure was weak and higher in the water column (15-20 m). Additionally, fewer mesostructure elements were observed during this period.

The density cross-section for the entire time series is shown in Figure 42. Stations 129A-130Z are equally spaced across the field from left to right. Superimposed on the isopycnals are bars showing the depths of the large and small deep mesostructure elements. The lengths of the bars cover the vertical extent of mesostructure in the water column. The large mesostructure elements (i.e., those previously defined

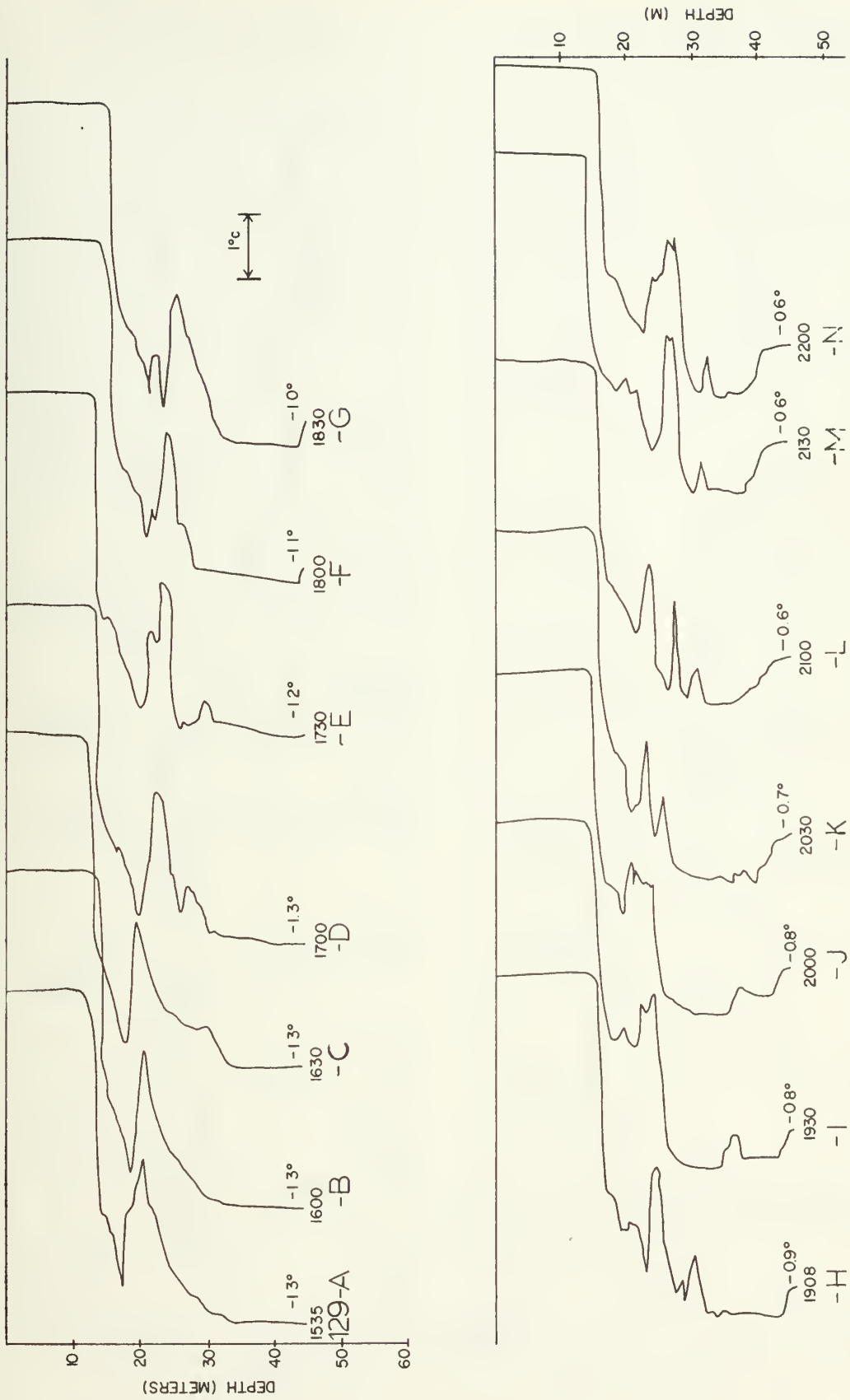


Figure 41a. Temperature profiles for 24-hr time series.

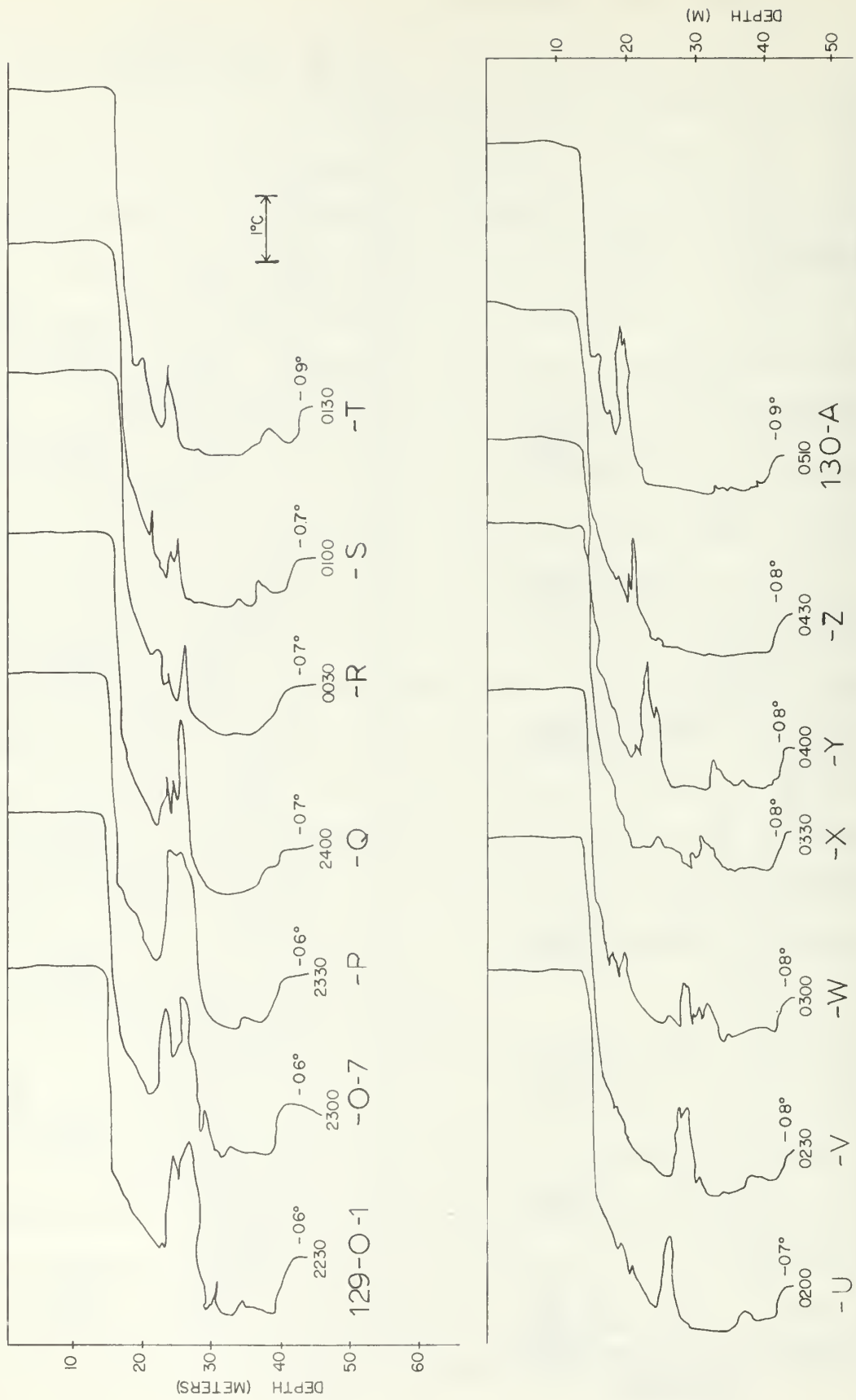


Figure 41b. Temperature profiles for 24-hr time series.

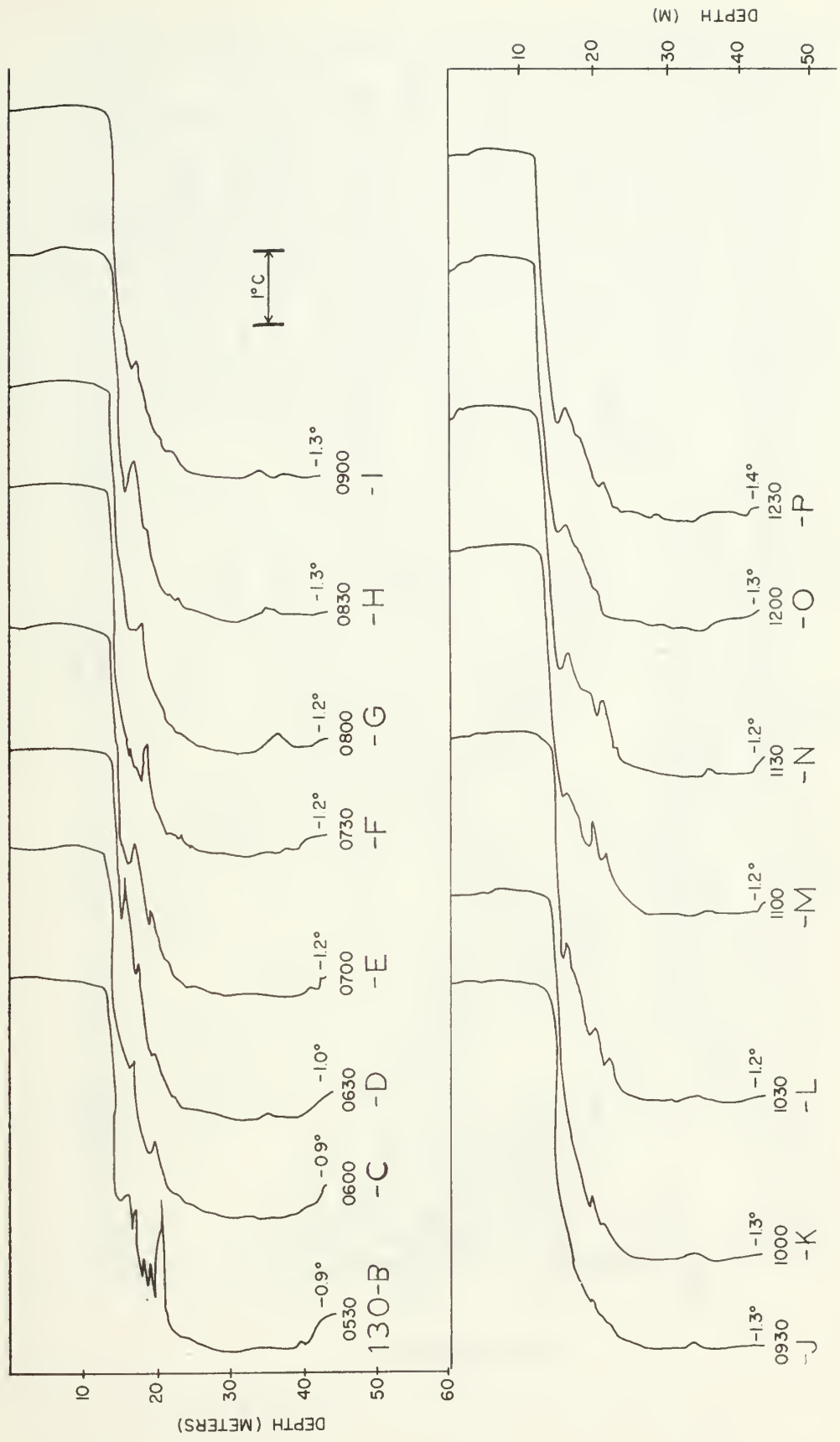


Figure 41c. Temperature profiles for 24-hr time series.

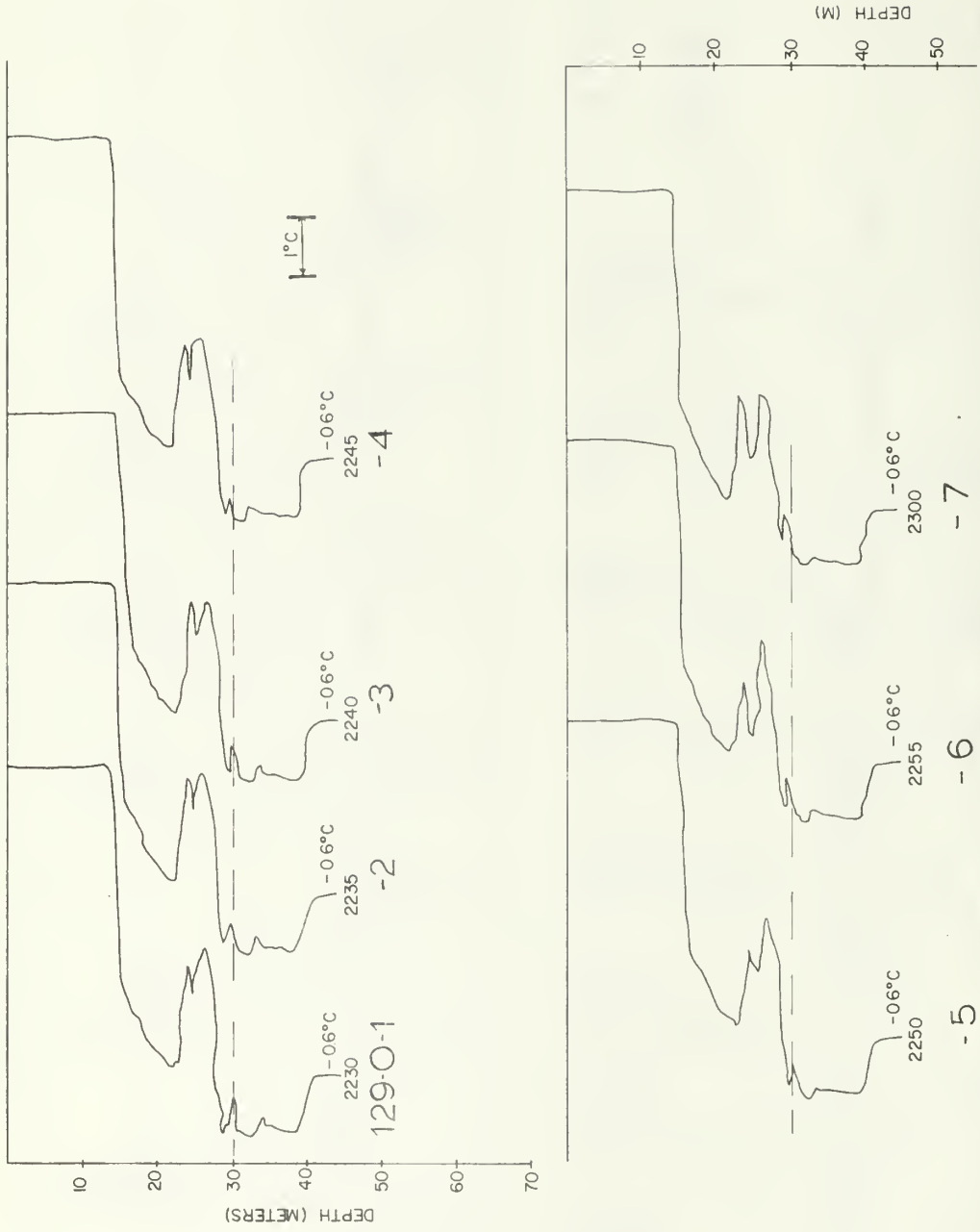


Figure 4ld. Temperature profiles for 24-hr time series.

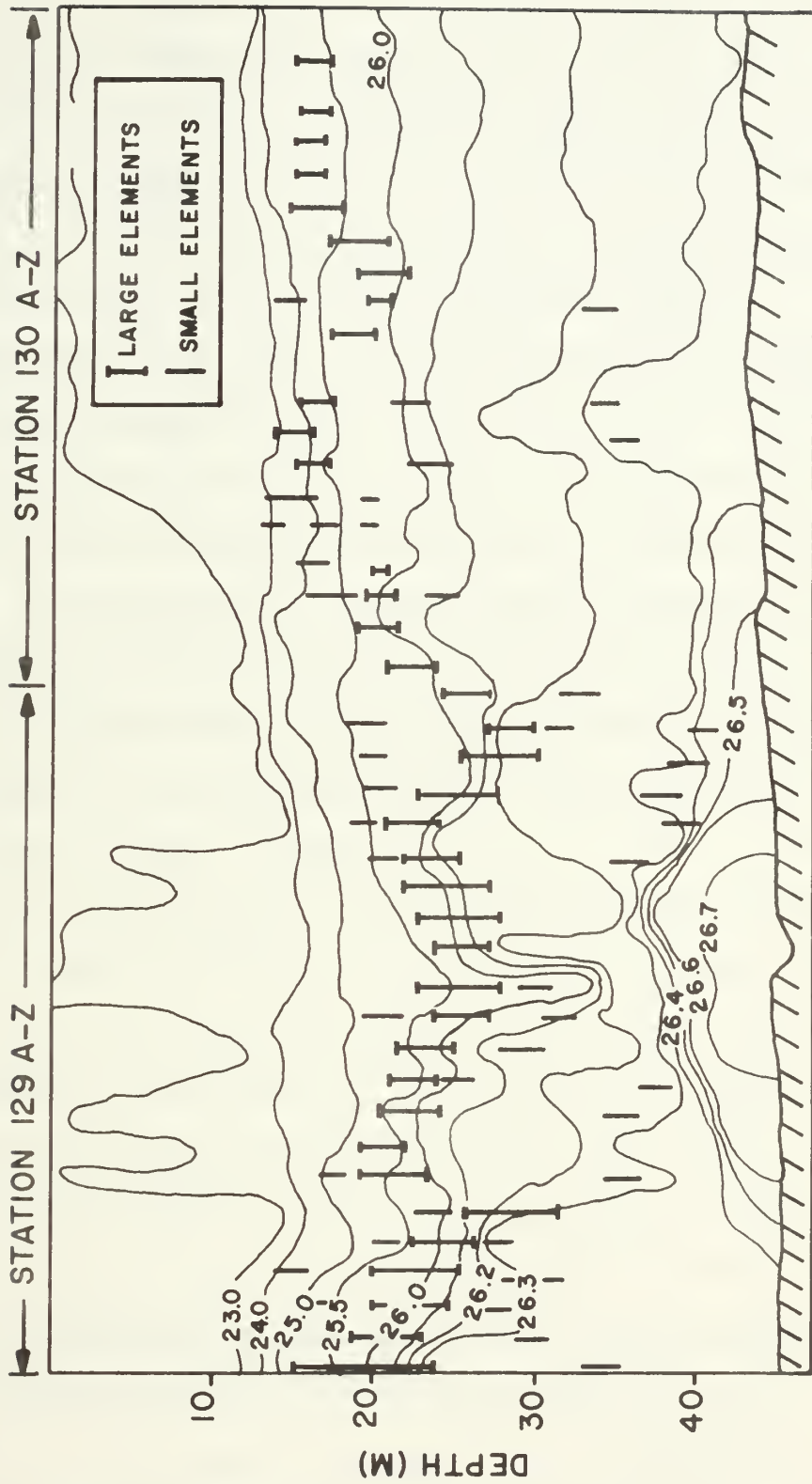


Figure 42. Sigma-t cross section for the 24-hr time series.

as strong) approximately follow the contour of the 26.0 sigma-t surface during the first half of the series. For the second half of the series, these elements are nearer the 25.5 sigma-t surface. Thus, they undulate more or less with the density surfaces as Corse found. The extremely complex nature of the density surfaces in Figure 42 is noteworthy.

Current measurements during the time series are shown in Figure 14, presented earlier. The seven measurements suggest the possible presence of an anti-cyclonic gyre situated in the region of Stations 129-130. The first 12 hours of the time series were conducted in waters flowing with an integrated average northward component from surface to bottom of 4.7 cm sec^{-1} . Conversely, the second 12-hour period was conducted in a region with a southward component of 3.65 cm sec^{-1} .

Mesostructure intensity weakened considerably during the last 12 hours of the time series. Due to the drifting of GLACIER during the time series, it is difficult to determine whether this was a temporal or a spatial effect. However the following points are pertinent:

- GLACIER drifted from 3 km south of the diffuse ice flow region to 19 km south at end of the time series.
- It is possible the ship drifted out of the area of mesostructure formation.
- The average flow direction shifted from a northward to a southward component as strong mesostructure disappeared.
- During the time series, conducted in the vicinity of scattered ice floes, deep mesostructure existed with

a moderate northward component of flow. This contrasts to those observations made during margin crossings where deep mesostructure was observed only with a strong northward component of flow.

3. Ice-Melt Zone

The previously mentioned region of ice melt-water, first noted by Paquette and Bourke (1976), assumes its importance due to the presence of mesostructure. The extent of this ice melt region can be seen in Figure 10. Mesostructure in this region was observed at Stations 26-36, 75-81, and 101-109. The mesostructure found in this open water region was exclusively deep structure, except where the average current flow in the water column was southerly, for which cases shallow as well as deep mesostructure may exist. The observance of mesostructure in this region was not reported in other MIZPAC cruises.

The station property profiles in the above stations (Appendix C) show that the deep mesostructure elements form in a band at depths from about 10 to 20 m. This occurs immediately below the main pycnocline which is typically strong in the ice-melt zone. The mesostructure of this region is fairly weak. This may be seen by examining the station profiles for Stations 31 and 33 in Appendix C.

This discovery of mesostructure in the melt-water area greatly expands the area where one may expect to find mesostructure. It also makes the categorization of mesostructure by class, formation process, or current pattern more difficult.

D. TIME AND SPACE VARIATIONS OF MESOSTRUCTURE

It is important to ascertain how mesostructure changes with time at a particular location because this can give an insight into the processes involved in its formation. An analysis of mesostructure variation, dependent strictly on time, is difficult because all oceanographic stations in MIZPAC 75 were conducted from a drifting ship. However, it was possible to revisit certain stations after a period of time and ascertain the time dependent changes, if any.

Variations in a strictly spatial sense also are important in order to determine the horizontal extent of the individual elements and to investigate the propagation of mesostructure from one station to another. This analysis met with limited success primarily because of the need of ice-margin crossings to be oriented along the line of mesostructure propagation to adequately prove either of the above characteristics and the ice-margin crossings probably were not so oriented.

We proceed first with an analysis of temporal variations. Three stations, 77, 78, and 111 (Appendix C), were revisited to determine if the mesostructure previously seen there had been altered or had disappeared. The revisited stations were then numbered 107, 101, and 129A, respectively. The paired station temperature profiles, along with their respective density profiles, are shown in Figure 43. The elapsed time between each pair was approximately two days. The reader will note that the class of mesostructure and the intensity over periods of time of up to 2 days had not changed notably. The

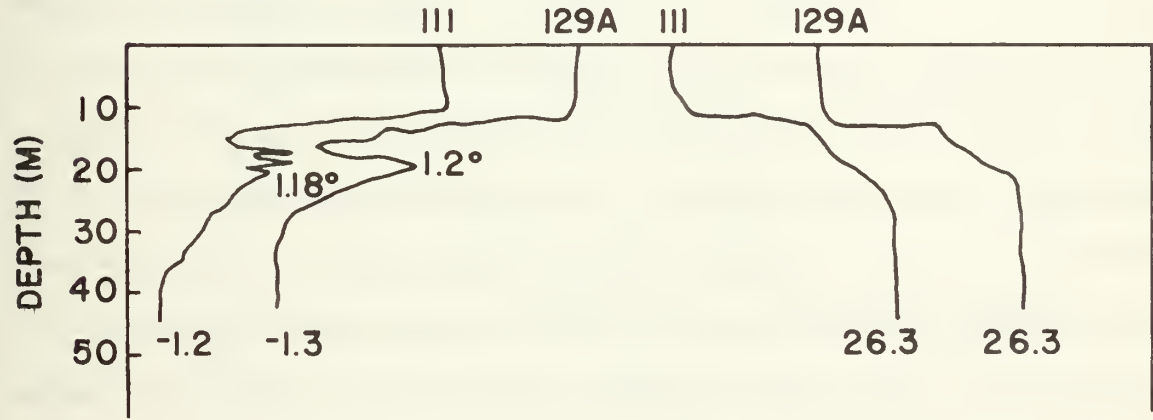
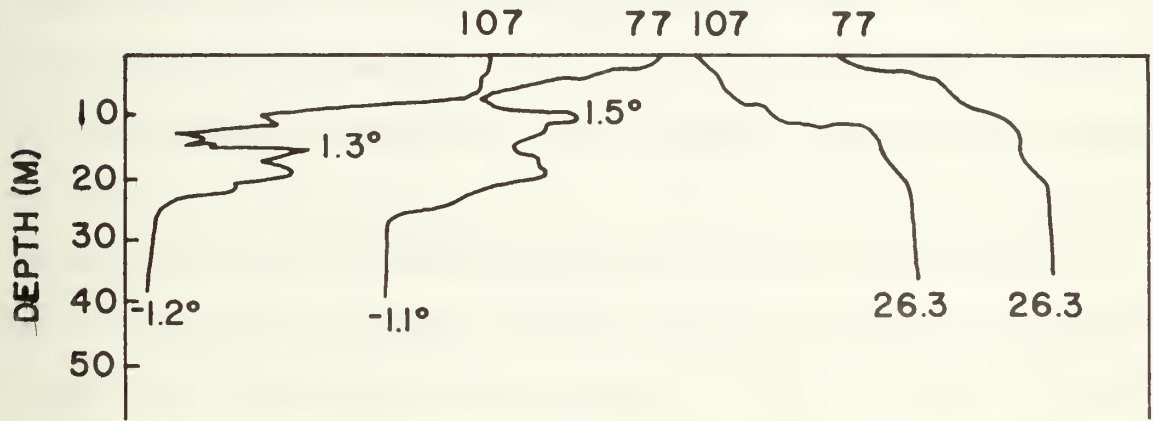
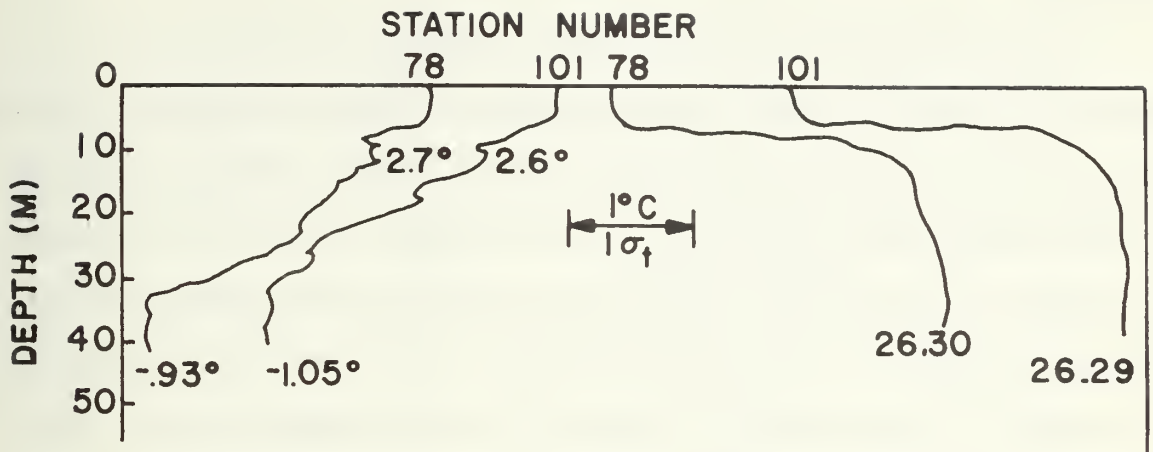


Figure 43. Temperature/density profiles for selected paired stations.

density gradients and density maximums remained closely similar.

It is remarkable that so little change occurred in two days in a region having appreciable currents of varying direction and in a region which is also influenced by the complex lateral pressures often existing near the ice. It is remarkable also in comparison with past results where coherence of mesostructure in space has seriously deteriorated within 1 or 2 km and in time within 4 hours. Still further, it is surprising that, even if the water were assumed quiescent in this area, the temperature structure had not been destroyed by double diffusion which usually is assumed to progress fast enough to essentially destroy the observed mesostructure within a few hours.

There are some possible explanations of these apparent anomalies. Never in previous MIZPAC cruises had stations been revisited after so short a time; perhaps properties are more constant at a point than has been assumed. Alternatively, there may be rapid spatial variation but slow temporal variation. In this connection, it must be remembered that all previous time series have been done from a drifting ship whose drift has been appreciable. Our speculations about double diffusion are qualitative; further analysis could show that the density gradients are so large as to prevent rapid double diffusion. Nevertheless, these observations strike at fundamental concepts which need further investigation.

For an analysis of spatial variation we find it appropriate to turn to the time series. Because of the drift of the ship, the changes which are observed during the time series are more spatial than temporal. Yet, it will be seen that, in common with earlier time series, there is a better station-to-station coherence in the temperature structure than in stations arbitrarily oriented along a line. This could result if the ship drifts more or less with the structure. The current-meter lowerings made during the time series (Figure 14) only partially support this view, but there seems to be no other explanation.

Figure 44 shows the isotherms of the time series plotted spatially along the line of drift which changed from easterly to southerly mid-way during the observations. This figure shows little or no correlation between most individual elements over periods greater than about 4 hours. The larger patches of warm water shown contain water of nearly constant density. These patches follow the depth fluctuations of the 25.5-26.0 sigma-t band.

We now look further into the idea of correlating meso-structure along density surfaces using the method of Howe and Tait (1972) working first with Crossing 3, and then with the time series. A description of this method follows.

Crossing 3 was chosen as it had the best developed meso-structure of all the crossings (Figure 19). The major temperature minima were numbered 1-4, starting at the bottom, and the major temperature maxima were labeled 5-7 starting

from the shallowest. After plotting each numbered point with the appropriate salinity on a temperature-salinity diagram, lines were drawn connecting adjacent cold points and warm points. The resulting diagram is shown in Figure 45. There appears to be only marginal correlation of the position of peaks and troughs along the line of stations between paired stations. This is not surprising if one realizes that the stations of this crossing are not aligned along the line of mesostructure propagation as shown by the current measurements. Analysis of current data shows at least two major current directions in evidence in the area of this margin crossing. Station 65 exhibited mainly west-northwesterly flow, while at Station 68 northeasterly flow predominated. Stations 64 and 66 are lacking current data, and Station 67 data was lost thus preventing definitive statements concerning mesostructure propagation along constant density surfaces. It appears, however, that Stations 64 and 65 and Stations 66 and 68 can be paired as being in the same flow regime. In this way, there is peak to peak and trough to trough correlation for these stations (Figure 45).

In spite of the lack of success of this analytical technique when applied to Crossing 3, it was decided to try this method on the 24 hour time series where the flow vectors were essentially constant for the first half of the series. It was hoped that this type of analysis would support the concept of tracing individual elements along constant density lines. Figure 46 presents the T-S diagram for the plotted mesostructure

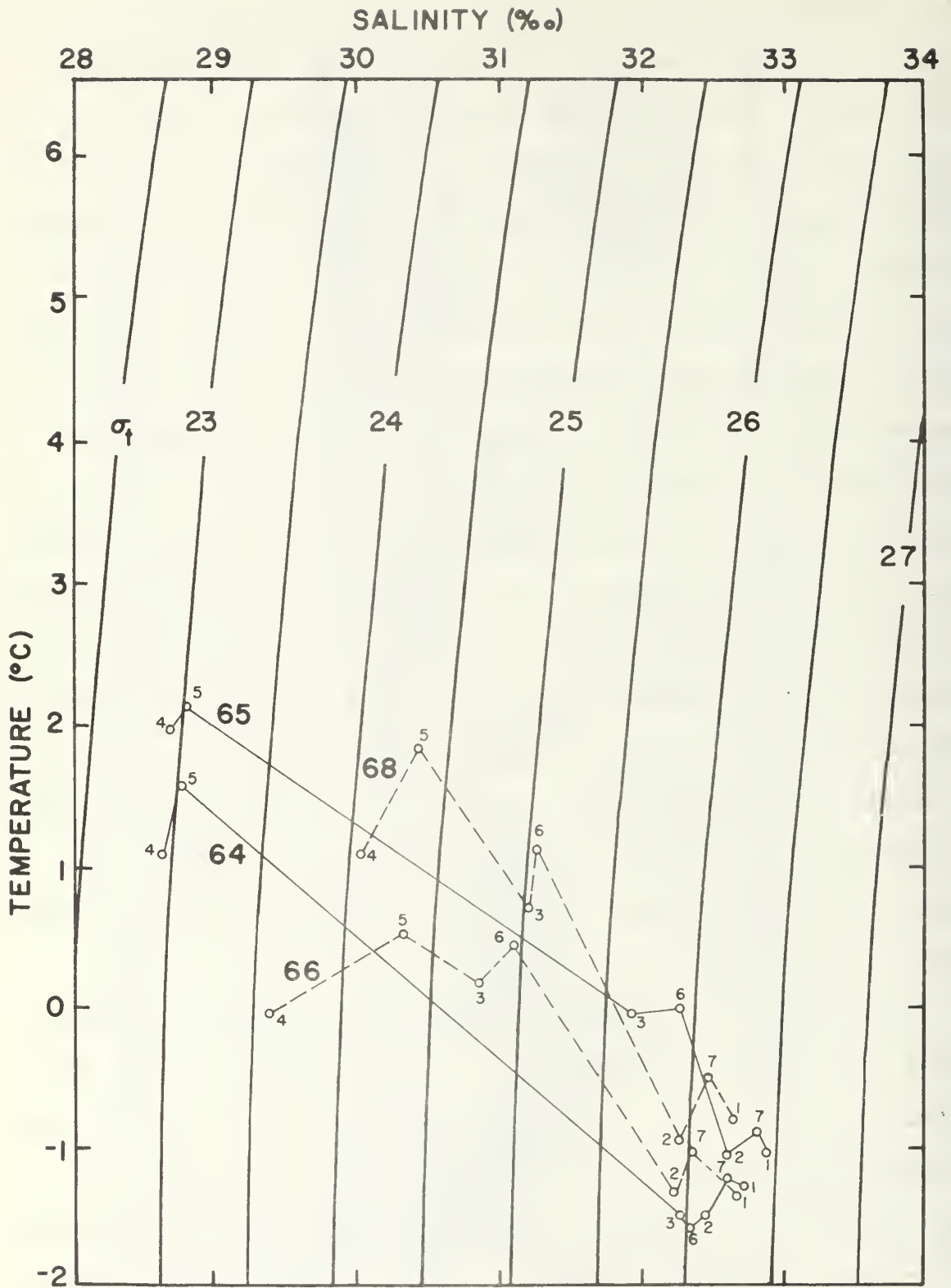


Figure 45. T-S grouping of Stations 64, 65, 66, 68.

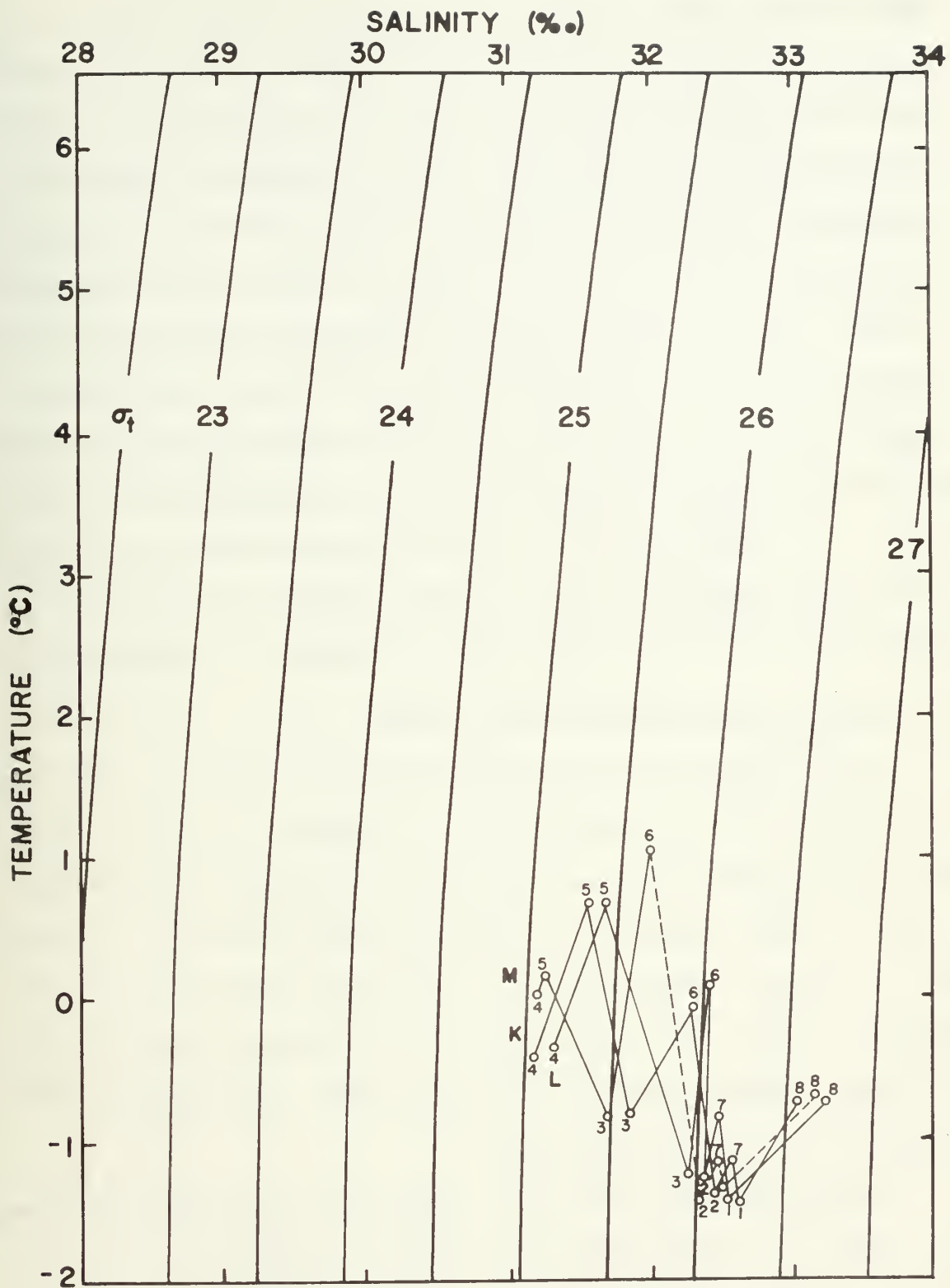


Figure 46. T-S grouping of Stations 129-K, 129-L, and 129-M.

maxima and minima for Stations 129-K, 129-L, and 129-M. These stations were chosen as they correspond to a warm lens of water following the 26.0 sigma-t surface. The flow pattern from current meter measurements made at each of these stations was essentially northeastward, with a spread of no more than 60 degrees. In contrast to the previous example, it is much easier to trace each elemental point along a constant density surface. The variability between points is higher (up to 0.5 sigma-t units) but, since this is a very high flow region (coastal current) and very dynamically active, one should expect some degree of turbulent mixing to be present which can account for this variation. This analysis enables us to conclude that individual mesostructure elements can be traced along the line of propagation for distances of about 4 km.

E. MESOSTRUCTURE-CURRENT CORRELATION

During MIZPAC 75 mesostructure was observed in three kinds of regions differing markedly with respect to ice cover: at six crossings of diffuse ice margins; during a 24 hour time series in the vicinity of a very diffuse ice flow (< 1 okta); and at several stations as far south as 96 km from the ice margin in the melt-water region. The class and intensity of the mesostructure varied considerably both from region to region, and within each region.

During analysis of the flow regime in the vicinity of the ice margin, it was determined that flow in relation to the local ice margin orientation was not related to the class of mesostructure observed. Further investigation of flow in

the vicinity of margin crossings suggested the possibility of an association between the northward component of flow and the existing class of mesostructure. This association was also suggested by Paquette and Bourke (1976).

After thorough analysis of all known variables, it appeared that the northward component of flow and ice character were the primary variables having a direct influence on the formation of various classes of mesostructure. The existence of various classes of mesostructure under such differing conditions of ice character led to an investigation of ice character and the northward component of flow in relation to the class of mesostructure observed.

As mentioned in an earlier section, the ice character encountered in MIZPAC 75 varied from a diffuse ice margin to an ice-free ice-melt region. Additionally, the diffuseness of the ice margin varied considerably from crossing to crossing. Table III presents a classification system for ice character utilized in this analysis. Ice margins were separated into six categories based on the distance from open water to the point where the ice concentration was four oktas. Four oktas was selected as the reference as it was the maximum concentration observed during margin crossings in MIZPAC 75. Several stations were made in areas where the ice concentration was 5 or 6 oktas, but these were not part of an ice margin crossing. Diffuse ice floe areas (< 1 okta) are classified as Diffuse 5, one step more diffuse than the most diffuse in the previous group. Gradations within this

category (Diffuse 5) are based on the amount of ice observed at a station. No gradient measurement was practicable due to the exceedingly low ice concentrations involved, 10^{-1} to 10^{-6} . The ice melt region is ice-free and is divided into three zones based upon distance from the ice margin. These are called Melt 1, Melt 2, and Melt 3.

TABLE III. ICE CHARACTER

<u>Ice Character</u>	<u>Ice Margin</u>
	Distance (km) from 0-4 oktas
Compact 1	0 - 1.5
Compact 2	1.5 - 3
Diffuse 1	3 - 9
Diffuse 2	9 - 15
Diffuse 3	15 - 21
Diffuse 4	21 - 27

<u>Ice Character</u>	<u>Diffuse Ice Floe Region</u>
<u>Diffuse 5</u>	<u>Ice Concentration</u>
	10^{-1} - 10^{-6}

<u>Ice Character</u>	<u>Distance (km) from margin</u>
Melt 1	0 - 30
Melt 2	30 - 60
Melt 3	60 - 90

An attempt to correlate graphically the class and strength of mesostructure with the flow regime is shown in the mesostructure-current correlation chart, Figure 47. The speed indicated is the integrated northward component averaged from surface to bottom. The symbol which indicates shallow and deep mesostructure does not specifically indicate a nose, although a nose is usually present in these instances. The line

ICE CHARACTER

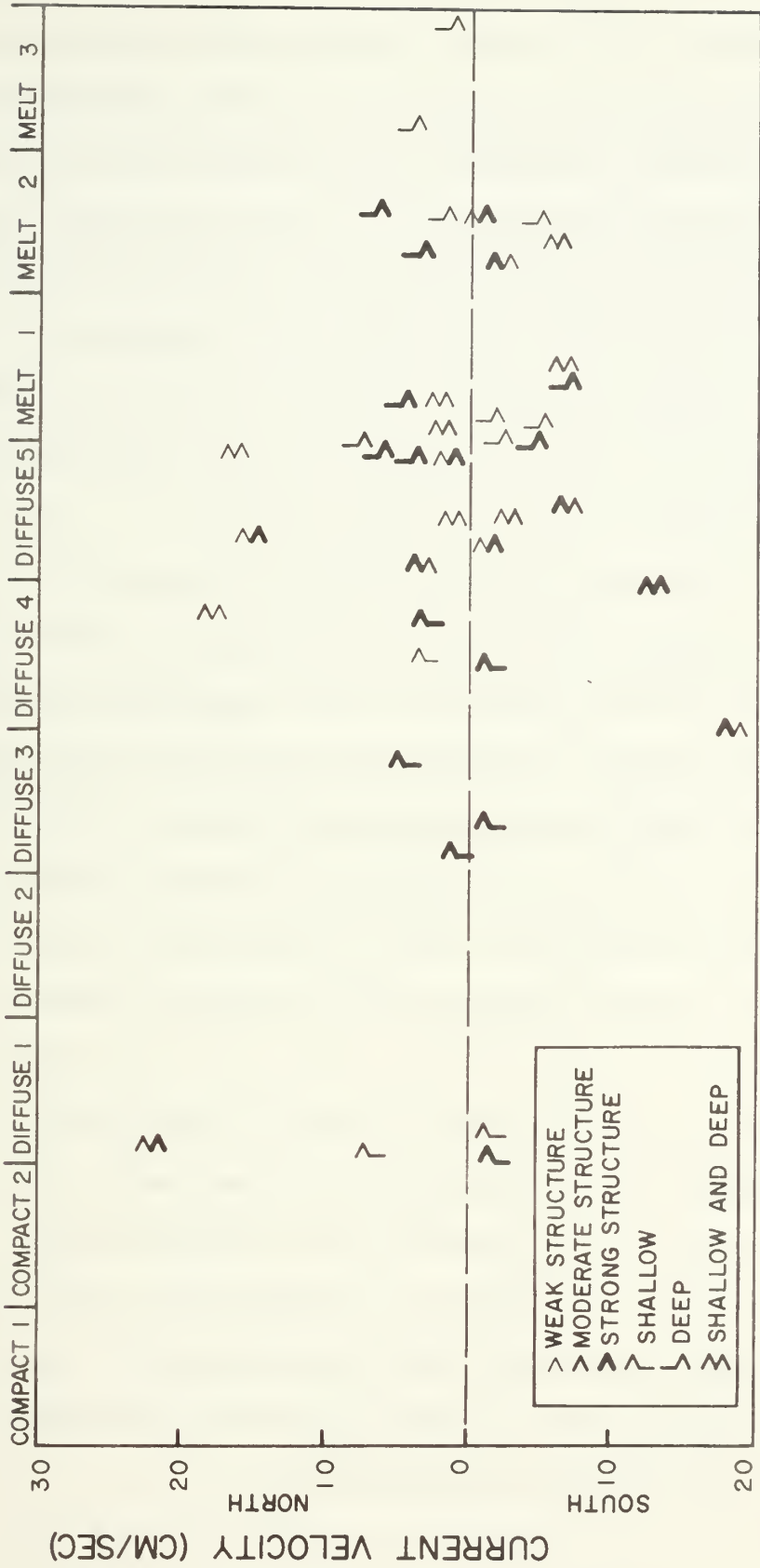


Figure 47. Mesostucture-current correlation.

thickness in the mesostructure symbols denotes the mesostructure intensity, the thickest symbol indicating strong mesostructure (temperature excursion $> 1.0^{\circ}\text{C}$). The next gradation in thickness indicates intermediate mesostructure (temperature excursion between $0.5^{\circ} - 1.0^{\circ}\text{C}$) and the thinnest symbol indicates weak mesostructure (temperature excursion between $0.1^{\circ} - 0.5^{\circ}\text{C}$). This chart includes all 44 stations in which current measurements were taken during MIZPAC 75. Two stations (51 and 121) did not exhibit mesostructure and are represented by short vertical lines.

In the vicinity of the diffuse ice margin (D1 through D4) shallow mesostructure strongly predominates and it is associated with a weak northward or weak southward component of flow. The average intensity of this shallow mesostructure is strong. As stations become more distant from the ice margin (D5-M3), shallow and deep mesostructure or deep mesostructure only were observed; flow at these stations was equally distributed between northward and southward components, showing no preference for either. This occurrence of deep mesostructure up to 96 km south of the ice margin contradicts past reasoning which concluded that deep mesostructure was closely related to the presence of the ice margin. It is evident that there is little correlation of mesostructure class with the north or south flow component. The observation that weaker north-south components are present near the ice may not be statistically valid.

The salient conclusions which can be reached from this analysis are summarized below:

- There appears to be no correlation of mesostructure class or intensity with a northward direction of flow. However, there is some correlation of combined shallow and deep mesostructure of moderate strength with high speed. This correlation might have been improved if time had allowed further analysis to investigate absolute speed instead of the northward component. The previous conclusion that strong mesostructure is correlated with strong flow toward the ice (north in a general sense) is not weakened by this finding because the short-term current measurement may not be a good indication of mean direction. The previous conclusion may even be regarded to be strengthened because one expects generally stronger interactions of water with the ice in those areas where the water speeds, even though rotary or random, are large.
- It is surprising, in view of previous theory, that there is a preponderance of moderate to strong deep and shallow mesostructure in the highly diffuse ice region (D5). This may be a correlation with ice concentration rather than distance. However, there seems no particular correlation of mesostructure with the diffuseness in the immediate vicinity of the margin, descriptions C1 to D4. A distance scale would have yielded similar results in this region.

- Mesostructure was found even in the melt-water zone, south of all ice. Deep mesostructure predominated but became weak toward the southern limit of the melt-water zone, 96 km from the ice. This mesostructure was less sharply layered than in the other areas. This is the first time that mesostructure has been recognized so far from the ice.

IV. CONCLUSIONS

The following conclusions resulted from analysis of MIZPAC 75 data:

- The existence of a two-layered region of ice-melt water, discovered in MIZPAC 74 data, was verified.
- The core of the warm northerly flowing coastal current was found 74 km off shore at latitude 71°N , much farther seaward than in previous years.
- The separation of the current flow with the appearance of northwest and northeast branches north of latitude $69^{\circ}45'\text{N}$ was supported by direct current measurements and temperatures.
- A new definition of shallow and deep mesostructure based upon their position relative to the thermocline was developed. The previous technique of separating these classes by an arbitrary density is believed to be unsuitable.
- A scale of mesostructure intensity was devised based on the extent of the lateral excursion of temperature.
- Mesostructure was found to exist in regions having three distinct ice characters: ice margins, diffuse ice floe region, and the ice melt-water region.
- Mesostructure was much more prevalent in highly diffuse ice areas rather than close to the ice margin. This had been observed before but was not regarded as typical.

- Mesostructure was found far out in the region of ice-melt water, which was not observed before. Mesostructure in this region was weak and the elements were thick and rounded.
- Shallow and deep mesostructure existed only during two margin crossings at isolated stations outside the ice margin. This was probably due to margin crossings not being made along the axis of mesostructure propagation. A strong northward component of flow seemed to be associated with the presence of shallow and deep mesostructure.
- During the remaining four margin crossings, only shallow mesostructure existed and was associated with a weak northerly or weak southerly flow.
- Mesostructure was observed in the same area south of the ice for at least two days. This lifetime was surprisingly long in view of rates suggested by others for the diffusion of heat.
- Mesostructure during a time series, conducted just south of the diffuse ice floe region, was typically better correlated station-to-station than in spatial arrays of stations. The correlations were found along constant density surfaces. Similar correlations were made in two other stations in the ice melt-water region.
- Currents were consistent with a mean northerly transport but were rather variable. Some evidence of a large gyre north of Cape Lisburne was evident.

- The bottom water was warmer this year and salinities were lower than in the past.
- Two patches of relatively warm Atlantic water were discovered on the bottom of the Chukchi Shelf. Why this water persisted on the shelf and did not return to the Arctic Ocean is unknown.
- Strong fronts were found at the ice margin in two locations.

BIBLIOGRAPHY

- Bourke, R. H. and R. G. Paquette. 1976. (Manuscript in preparation).
- Coachman, L. K. and K. Aagaard, 1966. On the Water Exchange Through Bering Strait, *Limnol. and Oceanog.* 11(1): 44-59.
- Coachman, L. K., K. Aagaard and R. B. Tripp. 1976. Bering Strait: The Regional Physical Oceanography, Seattle, University of Washington Press, 192 pp.
- Corse, W. R. 1974. An Oceanographic Investigation of Mesos-structure near Arctic Ice Margins, Master's Thesis, Naval Postgraduate School, Monterey, 54 pp.
- Garrison, G. R., E. Pence, H. Feldman, and S. Shah. 1973. Studies in the Marginal Ice Zone of the Chukchi Sea, Applied Physics Lab., University of Washington, Tech. Rpt. APL-UW 7309, 43 pp.
- Howe, M. R. and R. I. Tait. 1972. The Role of Temperature Inversions in the Mixing Processes of the Deep Ocean, *Deep-Sea Research* 19(11): 781-791.
- Karrer, A. E. 1975. The Descriptive and Dynamic Oceanography of the Mesosstructure near Arctic Ice Margins, Master's Thesis, Naval Postgraduate School, Monterey, 91 pp.
- LaFond, E. C. and D. W. Pritchard. 1952. Physical Oceanographic Investigations in the Eastern Bering and Chukchi Seas During the Summer of 1947, *J. Mar. Res.* 11(1): 69-86.
- Mountain, D. G. 1974. Bering Sea water on the North Alaskan Shelf, Ph.D. Thesis, University of Washington, Seattle. WA, 154 pp.
- Paquette, R. G. and R. H. Bourke. 1973. Oceanographic Measurements near the Arctic Ice Margins, Dept. of Oceanography, Naval Postgraduate School, Monterey, Tech. Rpt. NPS-58PA 73121A, 96 pp.
- Paquette, R. G. and R. H. Bourke. 1974. Observations of the Coastal Current on Northwestern Alaska, *J. Mar. Res.* 32(2): 195-207.
- Paquette, R. G. and R. H. Bourke. 1976. Oceanographic Investigation of the Marginal Sea Ice Zone of the Chukchi Sea --MIZPAC 74, Dept. of Oceanography, Naval Postgraduate School, Monterey, Tech. Rpt. NPS-58PA76051.

- Paquette, R. G., R. H. Bourke, and W. R. Corse. 1974. The Source of Temperature Mesostructure in the Ocean near the Arctic Ice Margin, paper presented at Fall Annual Meeting, American Geophys. Union, San Francisco, December.
- U. S. Naval Oceanographic Office. 1958. Oceanographic Atlas of the Polar Seas, Part II, Arctic, H. O. Pub. No. 705, 149 pp.

APPENDIX A

EXPLANATION OF HEADING CODES

The heading of the printed output uses the coding and format from NODC Publication M-2, August 1964, with a few exceptions. Heading entries which are not self-explanatory are as follows: MSQ is the Marsden Square, and DPTH is the water depth in meters. Wave source direction is in tens of degrees, but the direction 99 indicates no observation. The significant wave height is coded by Table 10 (Code $\div 2 \approx$ height in meters) and the wave period coded by Table 11 (Code $\div 2 \approx$ period in sec); in each case X indicates no observation. Wind speed, V, is coded as Beaufort force, Table 17. The barometer is in millibars, less 1000 if more than 3 digits; wet and dry bulb temperatures are in degrees C. The present weather is from Table 21 with cloud type and amount from Tables 25 and 26, respectively. The combination 4 X 9 indicates that clouds cannot be observed usually because of fog conditions. The visibility is from Table 27 which is roughly in powers of two with Code 4 = 1-2 km. The ice concentration, IC, is in oktas; amounts less than 1 okta are preceded by a minus sign and indicate concentrations in powers of ten, e.g., $10^{-4} = -4$.

The entry, COD, is a code to identify the accuracy of each station position based upon the navigation system used. Code 1 indicates a position determined by visual sightings or radar, Code 2 a position determined by navigation

satellite, and Code 3 a position determined by DR. SORD is a literal addendum to the 3-digit station number used, for example, in sequential stations listed in the time series.

APPENDIX B

HEADING DATA FOR MIZPAC 75 STATIONS

Heading data are listed on the following pages for MIZPAC 75. The coding conventions are those described in Appendix A.

MIZPAC 75 CTD STATIONS

NAT SHIP	LAT	LONG	MSQ	MO	DY	YR	HR	STA	DPTH	OBS	COD	IC	WVD	HT	PER	WVD	V	BAR	WTHR	CL	AMT	VIS	SORD
31	GL 64-30.0	165-25.0	233	07	30	75	18.2	001	28	1	0	99	0	09	1			0	0	0	8		
31	GL 64-17.1	166-12.5	233	07	30	75	22.5	002		1	0	34	2	34	4			0	0	0	8		
31	GL 64-04.0	167-04.5	233	07	31	75	01.5	03		2	0	33	2	33	5	012		0	0	0	8		
31	GL 63-49.4	167-52.7	233	07	31	75	05.4	004	37	2	0	29	1	29	4	012		0	0	0	8		
31	GL 63-38.7	168-46.6	233	07	31	75	09.8	005	32	1	0	27	2	27	3	012		0	0	0	8		
31	GL 64-03.6	168-42.5	233	07	31	75	13.7	006		3	0	30	2	30	3			4	X	9	7		
31	GL 64-30.8	168-42.0	233	07	31	75	17.0	007	27	2	0	25	1	35	2	013		0	0	0	8		
31	GL 64-54.5	168-45.0	233	07	31	75	19.6	008	45	1	0	25	0	32	2	015		1	3	1	8		
31	GL 65-18.5	168-46.0	233	07	31	75	22.5	009		3	0	26	0	25	2	015		0	0	0	8		
31	GL 65-43.0	168-31.0	233	08	01	75	02.5	010		1	0	03	0	36	2	012		1	3	6	8		
31	GL 66-20.4	168-40.0	233	08	01	75	07.5	011	48	1	0	03	1	06	1	017		1	3	6	8		
31	GL 66-57.6	168-41.0	233	08	01	75	11.0	012	45	2	0	34	0	34	2	019		2	4	8	7		
31	GL 67-14.0	168-41.0	233	08	01	75	12.0	013	45	3	0	34	0	34	3	019		2	4	8	7		
31	GL 67-32.8	168-40.8	233	08	01	75	14.2	014	48	2	0	34	0	34	2	018		2	4	8	7		
31	GL 68-02.5	168-40.0	233	08	01	75	16.5	015	61	3	0	02	0	32	2	017		5	7	9	8		
31	GL 68-24.5	168-40.5	233	08	01	75	18.6	016	52	2	0	04	0	36	2	017		2	7	8	8		
31	GL 68-28.0	168-25.0	233	08	01	75	21.0	017	54	3	0	04	0	36	2	017		1	7	4	8		
31	GL 68-28.0	168-10.0	233	08	01	75	22.0	018	48	3	0	04	1	04	3	017		1	3		7		
31	GL 68-28.2	167-57.0	233	08	01	75	23.0	019	50	3	0	04	1	04	3	017		1	3		7		
31	GL 68-29.0	167-43.0	233	08	02	75	00.8	020	45	3	0	25	2	25	3	017		1	3		7		

MIZPAC 75 CTD STATIONS

NAT SHIP	LAT	LONG	MSQ	MO	DY	YR	HR	STA	DEPTH	OBS	COD	IC	HVD	HT	PER	WIND	V	BAR	WTHR	CL	AMT	VIS	SORD	
31	GL 70-01.0	167-26.0	269	08	03	75	00.5	037E					1	00	0	07	4	020		4	X	9	3	E
31	GL 70-04.0	167-32.0	269	08	03	75	02.2	038	42															
31	GL 70-08.5	167-41.9	269	08	03	75	03.8	039	51	2			4	00	0	08	3	020		4	X	9	3	
31	GL 70-10.5	167-42.0	269	08	03	75	05.6	040	50	2			1	00	0	08	3	018		4	X	9	2	
31	GL 70-13.0	167-42.0	269	08	03	75	06.7	041	52	2			1	00	0	07	3	020		4	X	9	2	
31	GL 70-18.8	167-43.0	269	08	03	75	08.1	042A	52				2	00	0	06	3	021		1	7	2		A
31	GL 70-18.8	167-43.0	269	08	03	75	09.4	042B	52				2	00	0	06	3	021		1	7	2		8
31	GL 70-20.5	167-31.0	269	08	03	75	13.3	043A	52	3			4	09	2	09	4	020		1				A
31	GL 70-20.5	167-31.0	269	08	03	75	13.8	043B	52	3			5	00	0	09	4	020		1				P
31	GL 70-20.3	167-25.0	269	08	03	75	14.6	044		3			6	00	0	09	3	020		4	X	9	4	
31	GL 70-20.5	167-16.5	269	08	03	75	15.8	045	52	2			4	00	0	08	3	018		1	3	4	7	
31	GL 70-20.1	167-02.0	269	08	03	75	16.8	046	52	3			0	99	1	14	4	014		1	3			
31	GL 70-43.0	167-03.0	269	08	03	75	20.3	047	52	3			0	11	1	11	4	015		4	X	9	5	
31	GL 70-40.5	167-11.0	269	08	03	75	21.7	048	55				2	00	0	13	4	019		4	X	9	5	
31	GL 70-40.5	167-15.0	269	08	03	75	23.0	049	73	3			2	00	0	11	4	019		1				
31	GL 70-40.5	167-28.0	269	08	04	75	00.0	050	50	3			-2	00	0	12	3	018		4	X	9	5	
31	GL 70-42.5	168-02.5	269	08	04	75	02.0	051		2			-2	00	0	13	3	017		4	X	9	5	
31	GL 71-03.5	168-04.5	265	08	04	75	04.5	052	46	2			0	11	1	11	3	016		2	5	8	6	
31	GL 71-26.0	168-02.0	269	08	04	75	07.7	053	51				8	14	1	14	3	016		4	X	9	2	
31	GL 71-38.0	167-14.0	269	08	04	75	11.5	054	50	3			0			13	4	016		4	X	9	3	

MIZPAC 75 CTD STATIONS

NAT	SHIP	LAT	LONG	MSQ	MO	DY	YR	HR	STA	DPTH	OBS	COO	IC	MVD	HT	PER	WIND	V	BAR	WTHR	CL	AMT	VIS	SORD
31	GL	71-34.0	166-10.0	269	08	04	75	15.0	058		3						14	3	016	4	X	9	3	
31	GL	71-23.5	165-26.0	269	08	04	75	20.3	056	44	2	7	90	0			27	2	015	4	X	9	5	
31	GL	71-18.8	165-27.9	269	08	04	75	22.3	057	44	3	3	00	0			24	3	014	4	X	9	5	
31	GL	71-16.0	165-27.5	269	08	04	75	23.2	058	44	2	3	00	0			28	2	014	4	X	9	5	
31	GL	71-12.2	165-16.6	269	08	05	75	00.8	059	44	3	2	00	0			26	2	014	4	X	9	5	
31	GL	71-08.8	165-02.9	269	08	05	75	01.8	060	44	3	-2	00	0			24	2	013	4	X	9	5	
31	GL	71-02.0	164-25.0	269	08	05	75	05.5	061	36							25	3	012	5	6	8	8	
31	GL	70-49.1	164-22.9	269	08	05	75	08.7	062	46	2	1	00	0			02	3	011	3	7	8		
31	GL	70-40.5	164-11.7	269	08	05	75	12.5	062A	52	2	1	00	0			27	2	011	1				A
31	GL	70-40.5	164-11.7	269	08	05	75	13.3	063B	52	2	1	00	0			27	2	011	1				B
31	GL	70-39.0	164-09.0	269	08	05	75	13.8	064	52	2						30	2	011					
31	GL	70-36.0	164-09.0	269	08	05	75	15.0	065A	48	3	2	00	0			28	3	011	4	X	9	5	A
31	GL	70-36.0	164-09.0	269	08	05	75	16.0	065B	48	3	2	00	0			28	3		4	X	9	5	B
31	GL	70-33.0	164-07.5	269	08	05	75	16.5	066	48	2	0	35	0			35	3	011	4	X	9	4	
31	GL	70-29.5	164-04.5	269	08	05	75	17.3	067	47	2	0					00	4	012	5	7	8	8	
31	GL	70-24.0	164-00.0	269	08	05	75	18.3	068	37							00	3	012	2	7	8	8	
31	GL	70-21.5	163-15.5	269	08	05	75	20.4	069	35	2	-3	00	0			35	3	013	7	7	8	8	
31	GL	70-28.0	163-05.0	269	08	05	75	22.3	070	30	3	-6	00	0			24	4	013	1	7	6	8	
31	GL	70-24.0	163-03.0	269	08	05	75	23.8	071	35	2	-6	00	0			20	4	014					
31	GL	70-18.5	162-54.0	269	08	06	75	02.0	072	35	3	-3	34	0			34	4	015					

MIZPAC 75 CTD STATIONS

NAT	SHIP	LAT	LONG	MSQ	MO	DY	YR	HR	STA	DPTH	OBS	COD	IC	WVD	HT	PER	WVD	V	BAR	WTHR	CL	AMT	VIS	SORD
31	GL	70-16.6	163-11.4	269	08	06	75	03.1	075	33	2	-3	00	0	99					1	7	5	8	
31	GL	70-12.3	163-46.5	269	08	06	75	04.5	074	35	2	0	31	1	33	4			016	1	7	7	5	
31	GL	70-08.0	164-14.0	269	08	06	75	06.1	075	38	2	0	02	1	02	3			017	1	7	8		
31	GL	70-04.0	164-35.0	269	08	06	75	07.5	076		2	0	34	2	35	3			017	2	7	7	8	
31	GL	69-55.2	165-06.0	233	08	06	75	08.7	077	39	3	0	34	1	35	4			017	2	7	8	8	
31	GL	69-56.5	165-35.8	233	08	06	75	10.5	078	43	2	0	33	1	33	4			018	1				
31	GL	69-56.6	166-06.1	233	08	06	75	12.5	079	37	2	0	31	2	31	4			018	1			7	
31	GL	69-56.6	166-35.9	233	08	06	75	13.7	080	48	0	31	1	31	3				018					
31	GL	69-58.1	167-04.7	233	08	06	75	15.0	081	49	2	0	30	1	31	4			017	1	7	4	5	
31	GL	69-58.1	168-03.4	233	08	06	75	16.7	082	49	3	0	30	1	31	3			017	1	7	3	5	
31	GL	69-58.2	168-03.5	233	08	06	75	18.3	083	51	3	0	0	0	29	3			017	1	7	7	8	
31	GL	69-58.5	168-07.5	233	08	06	75	19.3	084	51	3	-2	00	0	29	3			017	1	7	7	7	
31	GL	70-03.8	168-16.3	269	08	06	75	21.2	085		3	-2	00	0	30	3			016	4	7	7	7	
31	GL	70-01.0	168-20.0	269	08	06	75	22.0	086	42	3	1	31	0	31	4			016	4	X	9	4	
31	GL	70-00.0	168-16.0	269	08	06	75	23.0	087	60	2	1	31	0	31	3			017	4	X	9	4	
31	GL	69-59.0	168-16.0	223	08	07	75	00.0	088	61	2	2	00	0	31	3			016	4	X	9	4	
31	GL	69-49.0	168-16.0	233	08	07	75	02.5	089	45		0	00	0	27	2			016	4	X	9	3	
31	GL	69-46.0	168-40.0	233	08	07	75	04.0	090	52	2	-2	00	0	33	2			016	1	4	2	8	
31	GL	69-40.5	169-07.5	233	08	07	75	06.8	091	54	3	0	26	1	26	3			016	0		0	8	
31	GL	69-47.8	169-29.8	233	08	07	75	09.3	092	40	2	0	0	1	34	4			016	0		0	8	

MILPAC 75 CTD STATIONS

NAT SHIP	LAT	LONG	MSQ	MO	DY	YR	HR	STA	DPTH	08S	COD	IC	MWD	HT	PER	WIND	V	BAR	WTHR	CL	AMT	VIS	SQRD
31	GL 69-49.4	169-10.0	233	08	07	75	10.3	093	46		2	2	00	0	33	2	016		1				
31	GL 69-50.5	169-05.0	233	08	07	75	11.2	094	40			4	00	0	33	3	016		1	4	1		
31	GL 69-52.6	169-00.0	233	08	07	75	11.8	095	38		2	5	00	0	34	3	016		1				
31	GL 69-52.6	169-00.0	233	08	07	75	12.5	096	43		2	5	00	0	31	2	016		1				
31	GL 69-46.0	169-03.0	233	08	07	75	14.0	097	53			0	00	0	28	3	017		1	4	3	8	
31	GL 69-44.5	169-00.0	233	08	07	75	14.8	098	53		2	-2	00	0	31	2	016		1	4	3	8	
31	GL 69-46.8	169-02.0	233	08	07	75	16.8	099	49		3	-2	00	0	31	2	016		1	4	3	8	
31	GL 69-43.5	168-55.8	233	08	07	75	18.7	100	54		2	-6	00	0	10	3	017		1	2	3	8	
31	GL 69-53.5	165-46.5	233	08	08	75	02.5	101	44		2	0	32	0	33	2	016		1	4	7	6	
31	GL 69-57.7	165-21.0	233	08	08	75	04.3	102	41		3	0	32	1	20	2	016		1	4	7		
31	GL 70-02.6	164-43.2	269	08	08	75	06.3	103	48		2	0	27	0	27	3	015		1	4	7	8	
31	GL 70-07.5	164-17.9	269	08	08	75	09.7	104	37		3	0	00	0	24	2	015		1	7	7	8	
31	GL 69-51.5	164-48.5	233	08	08	75	12.0	105	35		2	0	18	0	18	3	014		1				8
31	GL 69-50.0	164-51.0	233	08	08	75	13.3	106	40		2	0	18	0	18	4	014		1				
31	GL 70-01.0	164-52.0	269	08	08	75	14.2	107	40		3	0	20	0	21	3	013		1	3	7	6	
31	GL 70-06.2	164-52.0	269	08	08	75	15.4	108	41		3	0	20	1	21	4	011		1	3	7	6	
21	GL 70-11.8	164-56.0	269	08	08	75	16.5	109	44		3	0	20	2	21	4	011		1	3	7	6	
31	GL 70-19.0	164-52.0	269	08	08	75	17.6	110	46		3	0	20	2	21	5	010		1	3	5	6	
31	GL 70-21.0	164-50.0	269	08	08	75	18.5	111	46		2	0	23	2	23	5	009		1	3	3	7	
31	GL 70-26.4	164-50.0	269	08	08	75	20.1	112	47		3	-4	22	2	22	5	008		1	3	7		

MIZPAC 75 CTD STATIONS

NAT SHIP	LAT	LONG	MSQ	MO	DY	YR	HR	STA	DPHT	ORS	COD	IC	MVD	HT	PER	WIND	V	BAR	WTHR	CL	AMT	VIS	SGRD
31	GL 70-31.5	164-50.0	269	08	08	75	21.0	113	46	5	-2	22	0	22	5	007			1	6	2	8	
31	GL 70-43.6	164-45.3	269	08	08	75	22.3	114	42	2	-2	22	0	22	5	005			1				
31	GL 70-43.5	164-15.0	269	08	09	75	00.2	115	48	2	-6	22	1	22	5	005			1	6	2		
31	GL 70-44.0	163-42.0	269	08	09	75	01.9	116	50	3	4	00	0	23	5	004			2	7	8		
31	GL 70-35.0	163-13.0	265	08	09	75	04.3	117	44	3	3	00	0	25	3	003			2	7	9	5	
31	GL 70-40.9	162-42.4	269	08	09	75	06.3	118	39	2	2	00	0	24	5	012			2	7	8		
31	GL 70-39.1	162-14.2	265	08	09	75	07.7	119	35	2	2	00	0	25	5	012			2	7	9	6	
31	GL 70-39.0	161-45.0	269	08	09	75	09.5	120	43	3	2	00	0	24	4	012			5	7	8	2	
31	GL 70-39.0	161-05.0	233	08	09	75	13.5	121	47	2	6	00	0	26	4	001			4	X	9	4	
31	GL 70-35.5	160-31.5	269	08	09	75	16.9	122	47					29	4	001							
31	GL 70-30.0	162-23.0	269	08	09	75	20.7	123	35		0	0	1	31	5	013			1	6	3		
31	GL 70-22.3	162-52.2	269	08	09	75	22.7	124	38	2	0	0	2	31	5	005			1	4	3	7	
31	GL 70-28.0	162-34.0	265	08	10	75	00.7	125	37	3	-2	30	2	30	4	006			1	4	3	7	
31	GL 70-28.0	162-04.0	269	08	10	75	02.3	126	26	1				29	4	006							
31	GL 70-32.0	161-44.0	269	08	10	75	03.7	127	26	1	2	00	0	29	4	006			7	7	4	6	
31	GL 70-28.0	161-22.0	269	08	10	75	06.1	128	24	1	-2	00	0	30	4	007			1	7	6	5	
31	GL 70-20.6	164-50.9	269	08	10	75	15.6	129A	46	3	0	30	2	30	5	009			1	7	6	5	A
31	GL 70-20.6	164-50.0	269	08	10	75	16.0	129B	46	3	0	30	2	30	3	009			1	7	6	5	B
31	GL 70-20.5	164-45.0	269	08	10	75	16.5	129C	46	3	0	30	2	30	2								C
31	GL 70-20.5	164-47.5	269	08	10	75	17.0	129D	44	3	0	30	2	30	2								D

MIZPAC 75 CTD STATIONS

NAT SHIP	LAT	LONG	MSQ	MO	DY	YR	HR	STA	DPTH	OBS	CCD	IC	WVD	HT	PER	WND	V	BAR	WTHR	CL	AMT	VIS	SCRD
31	GL 70-20.4	164-46.0	269	08	10	75	17.5	129E	44		3	0	30	1	31	4	009		7	7	6	3	E
31	GL 70-20.3	164-45.0	269	08	10	75	18.0	129F		3	0	30	1	31	4	010							F
31	GL 70-20.0	164-43.0	269	08	10	75	18.5	129G			0	31	1	31	2	010			1	7	6	7	G
31	GL 70-19.6	164-41.5	269	08	10	75	19.1	129H		3	0	31	1	32	3	010							H
31	GL 70-19.6	164-40.0	269	08	10	75	19.5	129I			0	32	1						1	6	8	4	I
31	GL 70-19.6	164-38.0	269	08	10	75	20.0	129J		3	0	32	1	31	2	010							J
31	GL 70-19.5	164-37.0	269	08	10	75	20.5	129K			0	33	1										K
31	GL 70-19.5	164-35.8	269	08	10	75	21.0	129L		3	0	33	0	31	2	011			1	6	8	6	L
31	GL 70-19.0	164-36.0	269	08	10	75	21.5	129M			0	31	0	31	3	011							M
31	GL 70-18.5	164-37.0	269	08	10	75	22.0	129N			0	32	0	32	3	012							N
31	GL 70-18.0	164-37.0	269	08	10	75	22.5	129O	44	3	0	32	0										O
31	GL 70-17.7	164-37.5	269	08	10	75	23.5	129P	44		0	32	0										P
31	GL 70-17.2	164-36.0	269	08	11	75	00.0	129Q	43	3	0	52	0										Q
31	GL 70-17.1	164-35.0	269	08	11	75	00.5	129R			0	52	0										R
21	GL 70-17.0	164-35.5	269	08	11	75	01.0	129S			0	32	0										S
31	GL 70-17.0	164-40.5	269	08	11	75	01.5	129T			0	32	0										T
31	GL 70-16.0	164-40.2	269	08	11	75	02.0	129U			0	32	0										U
31	GL 70-15.5	164-40.0	269	08	11	75	02.5	129V		2	0	31	1	31	2	012			2	7	8	8	V
31	GL 70-15.3	164-41.0	269	08	11	75	03.0	129W			0	51	0	32	1	012			1	7	7	6	W
31	GL 70-15.0	164-41.2	269	08	11	75	03.5	129X		3	0	31	0	32	1	012							X

MIZPA 75 CTD STATIONS

NAT SHIP	LAT	LONG	MSQ	MO	DY	Yr	HR	STA.	DEPTH	OBS	CTD	IC	MWD	FT	PER	WIND	V	BAR	WTHR	CL	AMT	VIS	SORD	
31	GL 70-11.4	164-41.2	269	08	11	75	14.0	130S				0	30	0									S	
31	GL 70-11.3	164-42.1	269	08	11	75	14.5	130T				0	00	0	26	1	012			2	7	8	5	T
31	GL 70-11.1	164-42.0	269	08	11	75	15.0	130U				0	00	0									U	
31	GL 70-11.0	164-41.0	269	08	11	75	15.5	130V		3	0	00	0	23	1	012				1	7	7	4	V
31	GL 70-10.8	164-40.0	069	08	11	75	16.0	130W		2	0	00	0										W	
31	GL 70-10.6	164-35.0	269	08	11	75	16.5	130X				0	04	0	28	1	012			1	7	6	6	X
31	GL 70-10.4	164-38.0	269	08	11	75	17.0	130Y				0	00	0									Y	
31	GL 70-10.2	164-37.0	269	08	11	75	17.5	130Z				0	00	0	23	1	011			2	7	8	7	Z
31	GL 70-20.5	164-37.0	269	08	11	75	19.7	131	47			0	00	0	23	1				2	6	8	7	
31	GL 70-20.5	164-35.0	269	08	11	75	20.4	132		3	0	00	0	21	1									
31	GL 70-20.5	164-25.0	269	08	11	75	20.9	133	43	3	0	00	0	21	1	012				2	8	8	7	
31	GL 70-20.5	164-26.0	269	08	11	75	21.4	134	43	2	0	00	0	24	1					2	8	8		
31	GL 70-20.9	164-16.5	269	08	11	75	22.0	135		2	0	00	0	21	1	012								
31	GL 70-20.6	164-01.2	269	08	11	75	23.0	136	40	3	0	00	0	19	2	011				1	7		7	
31	GL 70-19.7	163-42.1	269	08	11	75	23.9	137	40	3	0	00	0											
31	GL 70-23.0	163-20.0	269	08	12	75	01.8	138		2	0	00	0	12	2	010								

APPENDIX C

CTD DATA FOR MIZPAC 75 STATIONS

The data for each station of MIZPAC 75 is presented in graphical format. Four stations appear on each page; the respective station number appears in the lower power of each plot. The scales for the horizontal axis are located at the top of each column and the symbols used are as follows:

ST, Sigma-t

SV, sound velocity (m sec^{-1})

S, salinity ($^{\circ}/\text{oo}$)

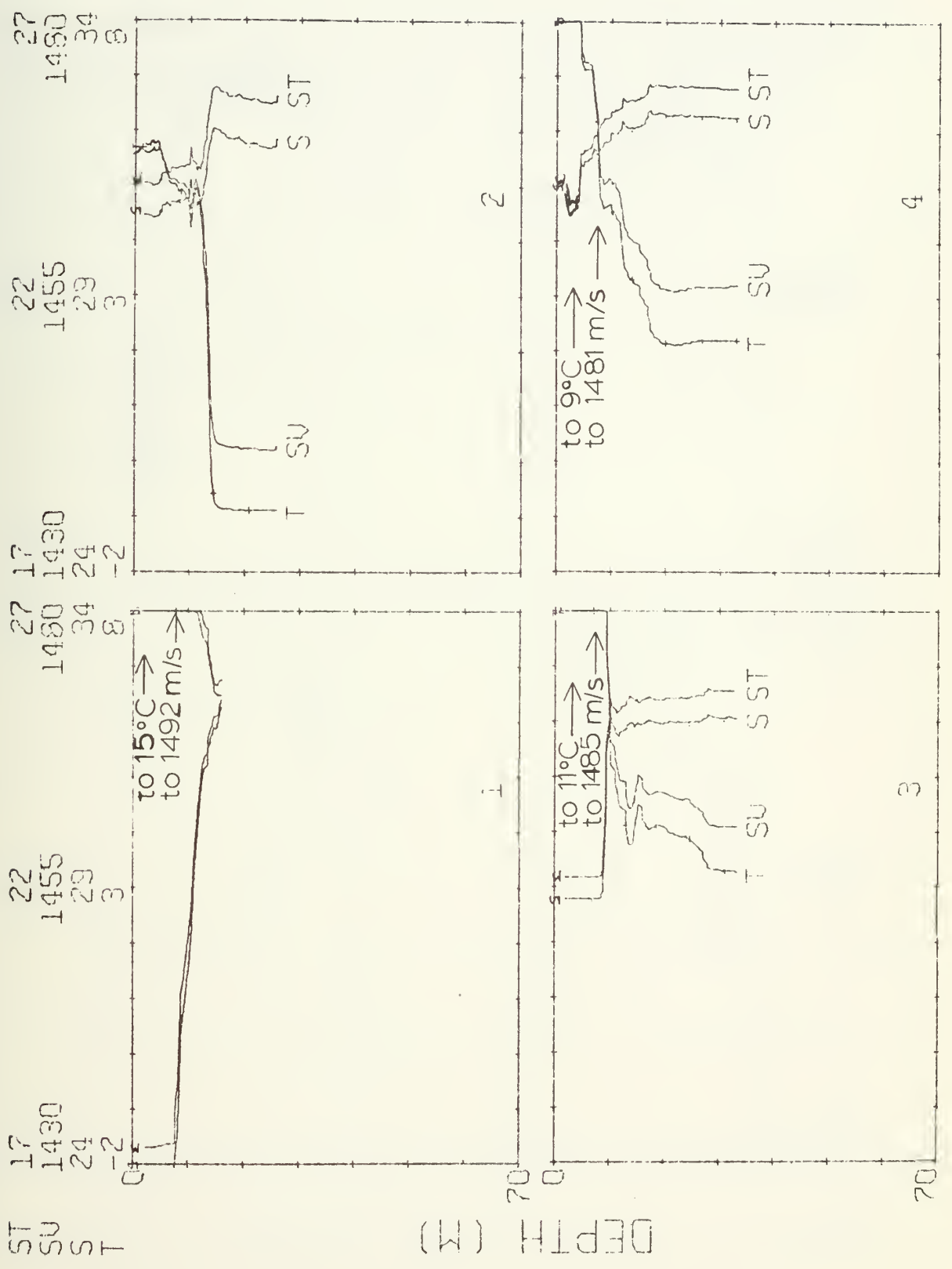
T, temperature ($^{\circ}\text{C}$)

The symbol for each of the above parameters is at the bottom of each trace and an S, T, or V (salinity, temperature, or sound velocity) appears at the top to help distinguish individual traces. Temperature traces are further distinguished by a cross about every 5 meters and salinity traces by similar tiny dots. Stations which were missing from the sequence were mostly those which were not recoverable when the data were reprocessed ashore. Nearly all of these eventually were recovered by tracing the original records with the Calma digitizer as was done in the past. The corrected temperature and salinity traces for these missing stations are included in the body of this appendix in their proper sequence. It will be noted that seven lowerings about 5 minutes apart were made at Station 129-0 during the time series. These are labelled 129-0-1, 129-0-2, etc. There is

a short time series at Station 37 and occasional duplicate lowerings at a station, also indicated by a literal suffix to the station number.

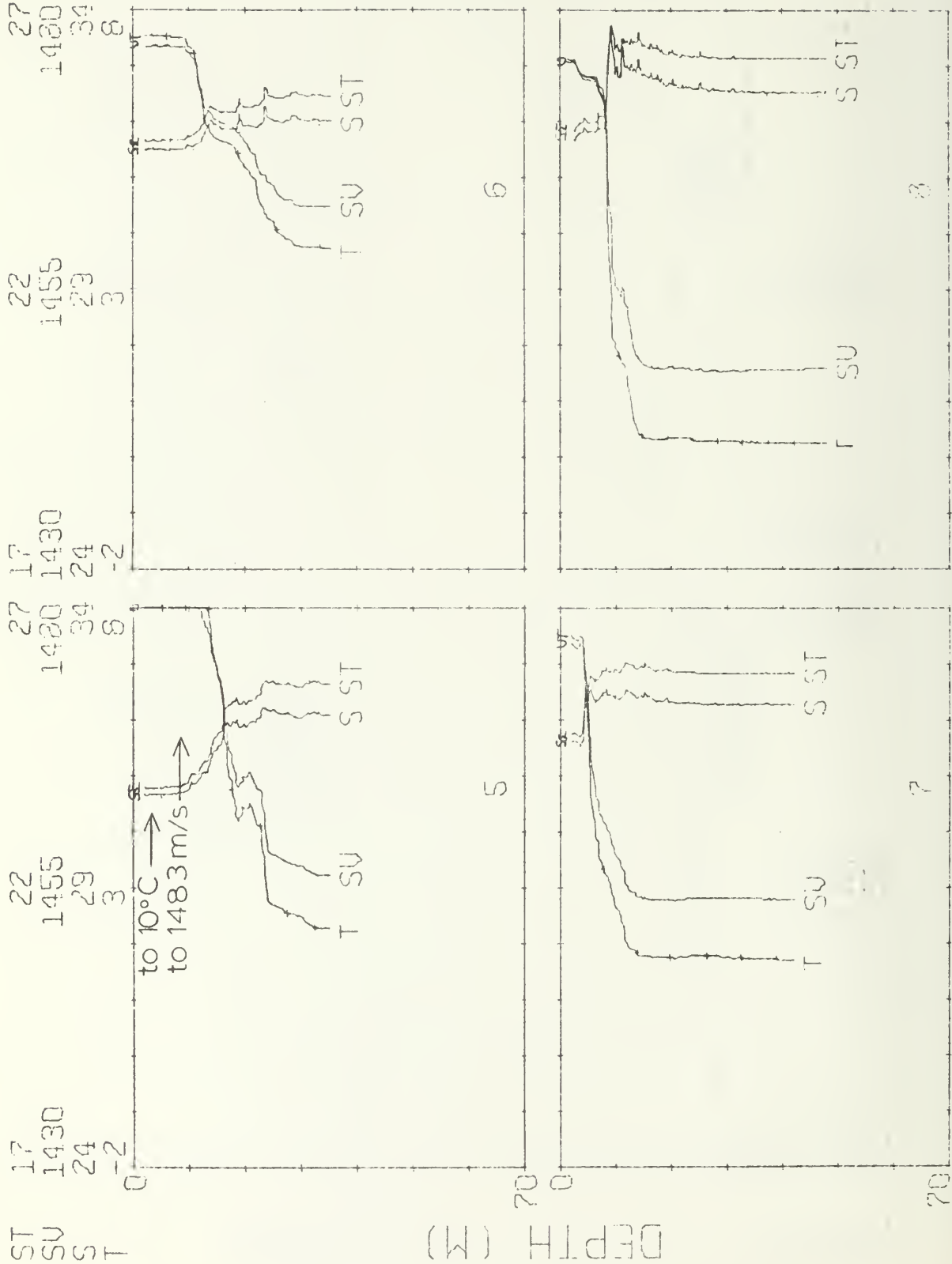
MG/CC
M/SEC
P.P.T.
DEG C

MIZPAC 75 CTD STATIONS



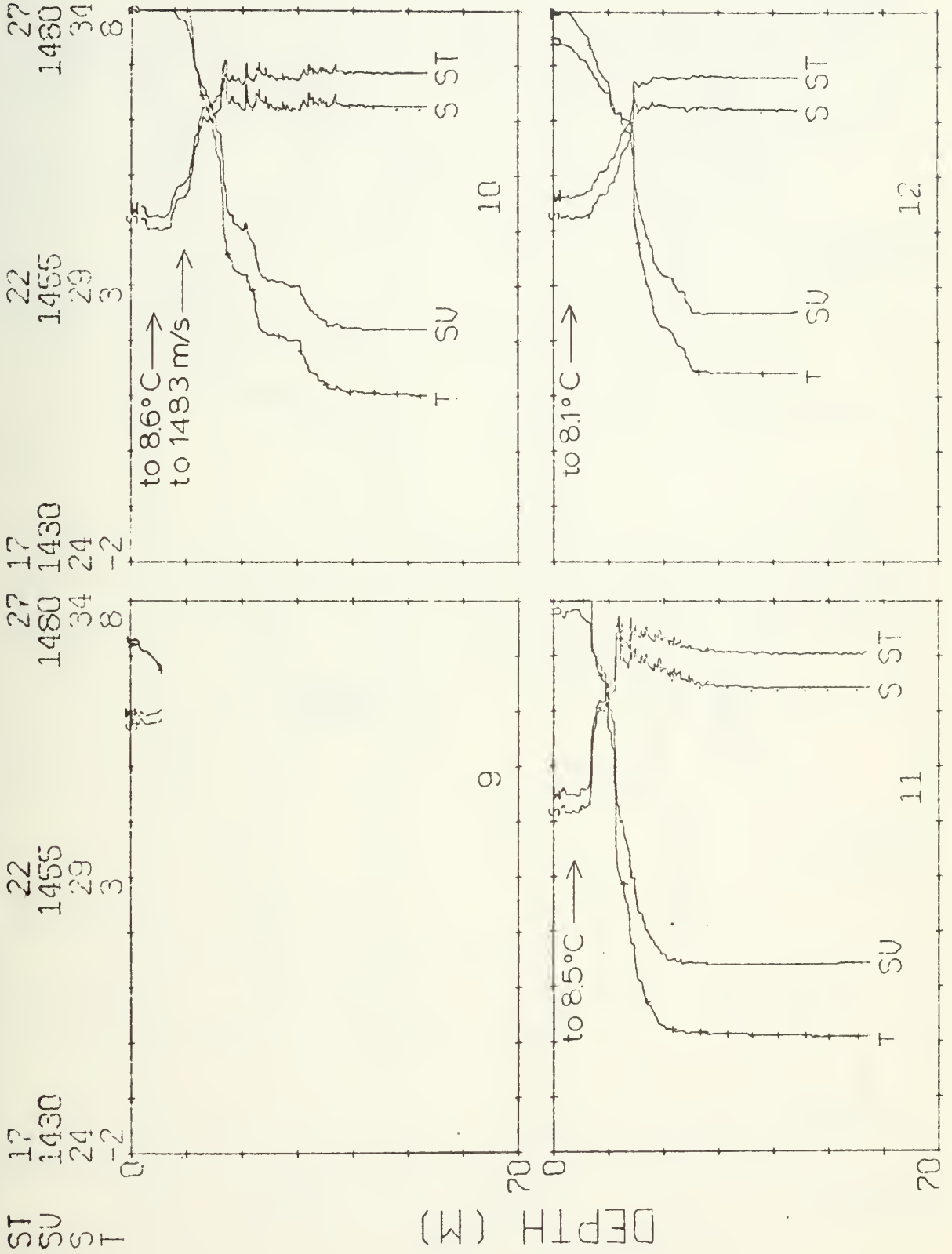
MG/CC
 M/SEC
 P.P.T.
 DEG C

MIZPAC 75 CTD STATIONS



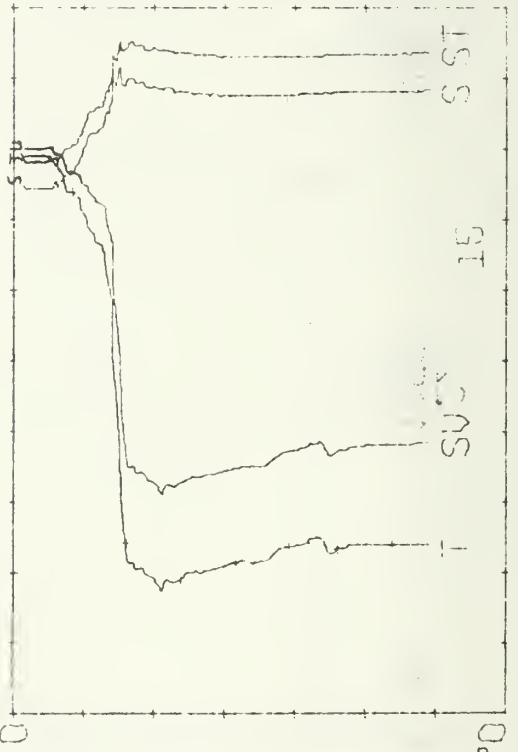
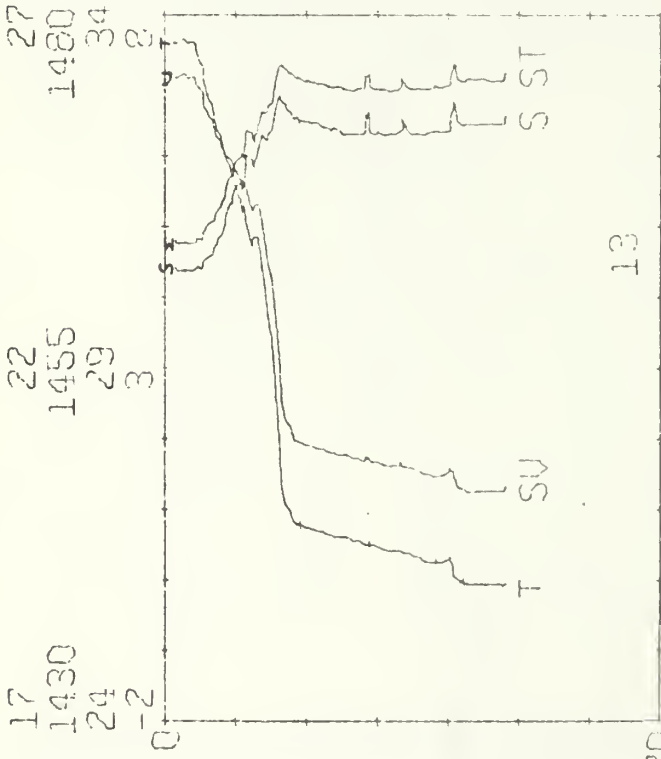
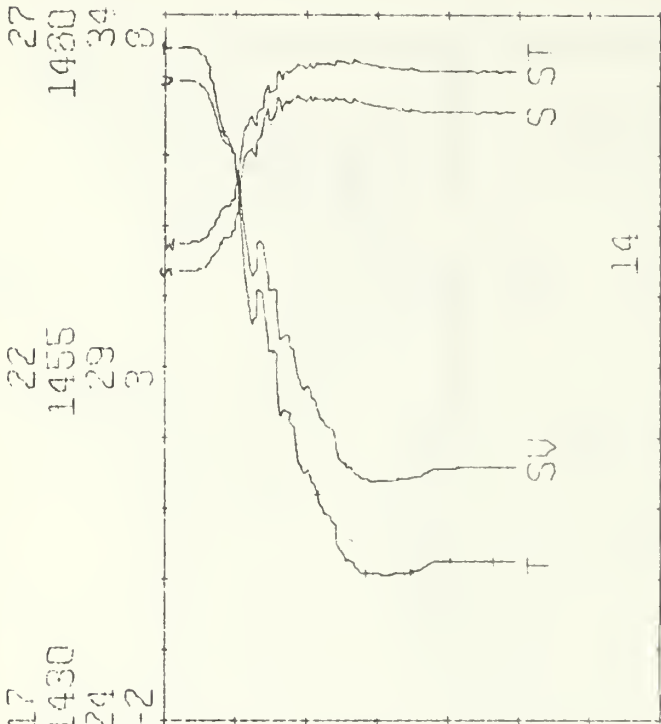
MG/CC
M/SEC
P.P.T.
DEG C

MIZPAC 75 CTD STATIONS



MG/CC
M/SEC
R.P.T.
DEG C

MIZPAC 75 CTD STATIONS

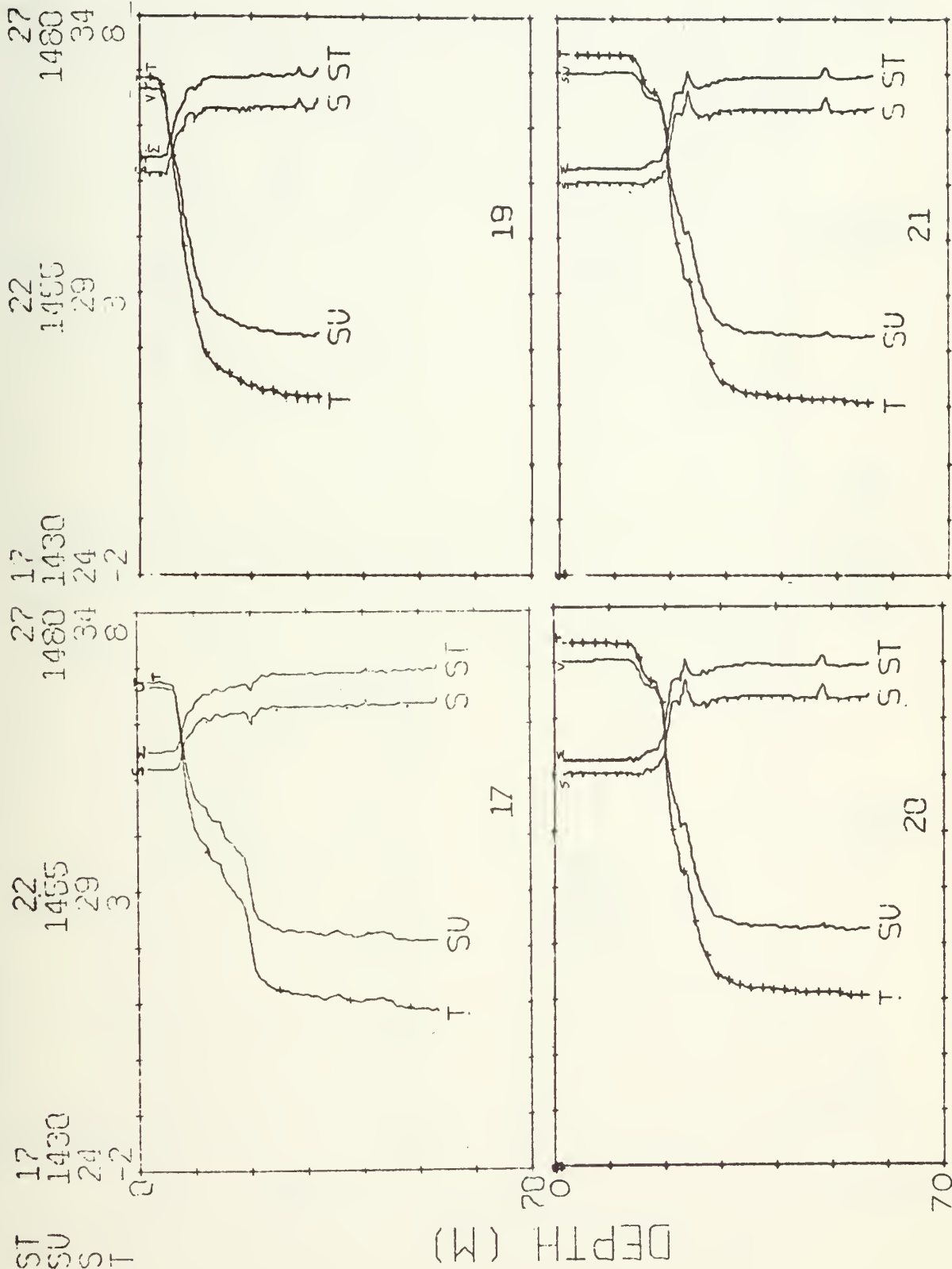


ST
SU
T

DEPTH (M)

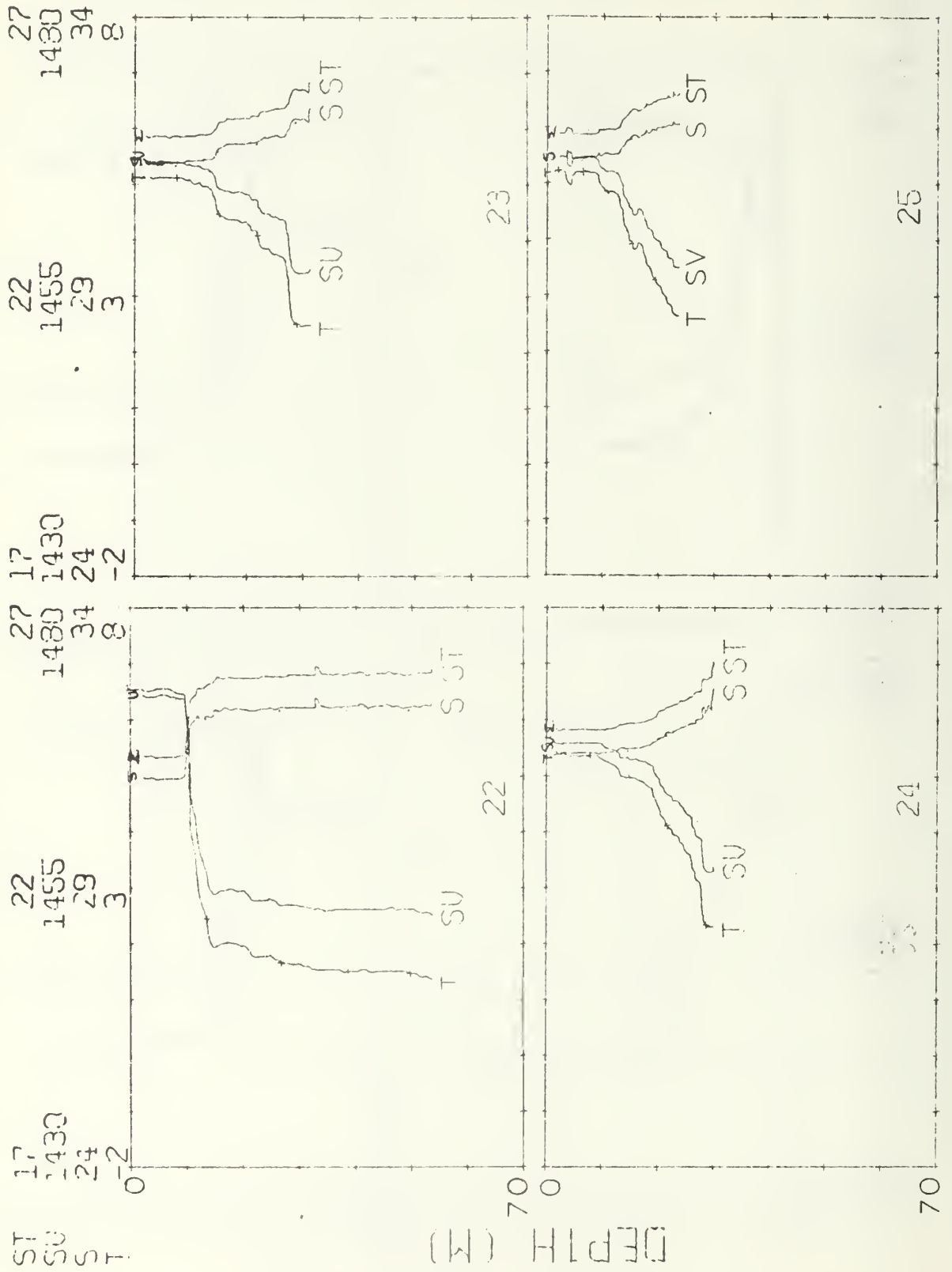
MG/CC
M/SEC
P.P.T.
DEG C

MIZPAC 75 CTD STATIONS



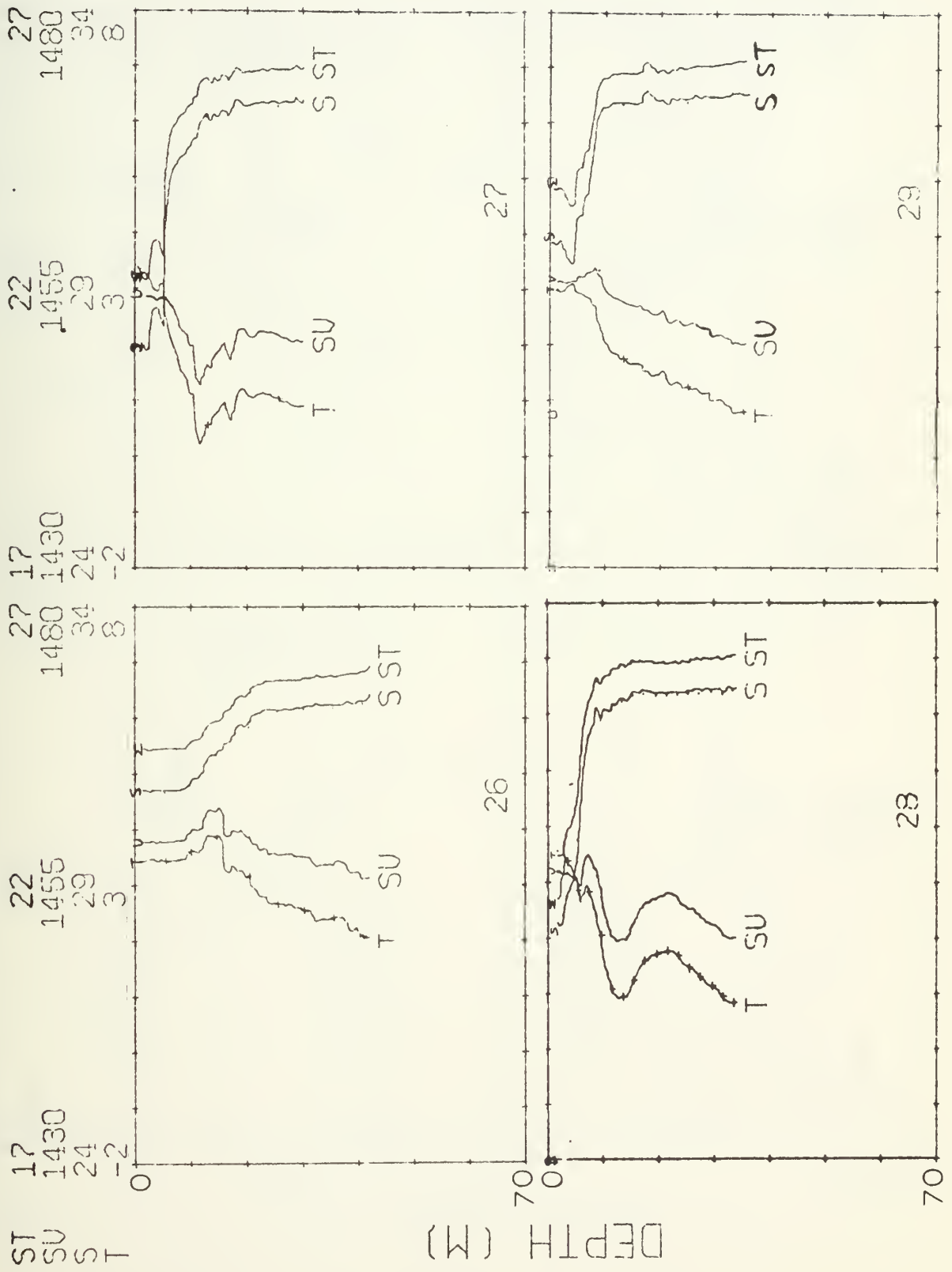
MG/CC
M/SEC
P.P.T.
DEG C

MIZPAC 75 STD STATIONS



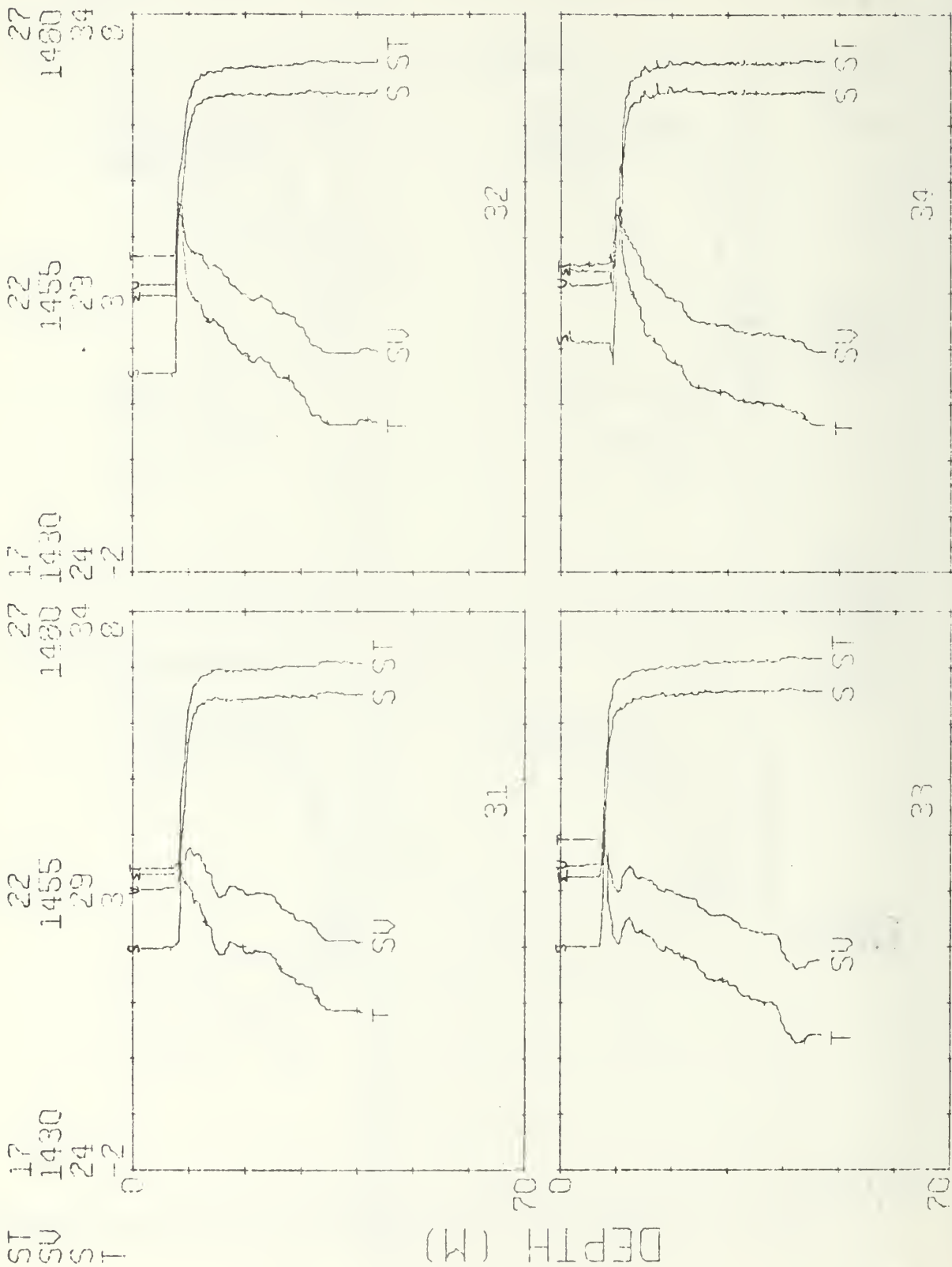
MG/CC
M/SEC
P.P.T.
DEG C

MIZPAC 75 CTD STATIONS



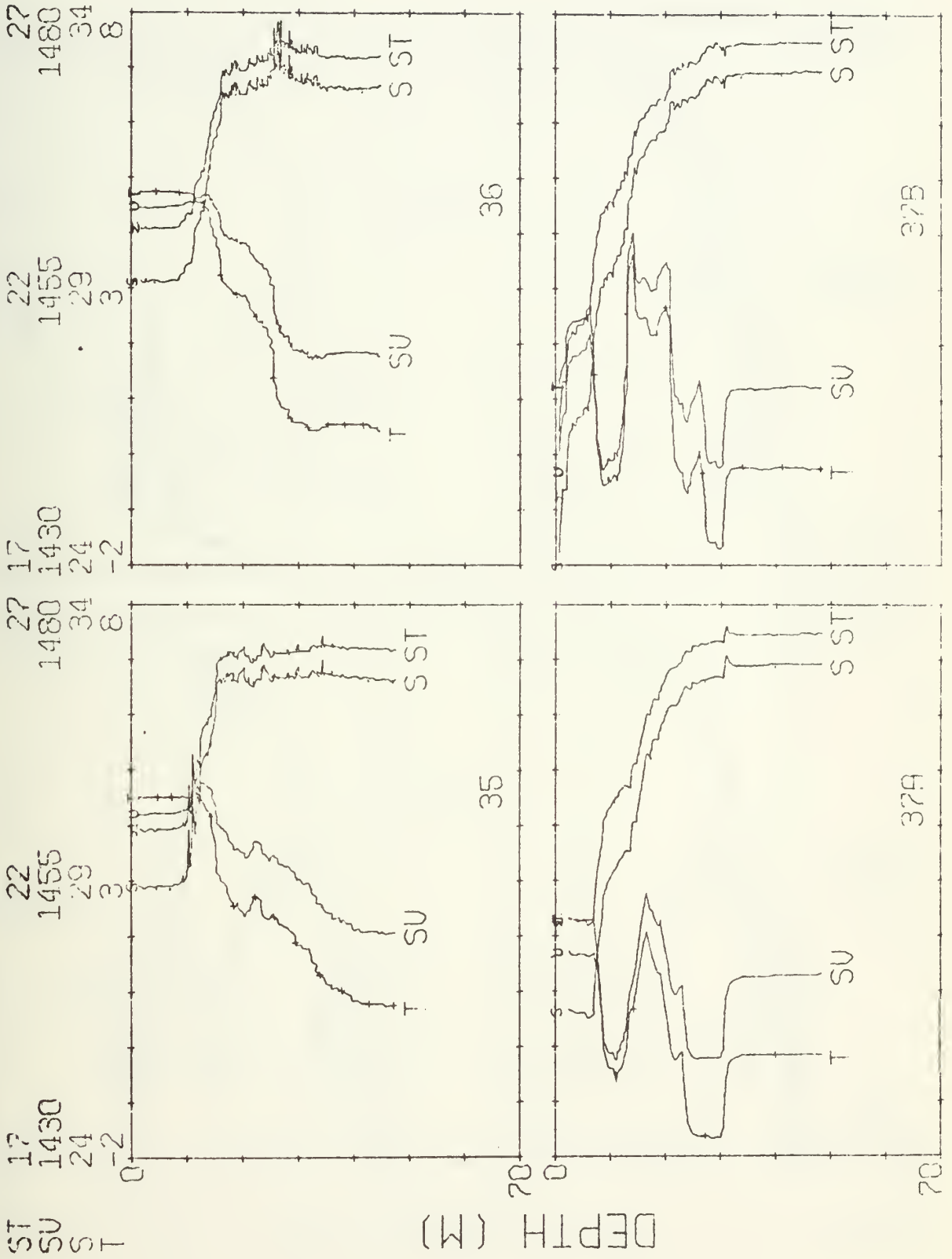
MG/CC
M/SEC
P.P.T.
DEC. C

MIZPAC 75 CTD STATIONS



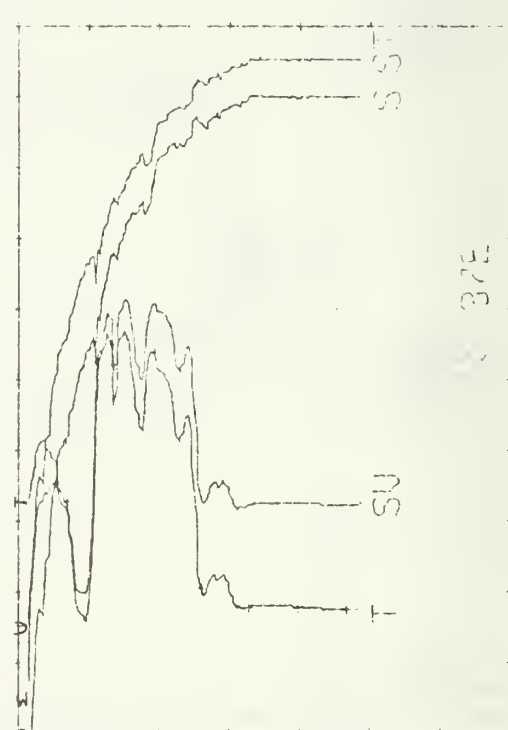
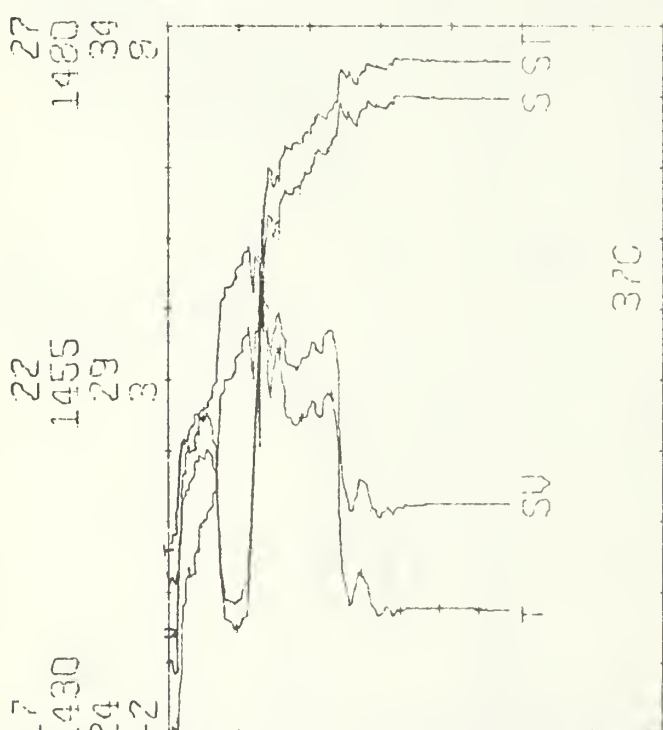
MG/CC
M/SEC
P.P.T.
DEG C

MIZPAC 75 CTD STATIONS



MG/CC
M-SEC
P.P.T.
DEC. C

MIZPAC 75 CTD STATIONS

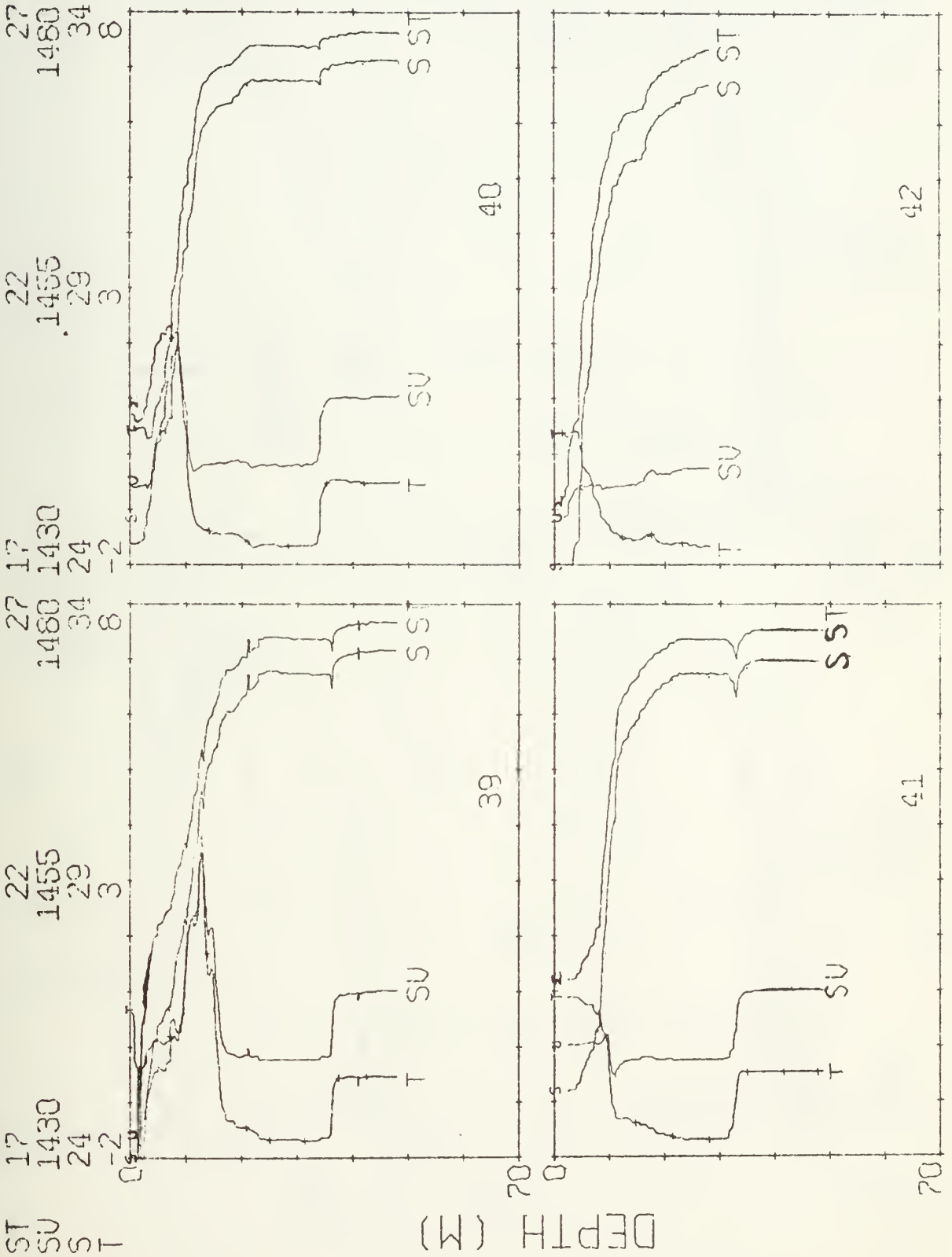


ST
SU
S
T

DEPTH (M)

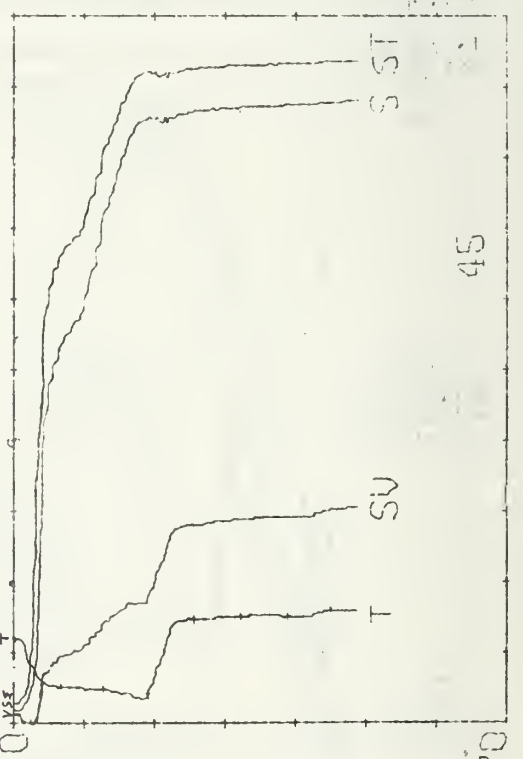
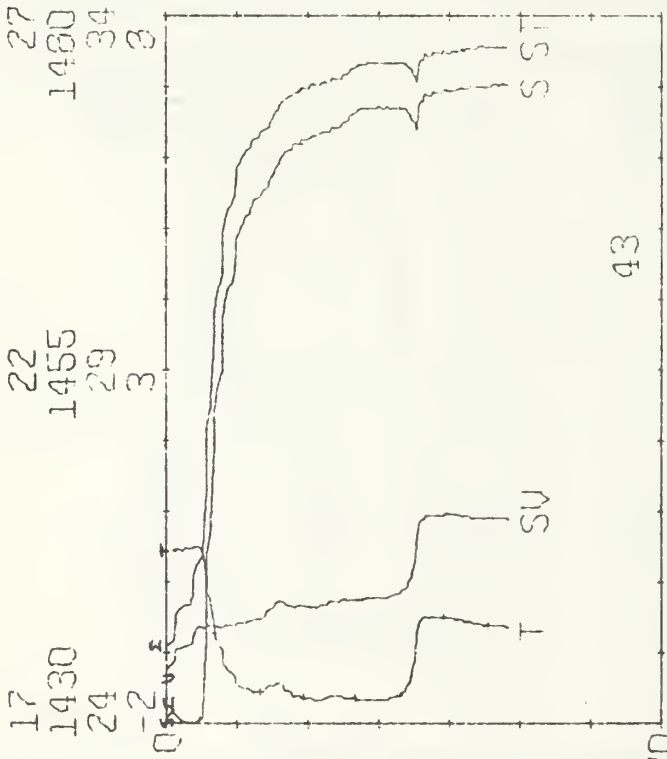
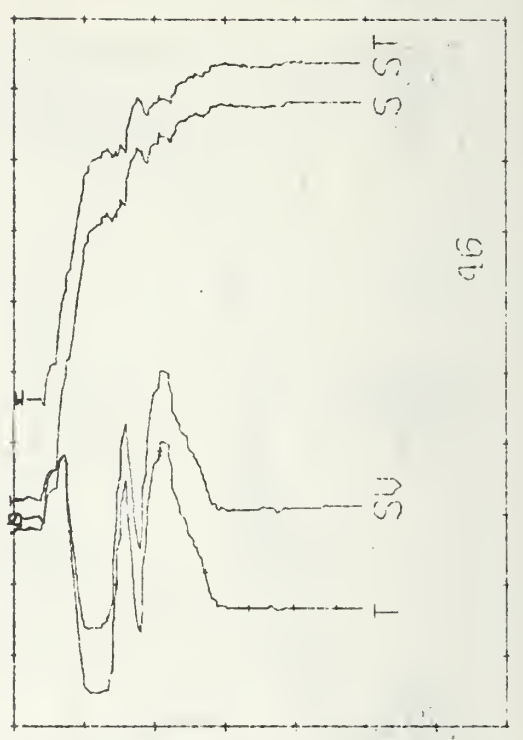
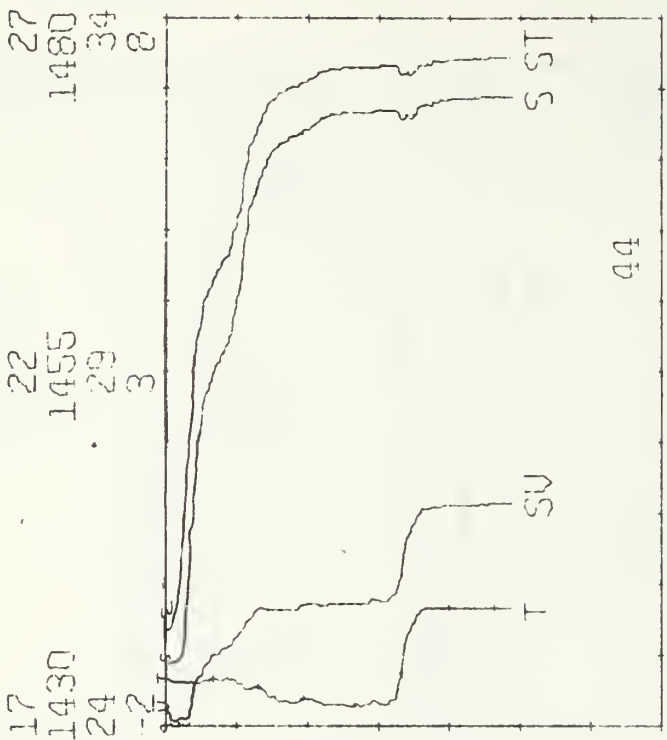
MG/CC
M/SEC
P.P.T.
DEC C

MIZPAC 75 CTD STATIONS



MG/CC
M/SEC
P.P.T.
DEG C

MIZPAC 75 CTD STATIONS

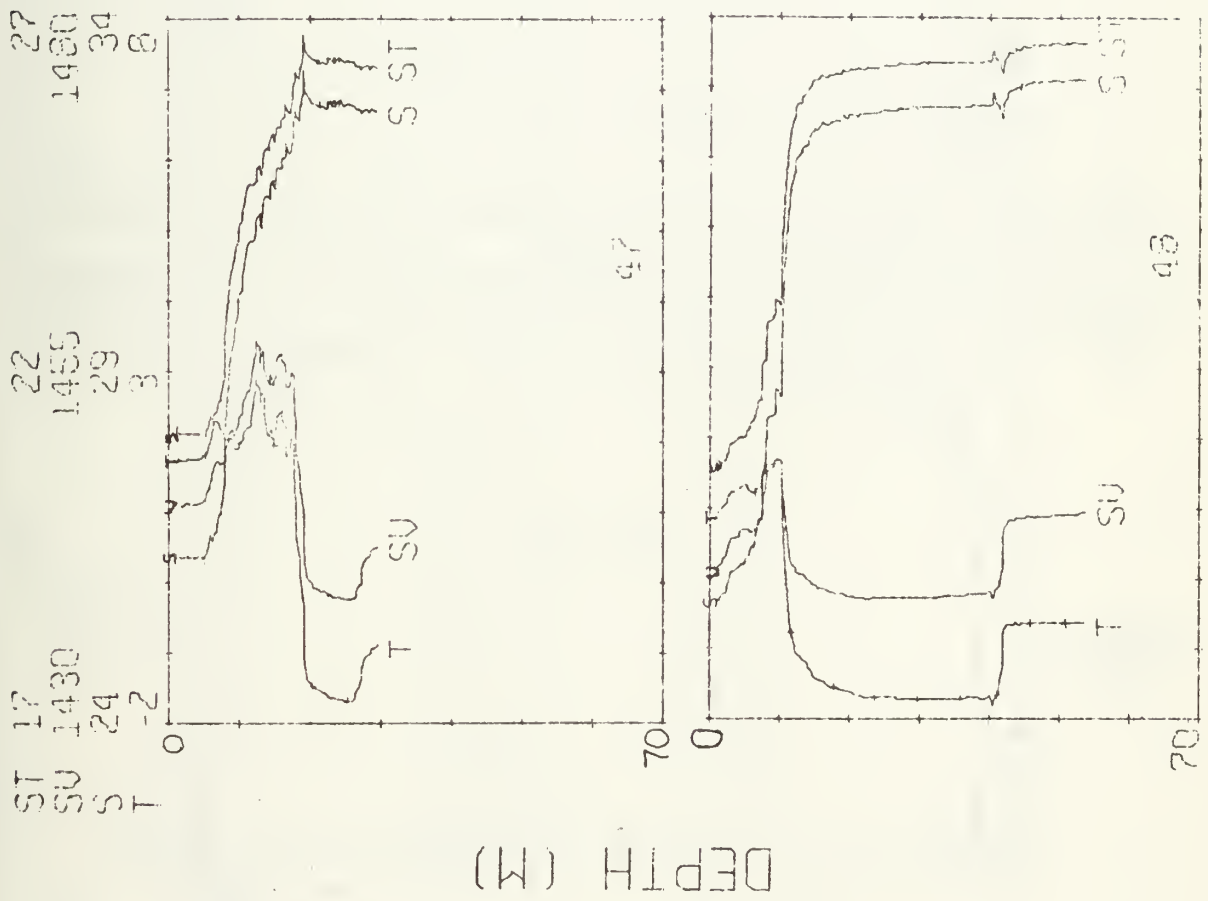


ST
SU
T

DEPTH (M)

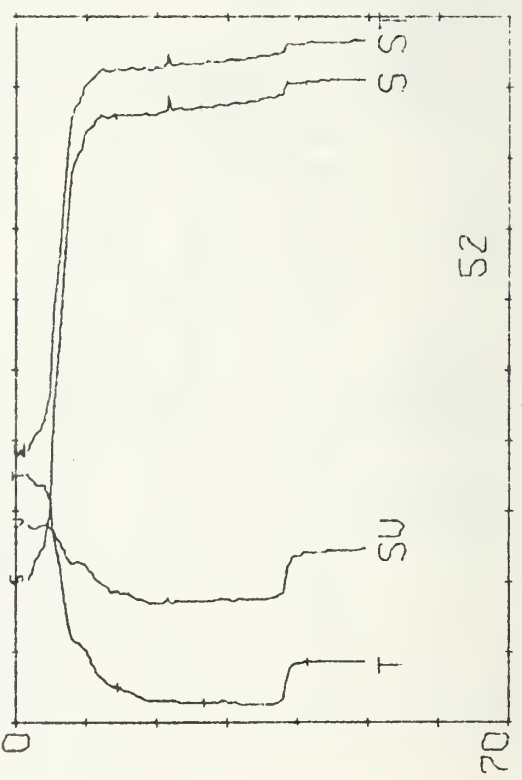
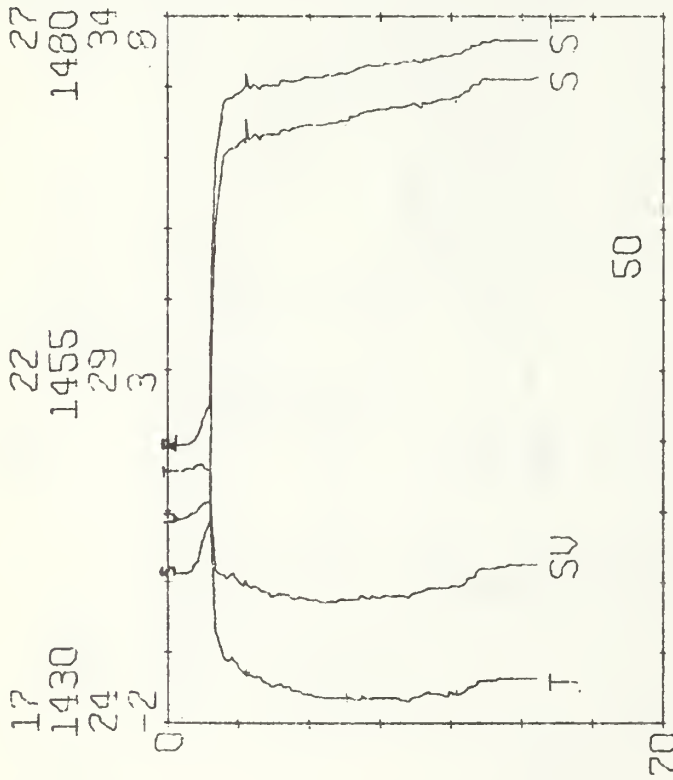
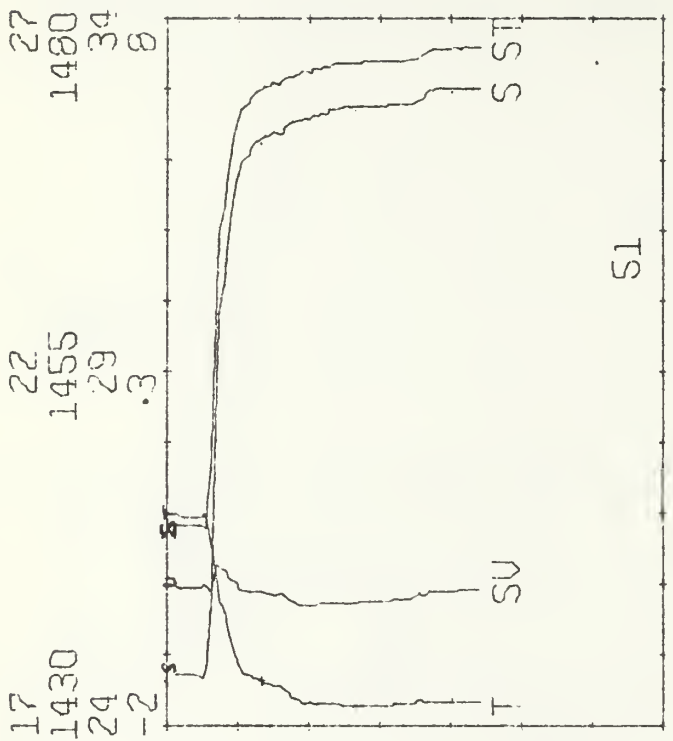
MIZPAC 75 CTD STATIONS

MG/GC
 M-SEC
 P.P.T.
 DEG C



MG/GC
M/SEC
P.P.T.
DEG C

MIZPAC 75 CTD STATIONS

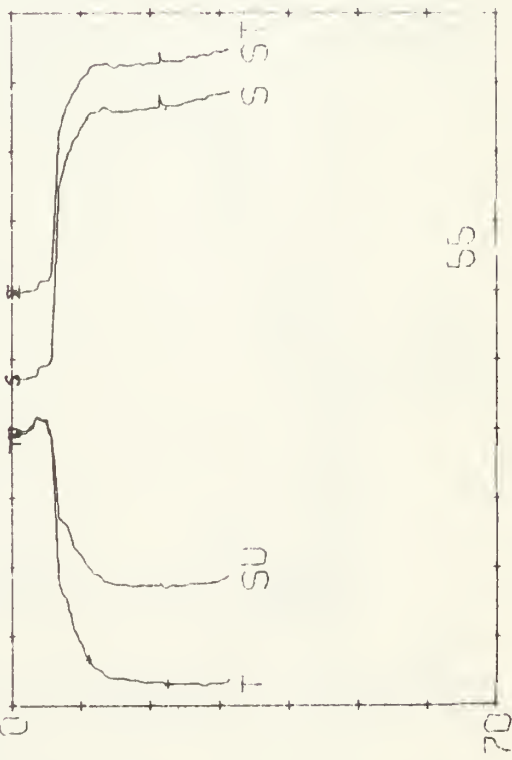
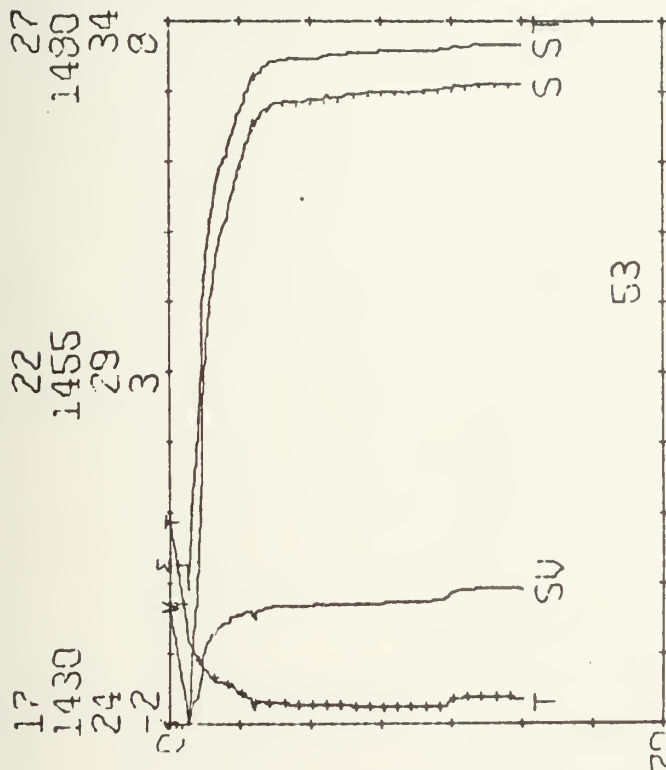
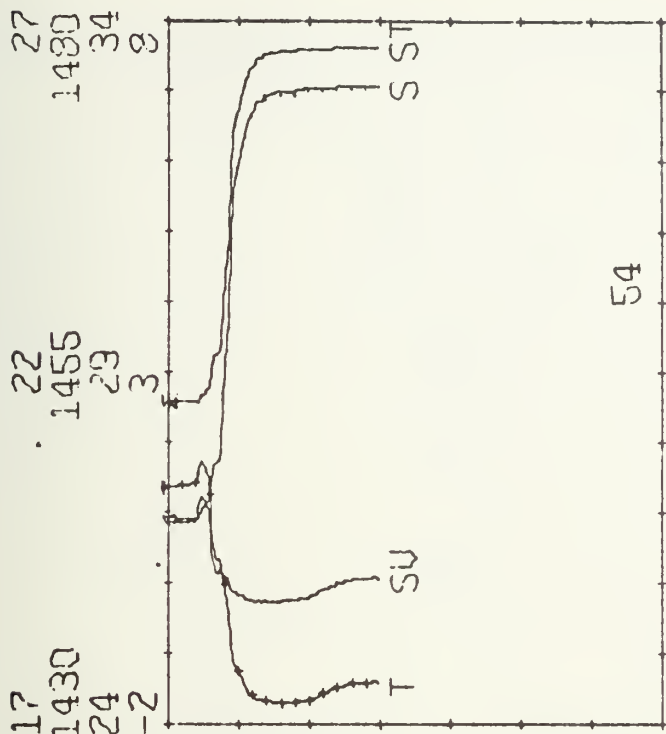


ST
SU
S
T

DEPTH (M)

MG/CC
M/SEC
P.P.T
DEG C

MIZPAC 75 STD STATIONS

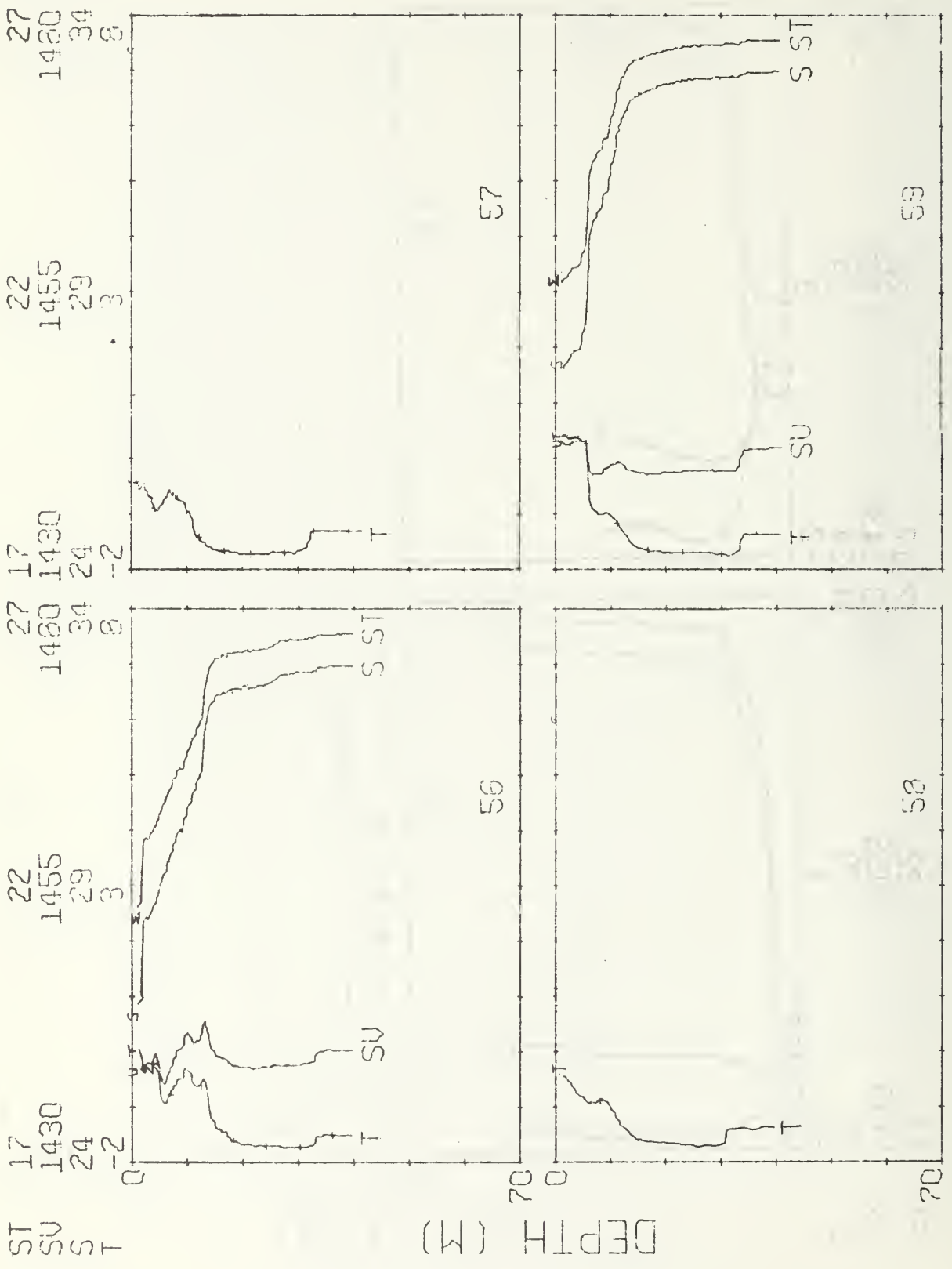


ST
SU
S
T

DEPTH (M)

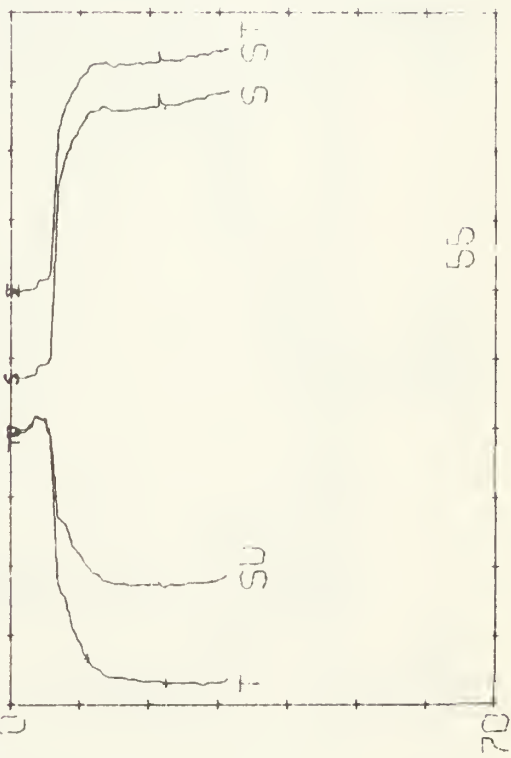
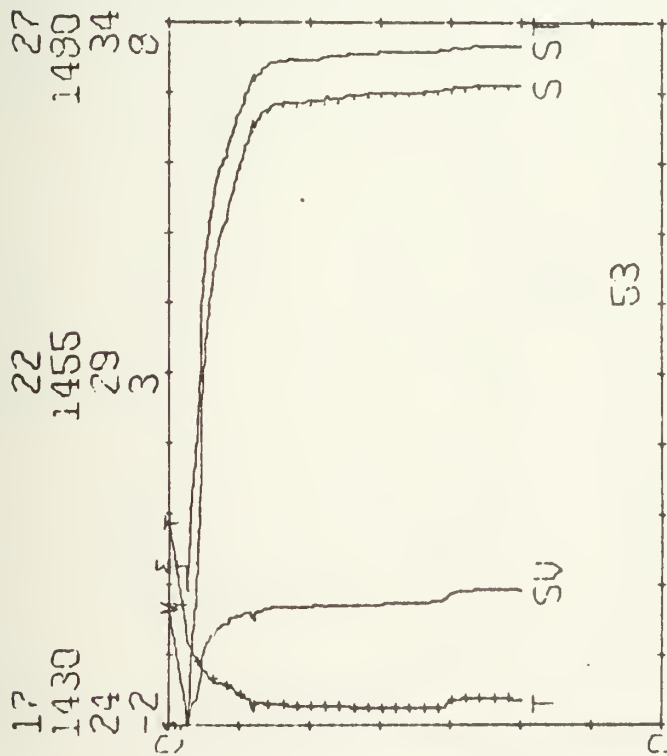
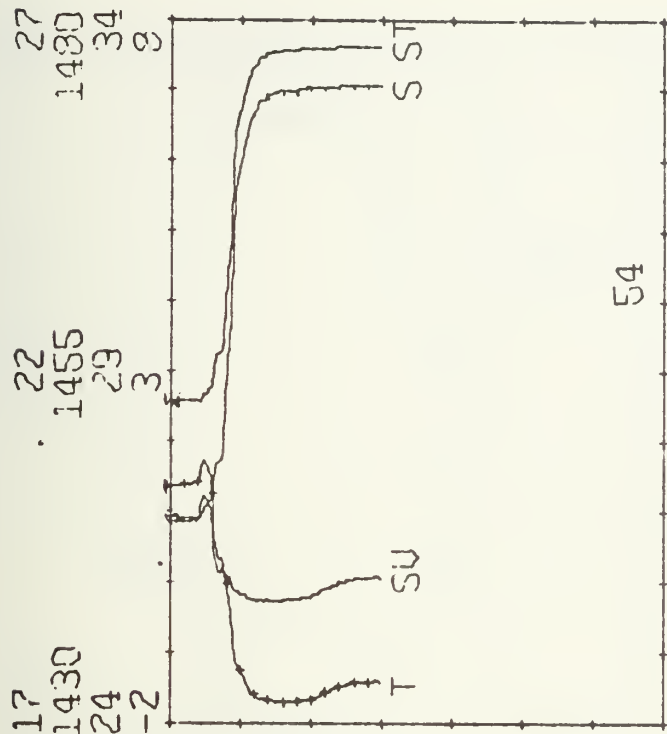
MG/CC
 M/SEC
 P.P.T.
 DEG C

MIZPAC 75 CTD STATIONS



MG/CC
M/SEC
P.P.T
DEG C

MIZPAC 75 STD STATIONS

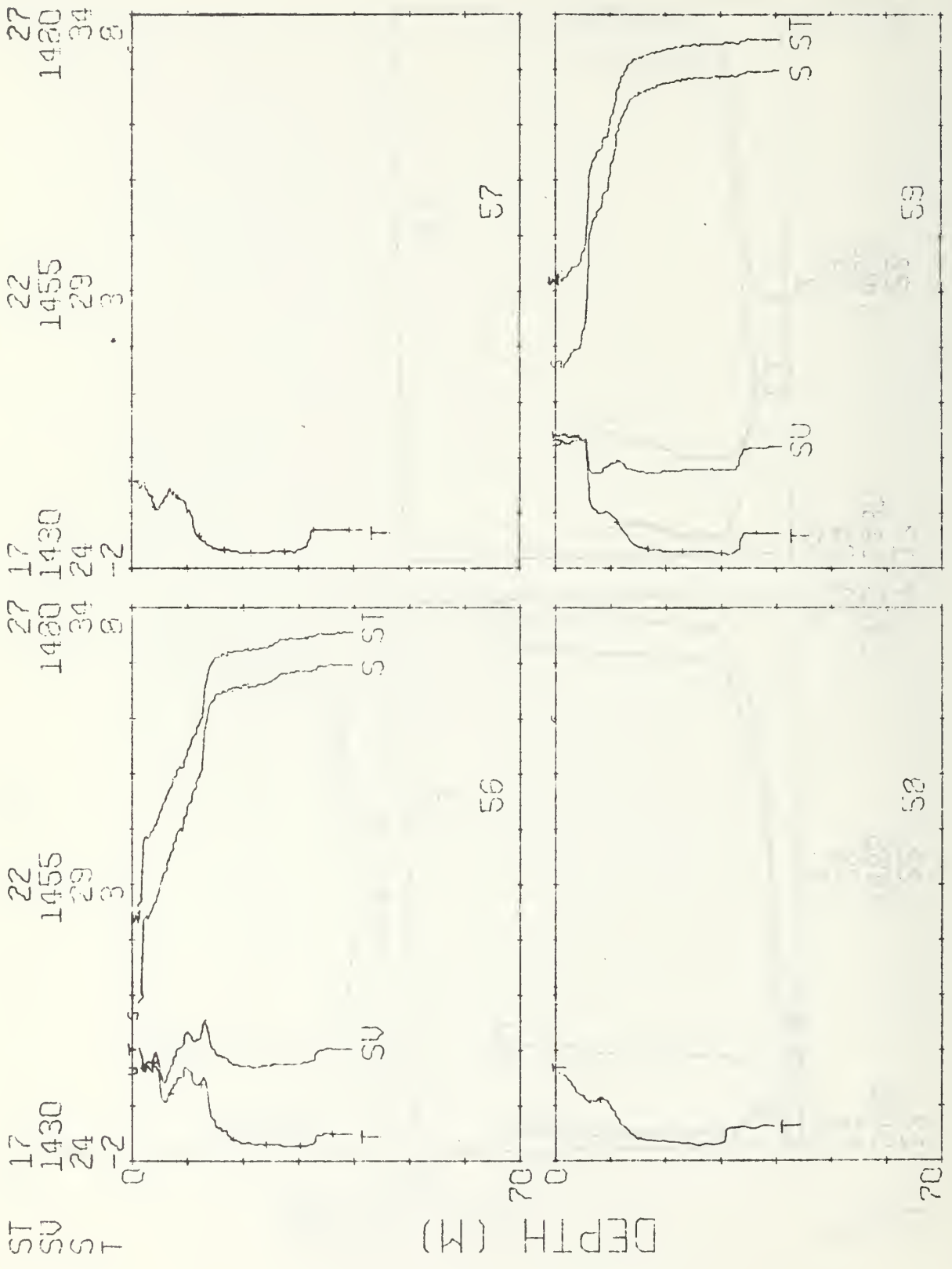


ST
SU
S
T

DEPTH (M)

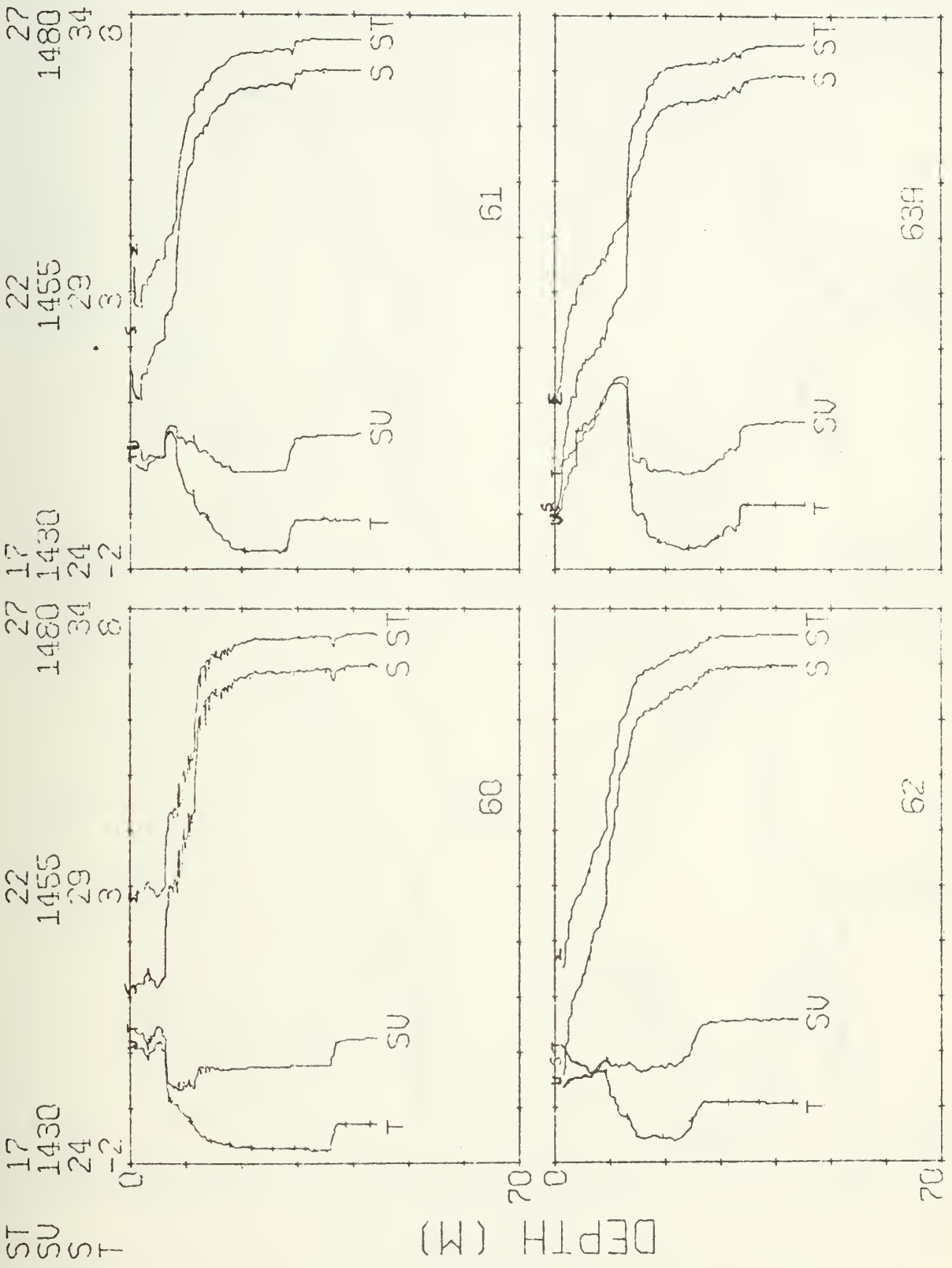
MS/CC
 M/SEC
 R.P.T.
 DEG C

MIZPAC 75 CTD STATIONS



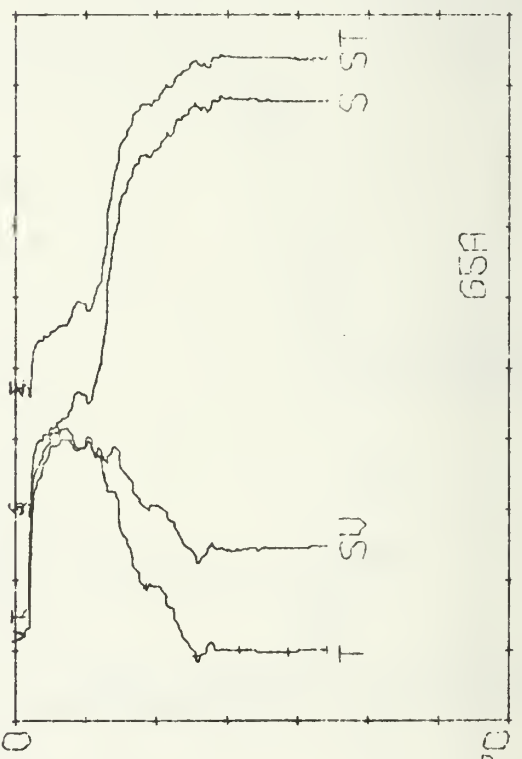
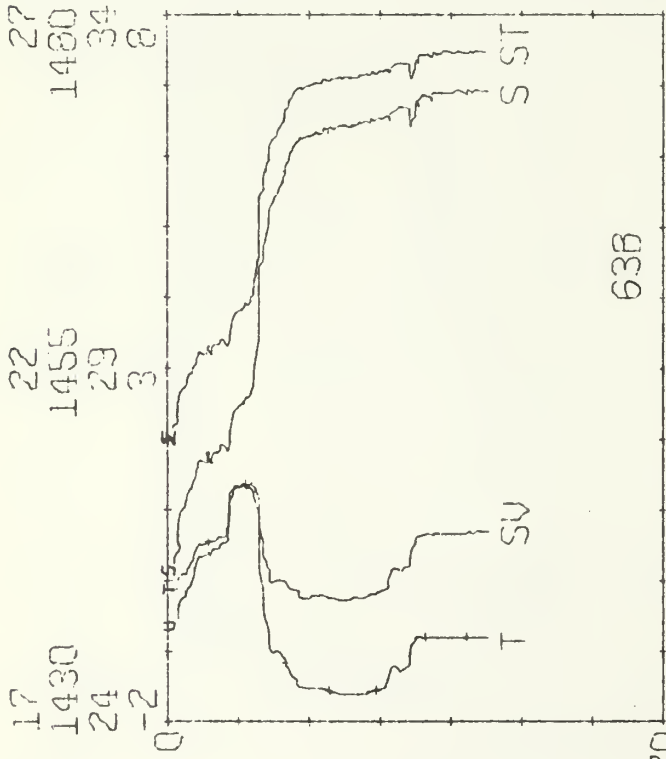
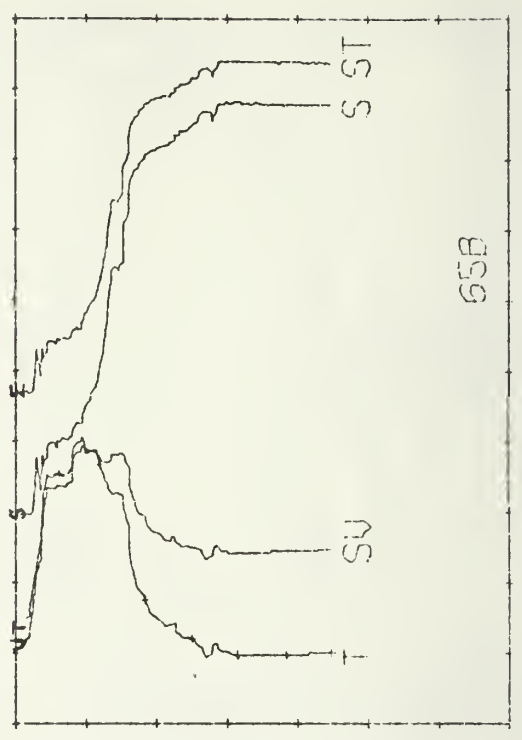
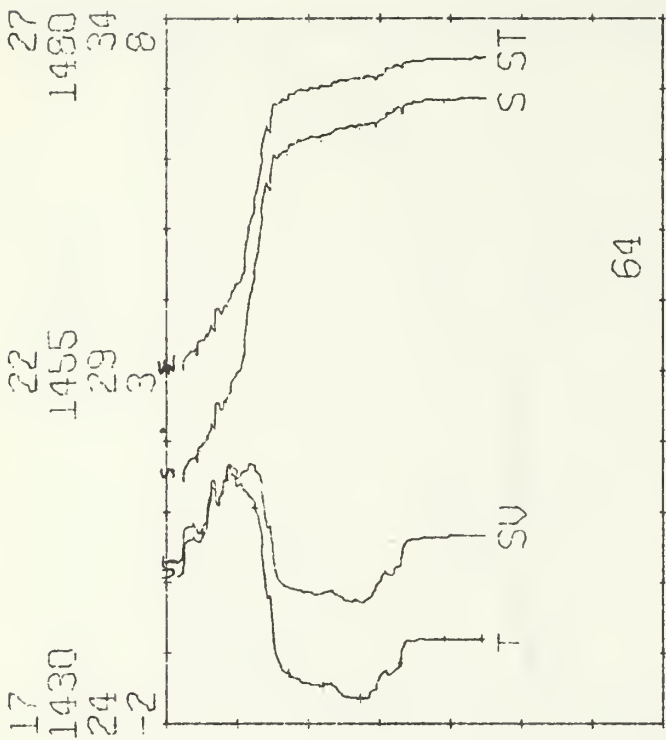
MG/CC
M/SEC
P.P.T.
DEG C

MIZPAC 75 CTD STATIONS



MG/CC
M/SEC
P.P.T.
DEG C

MIZPAC 75 CTD STATIONS

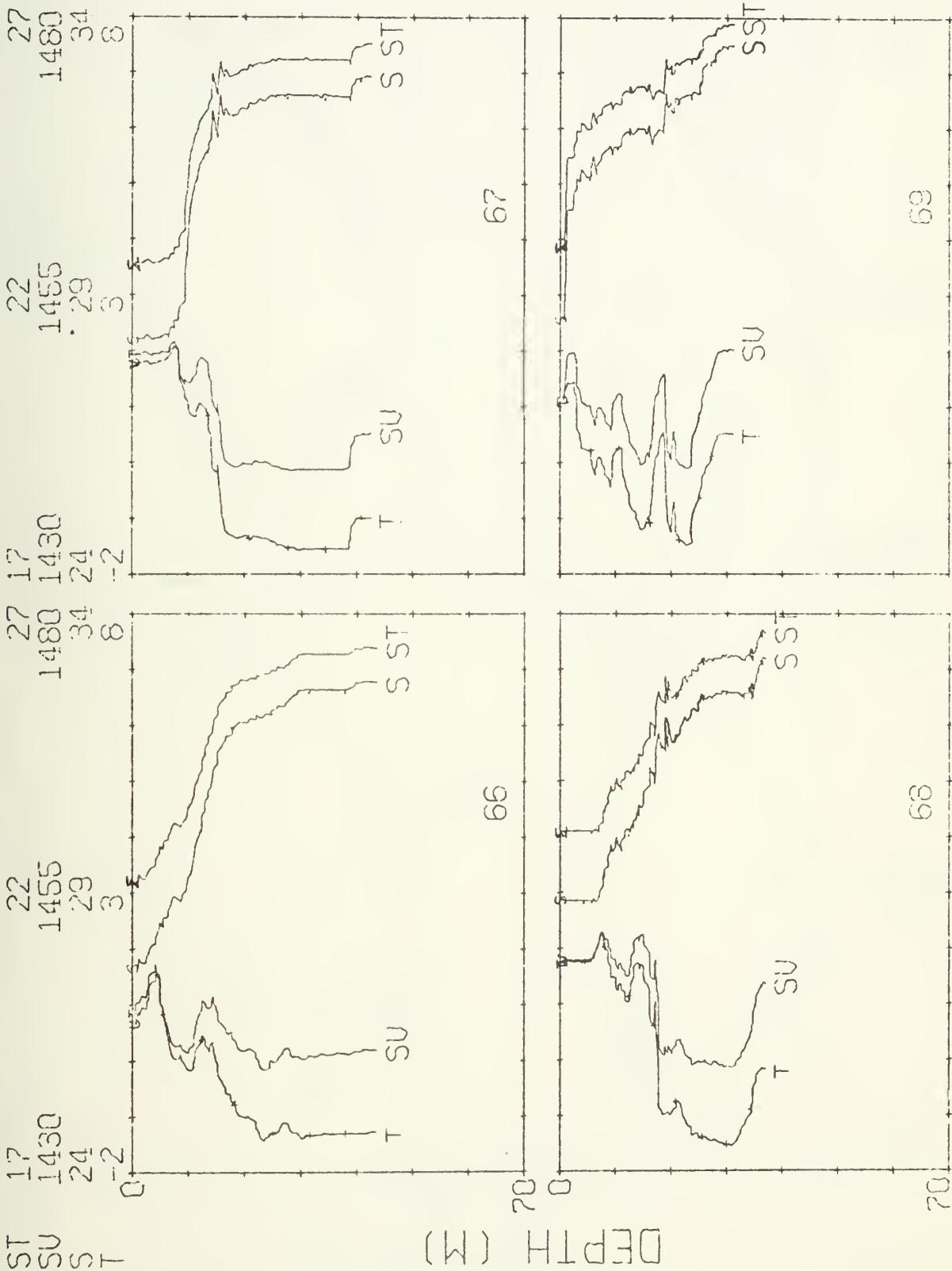


ST
SU
T

DEPTH (M)

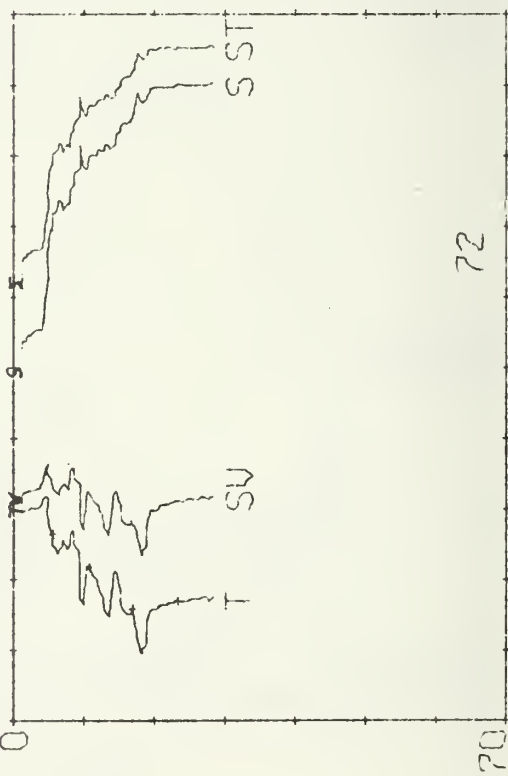
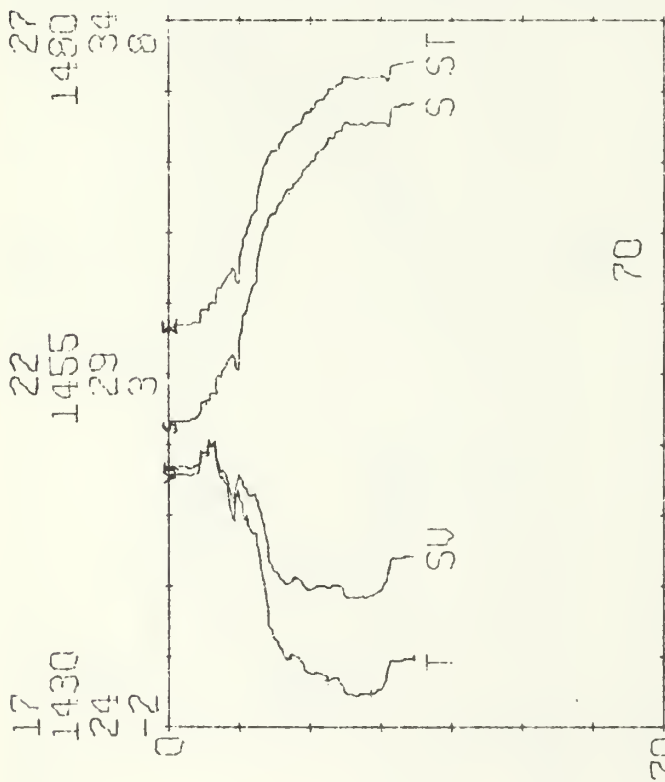
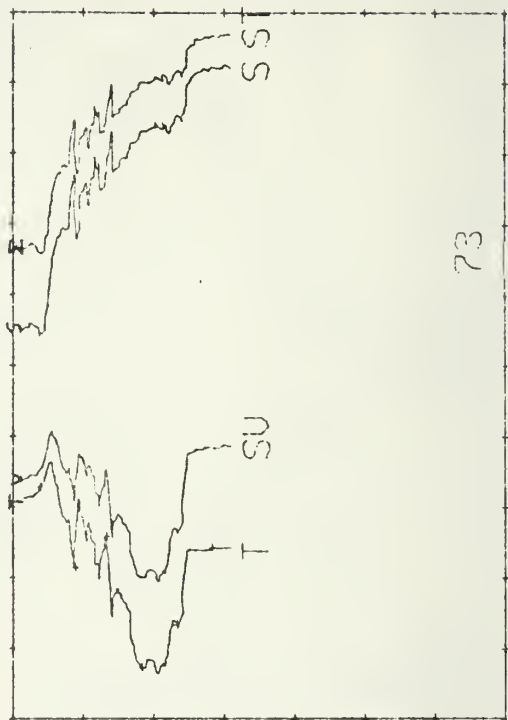
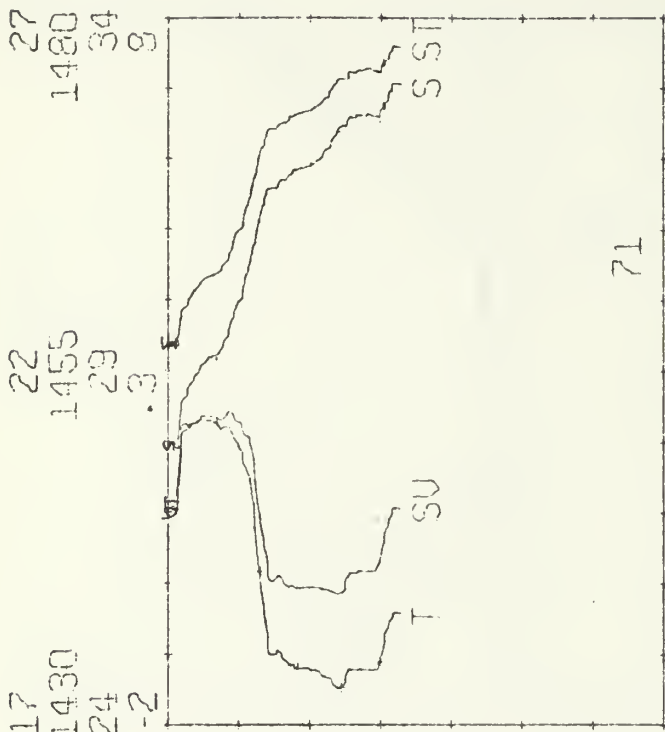
MG/CC
M/SEC
P.F.T.
DEG C

MIZPAC 75 CTD STATIONS



MG-00
M/SEC
P.P.T.
DEG C

MIZPAC 75 CTD STATIONS

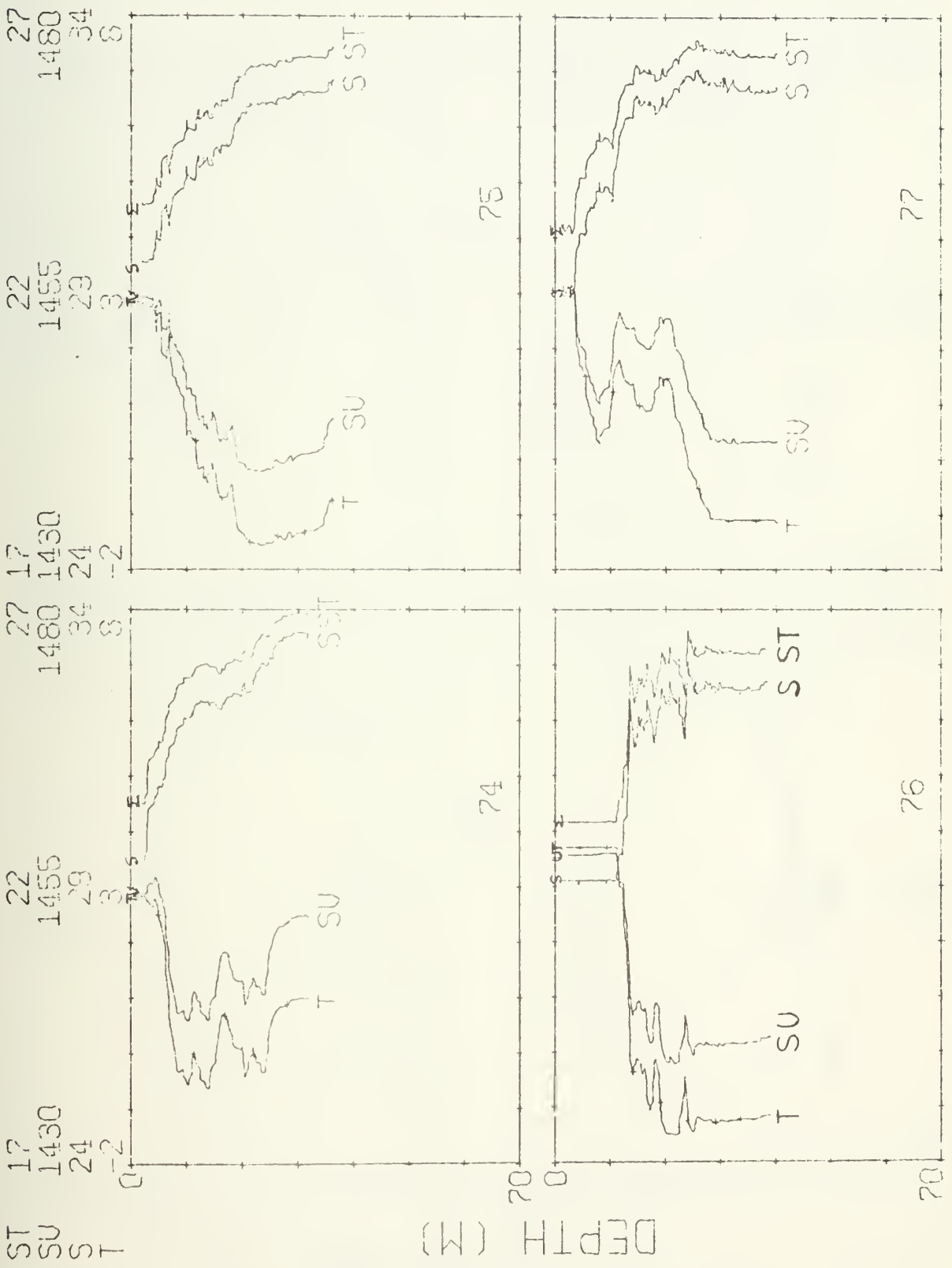


ST
SU
T

DEPTH (M)

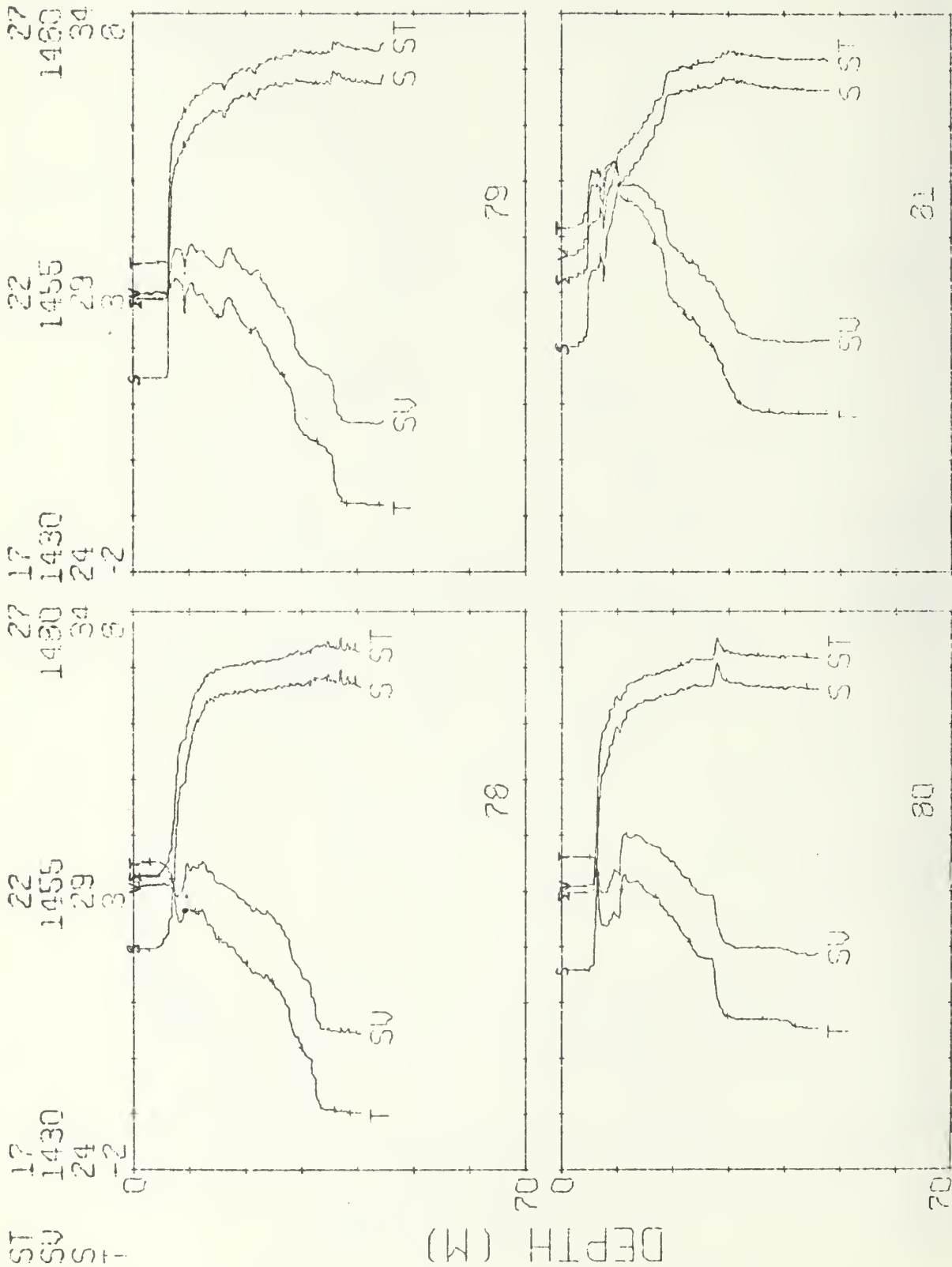
MG/CC
M/SEC
P.P.T.
DEG C

MIZPAC 75 CTD STATIONS



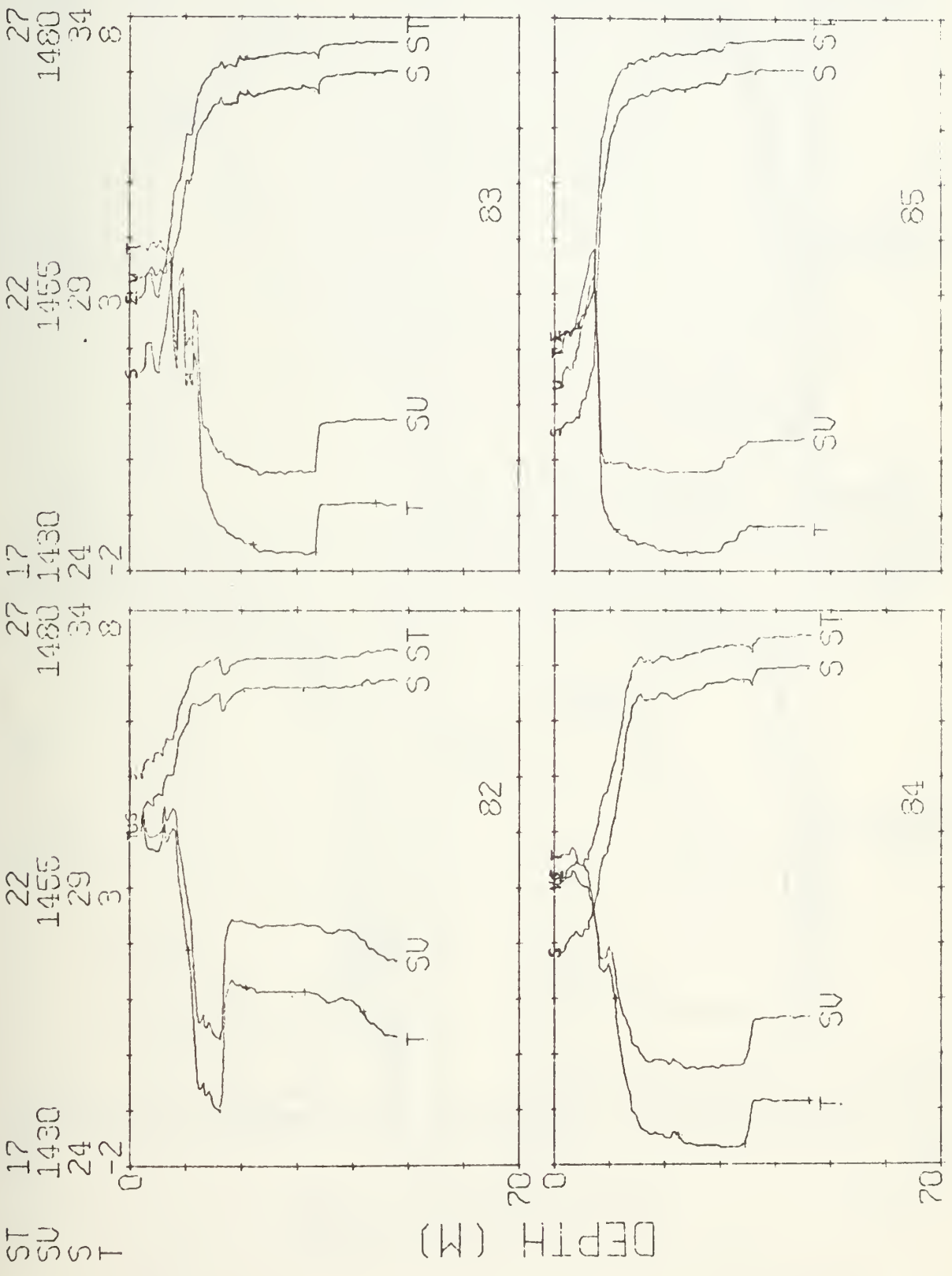
MG/CC
 M/SEC
 P.P.T.
 DEG C

MIZPAC 75 CTD STATIONS



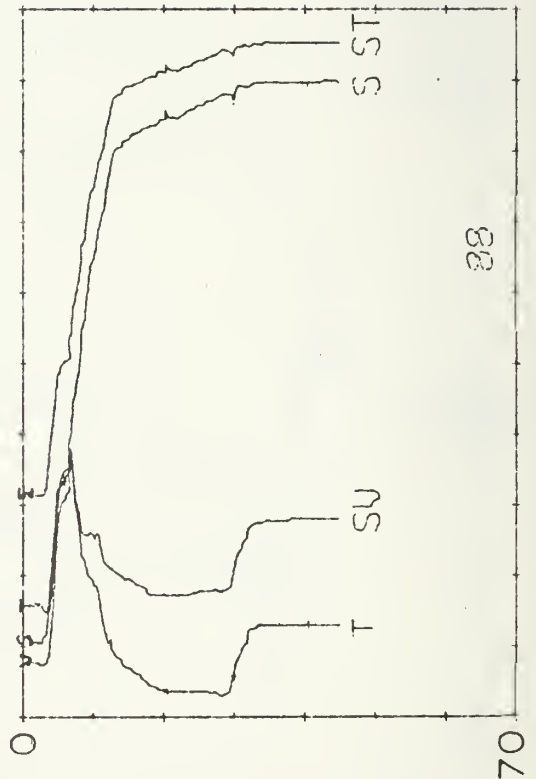
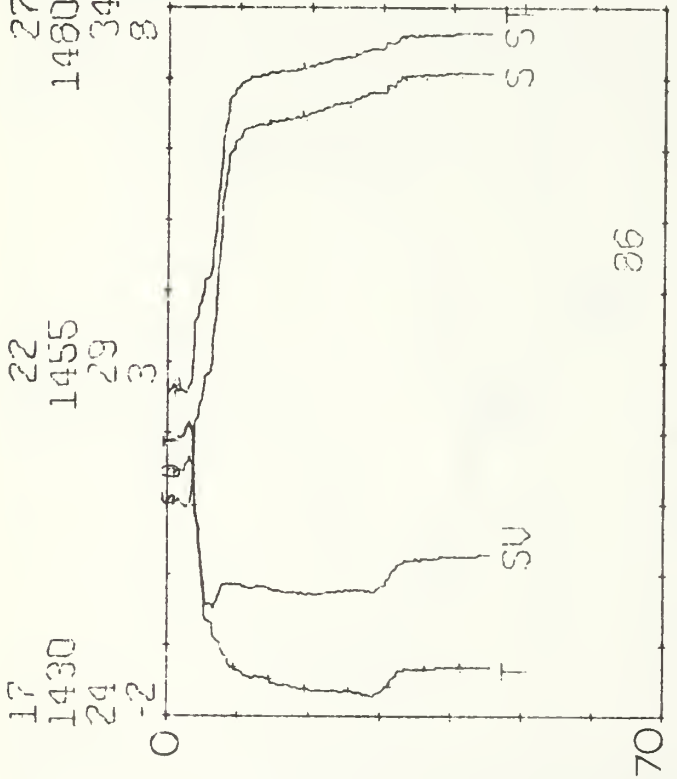
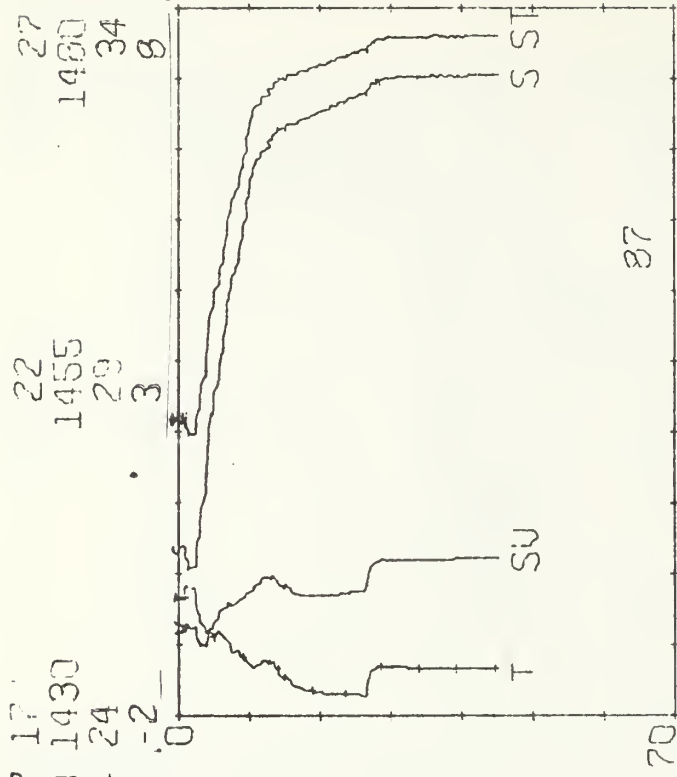
MG/CC
M/SEC
P.P.T.
DEG C

MIZPAC 75 CTD STATIONS



MIZPAC 75 CTD STATIONS

HG/CG 27
 M/SEC 1480
 P.P.T. 34
 DEG C 8



DEPTH (M)

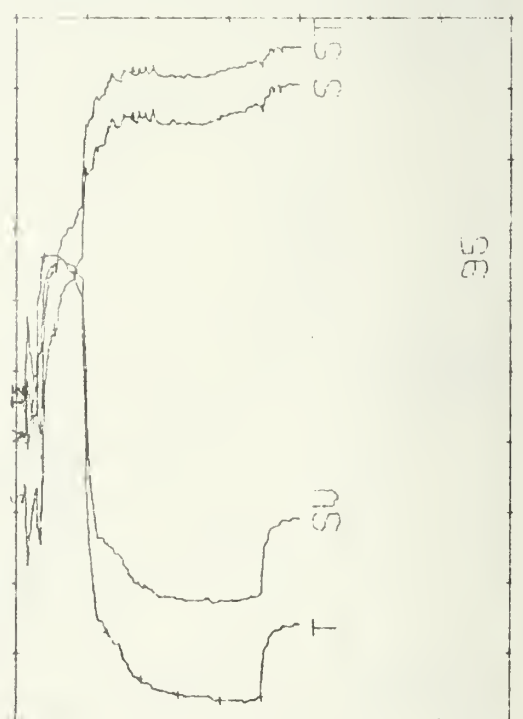
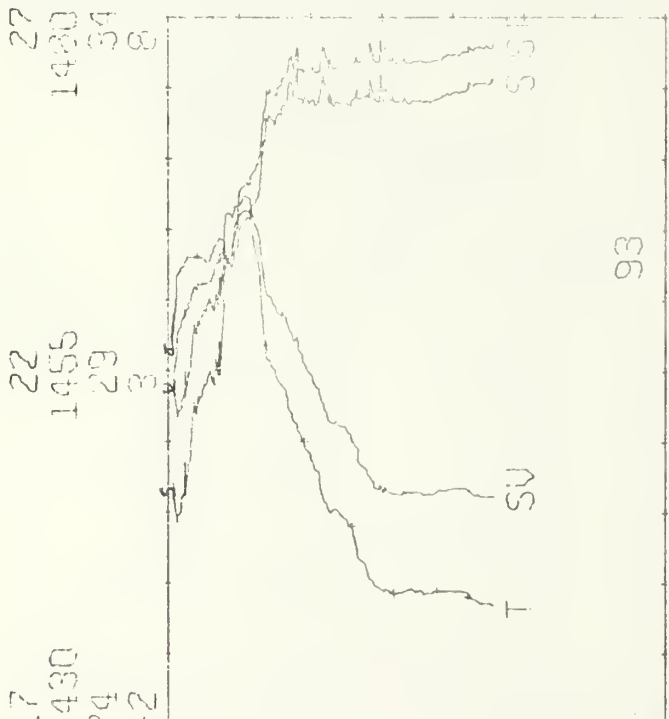
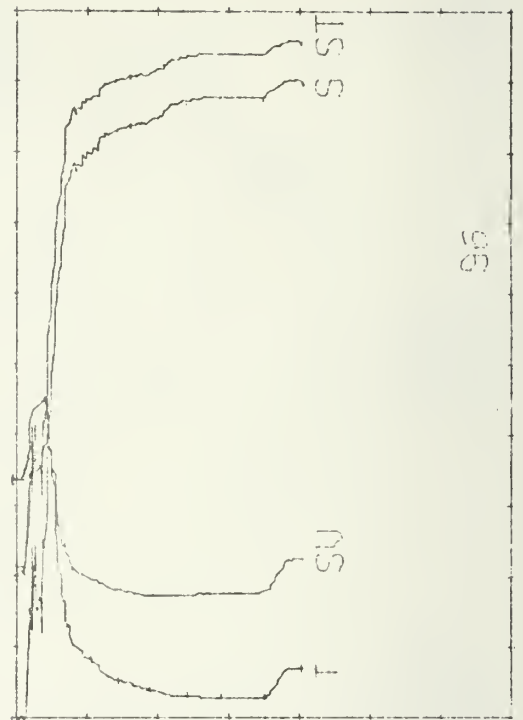
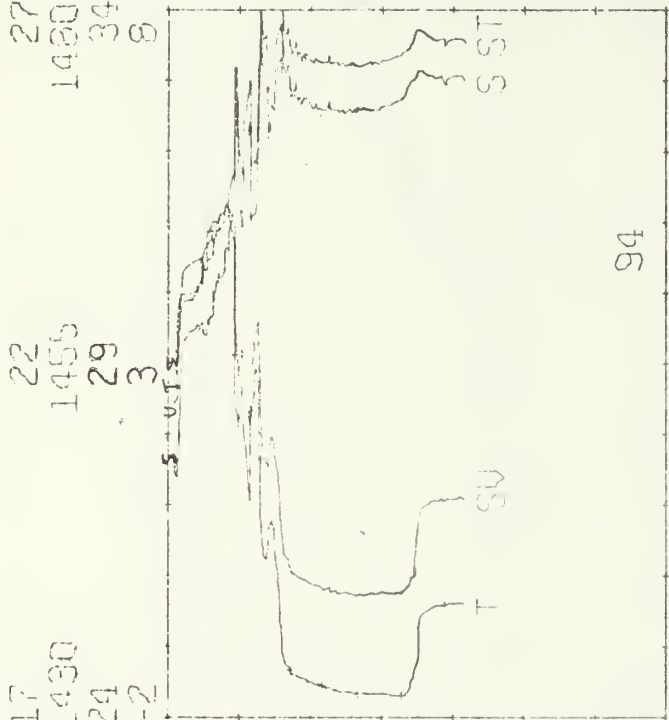
MG/CC
M/SEC
P.P.T.
DEG C

MIZPAC 75 CTD STATIONS



MG/CC 27
 M/SFC 1480
 P.S.T. 34
 DEG C 8

MIZPAC 75 CTD STATIONS

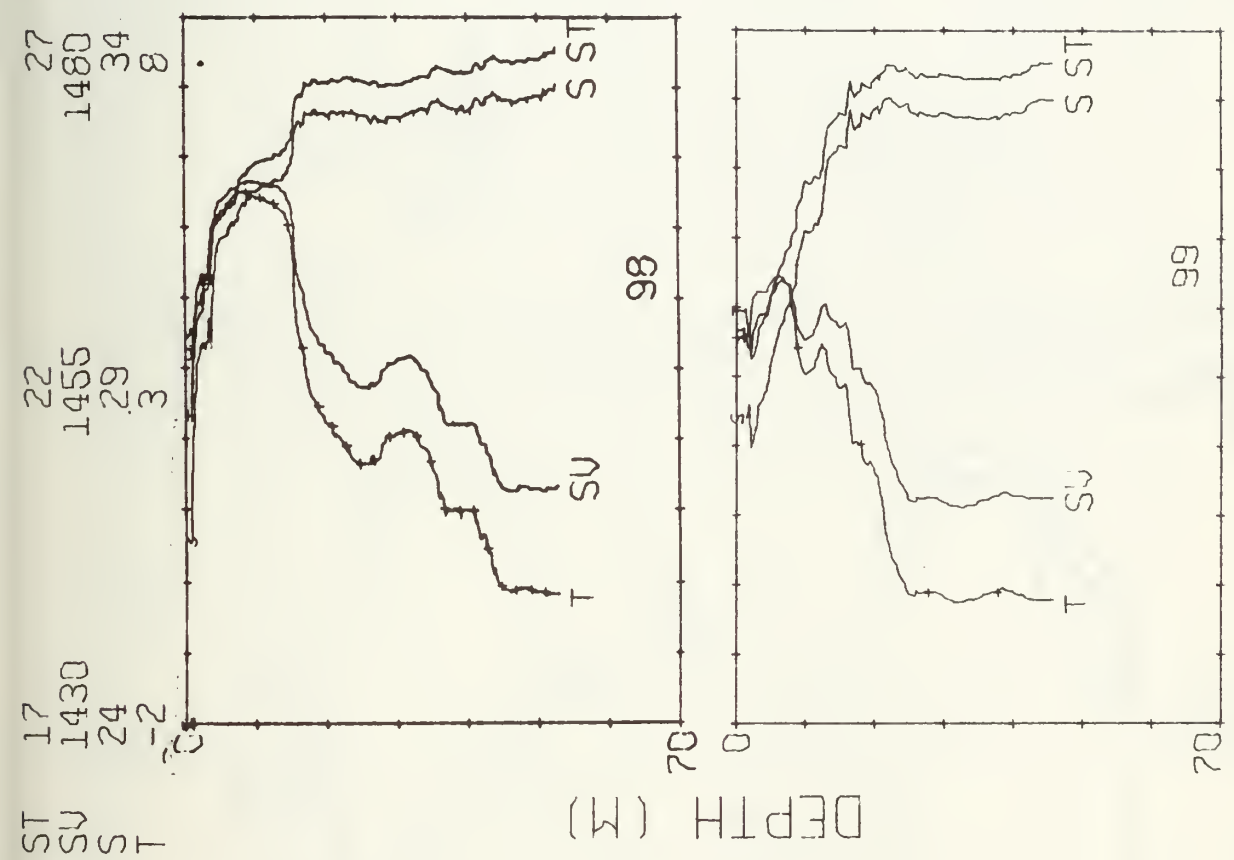


ST
 SU
 T

DEPTH (M)

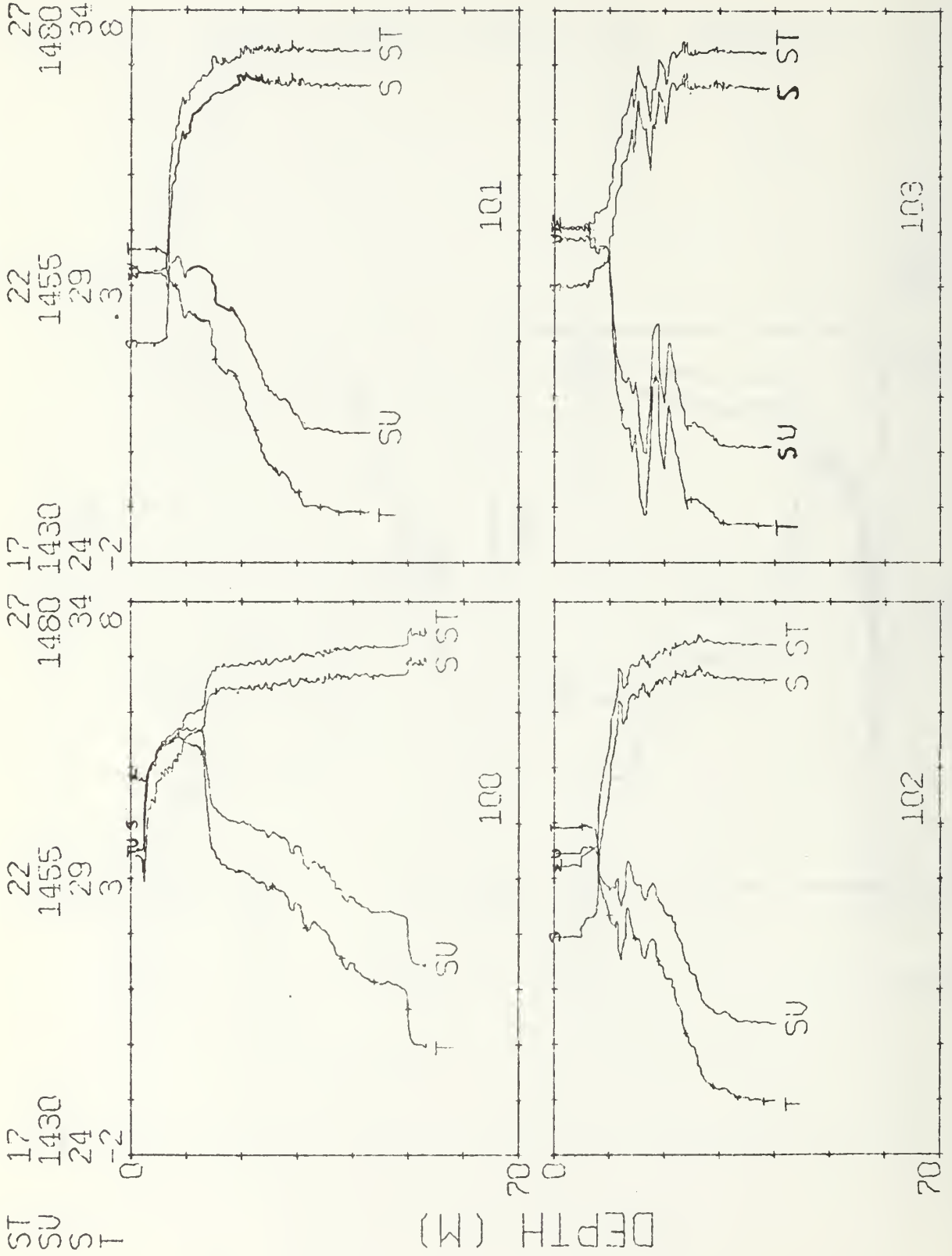
MIZPAC 75 CTD STATIONS

MG/CC
M/SEC
P.P.T.
DEG C



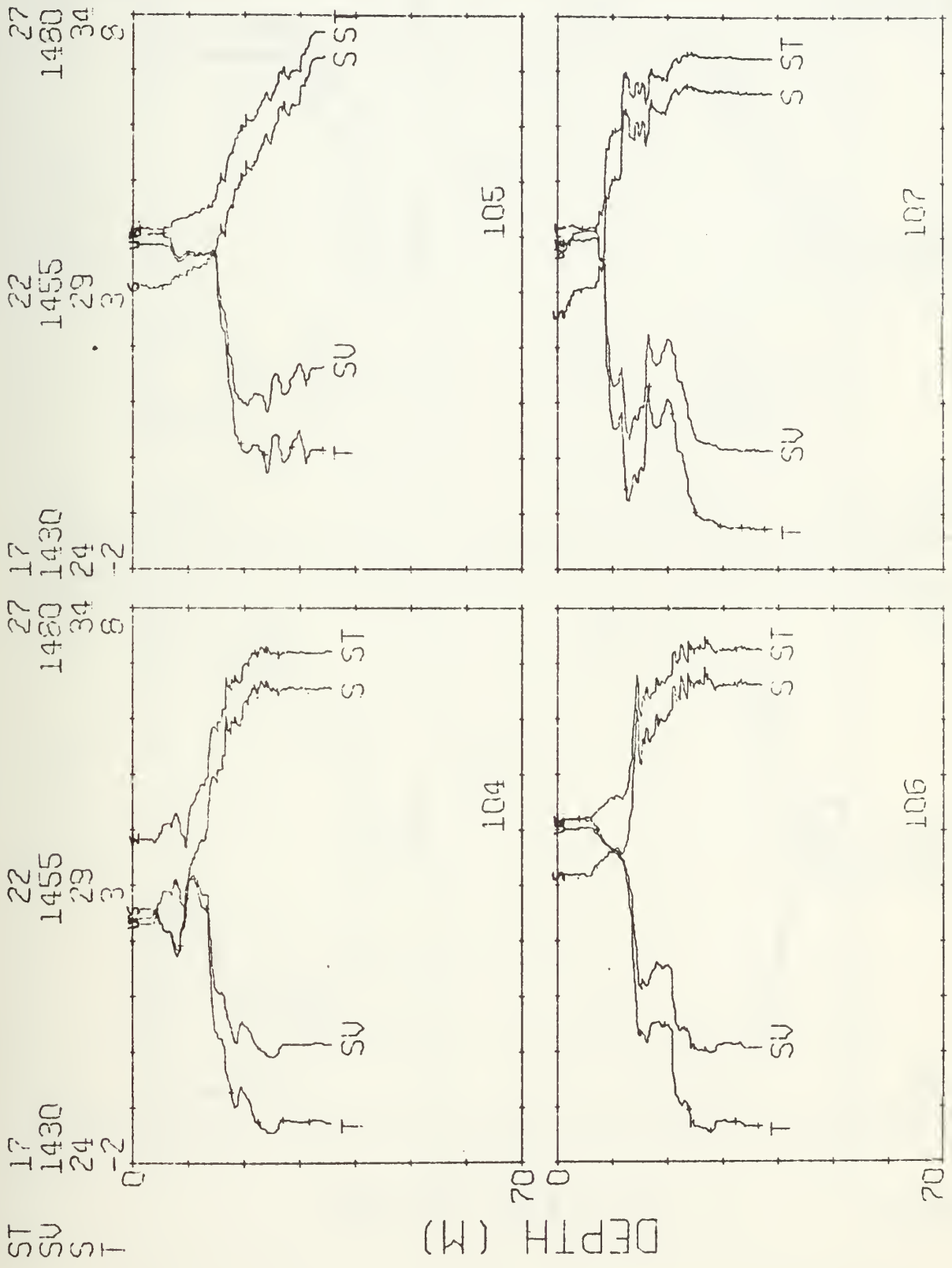
MG/GC
M/SEC
P.P.T.
DEG C

MIZPAC 75 CTD STATIONS



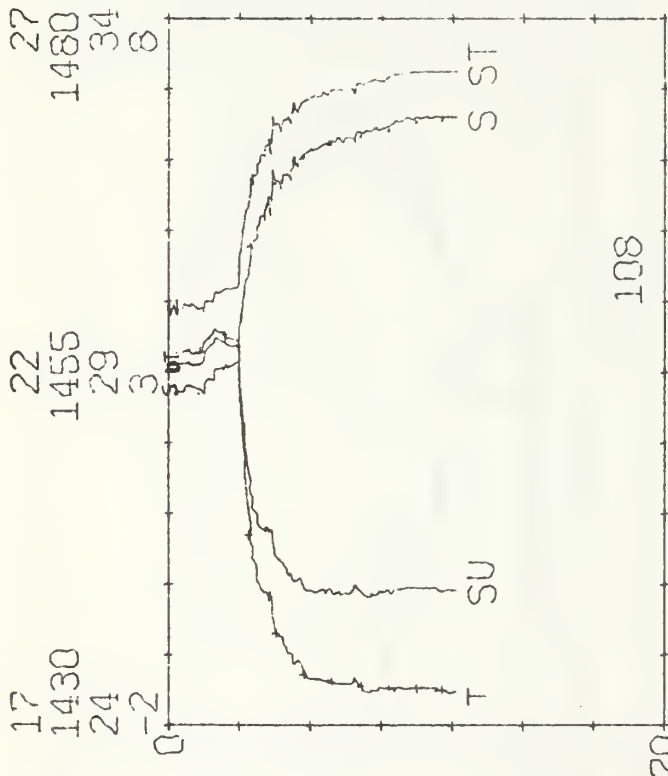
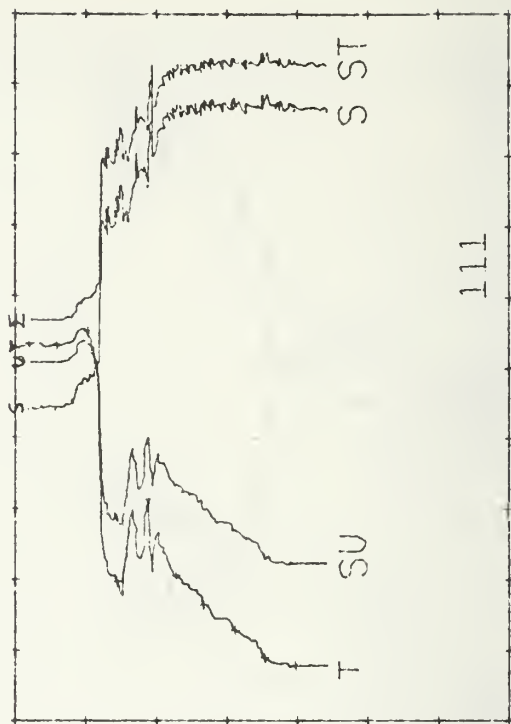
MG-CC
 M-SEC
 P.P.T.
 DEG C

MIZPAC 75 CTD STATIONS



MG/CC
M/SEC
P.P.T.
DEG C

MIZPAC 75 CTD STATIONS

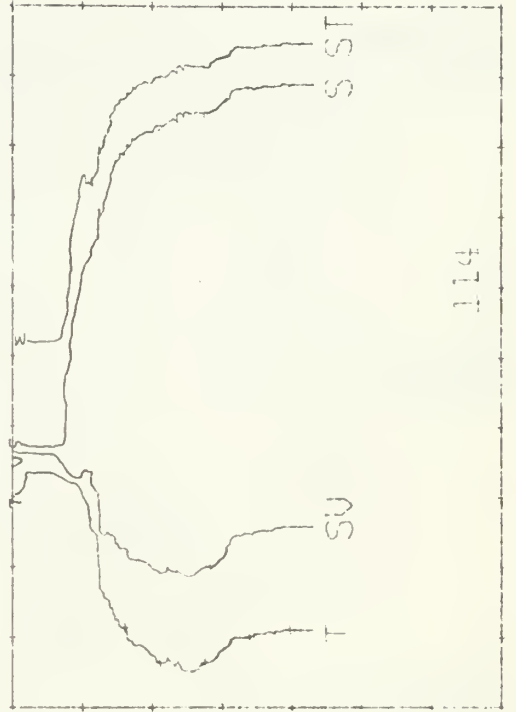


ST
SU
T

DEPTH (M)

MG/CC
M/SEC
P.P.T.
DEC C

MIZPAC 75 CTD STATIONS

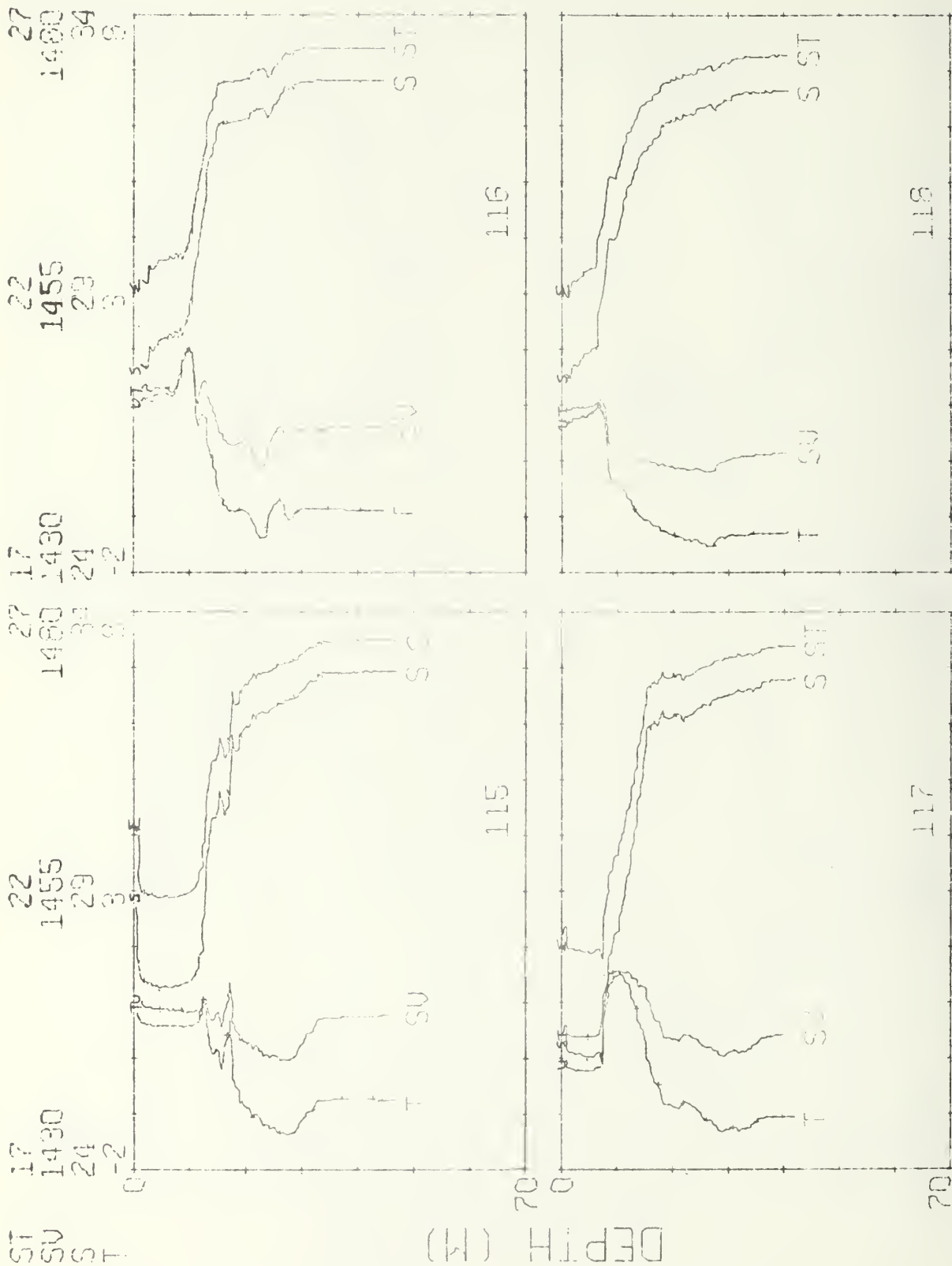


ST
SU
S
T

DEPTH (M)

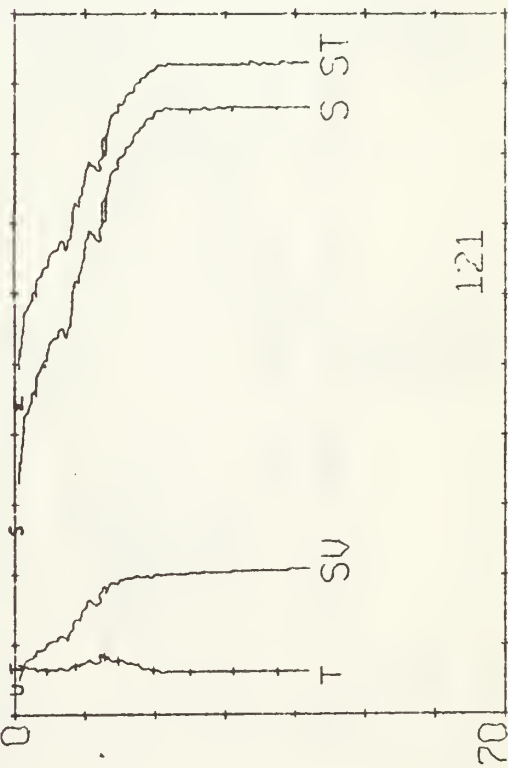
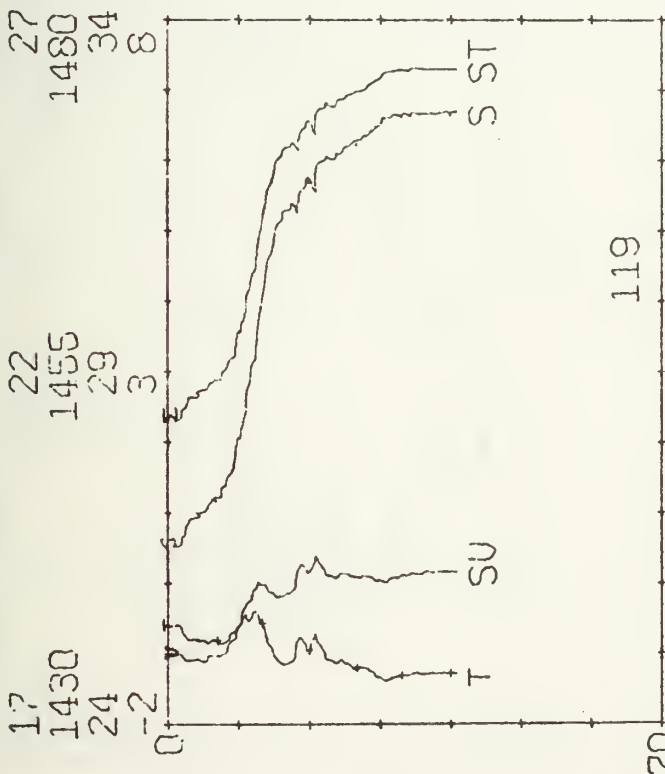
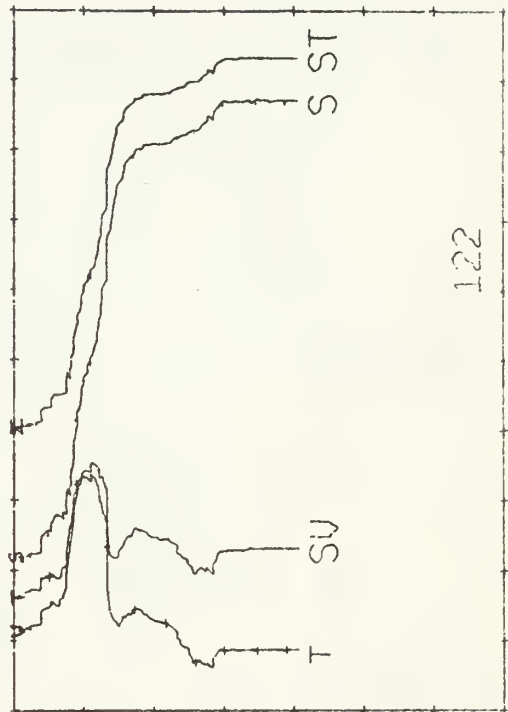
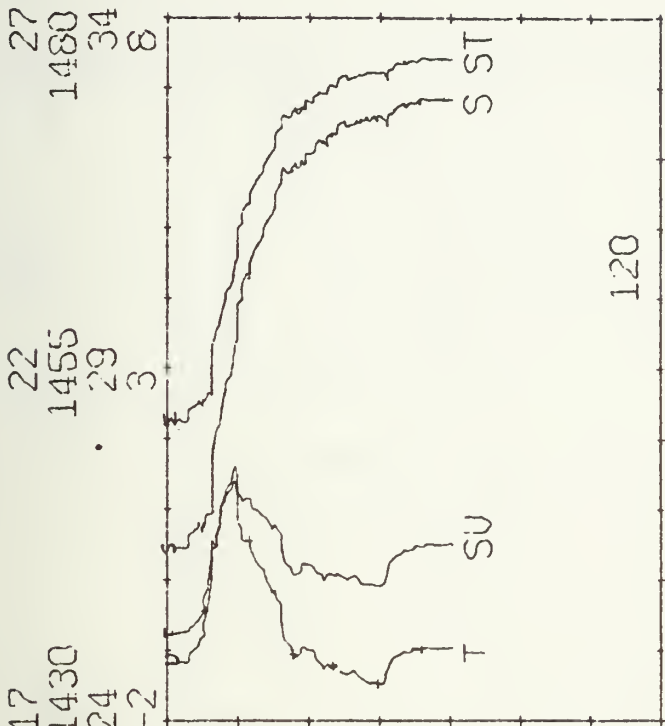
MS/C
M/SEC
P.P.T.
SEC/C

MIZPAC 75 CTD STATIONS



MG/CC
M/SEC
P.P.T.
DEG C

MIZPAC 75 CTD STATIONS

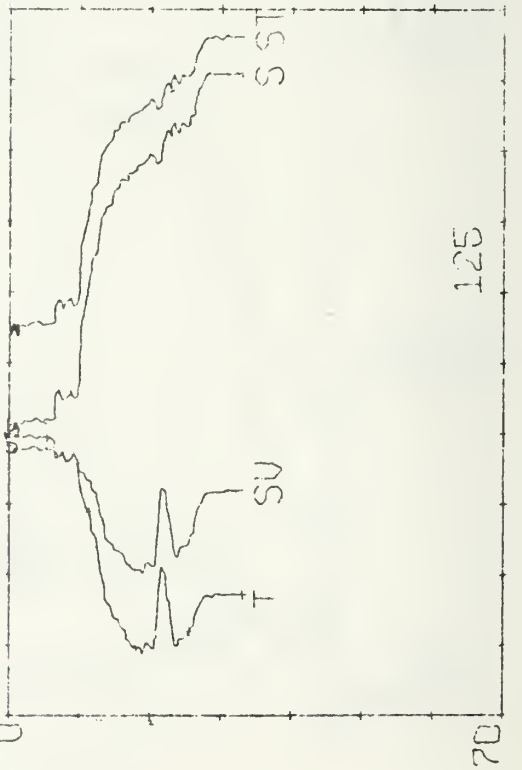
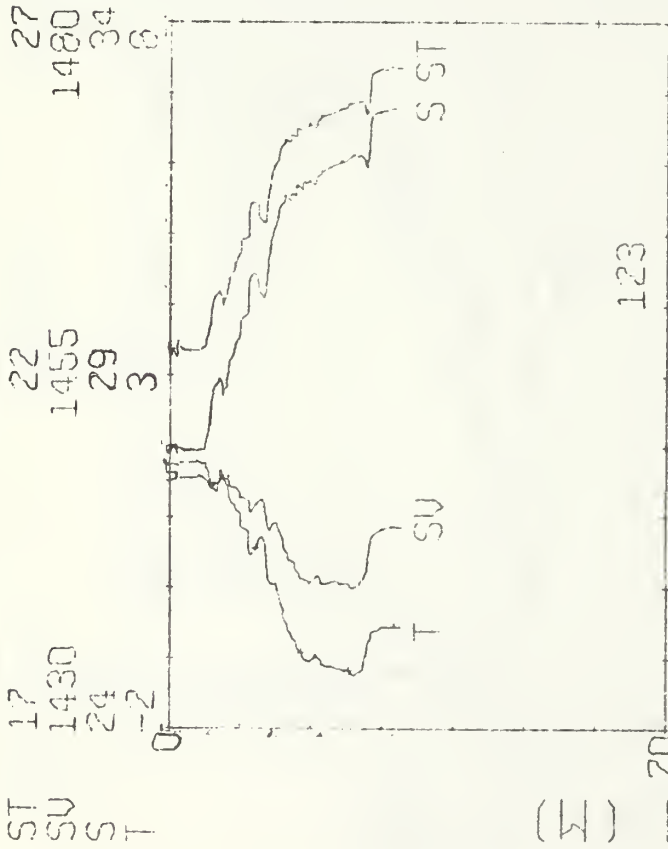
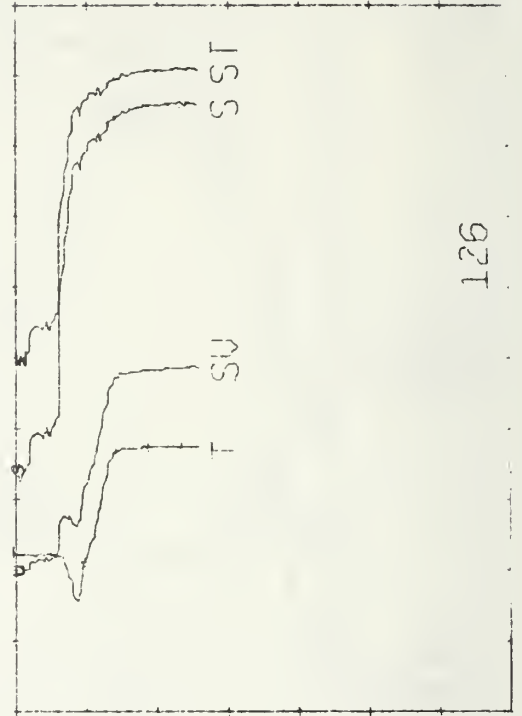
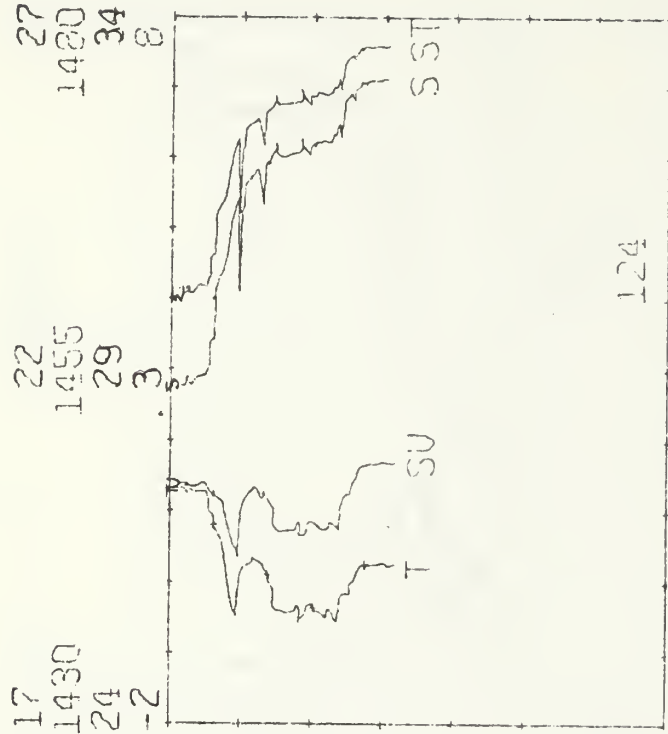


ST
SU
S
T

DEPTH (M)

MG/CC
M/SEC
P.P.T.
DEC C

MIZPAC 75 CTD STATIONS



MG/CC
M/SEC
P.P.T.
DEG C

MIZPAC 75 CTD STATIONS

27 1480 34 8

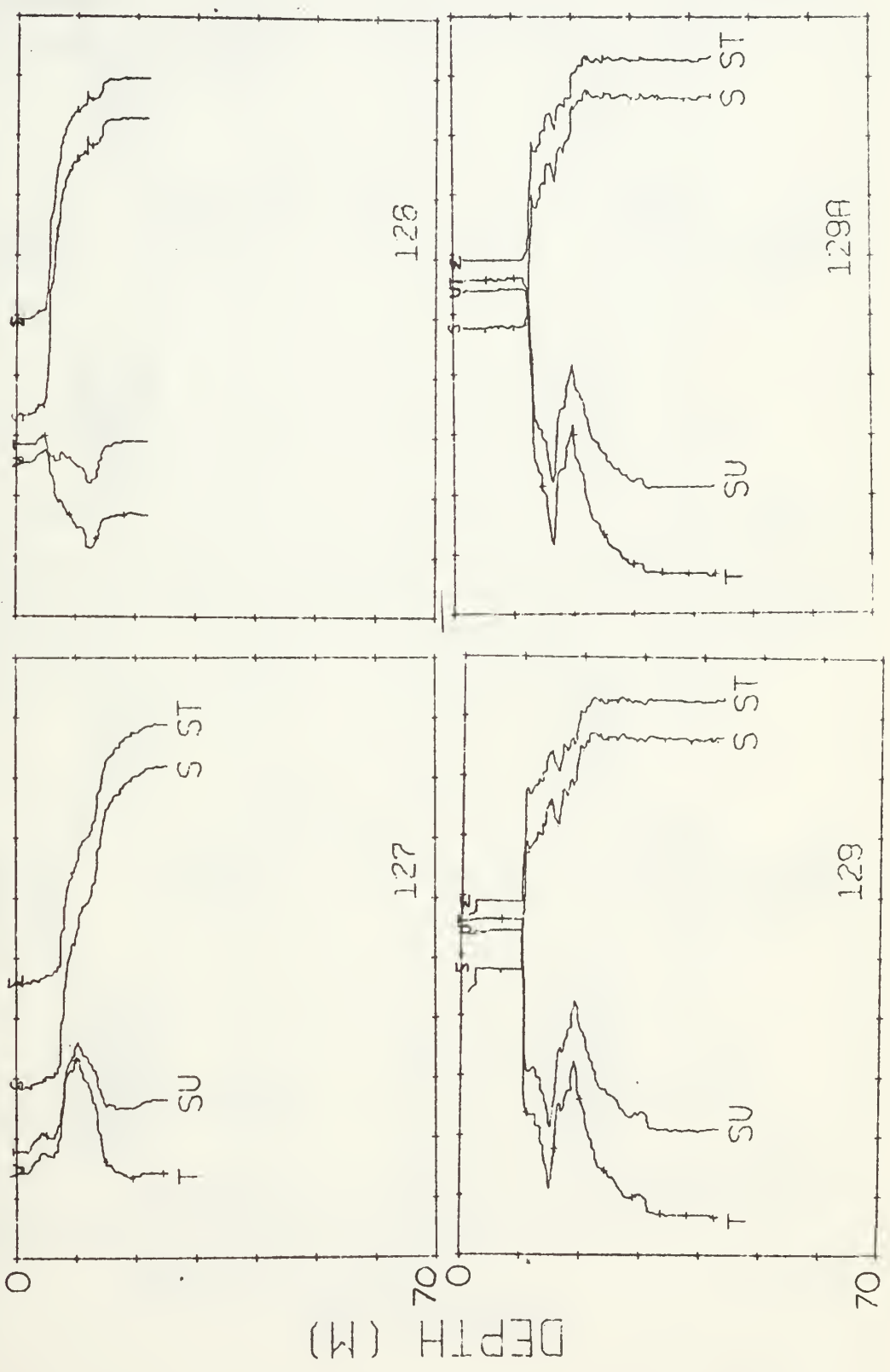
22 1455 29 3

27 17 1430 34 24 -2

22 1455 29 3

17 1430 24 -2

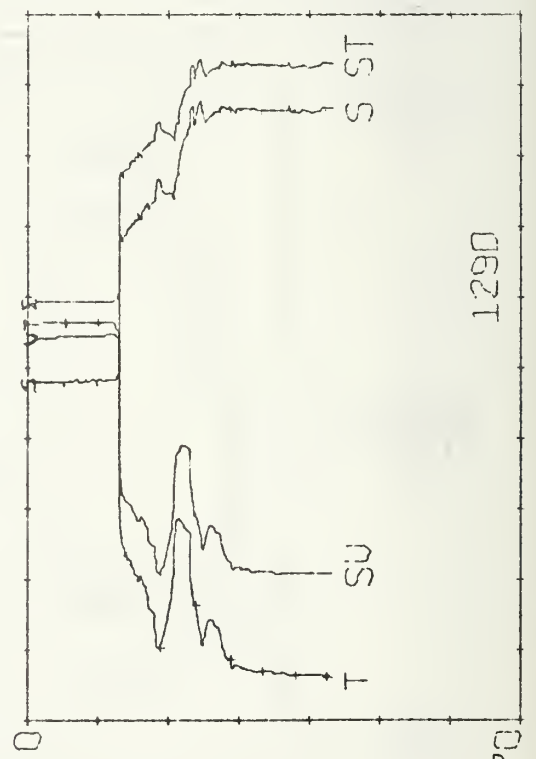
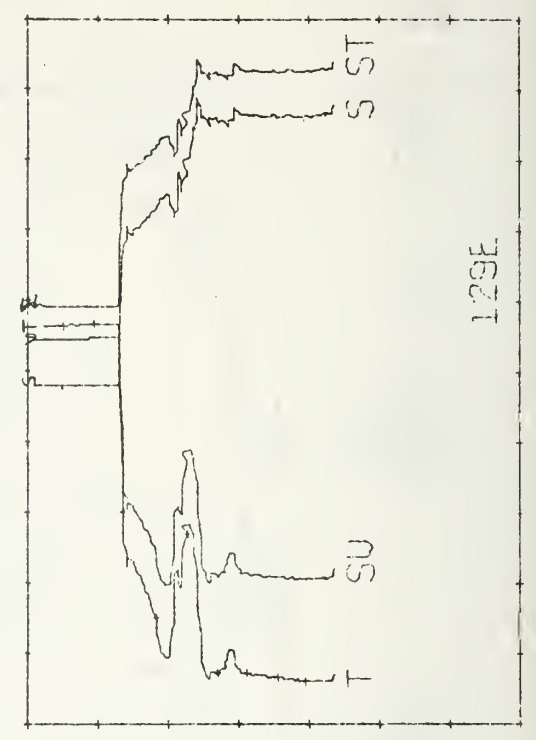
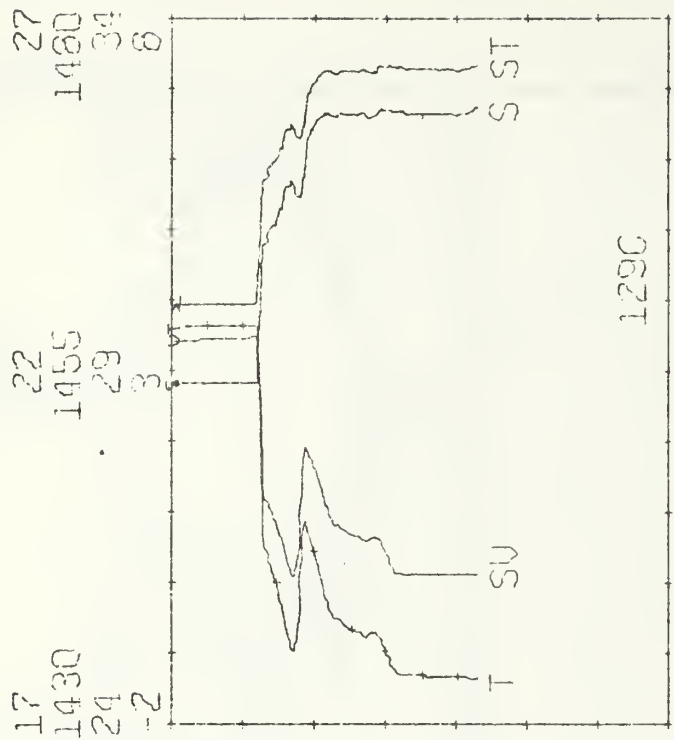
ST
SU
S
T



DEPTH (M)

MG/CC
 H/SEC
 P.P.T.
 DEG. C

MIZPAC 75 CTD STATIONS

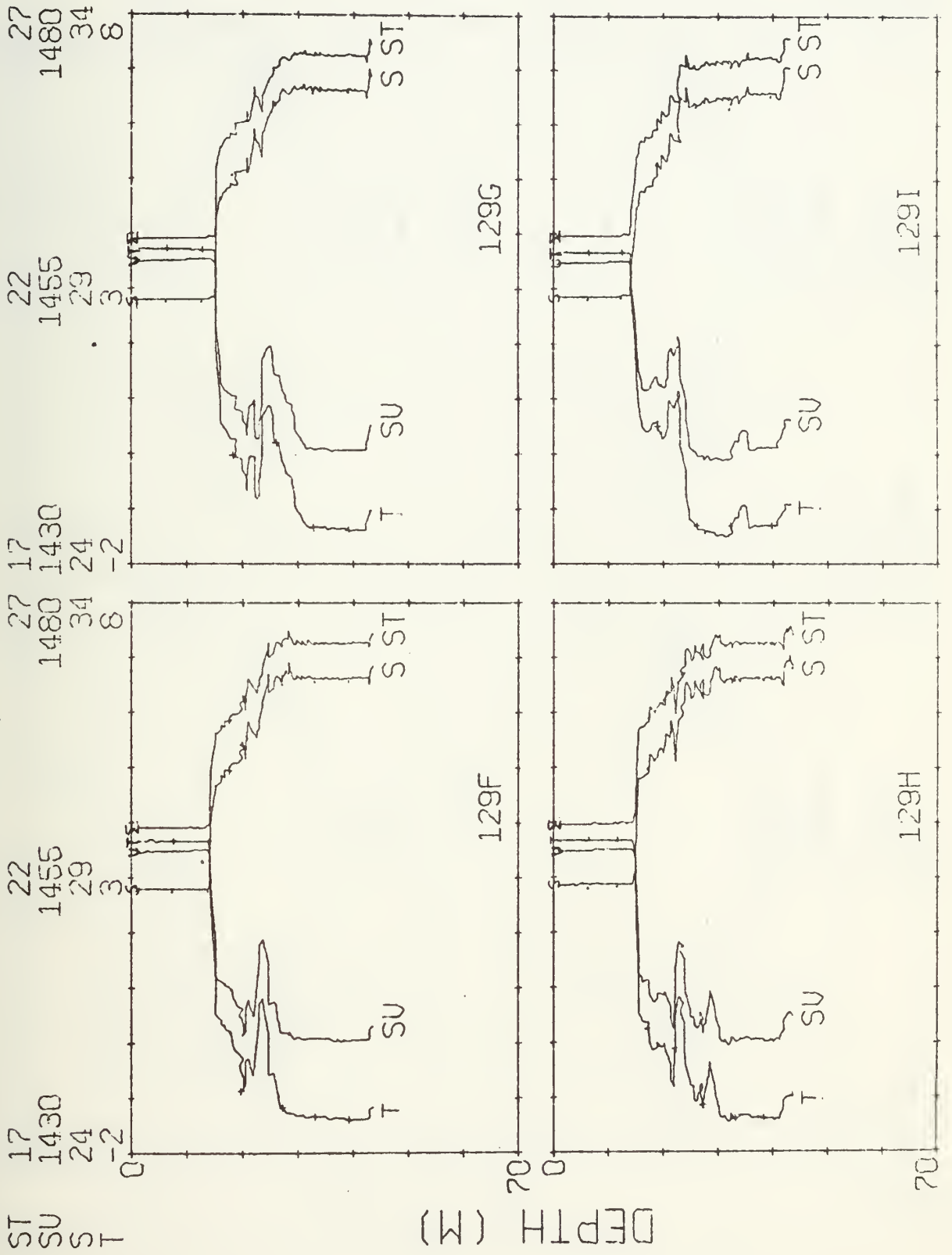


ST
 SU
 T

DEPTH (M)

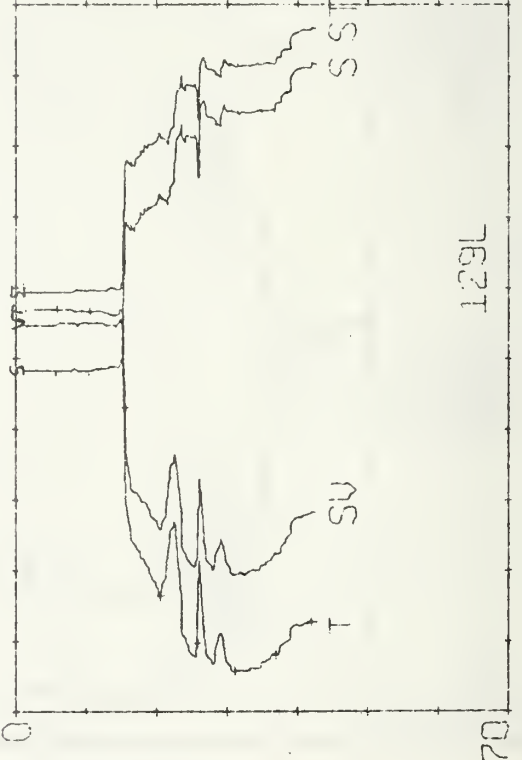
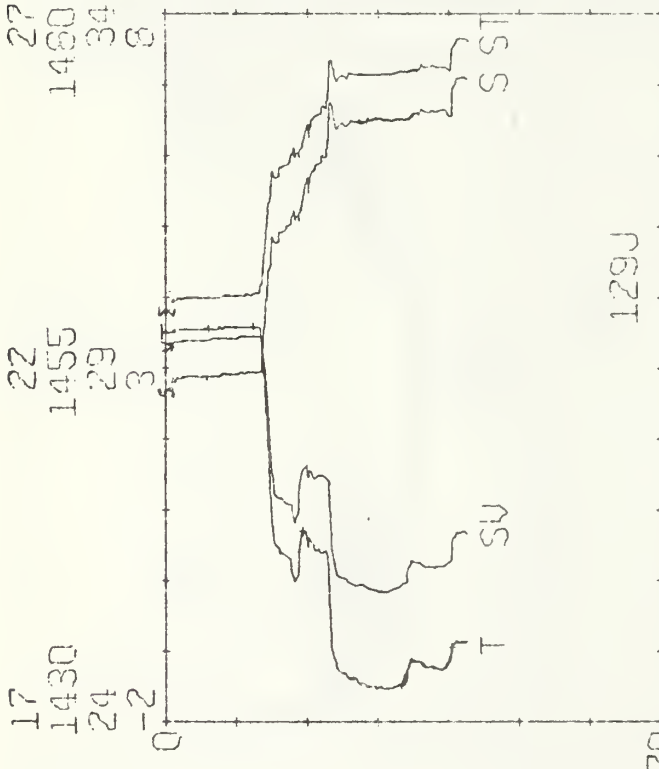
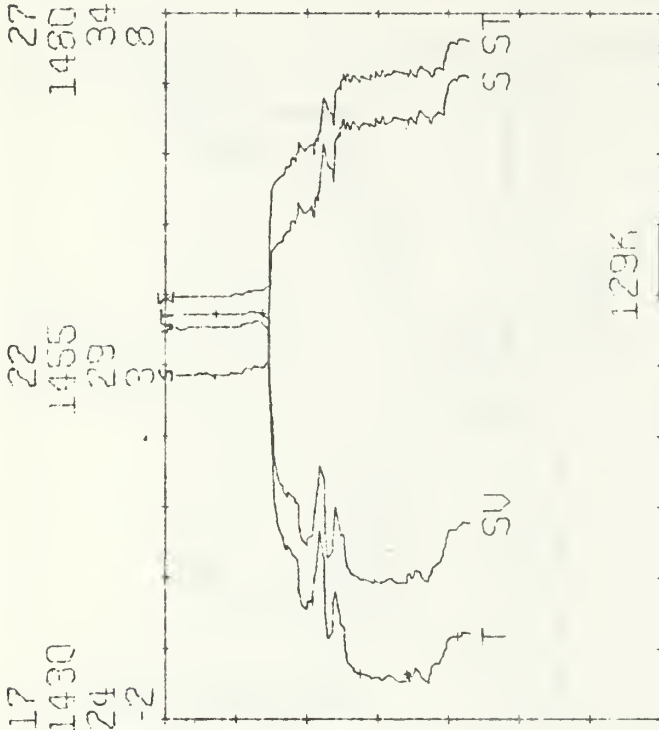
MG-CC
 M-SEC
 P.P.T.
 DEG C

MIZPAC 75 CTD STATIONS



MG/CC
M/SEC
P.P.T.
DEG C

MIZPAC 75 CTD STATIONS

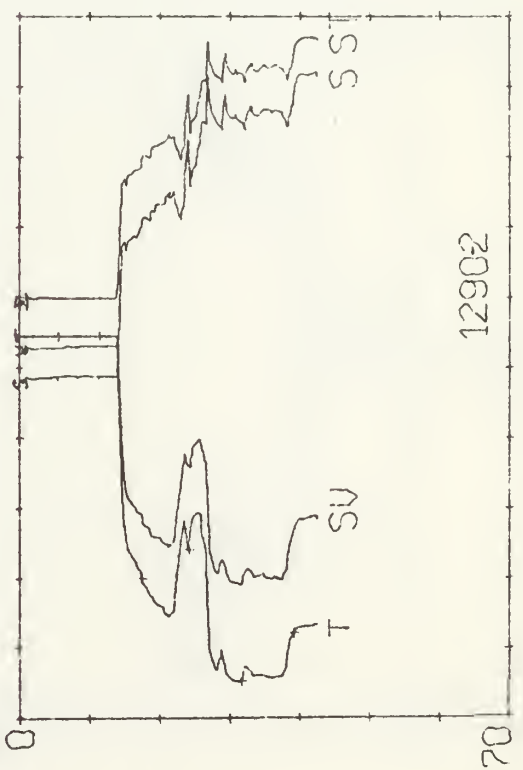
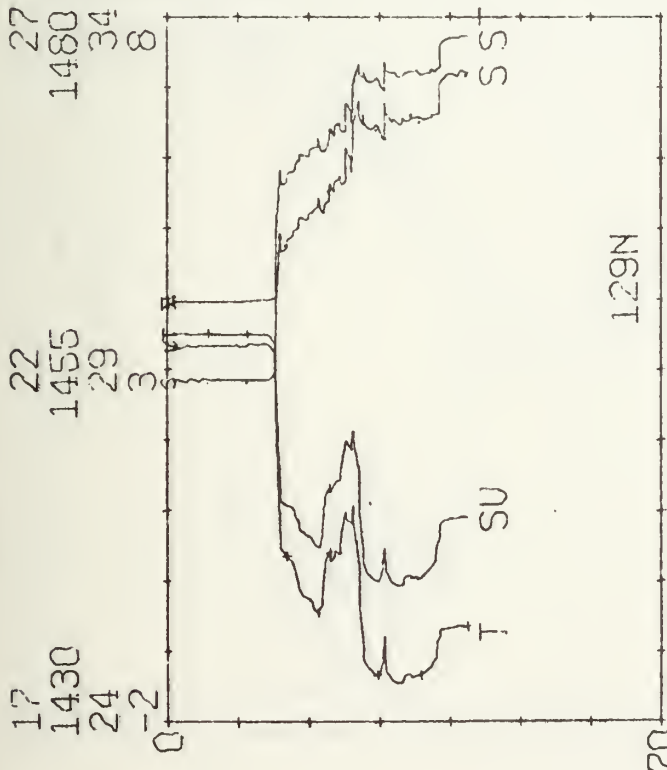
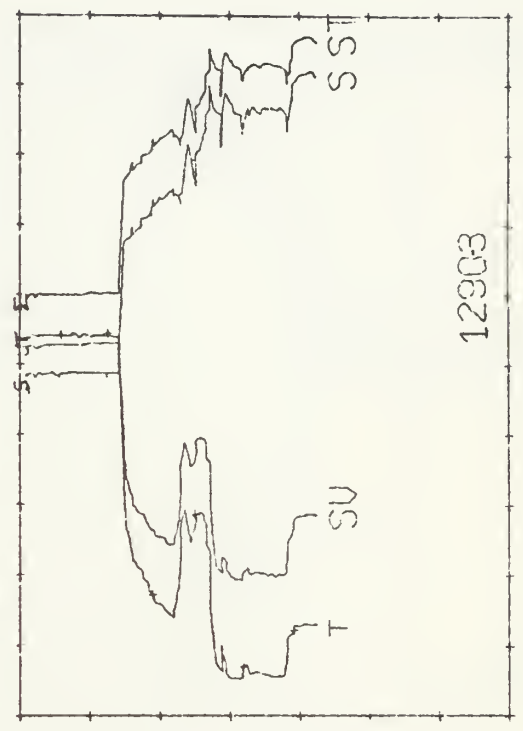
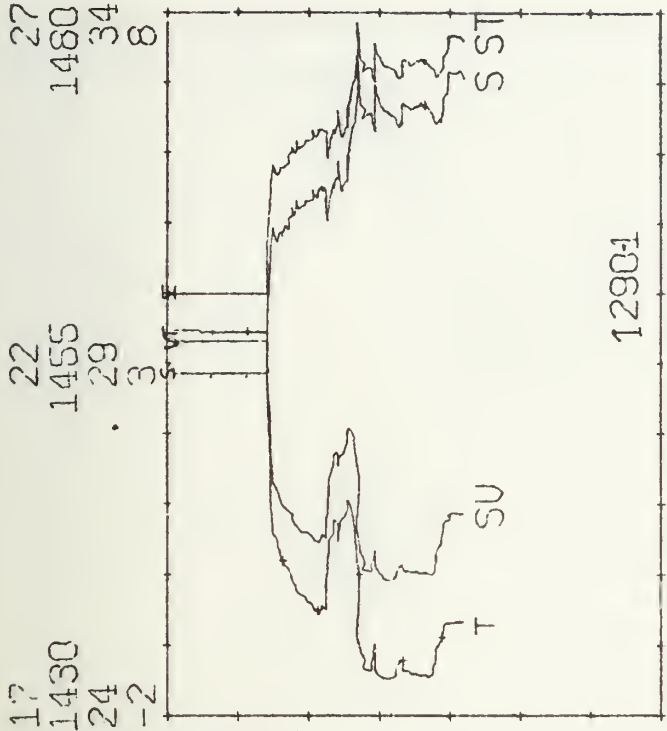


ST
SU
S T

DEPTH (M)

MG/CG
M/SEC
P.P.T.
DEG C

MIZPAC 75 CTD STATIONS

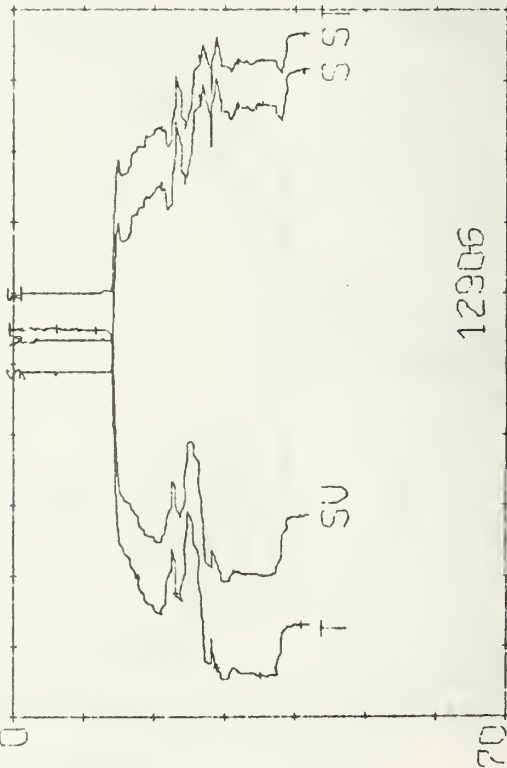
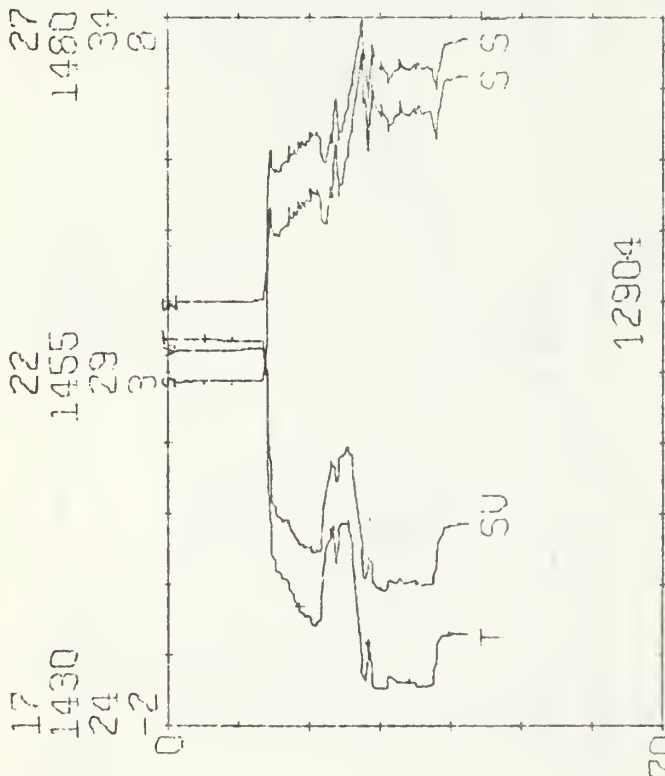
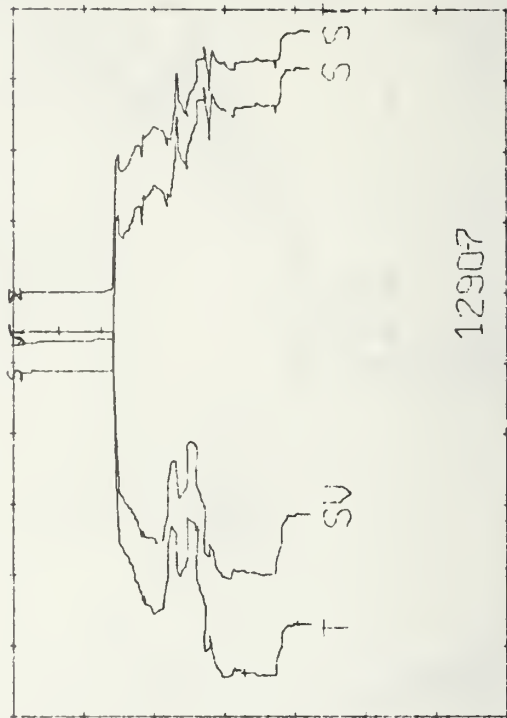
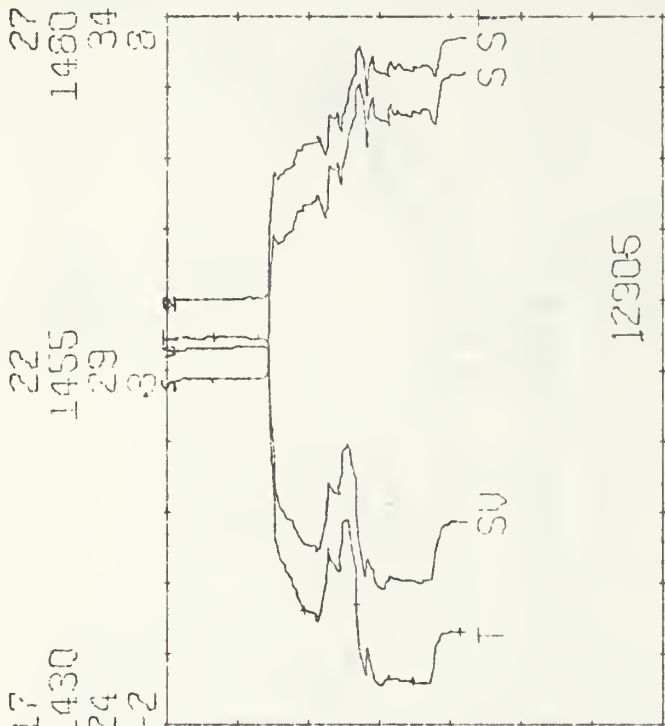


ST
SU
S
T

DEPTH (M)

MG/CC
M/SEC
P.P.T.
DEG C

MIZPAC 75 CTD STATIONS

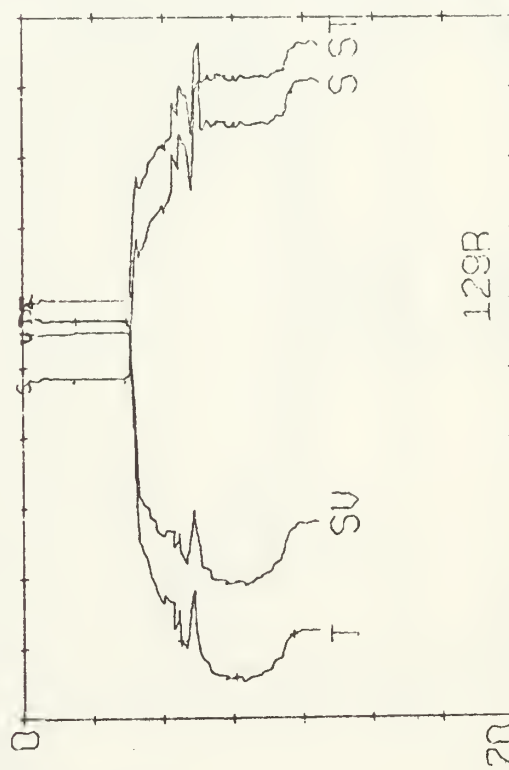
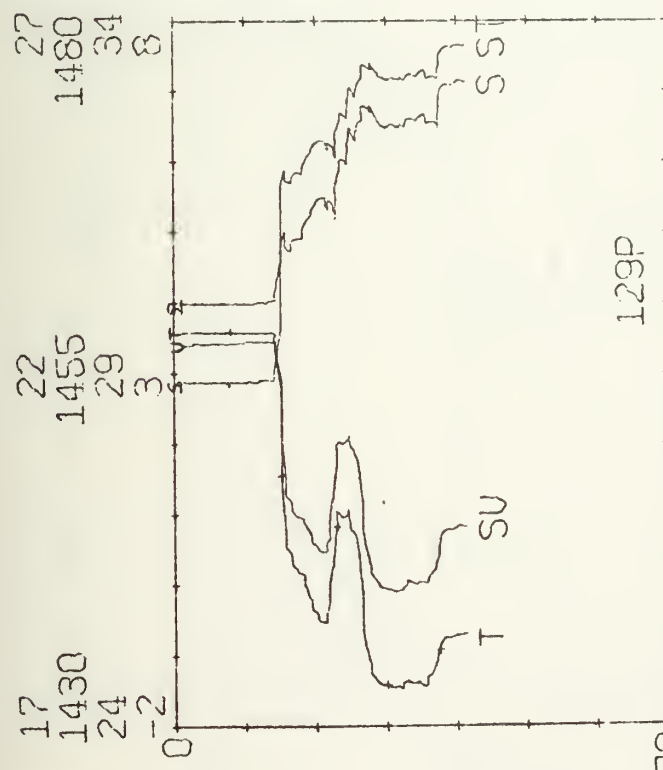
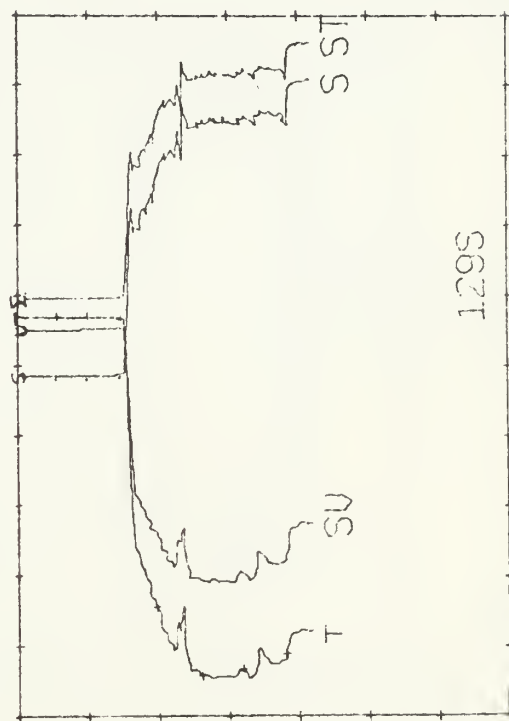
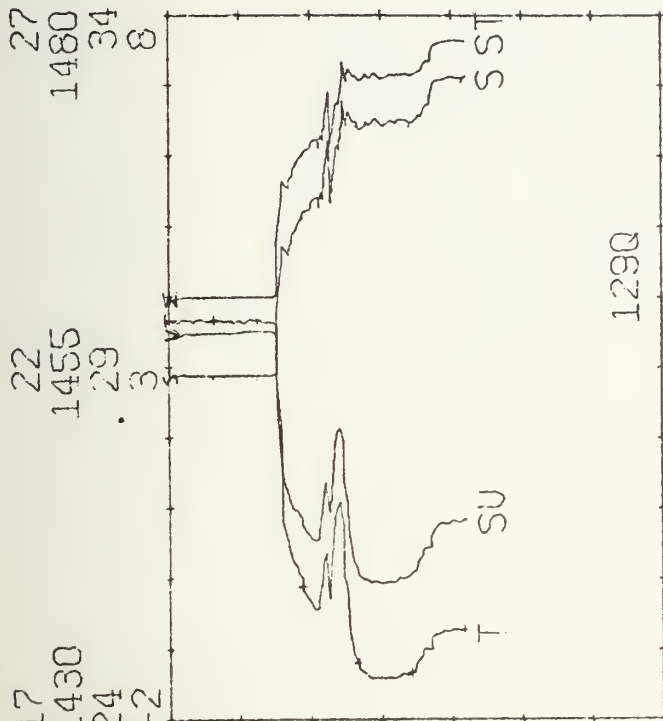


ST
SU
T

DEPTH (M)

MG/CC
M/SEC
P.P.T.
DEG C

MIZPAC 75 CTD STATIONS

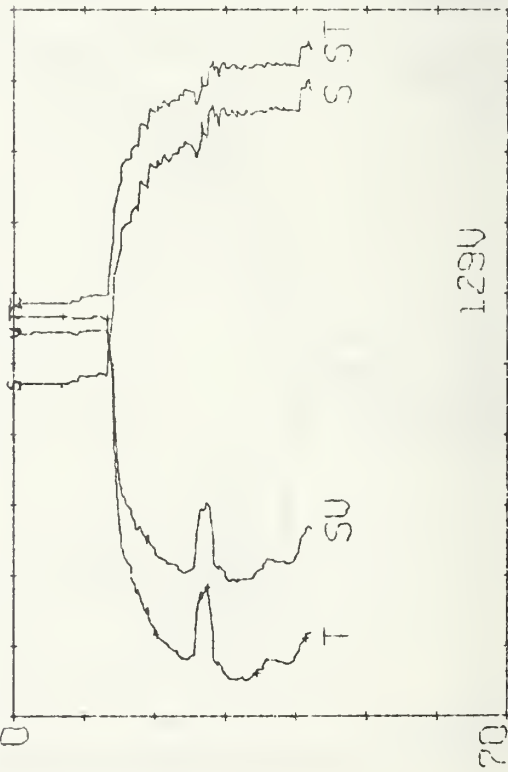
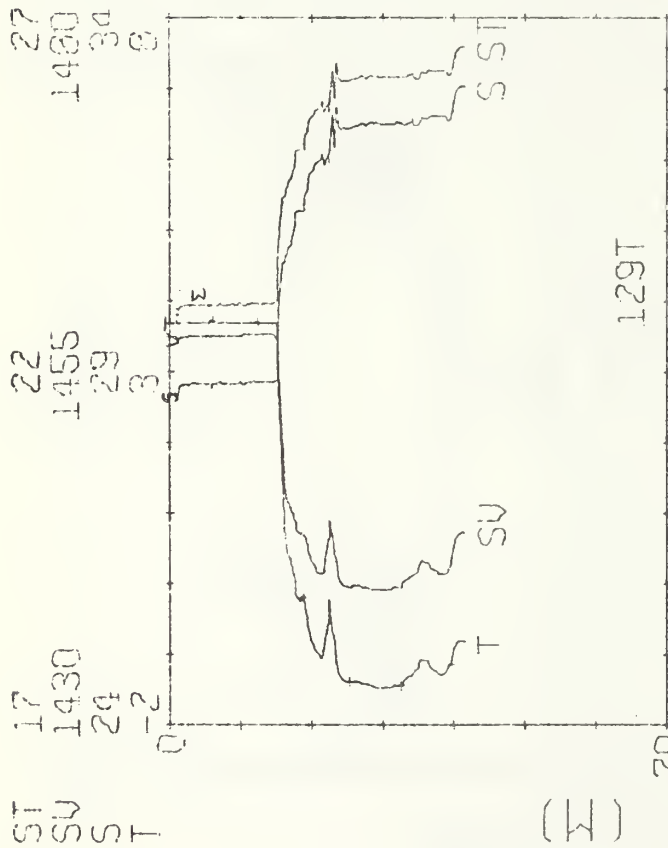
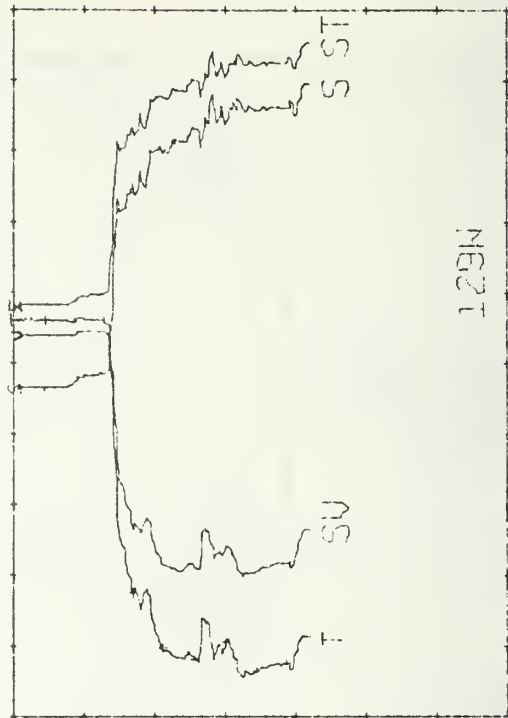
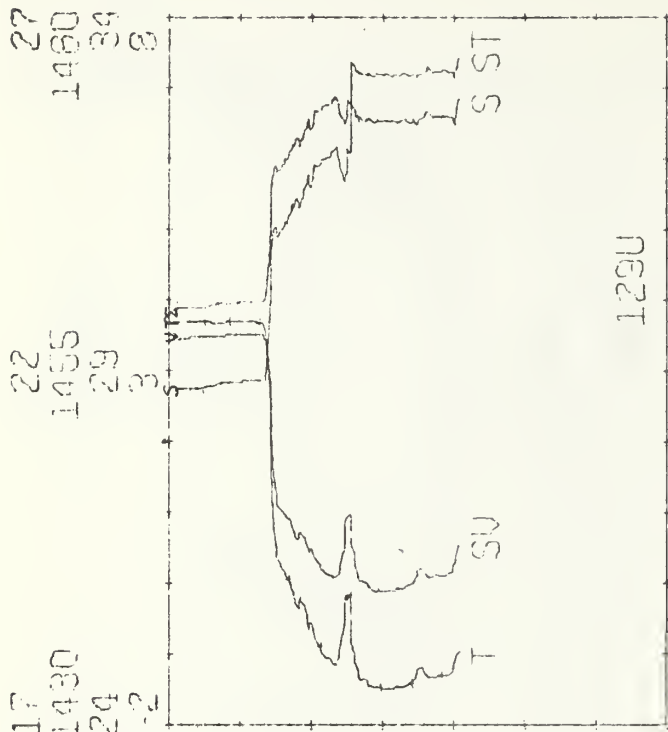


DEPTH (M)

ST
SU
S
T

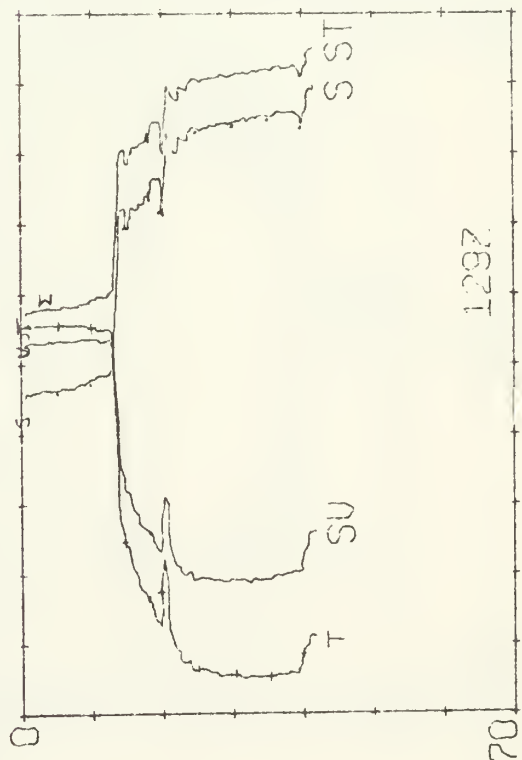
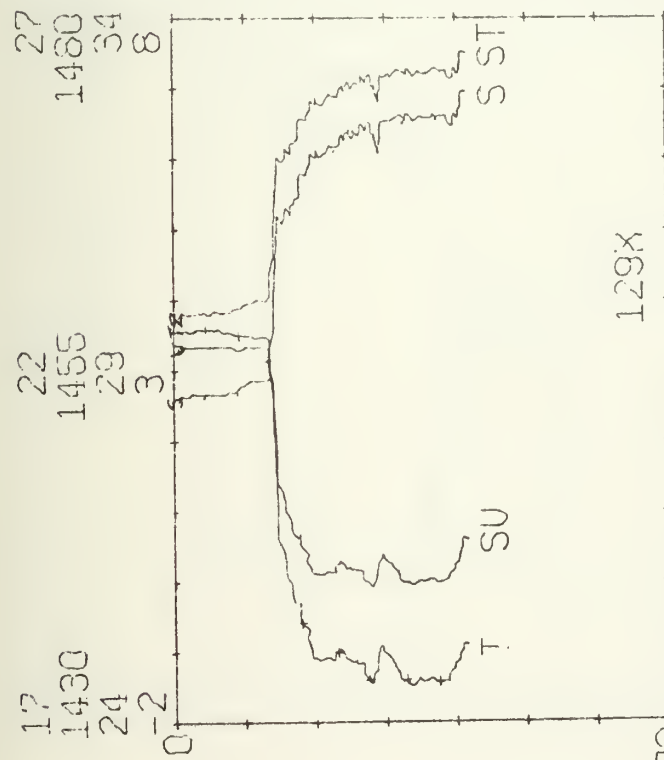
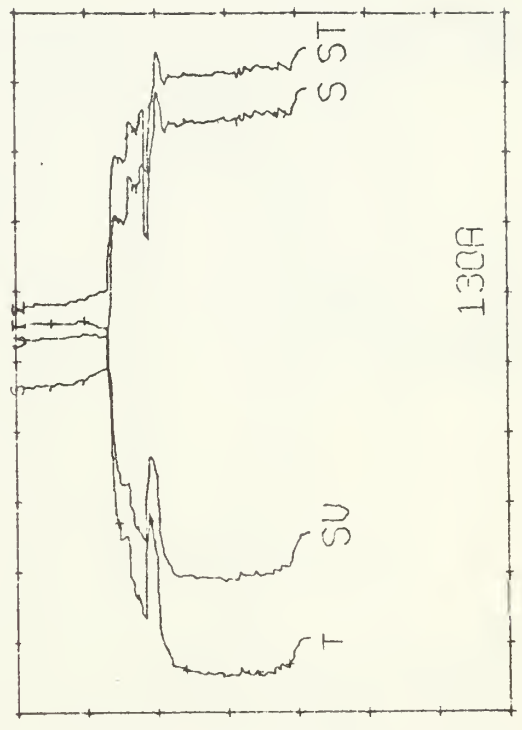
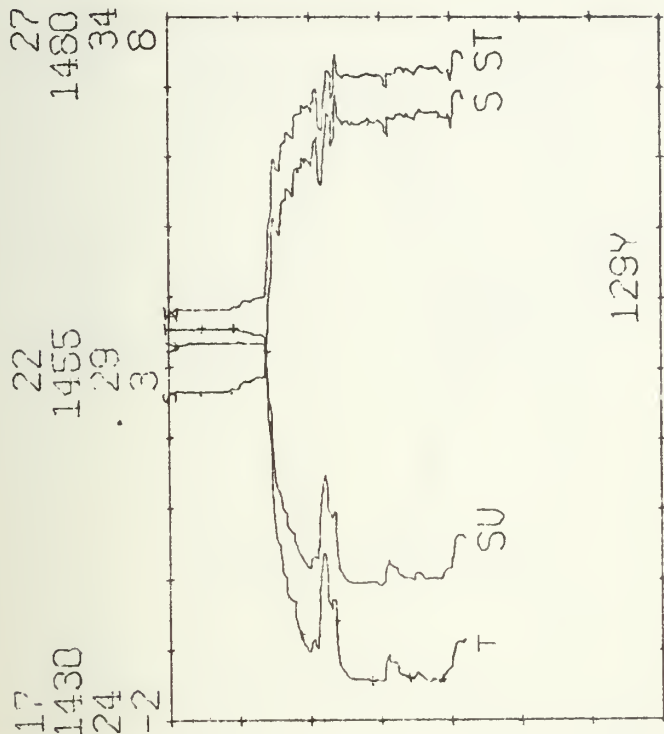
MO/00
 M/SEC
 P.P.T.
 DEG C

MIZPAC 75 CTD STATIONS



MG/CC
M/SEC
P.P.T.
DEG C

MIZPAC 75 CTD STATIONS

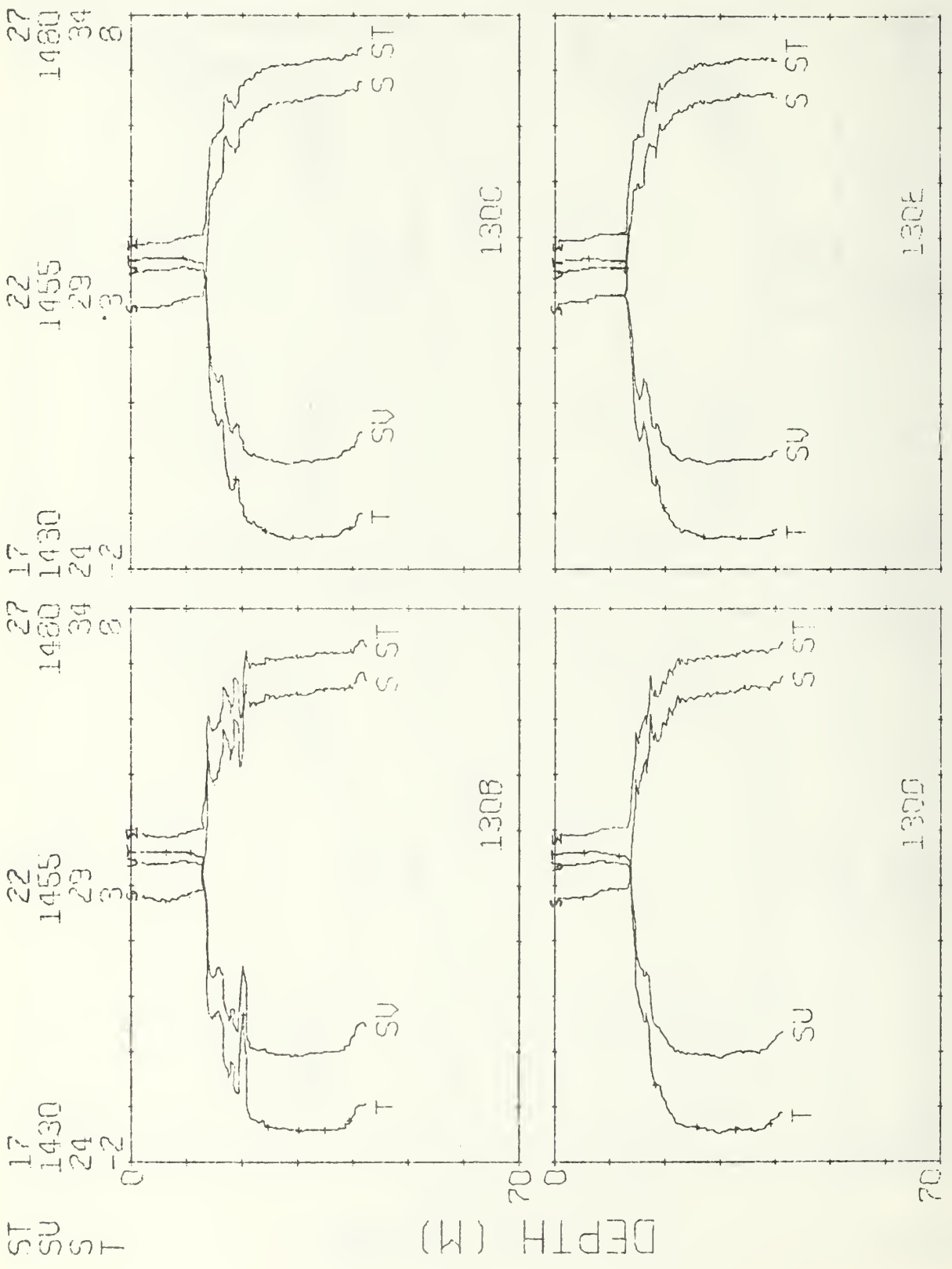


ST
SU
S T

DEPTH (M)

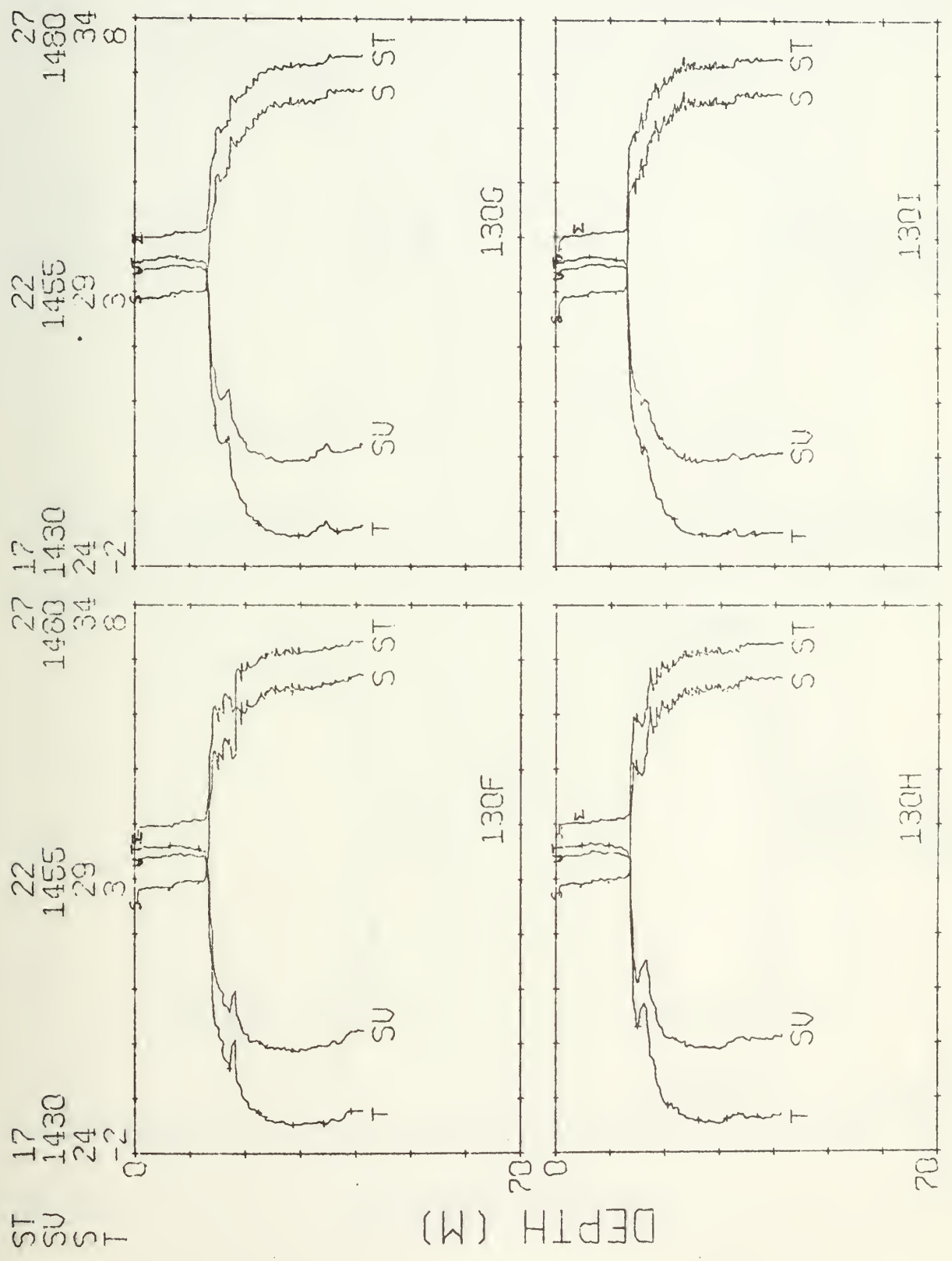
MG/CC 27
 M/SEC 1480
 P.P.T. 34
 DEG C 8

MIZPAC 75 CTD STATIONS



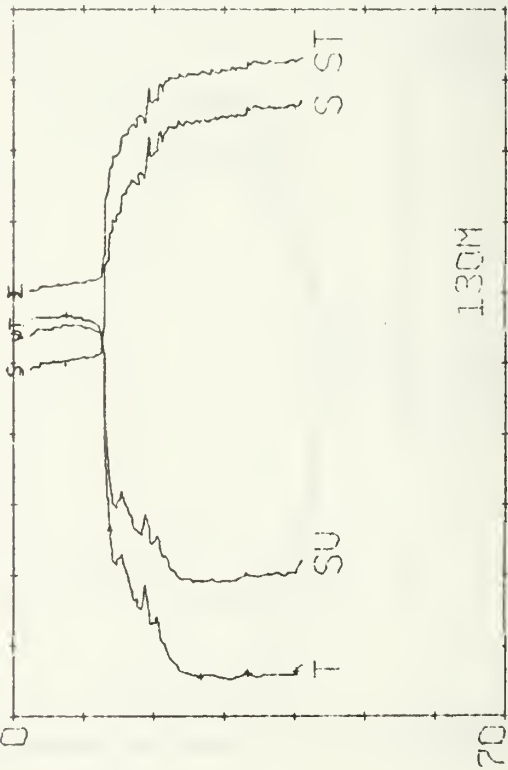
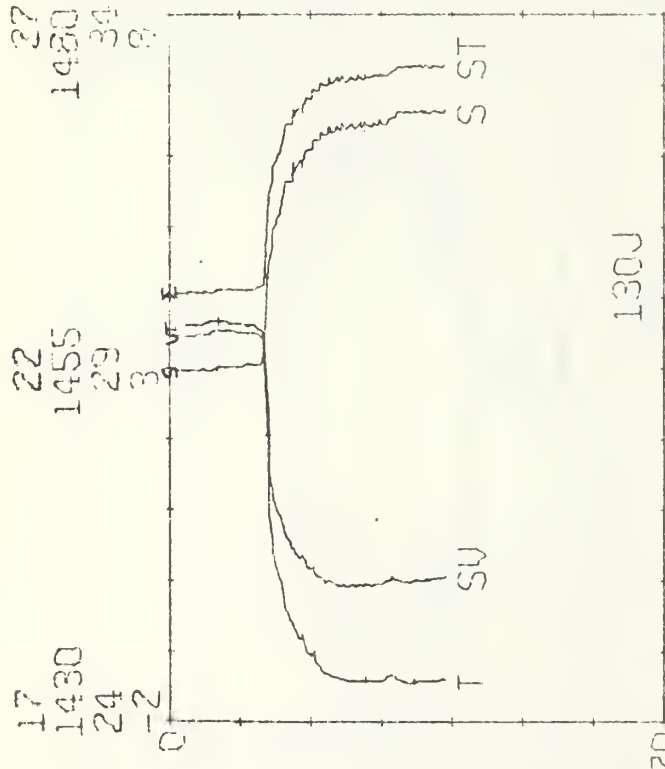
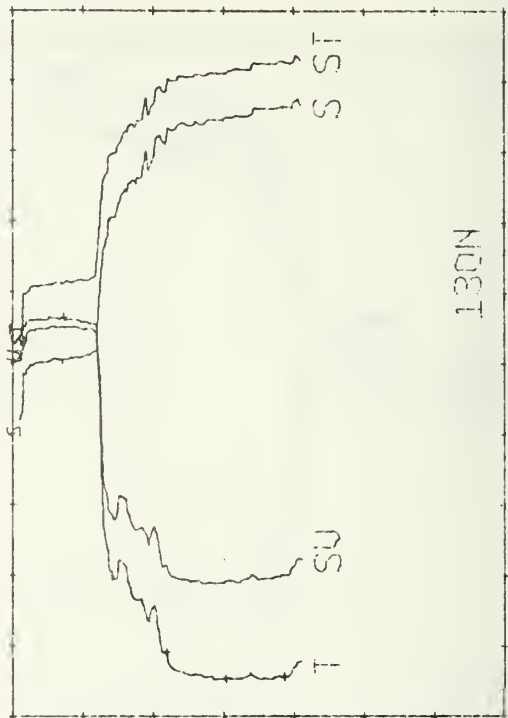
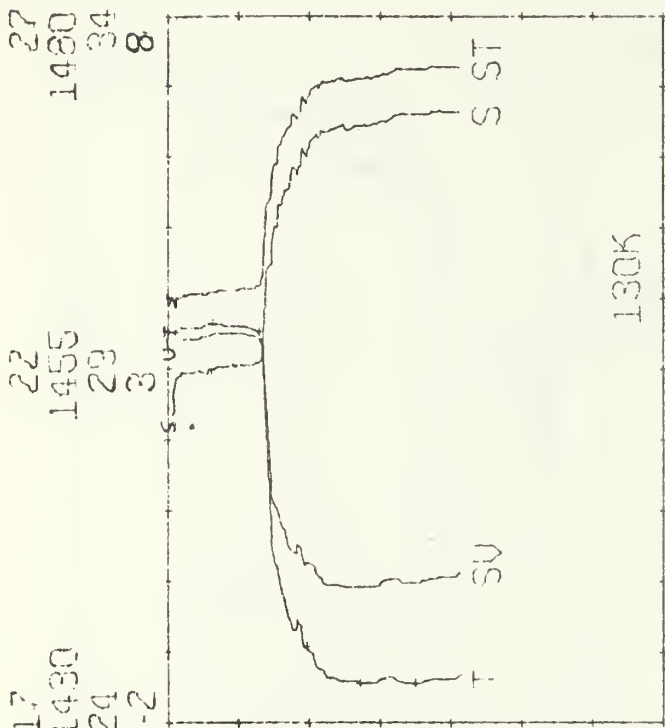
MG/GC
M/SEC
P.P.T.
DEG C

MIZPAC 75 CTD STATIONS



MG/CC 27
 M/SEC 1480
 P.P.T. 34
 DEG. C 8

MIZPAC 75 CTD STATIONS

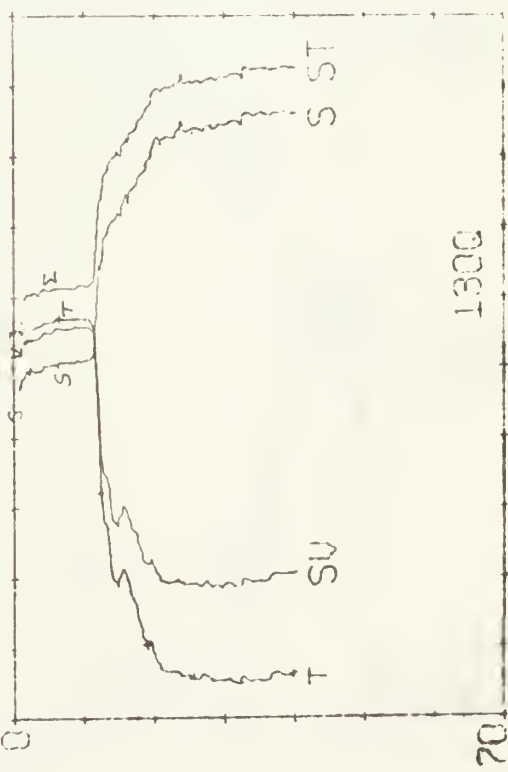
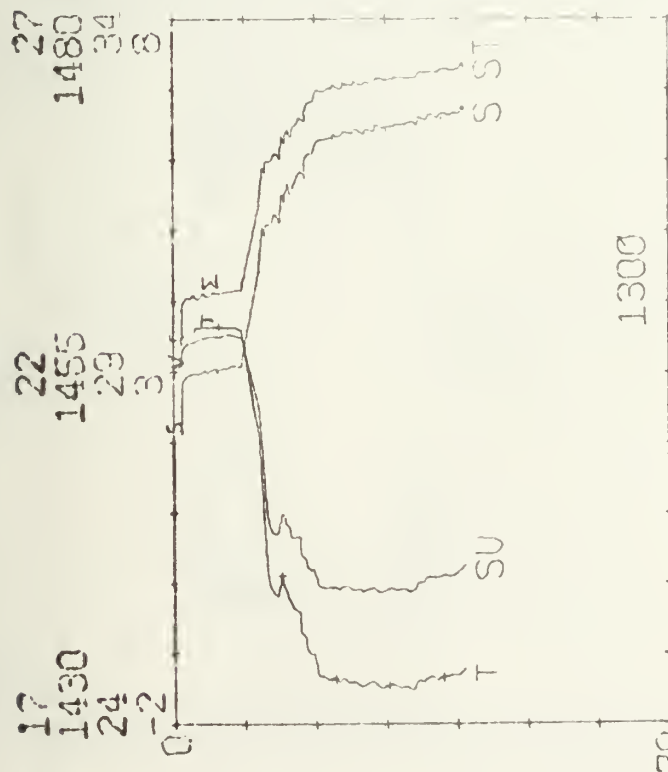
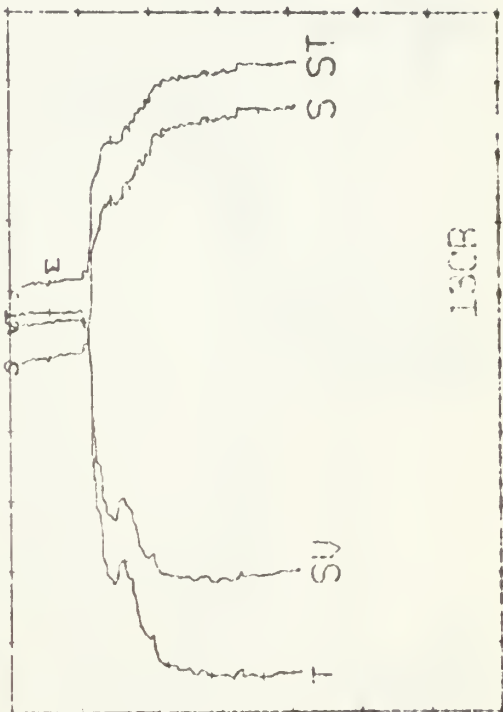
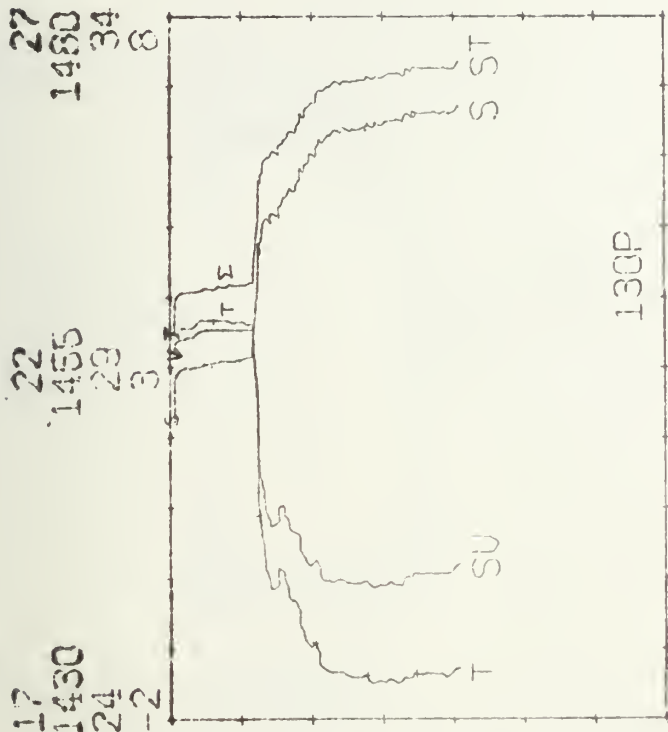


T SU S ST

DEPTH (M)

MG/CC 27
 M/SEC 1480
 P.P.T. 34
 DEG C 8

MIZPAC 75 CTD STATIONS

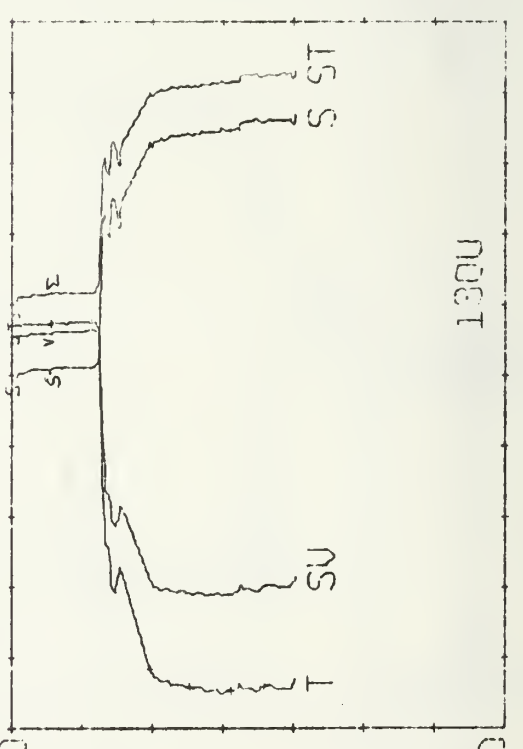
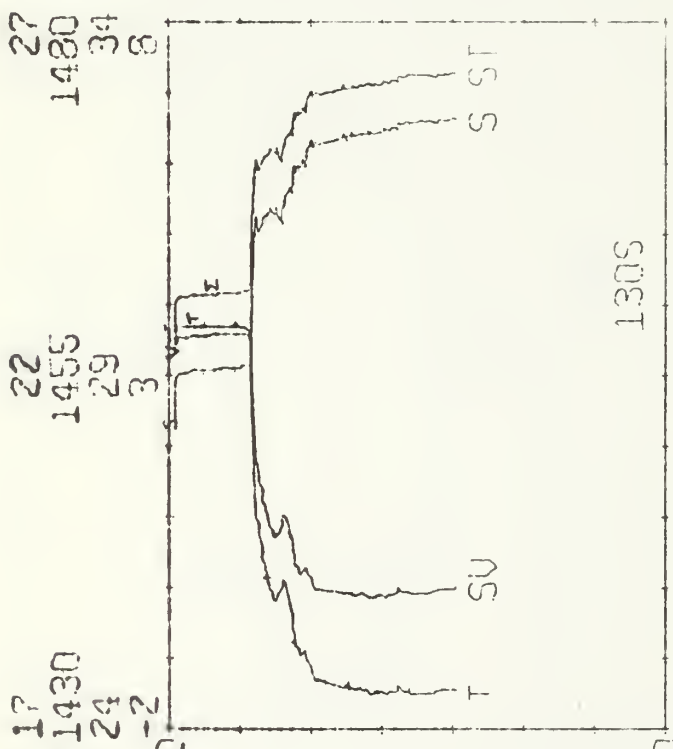
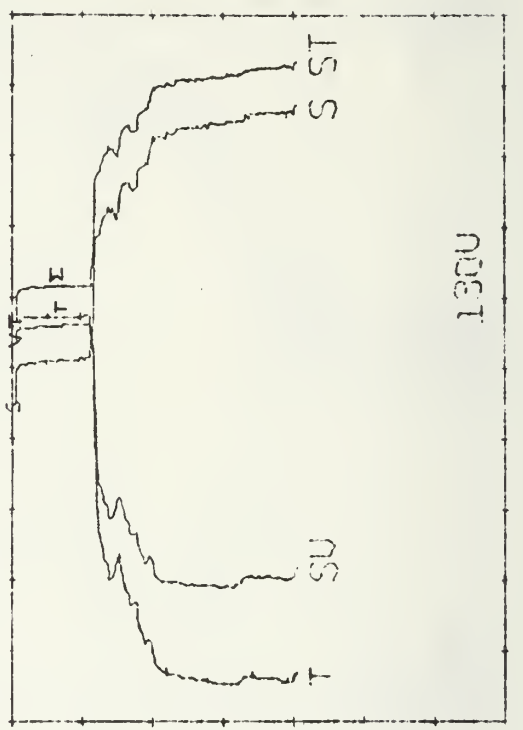
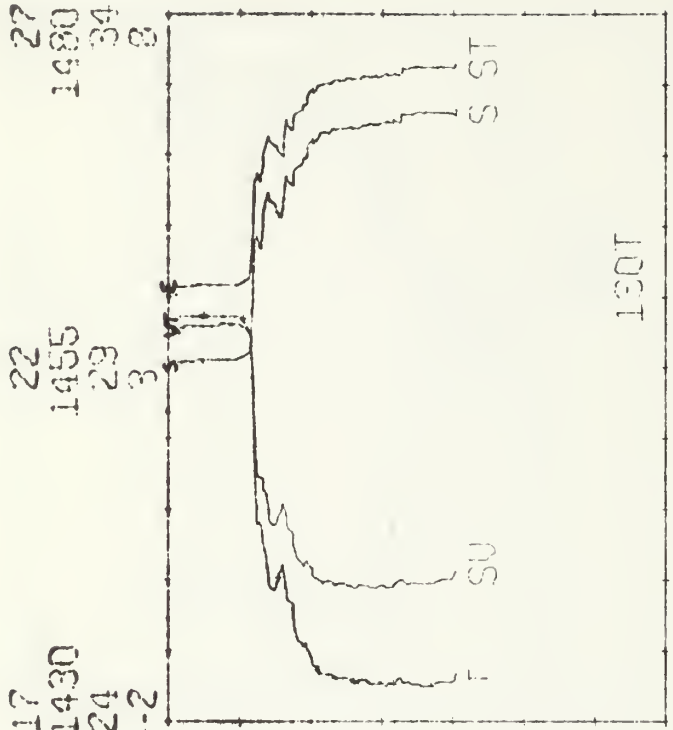


ST
 SU
 S
 T

DEPTH (M)

MG/CC
 M-SEC
 P.S.T.
 DEG C

MIZPAC 75 CTD STATIONS

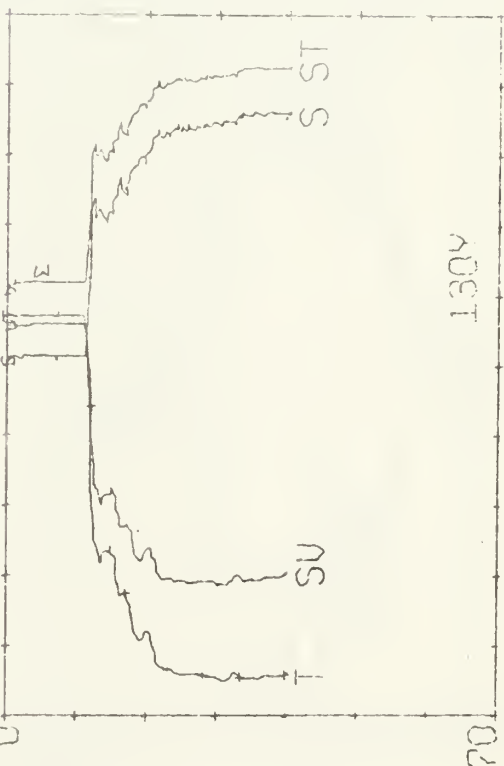
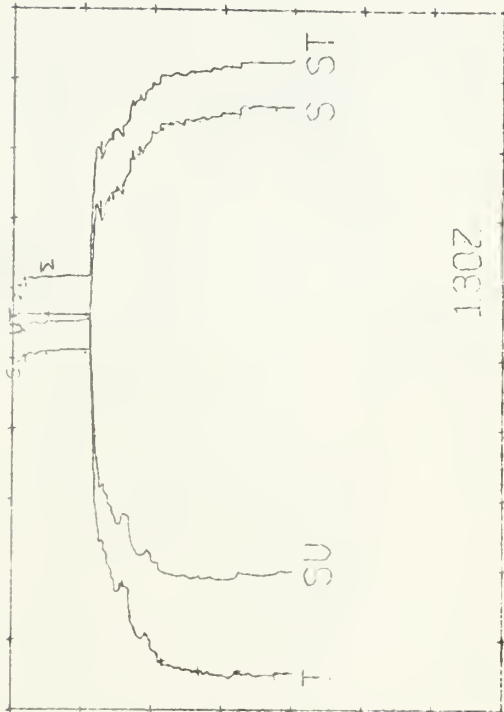
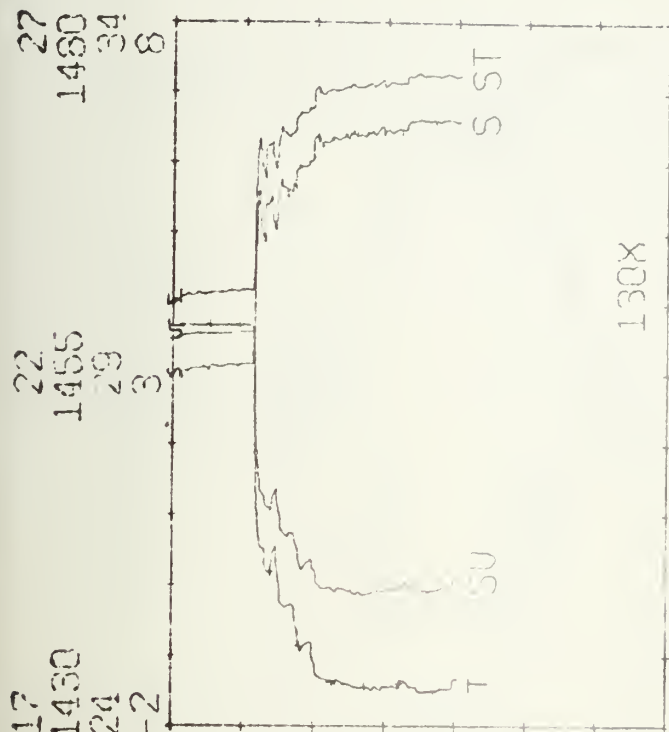


ST
 SU
 S
 T

DEPTH (M)

MG/GC 27
 M/SEC 1480
 P.P.T. 34
 DEG C 8

MIZPAC 75 CTD STATIONS

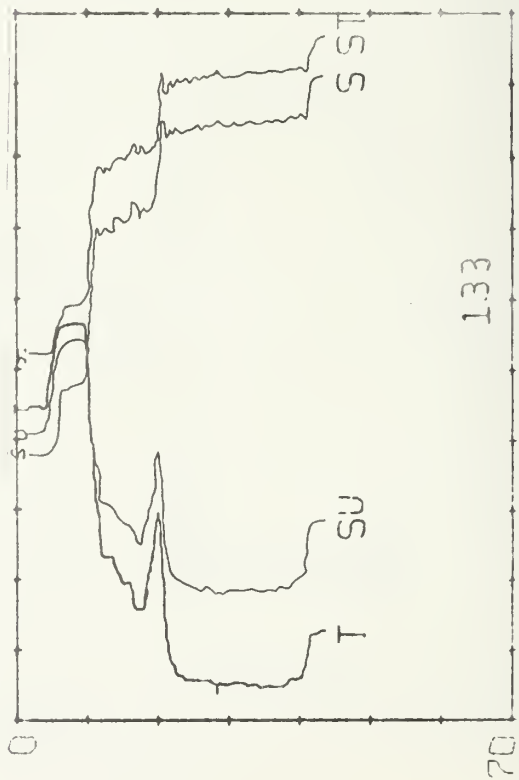
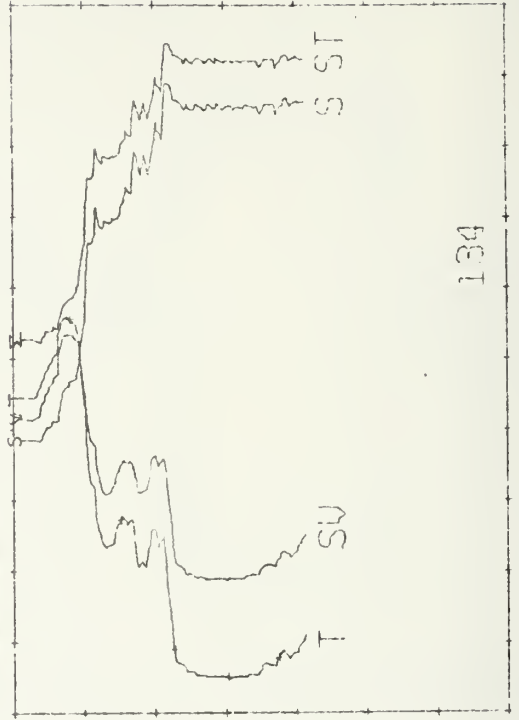
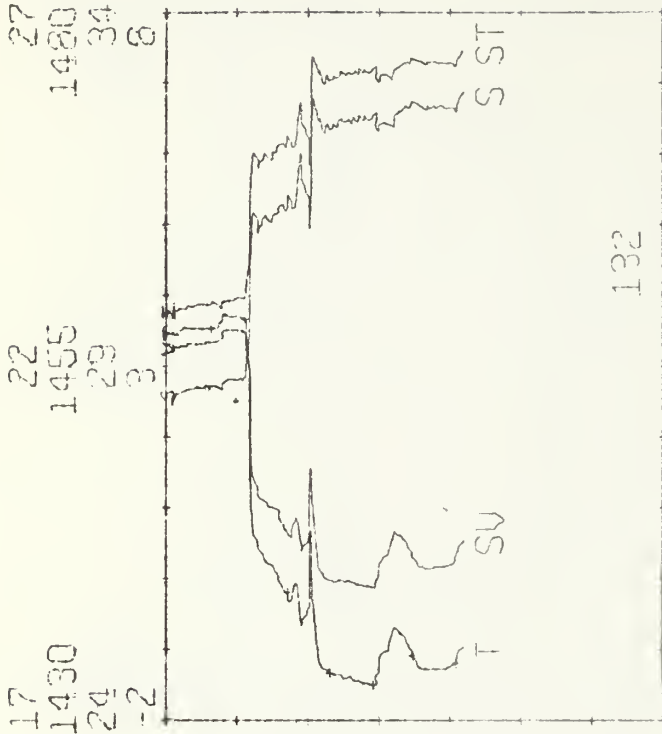


ST
 SU
 T

DEPTH (M)

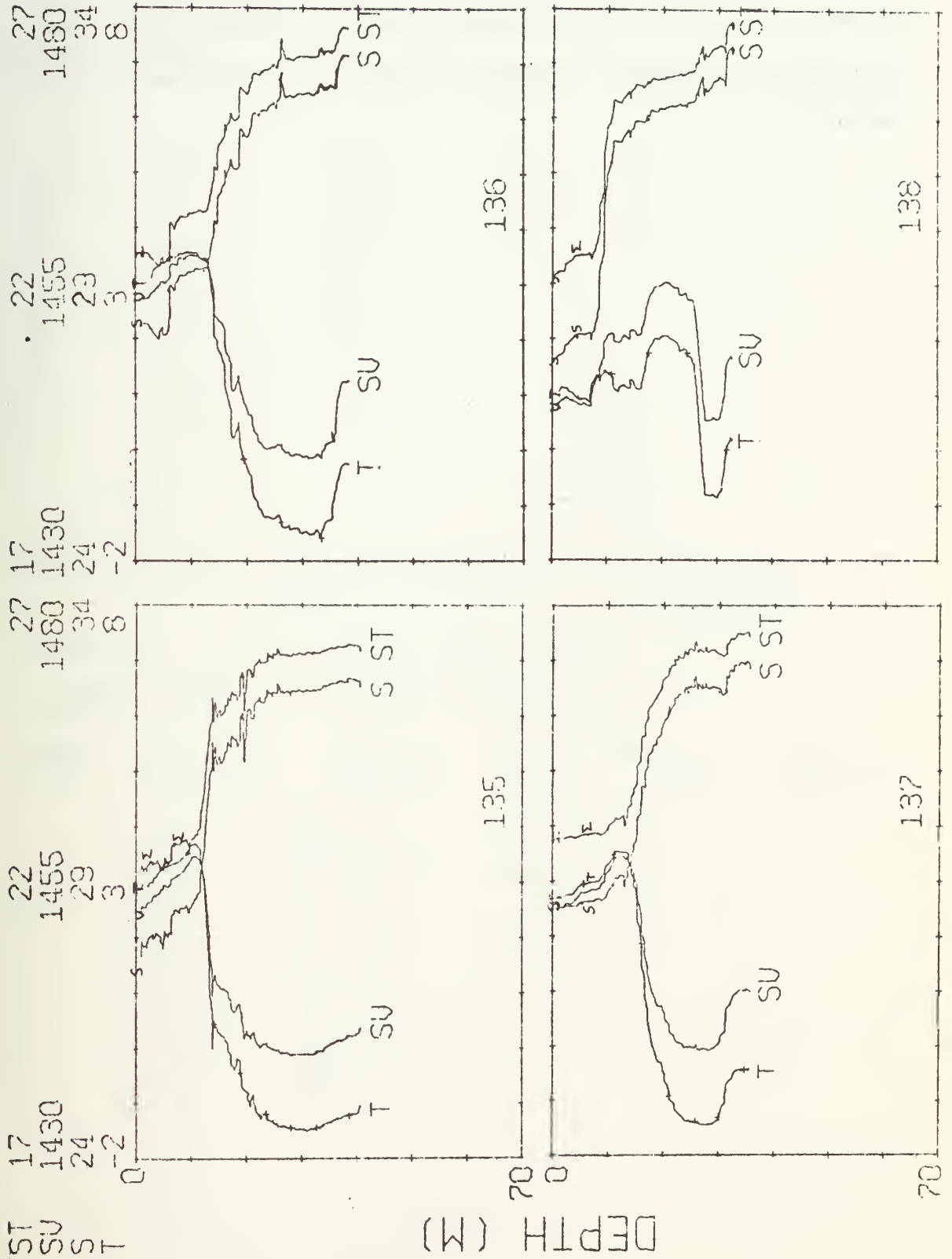
MG/CC
M/SEC
P.P.T.
DEG C

MIZPAC 75 CTD STATIONS



MG/CC
M/SEC
P.P.T.
DEG C

MIZPAC 75 CTD STATIONS



APPENDIX D

MIZPAC 75 CURRENT DATA

The data for the 44 current measurements follows. Two stations appear on each page. Data are presented at each depth measured and as averaged over 0-10m, 10-30m, and 30m-bottom.

MIZPAC

75

CURRENT DATA

Station: 16 Date: 1 Aug 75 Time: 1835ZLatitude: 68°-24.5' N Longitude: 168°-40.5' W

Depth (m)	N-Comp (cm sec ⁻¹)	E-Comp (cm sec ⁻¹)	Depth (M)	Direction (°T)	Speed (cm sec ⁻¹)
0	-0.16	8.81	0-10	103	8.2
5	0.52	6.81			
10	-5.85	8.28	10-30	112	12.0
15	-6.31	9.35			
19	-7.85	9.49	>30	068	12.4
24	-5.67	10.33			
29	1.63	15.26			
34	5.69	17.02			
39	5.99	17.54			
44	13.17	7.65			
49	-0.67	7.69			
54	-0.67	7.69			

MIZPAC

75

CURRENT DATA

Station: 37 Date: 2 Aug 75 Time: 2215ZLatitude: 69°-59'N Longitude: 167°-37'W

Depth (m)	N-Comp (cm sec ⁻¹)	E-Comp (cm sec ⁻¹)	Depth (M)	Direction (°T)	Speed (cm sec ⁻¹)
0	-2.10	-36.52	0-10	274	29.1
5	2.07	-33.50			
10	6.21	-17.04	10-30	203	18.6
15	-18.99	-6.39			
20	-19.18	-5.91	>30	222	22.8
25	-16.62	-3.42			
30	-13.93	-12.83			
35	-8.95	-13.95			
40	-15.48	-12.78			
45	-14.14	-16.67			
50	-22.91	-16.64			
51	-22.91	-16.64			

MIZPAC

75

CURRENT DATA

Station: 42 Date: 3 Aug 75 Time: 0804ZLatitude: 70°-18.8' N Longitude: 167°-43' W

Depth (m)	N-Comp (cm sec ⁻¹)	E-Comp (cm sec ⁻¹)	Depth (M)	Direction (°T)	Speed (cm sec ⁻¹)
0	-4.54	-18.57	0-10	278	16.2
5	-0.38	-15.54			
10	11.78	-13.86	10-30	256	4.5
15	-0.95	-4.08			
20	-0.87	-7.86	>30	246	6.4
25	0.80	-2.99			
30	-3.45	-2.65			
35	-1.07	-4.58			
40	-1.78	-5.48			
45	-3.73	-6.76			
48	-3.73	-6.76			

MIZPAC

75

CURRENT DATA

Station: 46 Date: 3 Aug 75 Time: 1650ZLatitude: 70°-20.1' N Longitude: 167°-02' W

Depth (m)	N-Comp (cm sec ⁻¹)	E-Comp (cm sec ⁻¹)	Depth (M)	Direction (°T)	Speed (cm sec ⁻¹)
0	46.97	18.76	0-10	003	31.3
5	25.67	-7.78			
10	21.14	-5.34	10-30	337	23.5
15	23.29	-8.12			
20	23.78	-8.28	>30	339	16.6
25	19.80	-10.06			
30	19.80	-10.06			
35	18.25	-11.09			
40	25.49	-5.41			
45	21.82	-3.37			
47	6.06	-4.79			
50	6.06	-4.79			

MIZPAC

75

CURRENT DATA

Station: 47 Date: 3 Aug 75 Time: 2015ZLatitude: 70°43.0' N Longitude: 167°03.0' W

Depth (m)	N-Comp (cm sec ⁻¹)	E-Comp (cm sec ⁻¹)	Depth (M)	Direction (°T)	Speed (cm sec ⁻¹)
0	5.07	35.19	0-10	080	26.2
5	4.48	17.14			
10	4.21	25.13	10-30	086	34.2
15	1.03	36.36			
20	2.35	34.21	>30	103	30.7
25	2.15	33.74			
30	3.37	32.02			
35	4.58	34.28			
40	-0.14	40.43			
45	-7.22	41.14			
50	-12.89	45.11			
55	-12.14	9.55			
60	-12.14	9.55			

MIZPAC

75

CURRENT DATA

Station: 48 Date: 3 Aug 75 Time: 2140ZLatitude: 70°40.5' N Longitude: 167° - 11.0' W

Depth (m)	N-Comp (cm sec ⁻¹)	E-Comp (cm sec ⁻¹)	Depth (M)	Direction (°T)	Speed (cm sec ⁻¹)
0	22.	-25.96	0-10	318	31.7
5	24.	-25.00			
8	22.	-18.76	10-30	298	9.3
10	24.	-15.36	>30	298	8.1
14	12.	-2.18			
16	1.	-8.75			
18	2.	-10.84			
20	5.	-11.57			
20	3.	-9.49			
24	3.	-7.56			
27	3.	-7.56			
30	3.	-7.56			
35	3.	-7.56			
40	2.	-6.93			
45	4.	-8.84			
50	4.	-6.57			
54	4.	-6.57			
55	4.	-6.57			

Station: 51 Date: 4 Aug 75 Time: 0200ZLatitude: 70°-43.5' N Longitude: 168°-02.5' W

Depth (m)	N-Comp (cm sec ⁻¹)	E-Comp (cm sec ⁻¹)	Depth (M)	Direction (°T)	Speed (cm sec ⁻¹)
0	35.20	-0.22	0-10	008	29.6
5	27.11	-0.38			
10	25.61	13.42	10-30	040	21.1
15	21.02	12.07			
20	15.64	13.89	>30	020	9.8
25	15.64	13.89			
30	12.23	14.46			
35	14.94	11.01			
40	14.34	9.80			
44	3.70	-3.58			
45	3.70	-3.58			

Station: 63 Date: 5 Aug 75 Time: 1230ZLatitude: 70°-40.5' N Longitude: 164°-11.7' W

Depth (m)	N-Comp (cm sec ⁻¹)	E-Comp (cm sec ⁻¹)	Depth (M)	Direction (°T)	Speed (cm sec ⁻¹)
0	3.92	12.22	0-10	062	11.8
2	3.38	13.43			
4	6.91	5.86	10-30	047	4.9
6	8.27	9.79			
8	5.22	10.72	>30	074	4.4
10	5.22	10.72			
12	4.95	12.30			
14	2.81	-2.21			
16	3.33	2.91			
18	4.21	1.83			
20	3.33	2.91			
25	7.15	2.17			
30	-2.36	5.36			
35	0.27	7.86			
40	1.43	2.75			
44	1.57	3.24			
45	1.57	3.24			

MIZPAC

75

CURRENT DATA

Station: 65 Date: 5 Aug 75 Time: 1500ZLatitude: 70°-36.0' N Longitude: 164°-09.0' W

Depth (m)	N-Comp (cm sec ⁻¹)	E-Comp (cm sec ⁻¹)	Depth (M)	Direction (°T)	Speed (cm sec ⁻¹)
0	-4.61	-3.04	0-10	346	5.1
5	12.83	-4.43	10-30	041	6.1
10	6.64	3.85	>30	047	10.5
15	3.01	-5.46			
20	-5.17	5.52			
25	9.76	8.67			
30	10.77	7.18			
35	10.29	7.95			
40	13.01	8.44			
44	2.74	7.22			
45	2.74	7.22			

MIZPAC

75

CURRENT DATA

Station: 68 Date: 5 Aug 75 Time: 1815ZLatitude: 70°-24.0' N Longitude: 164°-00.0' W

Depth (m)	N-Comp (cm sec ⁻¹)	E-Comp (cm sec ⁻¹)	Depth (M)	Direction (°T)	Speed (cm sec ⁻¹)
0	25.16	7.07	0-10	012	25.4
5	24.63	2.77	10-30	034	24.6
10	24.64	5.71	>30	028	12.7
15	23.51	12.43			
20	16.11	7.59			
25	19.41	18.34			
30	22.50	16.49			
35	25.17	18.18			
32	4.12	-0.07			
37	4.12	-0.07			

MIZPAC

75

CURRENT DATA

Station: 69 Date: 5 Aug 75 Time: 2025ZLatitude: 70°-21.5' N Longitude: 163°-19.5' W

Depth (m)	N-Comp (cm sec ⁻¹)	E-Comp (cm sec ⁻¹)	Depth (M)	Direction (°T)	Speed (cm sec ⁻¹)
0	4.97	-0.81	0-10	263	3.0
5	-4.72	-4.16			
10	-1.38	-3.97	10-30	226	4.3
15	-3.14	-8.84			
20	-4.60	-5.70	>30	055	1.5
25	-5.14	0.97			
30	0.89	1.26			
33	0.89	1.26			

MIZPAC

75

CURRENT DATA

Station: 70 Date: 5 Aug 75 Time: 2215ZLatitude: 70°-28.0' N Longitude: 163°-05.0' W

Depth (m)	N-Comp (cm sec ⁻¹)	E-Comp (cm sec ⁻¹)	Depth (M)	Direction (°T)	Speed (cm sec ⁻¹)
0	-15.43	2.62	0-10	035	5.4
5	23.94	1.24			
10	4.68	5.29	10-30	024	1.1
15	-0.03	2.83			
20	1.72	0.64	>30	036	0.5
25	1.75	-2.05			
30	0.42	0.30			
33	0.42	0.30			

MIZPAC

75

CURRENT DATA

Station: 72 Date: 6 Aug 75 Time: 0200ZLatitude: 70°-18.5' N Longitude: 162°-54.0' W

Depth (m)	N-Comp (cm sec ⁻¹)	E-Comp (cm sec ⁻¹)	Depth (M)	Direction (°T)	Speed (cm sec ⁻¹)
0	-24.85	-3.55			
5	-3.99	-7.09	0-10	205	11.6
10	-2.55	-4.06			
15	2.38	-4.22	10-29	321	1.7
20	0.63	-0.47			
24	1.80	-0.01			
26	0.97	-0.35			
29	0.97	-0.35			

MIZPAC

75

CURRENT DATA

Station: 74 Date: 6 Aug 75 Time: 0430ZLatitude: 70°-12.3' N Longitude: 163°-46.5' W

Depth (m)	N-Comp (cm sec ⁻¹)	E-Comp (cm sec ⁻¹)	Depth (M)	Direction (°T)	Speed (cm sec ⁻¹)
0	-0.50	14.90	0-10	098	5.0
5	2.22	13.33			
10	-3.71	-13.52	10-30	218	13.7
15	-6.41	-20.92			
20	-10.75	-8.69	>30	190	12.9
25	-13.18	-2.32			
30	-12.67	-2.23			
31	-12.67	-2.23			

MIZPAC

75

CURRENT DATA

Station: 77 Date: 6 Aug 75 Time: 0845ZLatitude: 69°-59.2' N Longitude: 165°-06' W

Depth (m)	N-Comp (cm sec ⁻¹)	E-Comp (cm sec ⁻¹)	Depth (M)	Direction (°T)	Speed (cm sec ⁻¹)
0	-8.41	20.49	0-10	112	12.7
5	0.68	9.79			
10	-6.61	5.05	10-30	087	7.2
15	0.08	7.82			
20	-0.42	8.48	>30	048	5.2
25	-0.22	6.83			
30	2.11	5.52			
37	3.44	3.83			
39	3.44	3.83			

MIZPAC

75

CURRENT DATA

Station: 79 Date: 6 Aug 75 Time: 1230ZLatitude: 69°-56.6' N Longitude: 166°-06.1' W

Depth (m)	N-Comp (cm sec ⁻¹)	E-Comp (cm sec ⁻¹)	Depth (M)	Direction (°T)	Speed (cm sec ⁻¹)
0	15.08	-6.76	0-10	351	9.9
5	11.71	-4.82			
10	2.66	6.83	10-30	058	6.3
15	3.57	6.36			
20	4.94	5.65	>30	337	3.9
25	2.18	5.82			
30	2.51	3.45			
35	-0.22	-0.99			
40	4.56	-3.05			
42	5.03	-1.11			
44	5.03	-1.11			

MIZPAC

75

CURRENT DATA

Station: 81 Date: 6 Aug 75 Time: 1500ZLatitude: 69°58.1' N Longitude: 167°04.7' W

Depth (m)	N-Comp (cm sec ⁻¹)	E-Comp (cm sec ⁻¹)	Depth (M)	Direction (°T)	Speed (cm sec ⁻¹)
0	-30.71	3.16	0-10	164	21.5
5	-8.47	-1.62			
10	-22.62	16.68	10-30	123	10.8
15	-15.49	17.41			
20	-3.26	10.89	>30	079	5.7
25	-3.76	4.19			
30	-0.77	3.94			
35	1.50	7.43			
40	-0.21	5.22			
44	1.62	4.88			
45	1.62	4.88			

MIZPAC

75

CURRENT DATA

Station: 83 Date: 6 Aug 75 Time: 1820ZLatitude: 69°58.2' N Longitude: 168°03.5' W

Depth (m)	N-Comp (cm sec ⁻¹)	E-Comp (cm sec ⁻¹)	Depth (M)	Direction (°T)	Speed (cm sec ⁻¹)
0	2.69	5.62	0-10	038	6.8
5	7.05	0.50			
10	6.27	6.27	10-30	031	6.2
15	7.05	0.50			
20	6.05	4.67	>30	024	6.3
25	3.20	4.00			
30	5.00	3.46			
35	6.97	4.12			
40	4.08	2.72			
44	5.95	1.67			
45	5.95	1.67			

Station: 86 Date: 6 Aug 75 Time: 2200ZLatitude: 70°-01.0' N Longitude: 168°-20.0' W

Depth (m)	N-Comp (cm sec ⁻¹)	E-Comp (cm sec ⁻¹)	Depth (M)	Direction (°T)	Speed (cm sec ⁻¹)
0	4.21	-11.01	0-10	292	10.9
5	6.45	-11.05			
10	1.41	-8.32	10-30	314	7.6
15	4.35	-7.21			
20	4.51	-10.36	>30	322	5.7
25	7.28	-3.30			
30	5.19	-0.92			
35	5.87	-2.63			
40	4.56	-4.22			
43	3.67	-3.61			
44	3.67	-3.61			

Station: 88 Date: 7 Aug 75 Time: 0001ZLatitude: 69°-59.0' N Longitude: 168°-16.6' W

Depth (m)	N-Comp (cm sec ⁻¹)	E-Comp (cm sec ⁻¹)	Depth (M)	Direction (°T)	Speed (cm sec ⁻¹)
0	-4.65	21.79	0-10	090	20.5
5	0.98	17.32			
10	3.50	22.31	10-30	113	13.3
15	-10.89	11.82			
20	-3.54	14.91	>30	106	8.4
25	-3.15	10.81			
30	-3.20	11.33			
35	-1.84	8.92			
40	-7.15	10.11			
44	-0.06	6.69			
45	-0.06	6.69			

MIZPAC

75

CURRENT DATA

Station: 90 Date: 7 Aug 75 Time: 0400ZLatitude: 69°-46.0' N Longitude: 168°-40.0' W

Depth (m)	N-Comp (cm sec ⁻¹)	E-Comp (cm sec ⁻¹)	Depth (M)	Direction (°T)	Speed (cm sec ⁻¹)
0	-2.77	13.40	0-10	029	3.8
5	4.79	-3.08			
10	7.92	-4.88	10-30	328	7.6
15	10.15	-6.15			
20	7.92	-4.88	>30	047	3.1
25	4.34	-2.83			
30	3.45	-2.32			
35	3.99	1.29			
40	1.08	2.34			
45	3.50	3.18			
48	1.08	2.34			
50	1.08	2.34			

MIZPAC

75

CURRENT DATA

Station: 91 Date: 7 Aug 75 Time: 0645ZLatitude: 69°-40.5' N Longitude: 169°-07.5' W

Depth (m)	N-Comp (cm sec ⁻¹)	E-Comp (cm sec ⁻¹)	Depth (M)	Direction (°T)	Speed (cm sec ⁻¹)
0	-12.58	9.24	0-10	111	5.0
5	4.04	-1.07			
10	3.07	5.75	10-30	016	6.6
15	3.94	7.83			
20	8.44	-2.02	>30	014	4.9
25	7.19	0.67			
30	6.01	0.73			
35	6.47	-0.36			
40	5.17	1.32			
45	5.41	1.70			
50	3.27	1.52			
53	3.27	1.52			

MIZPAC

75

CURRENT DATA

Station: 92 Date: 7 Aug 75 Time: 0915ZLatitude: 69°-47.8' N Longitude: 169°-29.8' W

Depth (m)	N-Comp (cm sec ⁻¹)	E-Comp (cm sec ⁻¹)	Depth (M)	Direction (°T)	Speed (cm sec ⁻¹)
0	5.79	-11.39	0-10	329	3.7
5	-0.32	4.01			
10	3.97	1.71	10-30	243	3.8
15	-4.16	-2.73			
20	-0.57	-4.25	>30	320	1.2
25	-1.32	-4.38			
30	-0.74	-2.18			
35	-0.12	-0.45			
40	-0.37	-1.82			
44	2.02	-0.38			
45	2.02	-0.38			

MIZPAC

75

CURRENT DATA

Station: 94 Date: 7 Aug 75 Time: 1110ZLatitude: 69°-50.5' N Longitude: 169°-05.0' W

Depth (m)	N-Comp (cm sec ⁻¹)	E-Comp (cm sec ⁻¹)	Depth (M)	Direction (°T)	Speed (cm sec ⁻¹)
0	-5.89	1.08	0-10	130	2.5
2	-2.90	0.74			
4	0.06	2.85	10-30	239	5.6
6	-0.31	4.95			
8	-1.18	3.26	>30	120	3.0
10	0.44	-1.20			
12	1.78	-2.87			
15	0.43	-4.60			
18	-4.59	-6.60			
20	-4.59	-6.50			
25	-4.59	-6.50			
30	-5.72	-1.56			
35	-2.67	2.87			
40	-0.88	2.42			
41	-0.88	2.42			

MIZPAC

75

CURRENT DATA

Station: 98 Date: 7 Aug 75 Time: 1445ZLatitude: 69°-44.5' N Longitude: 169°-00.0' W

Depth (m)	N-Comp (cm sec ⁻¹)	E-Comp (cm sec ⁻¹)	Depth (M)	Direction (°T)	Speed (cm sec ⁻¹)
0	-15.62	17.82	0-10	134	18.3
5	-10.17	11.19			
10	-12.29	10.54	10-30	127	16.8
15	-13.63	12.99			
20	-10.50	15.53	>30	099	7.6
25	-8.59	13.32			
30	-7.56	12.14			
35	-7.27	12.56			
40	-4.01	15.25			
46	3.32	14.40			
48	1.09	-2.33			
52	1.09	-2.33			

MIZPAC

75

CURRENT DATA

Station: 101 Date: 8 Aug 75 Time: 0232ZLatitude: 69°-55.5' N Longitude: 165°-46.5' W

Depth (m)	N-Comp (cm sec ⁻¹)	E-Comp (cm sec ⁻¹)	Depth (M)	Direction (°T)	Speed (cm sec ⁻¹)
0	2.05	-13.03	0-10	309	6.7
5	5.70	0.92			
10	4.80	-3.60	10-30	309	4.4
15	2.94	-4.83			
20	3.85	-2.37	>30	279	1.8
25	2.82	-3.09			
30	1.50	-3.27			
35	0.20	-3.30			
40	0.31	-0.98			
43	0.31	-0.98			

MIZPAC

75

CURRENT DATA

Station: 102 Date: 8 Aug 75 Time: 0420ZLatitude: 69°-57.7'N Longitude: 165°-21.0'W

Depth (m)	N-Comp (cm sec ⁻¹)	E-Comp (cm sec ⁻¹)	Depth (M)	Direction (°T)	Speed (cm sec ⁻¹)
0	-3.19	-1.41	0-10	215	4.8
5	-0.38	-2.01			
10	-8.20	-4.91	10-30	223	8.0
15	-4.55	-5.84			
20	-6.48	-5.70	>30	218	7.7
25	-6.29	-5.22			
30	-6.09	-4.74			
35	-6.09	-4.74			
39	-6.09	-4.74			

MIZPAC

75

CURRENT DATA

Station: 103 Date: 8 Aug 75 Time: 0615ZLatitude: 70°-02.6' N Longitude: 164°-43.2' W

Depth (m)	N-Comp (cm sec ⁻¹)	E-Comp (cm sec ⁻¹)	Depth (M)	Direction (°T)	Speed (cm sec ⁻¹)
0	18.43	6.86			
5	5.52	-2.78	0-10	010	13.9
10	17.06	2.93			
15	13.87	5.15	10-30	057	6.0
20	6.46	6.75			
25	-2.30	5.82	>30	153	5.7
30	-5.06	2.54			
39	-5.06	2.54			

MIZPAC

75

CURRENT DATA

Station: 104 Date: 8 Aug 75 Time: 0900ZLatitude: 70°-07.5' N Longitude: 164°-17.9' W

Depth (m)	N-Comp (cm sec ⁻¹)	E-Comp (cm sec ⁻¹)	Depth (M)	Direction (°T)	Speed (cm sec ⁻¹)
0	-0.66	-1.45	0-10	196	3.0
5	-5.51	-0.01			
10	-2.55	-1.04	10-30	117	0.7
15	1.89	4.13			
20	-0.86	-0.98	>30	163	1.5
25	-0.86	-0.98			
30	-1.48	0.44			
35	-1.48	0.44			

MIZPAC

75

CURRENT DATA

Station: 105 Date: 8 Aug 75 Time: 1159ZLatitude: 69°-51.5' N Longitude: 164°-48.5' W

Depth (m)	N-Comp (cm sec ⁻¹)	E-Comp (cm sec ⁻¹)	Depth (M)	Direction (°T)	Speed (cm sec ⁻¹)
0	-0.85	-12.83	0-10	249	17.6
5	-8.97	-19.11			
10	-8.96	-17.40	10-30	254	5.8
15	-9.05	-16.29			
20	2.00	-9.35	>30	123	3.1
25	-4.71	0.62			
30	5.26	2.64			
33	-1.69	2.59			
35	-1.69	2.59			

Station: 107 Date: 8 Aug 75 Time: 1412ZLatitude: 70°-01.0' N Longitude: 164°-52.0' W

Depth (m)	N-Comp (cm sec ⁻¹)	E-Comp (cm sec ⁻¹)	Depth (M)	Direction (°T)	Speed (cm sec ⁻¹)
0	-15.76	-11.98	0-10	315	19.1
5	14.26	8.69			
10	14.72	-10.17	10-30	002	14.6
15	24.69	-2.68			
20	17.54	-0.81	>30	304	3.0
25	6.34	0.74			
30	9.90	4.50			
35	2.19	-1.36			
37	2.19	-1.36			

Station: 109 Date: 8 Aug 75 Time: 1630ZLatitude: 70°-11.8' N Longitude: 164°-56.0' W

Depth (m)	N-Comp (cm sec ⁻¹)	E-Comp (cm sec ⁻¹)	Depth (M)	Direction (°T)	Speed (cm sec ⁻¹)
0	17.13	-3.87	0-10	322	3.3
5	-14.53	2.15			
10	5.18	-4.46	10-30	292	16.2
15	8.44	-14.82			
20	5.95	-18.33	>30	280	7.7
25	5.75	-14.74			
30	4.04	-12.32			
35	2.50	-12.61			
40	0.73	-5.10			
43	0.73	-5.10			

MIZPAC

75

CURRENT DATA

Station: 111 Date: 8 Aug 75 Time: 1830ZLatitude: 70°-21.0' N Longitude: 164°-50.0' W

Depth (m)	N-Comp (cm sec ⁻¹)	E-Comp (cm sec ⁻¹)	Depth (M)	Direction (°T)	Speed (cm sec ⁻¹)
5	49.83	16.57	0-10	038	50.8
10	30.67	45.33			
15	26.09	68.36	10-30	099	29.5
20	-11.27	42.29			
25	-17.15	5.60	>30	179	8.6
30	-16.13	0.31			
35	-6.12	2.69			
40	-11.12	1.50			
45	-6.12	2.69			
50	-9.77	-3.25			
55	-9.77	-3.25			

MIZPAC

75

CURRENT DATA

Station: 114 Date: 8 Aug 75 Time: 2215ZLatitude: 70°-43.6' N Longitude: 164°-45.3' W

Depth (m)	N-Comp (cm sec ⁻¹)	E-Comp (cm sec ⁻¹)	Depth (M)	Direction (°T)	Speed (cm sec ⁻¹)
0	7.89	32.63			
5	57.79	-27.68	0-10	013	25.5
10	8.84	12.52			
15	26.29	-12.04	10-30	006	17.1
20	11.81	10.39			
25	12.56	8.57	>30	347	20.3
30	17.27	-0.11			
35	19.37	-4.75			
40	19.37	-4.75			
44	20.18	-4.11			
45	20.18	-4.11			

MIZPAC

75

CURRENT DATA

Station: 115 Date: 9 Aug 75 Time: 0013ZLatitude: 70°-43.5' N Longitude: 164°-15.0' W

Depth (m)	N-Comp (cm sec ⁻¹)	E-Comp (cm sec ⁻¹)	Depth (M)	Direction (°T)	Speed (cm sec ⁻¹)
0	40.23	38.67	0-10	049	36.7
5	16.33	28.77			
10	19.93	20.53	10-30	055	27.1
15	18.51	23.72			
20	14.65	20.91	>30	053	21.8
25	17.96	22.27			
30	13.15	23.48			
35	15.32	22.30			
40	14.19	19.98			
45	10.13	11.66			
48	10.13	11.66			

MIZPAC

75

CURRENT DATA

Station: 120 Date: 9 Aug 75 Time: 0930ZLatitude: 70°-39.0' N Longitude: 161°-45.0' W

Depth (m)	N-Comp (cm sec ⁻¹)	E-Comp (cm sec ⁻¹)	Depth (M)	Direction (°T)	Speed (cm sec ⁻¹)
0	-32.31	-11.30	0-10	203	34.5
5	-39.42	-17.99			
10	-23.70	-10.36	10-30	213	25.9
15	-20.51	-19.60			
20	-20.75	-13.14	>30	178	16.5
25	-20.37	-11.64			
30	-24.87	-12.24			
35	-27.57	-3.63			
38	-10.98	2.76			
41	-10.98	2.76			

MIZPAC

75

CURRENT DATA

Station: 121 Date: 9 Aug 75 Time: 1350ZLatitude: 70°-39.0' N Longitude: 161°-05.0' W

Depth (m)	N-Comp (cm sec ⁻¹)	E-Comp (cm sec ⁻¹)	Depth (M)	Direction (°T)	Speed (cm sec ⁻¹)
0	-2.31	8.00	0-10	115	7.4
5	-5.37	6.64			
10	-1.81	5.48	10-30	094	12.7
15	-10.85	8.46			
20	-4.71	13.76	>30	069	6.0
25	5.40	14.58			
30	6.61	13.99			
35	2.30	7.51			
40	2.06	4.72			
41	2.06	4.72			

MIZPAC

75

CURRENT DATA

Station: 129B Date: 10 Aug 75 Time: 1600ZLatitude: 70°-20.6' N Longitude: 164°-50.0' W

Depth (m)	N-Comp (cm sec ⁻¹)	E-Comp (cm sec ⁻¹)	Depth (M)	Direction (°T)	Speed (cm sec ⁻¹)
0	6.79	10.94	0-10	061	12.5
5	5.64	11.97			
10	5.70	9.81	10-30	022	5.3
15	-0.68	4.84			
20	7.25	-2.91	>30	054	4.2
25	6.91	2.27			
30	6.06	3.56			
35	3.59	3.89			
40	1.89	3.07			
42	1.89	3.07			

MIZPAC

75

CURRENT DATA

Station: 129D Date: 10Aug 75 Time: 1700ZLatitude: 70°-20.5' N Longitude: 164°-47.5' W

Depth (m)	N-Comp (cm sec ⁻¹)	E-Comp (cm sec ⁻¹)	Depth (M)	Direction (°T)	Speed (cm sec ⁻¹)
0	16.34	14.66	0-10	040	14.0
5	8.33	7.77			
10	7.57	4.59	10-30	057	9.3
15	1.91	8.81			
20	7.45	6.64	>30	074	6.3
25	5.45	7.22			
30	5.57	8.24			
35	8.26	8.28			
40	-1.62	4.89			
42	-1.62	4.89			

MIZPAC

75

CURRENT DATA

Station: 129J Date: 10Aug 75 Time: 2000ZLatitude: 70°-19.6' N Longitude: 164°-37.0' W

Depth (m)	N-Comp (cm sec ⁻¹)	E-Comp (cm sec ⁻¹)	Depth (M)	Direction (°T)	Speed (cm sec ⁻¹)
0	-0.90	24.41	0-10	087	23.5
5	1.09	23.13			
10	9.92	22.82	10-30	034	12.6
15	15.99	12.11			
20	13.89	4.32	>30	040	5.6
25	8.16	5.47			
30	3.45	6.49			
35	4.87	4.35			
40	4.03	3.20			
44	4.03	3.20			

MIZPAC

75

CURRENT DATA

Station: 129P Date: 10Aug75 Time: 2330ZLatitude: 70°-17.7' N Longitude: 164°-37.5' W

Depth (m)	N-Comp (cm sec ⁻¹)	E-Comp (cm sec ⁻¹)	Depth (M)	Direction (°T)	Speed (cm sec ⁻¹)
0	-3.27	22.23	0-10	121	20.2
5	-14.60	17.30			
10	-13.66	12.08	10-30	127	10.6
15	-10.89	5.49			
20	-5.36	6.15	>30	110	8.0
25	-3.56	10.23			
30	-5.61	12.11			
35	-3.67	9.60			
40	-2.79	7.74			
41	-2.12	6.35			
42	-2.12	6.35			

MIZPAC

75

CURRENT DATA

Station: 130G Date: 11Aug75 Time: 0800ZLatitude: 70°-14.1' N Longitude: 164°-41.4' W

Depth (m)	N-Comp (cm sec ⁻¹)	E-Comp (cm sec ⁻¹)	Depth (M)	Direction (°T)	Speed (cm sec ⁻¹)
0	1.49	10.94	0-10	103	11.1
5	-5.58	7.88			
10	-3.20	13.65	10-30	180	4.8
15	-6.10	-0.47			
20	-5.36	-0.61	>30	146	2.1
25	-5.28	-0.10			
30	-2.30	1.15			
35	-0.60	1.18			
37	-2.30	1.15			
40	-2.30	1.15			

Station: 130N Date: 11Aug75 Time: 1130ZLatitude: 70°-12.2' N Longitude: 164°-37.3' W

Depth (m)	N-Comp (cm sec ⁻¹)	E-Comp (cm sec ⁻¹)	Depth (M)	Direction (°T)	Speed (cm sec ⁻¹)
0	-6.20	13.44	0-10	121	13.2
5	-6.53	11.62			
10	-7.77	8.74	10-30	128	5.1
15	-4.75	9.00			
20	-4.27	3.16	>30	137	1.9
25	-1.88	2.39			
30	-1.47	1.44			
35	-1.26	0.97			
40	-1.47	1.44			
45	-1.47	1.44			

Station: 130W Date: 11Aug75 Time: 1600ZLatitude: 70°-10.8' N Longitude: 164°-40.0' W

Depth (m)	N-Comp (cm sec ⁻¹)	E-Comp (cm sec ⁻¹)	Depth (M)	Direction (°T)	Speed (cm sec ⁻¹)
0	-1.02	-1.12	0-10	199	3.4
5	-4.95	-0.84			
10	-3.68	-1.28	10-30	170	0.5
15	-0.73	2.06			
20	-1.22	0.46	>30	114	1.0
25	-1.02	-1.12			
30	1.19	-1.07			
35	-0.41	0.94			
39	-0.41	0.94			

DISTRIBUTION LIST

<u>ADDRESSEE</u>	<u>NO. OF COPIES</u>
Director Applied Physics Laboratory University of Washington 1013 Northeast 40th Street Seattle, Washington 98195	
Mr. Robert E. Francois	1
Mr. E. A. Pence	1
Mr. G. R. Garrison	1
Library	1
Director Arctic Submarine Laboratory Code 90, Building 371 Naval Undersea Center San Diego, California 92132	25
Superintendent Naval Postgraduate School Monterey, California 93940	
Library	2
Dr. R. G. Paquette	5
Dr. R. H. Bourke	5
Polar Research Laboratory, Inc. 123 Santa Barbara Street Santa Barbara, California 93101	2
Chief of Naval Operations Department of the Navy Washington, D. C. 20350	
NOP-02	1
NOP-22	1
NOP-946D2	1
NOP-095	1
NOP-098	1
Commander Submarine Squadron THREE Fleet Station Post Office San Diego, California 92132	1
Commander Submarine Group FIVE Fleet Station Post Office San Diego, California 92132	1

DISTRIBUTION LIST

<u>ADDRESSEE</u>	<u>NO. OF COPIES</u>
Director Marine Physical Laboratory Scripps Institution of Oceanography San Diego, California 92132	1
Commanding Officer Naval Intelligence Support Center 4301 Suitland Road Washington, D. C. 20390	1
Commander Naval Electronic Systems Command Naval Electronics System Command Headquarters Department of the Navy Washington, D. C. 20360 NESC 03 PME 124	1 1 1
Director Woods Hole Oceanographic Institution Woods Hole, Massachusetts 02543	1
Commanding Officer Naval Coastal Systems Laboratory Panama City, Florida 32401	1
Commanding Officer Naval Submarine School Box 700, Naval Submarine Base, New London Groton, Connecticut 06340	1
Assistant Secretary of the Navy (Research and Development) Department of the Navy Washington, D. C. 20350	2
Director of Defense Research and Engineering Office of Assistant Director (Ocean Control) The Pentagon Washington, D. C. 20301	1
Commander, Naval Sea Systems Command Naval Sea Systems Command Headquarters Department of the Navy Washington, D. C. 20362	4

DISTRIBUTION LIST

<u>ADDRESSEE</u>	<u>NO. OF COPIES</u>
Chief of Naval Research Department of the Navy 800 North Quincy Street Arlington, Virginia 22217	1
Code 102-OS	1
Code 220	1
Code 461	1
Code 480	1
Project Manager Anti-Submarine Warfare Systems Project Office (PM4) Department of the Navy Washington, D. C. 20360	1
Commanding Officer Naval Underwater Systems Center Newport, Rhode Island 02840	1
Commander Naval Air Systems Command Headquarters Department of the Navy Washington, D. C. 20361	2
Commander Naval Oceanographic Office Washington, D. C. Attention: Library	2
Director Defense Supply Agency Defense Documentation Center Cameron Station Alexandria, Virginia 22314	2
Director Advanced Research Project Agency 1400 Wilson Boulevard Arlington, Virginia 22209	1
Commander SECOND Fleet Fleet Post Office New York, New York 09501	1
Commander THIRD Fleet Fleet Post Office San Francisco, California 96601	1

DISTRIBUTION LIST

<u>ADDRESSEE</u>	<u>NO. OF COPIES</u>
Commander Naval Surface Weapons Center White Oak Silver Spring, Maryland 20910 Mr. M. M. Kleinerman Library	1 1
Officer-in-Charge New London Laboratory Naval Underwater Systems Center New London, Connecticut 06320	1
Commander Submarine Development Group TWO Box 70 Naval Submarine Base New London Groton, Connecticut 06340	1
Oceanographer of the Navy Hoffman II 200 Stovall Street Alexandria, Virginia 22332	1

ADDRESSEENO. OF COPIES

Commandant
U. S. Coast Guard Headquarters
400 Seventh Street, S.W.
Washington, D. C. 20590 2

Commander
Pacific Area, U. S. Coast Guard
630 Sansome Street
San Francisco, California 94126 1

Commander
Atlantic Area, U. S. Coast Guard
Governors Island
New York, New York 10004 1

DISTRIBUTION LIST

<u>ADDRESSEE</u>	<u>NO. OF COPIES</u>
Commander Naval Weapons Center China Lake, California 93555 Attention: Library	1
Commander Naval Electronics Laboratory Center 271 Catalina Boulevard San Diego, California 92152 Attention: Library	1
Director Naval Research Laboratory Washington, D. C. 20375 Attention: Technical Information Division	3
Director Ordnance Research Laboratory Pennsylvania State University State College, Pennsylvania 16801	1
Commander Submarine Force U. S. Atlantic Fleet Norfolk, Virginia 23511	1
Commander Submarine Force U. S. Pacific Fleet N-21 FPO San Francisco, California 96610	1 1
Commander Naval Air Development Center Warminster, Pennsylvania 18974	1
Commander Naval Ship Research and Development Center Bethesda, Maryland 20084	1
Chief of Naval Material Department of the Navy Washington, D. C. 20360 NMAT 03 NMAT 034 NMAT 0345	2 1 1

DISTRIBUTION LIST

<u>ADDRESSEE</u>	<u>NO. OF COPIES</u>
Department of Oceanography, Code 68 Naval Postgraduate School Monterey, California 93940	3
Commander Naval Weather Service Command Washington Navy Yard Washington, D. C. 20390	1
Dr. Robert E. Stevenson Scientific Liaison Office, ONR Scripps Institution of Oceanography La Jolla, California 92037	1
SIO Library University of California, San Diego P. O. Box 2367 La Jolla, California 92037	1
Department of Oceanography Library University of Washington Seattle, Washington 98105	1
Department of Oceanography Library Oregon State University Corvallis, Oregon 97331	1
Commanding Officer Fleet Numerical Weather Central Monterey, California 93940	1
Commanding Officer Navy Environmental Prediction Research Facility Monterey, California 93940	1
LCDR W. Zuberbuhler 2775 Brookwood Orange Park, Florida 32073	2
LT John Roeder 125 E. Oakshire Dr. Embassy Hills Port Richey, Florida 33568	2
LCDR John Pfeiffer 77 Adams Place Apt 407 Quincy, Massachusetts 02169	1

Thesis
Z76 Zuberbuhler 166713
c.1 Oceanography, meso-
structure, and currents
of the pacific marginal
sea-ice zone - MIZPAC
75.

Thesis
Z76 Zuberbuhler 166713
c.1 Oceanography, meso-
structure, and currents
of the pacific marginal
sea-ice zone - MIZPAC
75.

thesZ76

Oceanography, mesostructure, and current



3 2768 001 90440 2

DUDLEY KNOX LIBRARY